EXPERIMENTAL MODELING AND INTELLIGENT CONTROL OF A WOOD-DRYING KILN

GIVON CHUEN KEE YAN

B.A.Sc. in Mechanical Engineering, University of Manitoba, Canada, 1997

A THESIS SUBMITTED IN PARTIAL FULFILMENT OF
THE REQUIREMENTS FOR THE DEGREE OF

MASTER OF APPLIED SCIENCE

in

THE FACULTY OF GRADUATE STUDIES
DEPARTMENT OF MECHANICAL ENGINEERING

We accept the thesis as conforming
to the required standard

THE UNIVERSITY OF BRITISH COLUMBIA

May 2000

Department of MECHANICAL ENGINEERING

The University of British Columbia
Vancouver, Canada

Date 28 APRIL 2000

DE-6 (2/88)

ABSTRACT

This thesis focuses on the development, implementation, and evaluation of a control system for a lumber drying kiln process. The control system uses sensory feedback from the moisture content sensors of the wood pieces and from the temperature sensors of the kiln interior. Both conventional and fuzzy-logic proportional-integral-derivative control are developed. In order to achieve the research goals, this investigation is divided into two parts. The first part of the thesis consists of the system modeling and validation where experimental modeling is emphasized. The second part presents the controller design, development, and implementation. Both simulation studies and experimental studies on a prototype wood-drying kiln are carried out.

System modeling is performed by system identification scheme using experimental data and recursive least squares algorithm for parameter estimation. Process models are developed based on the assumptions that the process is a linear, time invariant, and single-input-single-output (SISO) uncoupled one with no time delay. Two different approaches are utilized in constructing the system model. The first approach is to obtain the system model directly as a single model structure, while the second approach is to obtain the system model through separating the overall system into two subsystems. Models are built assuming different dynamic orders and then validated by comparing the model response with the actual kiln response, based on experimental data. Extensive computer simulations are carried out to investigate the validity of the dynamic models. Results illustrate nonlinear, time-varying, and time delay characteristics of the process.

In the context of controller design and development, two different control methodologies are developed: a conventional proportional-integral-derivative (PID) controller and a direct fuzzy logic controller (FLC). Simulations are performed using the model developed through system identification. System performance is evaluated through simulations performed using Matlab Simulink.

The developed control system is then implemented in a downscaled industrial kiln which is located at the Innovation Centre of National Research Council (NRC) of Canada. This experimental setup is equipped with a variety of sensors, which include

thermocouples for temperature feedback, an air velocity transmitter for measuring airflow speed in the plenum, relative humidity sensors for measuring the relative humidity inside the kiln, and wood moisture content sensors for measuring the moisture content of the wood pieces. The actuators of the experimental kiln system include an on/off electric heater and a variable-speed fan. All communications between actuators, sensors, and controllers are supported by software programming developed in Delphi, and located with the control computer. Extensive experimental studies are carried out on-line using the two controllers, and the results are evaluated to tune the controller parameters for achieving good performance in the wood drying kiln. The control system developed in this research may be applied in industrial wood drying kilns, with a clear potential for improved quality and increased speed of drying.

TABLE OF CONTENTS

LIST OF SYMBOLS

$e_{moisture}$	moisture error (Eq. 6.3)
EL	extremely Large
H	high
join	join operator (Eq. 3.26)
KD, KI, KP	derivative, integral and proportional gains, respectively
L	low
max	union operator (Eq. 3.11)
min	intersection operator (Eq. 3.12)
M	medium
NS	negative small
PL	positive large
PM	positive medium
PS	positive small
proj	projection operator
sup	supremum operator (Eq. 3.24, Eq. 3.29)
ZR	zero
o	composition operator (Eq. 3.30)
$\otimes$	transitional operator (Eq. 1.2)
$\oplus$	combinational operator (Eq. 1.2)

Greek Symbols

μ	membership function (Eq. 3.6)
ϕ_k	row vector containing system outputs and inputs computed at k
Φ_N	square matrix of $N{\times}N$ composed of ϕ
θ	column vector containing the estimated parameters of a and b

Abbreviations, Acronyms

AI	Artificial Intelligent
DAM	Data Acquisition Module
DAQ	Data Acquisition and Analogue Output
DFC	Direct Fuzzy Control
DFL	Direct Fuzzy Logic
DFLC	Direct Fuzzy Logic Controller
EMC	Equilibrium Moisture Content
FLC	Fuzzy Logic Control
FSP	Fiber Saturation Point
HFC	Hierarchical Fuzzy Logic Control
KB	Knowledge Base
LQG	Linear Quadratic Qaussian
LQR	Linear Quadratic Regulator
MC	Moisture Content
MDM	Mamdani's Direct Method
MI	Model Index
M-PID	Moisture Proportional-Integral-Derivative
NRC	National Research Council
PC	Personal Computer
PID	Proportional-Integral-Derivative
RLS	Recursive Least Squared
RMS	Root Mean Square
RPM	Revolution Per Minute
SISO	Single-Input-Single-Output
T-PID	Temperature Proportional-Integral-Derivative

LIST OF FIGURES

LIST OF TABLES

ACKNOWLEDGEMENT

Wong. Besides, I wish to especially thank Wing Hang Poon for his continuous support and encouragement during my stay in Vancouver. His generous care and support really touched my heart and brighten up my life.

I wish to thank my best friends in Hong Kong who always invited me for delicious dinners, and entertained me with fancy and spectacular events during my school breaks throughout the years. I sincerely thank: Karl Chung, Joseph Ip, Sandy Lai, Kai Man Lam, Benedict Leung and Family, Dr. Chi Min Shiu, and Simon Wong. I specially express my sincere thanks to Steve Mak for his unconditional friendship, care, support, and in the way he treats me as a very good friend, especially during hard periods of my life. Finally and most importantly, I express my sincere appreciation for the patience, support, love and encouragement of my very best friend Janet Leung throughout the years of my study in Canada. Thank God for introducing all these people into my life, and without you my life would have been incomplete. May God bless all these people. Thank you Father, I love you.

To my mother whom I love forever;
To my very best friend Janet for the love and encouragement she brings to my life;
To my undergraduate professor Rudy Schilling for his support and caring that deeply
touches my heart and brightens up my life;
To my graduate professor Clarence de Silva for his continuous support and supervision
that will last forever in my memory.

I wish to dedicate this thesis to the above people, for the success and completion of my
study in the University of British Columbia. They fill my life with joy and love. Their
support and encouragement mean so much to me, and make my life quite fulfilling.
— Givon Yan, 2000

Chapter 1

INTRODUCTION

The main objective of the research described in the thesis is to develop, implement, and evaluate an appropriate control scheme for an industrial kiln used in wood drying. In this chapter, first the background of the wood drying process is discussed, which includes some fundamental knowledge of the structure of wood in relation to the process of wood drying, the objectives of wood drying, and factors affecting the performance of lumber drying kilns. Next, the process goals and the related problems and difficulties in achieving these goals are discussed. Then the motivation for the present study is outlined. This is followed by an overview of the experimental setup that is used in the present work. The approach that has been taken in achieving the research goal is indicated, which includes the use of a conventional control scheme in conjunction with model-free intelligent control. Knowledge-based control and hierarchical control, which fall into the general area of intelligent control, are also discussed. The objectives and the scope of the research are outlined. The chapter concludes by indicating the contributions of this research and by giving a brief overview of the thesis.

1.1 Background

Industrial wood drying kilns are built for high-volume drying. They are constructed in warehouse sizes with the length ranging from 40 to 120 feet, and the width which mainly depends on the stack of lumber, ranging approximately from 6 to 9 feet. Wood drying is both a time consuming and energy consuming process that is carried out based on a pre-determined schedule. Current kiln operations in sawmills are executed as open-loop processes in the sense that they do not employ direct feedback of information from the wood pieces in the kiln. However, in some sense, the human operator may provide a link for information feedback, through manual adjustments of the kiln during the drying process. Industrial sawmills employ experienced kiln operators to work on-line with the entire drying operation, who frequently provide the required monitoring and supervision.

The way that industrial sawmills carry out the drying process is by executing an appropriate drying schedule according to the particular species of wood. Drying schedule is a chart that indicates all the necessary conditions for each drying step; specifically, operating temperature, time duration of drying, both dry bulb and wet bulb temperatures, equilibrium moisture content, and the relative humidity, which combined together is expected to give good drying result. Past information from kilns, existing drying schedules of similar wood species, and initial moisture conditions of wood are used in developing schedules for lumber drying.

In Canada, forestry is a major industry in the province of British Columbia (B.C.), a leading region in the world for wood production. Billion tons of wood are produced in the province annually. Improvements in process efficiency and product quality will bring about direct economic benefits and also would lead to growth of the industry.

1.1.1 Structure of Wood in Relation to Drying

Lumber drying is an important and complicated process, which consumes much time and energy. The complex material structure of wood and the sensitivity of the material characteristics to the stresses that buildup are known to limit the speed of drying. The variation in the properties of wood from species to species further complicates the drying process. Therefore, a good understanding of the fundamental properties of wood is important for understanding and controlling the drying process of lumber. The next section will discuss the species, structure, moisture relation, mechanism of drying, shrinkage, and the stress development during drying of wood.

<u>Wood species and structure</u>

The change of moisture content of wood is directly related to its structural features. Trees may be broadly divided into two groups: softwood and hardwood, but this is not directly related to the softness or hardness of their wood. Softwood denotes trees with needle or scale-like leaves; for example, pine, fir, spruce, hemlock and cedar. Hardwood denotes trees with broad leaves; for example, aspen, alder, birch, and broadleaf maple. Properties of wood drying are different in sapwood compared to heartwood mainly due to

their structural differences. Sapwood is the layer in the trunk that is located next to the bark, which contains living cells that transport water and nutrients to support the life of the tree. For softwood species, sapwood has a higher moisture content than in heartwood. For hardwood species, the sapwood has a slightly higher or almost the same moisture content compared to that of heartwood. This is because sapwood contains living cells and is therefore more permeable to water. As the tree grows layers of sapwood are added and the trunk diameter increases. The inner layer of sapwood dies and becomes infiltrated with gums and resins in the process [1]. This inner layer is what becomes heartwood, and has a greater resistance to moisture flow compared to sapwood. It is less permeable to water due to the presence of gums and resins within its structure, and therefore requires a longer drying time. Heartwood is harder to dry and more susceptible to drying defects. Consequently, milder drying conditions or comparatively lower temperature drying would be desirable.

Wood-moisture relation

Wood gains or loses moisture in an attempt to reach a state of equilibrium with the surrounding conditions or its environment (atmosphere). In wood drying, the amount of moisture present in the wood at this state of balance is called the equilibrium moisture content (EMC), and it primarily depends on the relative humidity and temperature inside the kiln. In kiln drying, it is crucial to control the EMC, which boils down to maintaining an optimum relative humidity and proper operating temperature, together with uniform and sufficient air circulation within the kiln. Control of these parameters is key to producing good drying results. In the initial stage of wood drying water is removed primarily from the cell cavities. This is called free water and is less tightly held within cell cavities and is easier to remove compared to bound water, which is the water held within the cell walls. It follows that relatively more heat energy is required to remove bound water. Once the water in the cell cavities is almost completely removed during a drying process, further drying would remove water from the cell wall. The wood at this stage reaches the fiber saturation point, and requires more attention. Fiber saturation point (FSP) is defined as the stage at which free water has been removed from the wood, but the cell walls are still rigid and fully saturated with water [1]. The FSP is important in

wood drying since it represents the beginning of water withdrawal from the cell walls, which results in changes of physical and mechanical properties; for example, increase of wood strength, onset of wood shrinkage, and development of internal stresses.

Mechanism of wood drying

In wood drying, several forces act simultaneously to move the water during evaporation [1]. These forces can be generally grouped into the following categories:

- Forces due to capillary action
- Forces of diffusion due to relative humidity gradient
- Forces of diffusion due to moisture content gradient

In the beginning of the wood drying process, water is removed from the surface by evaporation. The cells at the surface of wood will start to draw water from the neighboring cells and set up capillary forces. Free water will move from the cell cavity to an adjoining cell that is located closer to the surface, and a flow results by the so-called capillary action. The force that maintains this flow of water is a suction force caused by the capillary action.

Water is also moved by diffusion as a result of both the relative humidity gradient and the moisture content gradient. When water in the cell cavity of a surface cell is evaporated, its moisture concentration will decrease. The neighboring cells will then have a higher moisture concentration compared to the surface cells. Water moves from a higher water concentration to a lower water concentration by the mechanism known as diffusion. Since cell walls are a source of water vapor in the drying environment, water would evaporate from the cell walls into the cell cavities along the relative humidity gradient created by the adjacent cells by diffusion, during the drying process. Similarly, bound water within a cell wall would also move through the cell wall by diffusion due to the moisture content gradient being set by evaporation from the surface.

4

Wood shrinkage and stress development

Wood starts to shrink once all the water has been taken away from the cell cavities, and starting to lose water from the cell walls. Specifically, wood begins to shrink when the cell walls begin to lose water, at a moisture content of about 20% to 30% [1]. Precautions have to be taken during this drying period since internal stresses are more likely to develop when the drying temperature is too high, or the drying rate is too fast. Stresses normally develop when wood shrinks by different amounts in the three orthogonal directions (tangential, radial, and longitudinal). Since during the drying process, shrinkage begins in the outer fibers before it happens in the inner fibers, drying defects like warp and cracks are likely to occur.

The two main causes of stress development are:

1. Differential shrinkage
2. Hydrostatic tension.

Drying defects like surface checks and internal cracks can occur in the early stages of drying which are caused by either differential shrinkage or hydrostatic tension. Surface checks occur in the shell (surface of the wood) and the internal cracks occur in the core (inside part of the wood). During the early stages of drying, the fibers in the shell of the board start to dry first while the inner core is still wet. The outer shell begins to shrink and is resisted by the inner core. As a result the shell goes into tension while the core into compression. If the drying is too rapid, the shell will go into a permanently set condition without attaining full shrinkage and surface checks occur during the early stages of wood drying. When the drying progresses, the inner core starts to dry and shrink. However, the shrinkage of the inner core is prevented by the permanently expanded (set) condition of the shell, which causes the stresses to reverse. In this case, the core goes into tension and the shell into compression. This internal tension of the core could be severe enough to cause internal cracking.

Hydrostatic tension forces develop due to capillary action during the flow of water. As water is evaporated from the cell cavities near the surface, a tension pull is developed along the adjacent cells and is propagated deep into the wood. This tension pull is an inward force acting at the cell walls whose cavities are filled with water and can cause an inward collapse of these cell walls. The likelihood of occurrence of such inward collapse

is the greatest in the early stages of drying when many cell cavities are still full of water. Moreover, the collapse is more likely to occur if the drying temperature is very high.

1.1.2 Objective of Wood Drying

Wood drying is the final process before a batch of lumber is used in manufacturing. More importantly, the final moisture content of the wood pieces determines its value and the application. The manufacture of a high quality finished product like furniture requires a final moisture content of 12% or lower. The drying process is used to remove the moisture content of wood to assure high product quality. Besides, wood drying is also necessary for the following reasons [1]:

- To increase dimensional stability. Wood shrinks when it dries, and if it is cut before drying, it will appear undersized in the final form.
- To reduce or eliminate biological decay. Wood that is dried below 20% of its moisture content will not be susceptible to decay or insect attack.
- To increase the strength, stiffness and hardness of wood. The strength of wood can increase by 50% or more during the process of drying to a moisture content of 15%.
- To improve the ease of processing of wood. Properly dried wood is much easier to machine, glue, and finish.
- To increase the profit margin. The success and profitability of the drying process critically depends on the final quality of the dried wood since the commanded price increases with the drying quality.
- To reduce the weight for transportation. A weight reduction of 35% or more may result by removing the moisture in wood. This will reduce the shipping and handling costs.

1.1.3 Factors Affecting the Performance of Wood Drying Kilns

Wood is dried in a lumber drying kiln, which consists of one or more chambers designated to control the drying conditions. An overview of an industrial drying kiln is

shown in Figure 1-1. The operation efficiency, quality of the dried wood, and drying duration of the lumber drying process are all directly related to the design of the kiln. These design considerations include the geometry of the kiln setup, the mechanism of heat supply, the type and arrangement of fans, the operating temperature and relative humidity, control of the interior temperature and relative humidity, and the types of building material. There is always a trade-off between the initial setup cost and the drying quality. The performance of an industrial lumber drying kiln is mainly determined by the following factors [1]:

- Variation in the moisture content along individual wood pieces and within the wood stack
- Kiln charge preparation [i.e., stickering (placing different sizes of sticker in between layers of wood for air circulation), stacking (arranging wood pieces into different sizes of stack), sample selection (loading similar wood species of similar moisture content into the kiln for drying)]
- Capability and accuracy of kiln controller
- Controllability and uniformity of kiln conditions (kiln design)
- Skills, experience and reliability of kiln operator
- Dependability and maintenance of kiln equipment

1.1.4   Goals of the Present Work

The main objective of the work reported in this thesis is to develop a control system for an automated lumber drying process, aimed at reducing the drying time (efficient drying) and the energy consumption (effective use of energy), while maintaining or improving the quality of dried wood. In order to achieve this goal, the development of a control system with conventional and intelligent features is undertaken.

7
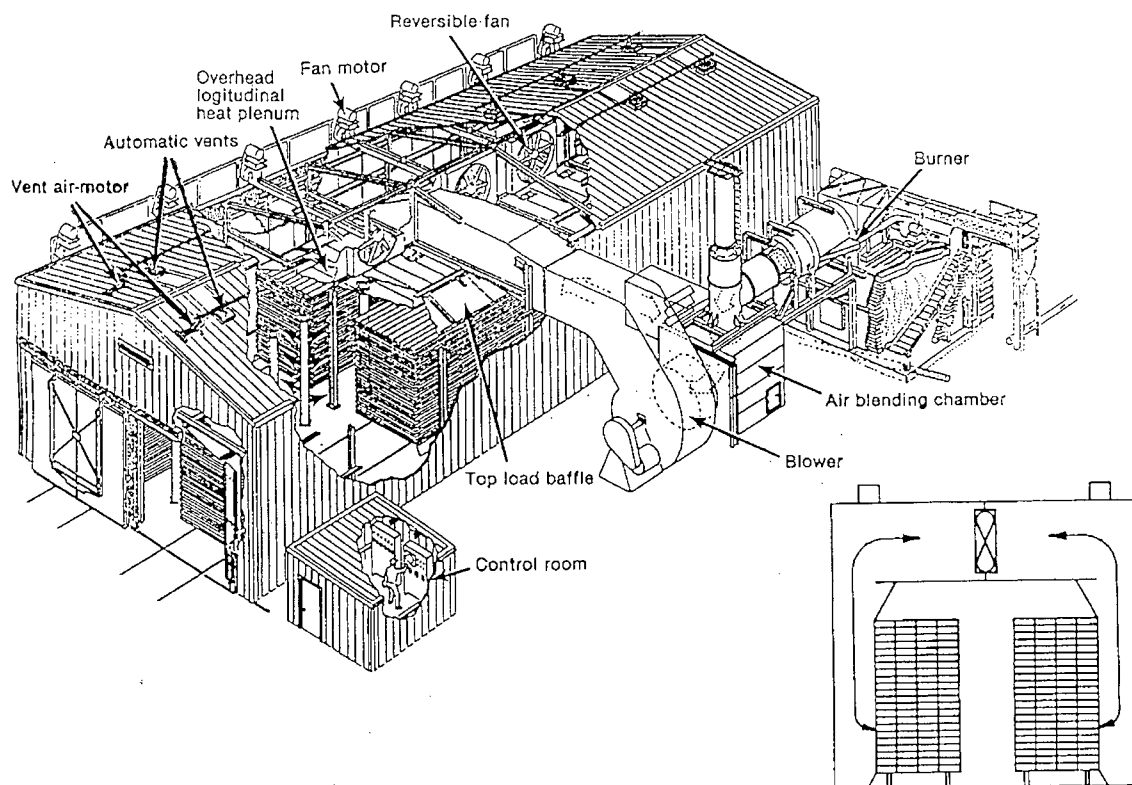
Figure 1-1   Layout of an industrial wood drying kiln.

1.1.5 Problems and Difficulties

Industrial lumber drying process is carried out using a pre-determined schedule, relying on the kiln operator for providing some degree of performance feedback. Problems would arise when the drying kiln is left unattended during off-hours. The common practice of lowering the desired operating temperature during off-hours would lead to energy inefficiency. Also, an unexpected situation may occur during the unattended period, and may lead to undesirable defects in the drying boards.

Another problem of industrial drying of lumber is the poor management of the selection of drying boards. Different species and wood pieces with various initial moisture content are sometimes included in the same drying batch due to time constraints and economic reasons. Clearly, this will lead to non-uniform quality of drying. There is always a trade off between cost reduction and the product quality.

1.2 Motivation for the Present Study

Kilns are perhaps the only practical means of rapid and high-volume drying of fresh forest lumber. They are widely used for drying industrial lumber to achieve the required serviceability in furniture manufacture, building, millwork and other wood product processes.

Lumber drying is considered an art rather than a science since the drying result is not accurately predictable and may even be completely unsatisfactory. Kiln drying requires dedicated attention of experienced kiln operators. Kiln operators require years of training and experience before they can satisfactorily undertake a wood drying process. Nevertheless, in view of the complexity, nonlinearity, and the distributed nature of the drying process, the quality of the dried wood may not be uniformly satisfactory.

Most research studies have mainly focused on developing models of heat flow and heat transfer, design of the kiln geometry, and arrangement of fans in order to provide a uniform air circulation. Clearly, it is useful to develop a fully automatic kiln system that will improve the quality of dried wood and will reduce the drying time. The process efficiency, reliability and predictability of product quality can also be greatly improved

9

through automation. Applying appropriate automation technology to the lumber drying industry is of key importance in the proper utilization of our nation's forest resource. The present research is aimed at making an important contribution towards this goal.

1.3 Overview of the Experimental Setup

The development and experimental work associated with the present work is carried out using the wood drying kiln at the Innovation centre of the National Research Council (NRC). This experimental setup is a downscaled industrial kiln which is appropriate for laboratory experimentation. A view of the kiln is shown in Figure 1-2. The test kiln is an insulated structure with dimension of 107"x38"x44". Wood is loaded into the kiln through the front door and is stacked into layers with a sticker thickness of 2.5". A sticker is a wooden strip placed between the lumber layers of a kiln load to permit air circulation. For the existing setup, 8 pieces of wood are used in a drying test. Wood is stacked into two layers and with 4 pieces of wood in each layer.
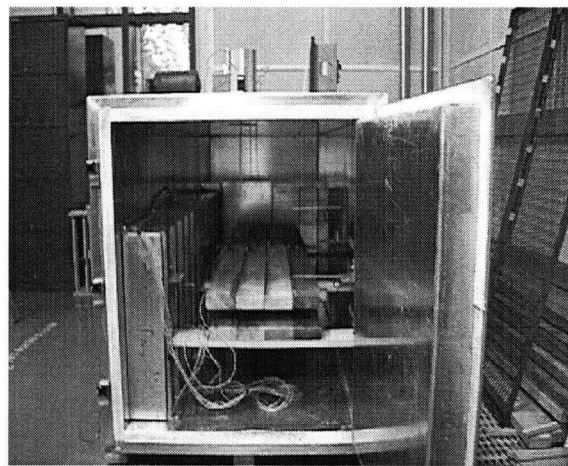
Figure 1-2   A view of the test kiln.

The kiln setup has two actuators and four output variables. Sensors for the output variables include 12 thermocouples, 2 relative humidity sensors, 1 air velocity transmitter and 8 pairs of wood moisture content sensors. They are located throughout the kiln as shown in figure 1-3. The heater consists of a heater filament and it is an electrical on/off

type. The variable speed fan draws air through the heater filament and then blows it out of the plenum through the slots that are equally spaced within the plenum. These two actuators are located in a small chamber situated at the back of the kiln.
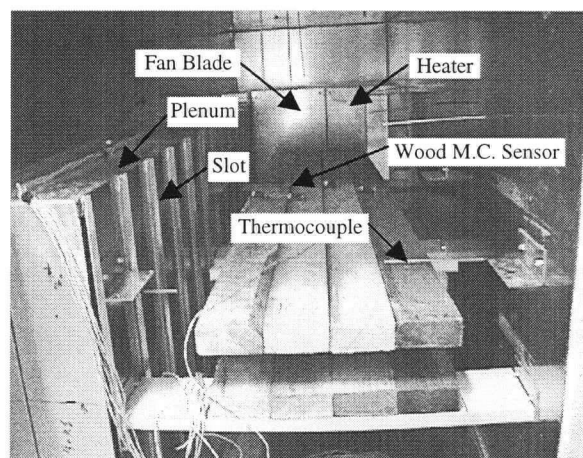
Figure 1-3   System instrumentation.

The system outputs are connected to a personal computer (PC) through a data acquisition and analogue output board (DAQ), excluding the 8 pairs of wood moisture content sensors. The wood moisture content sensors are connected to a data acquisition module (DAM) which then separately communicates with the PC. The PC in return provides control signals to both actuators on the basis of monitored system variables. All interactions are supported by software programming and interface developed in Delphi 3.0. These items are illustrated in Figure 1-4.

For experimentation, the 12 thermocouples are arranged into four different zones for acquiring the operating temperature. These four zones are denoted by zone 1 through zone 4. The location of each numbered thermocouple and relative humidity sensor is shown in Figure 1-5.
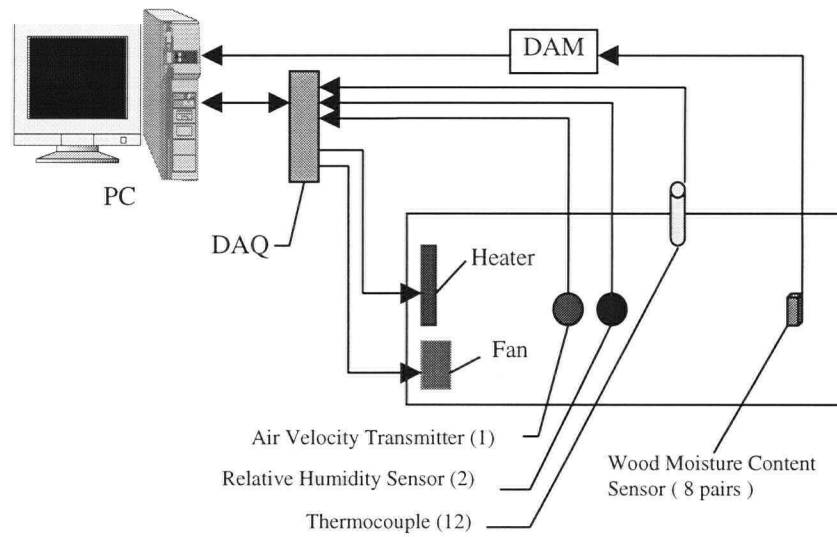
Figure 1-4   An overview of the experimental system.
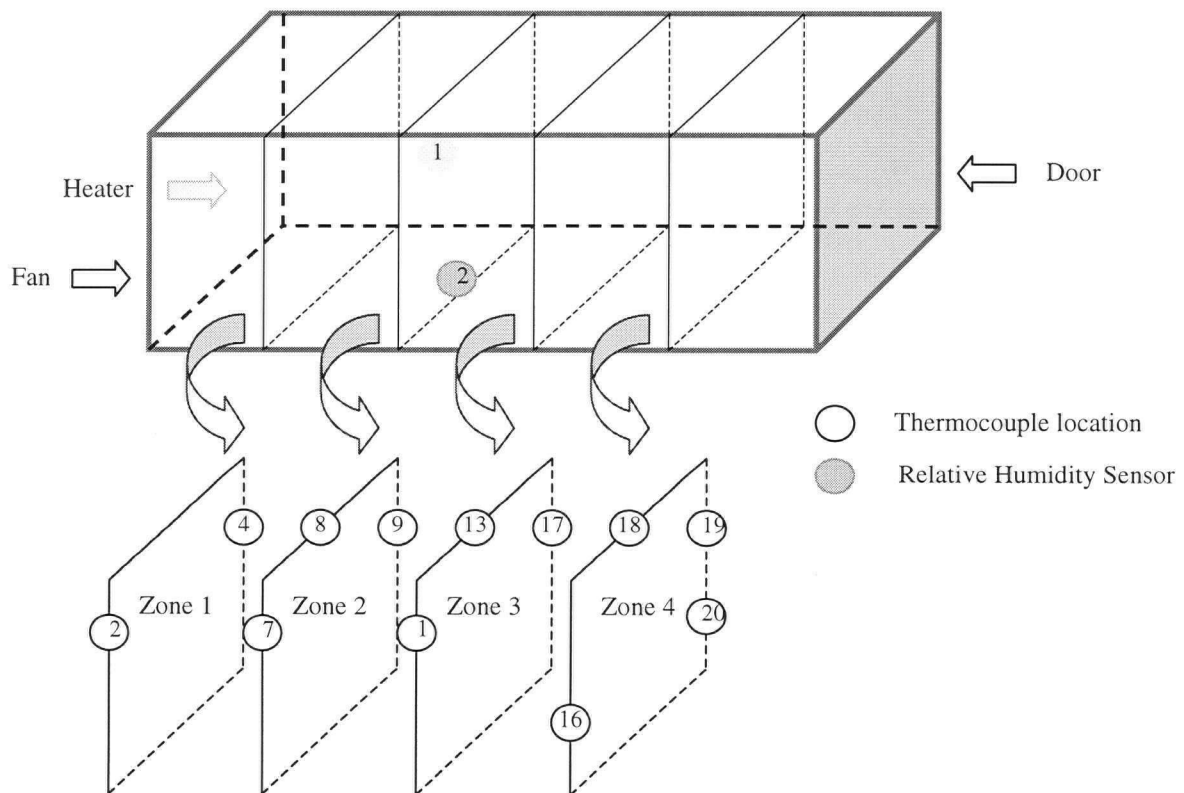
Figure 1-5   Sensor locations and their zone assignment within the drying kiln.

1.4 Proposed Approach

The proposed control system for the kiln is given a hierarchical control structure consisting of three layers, which combines conventional and intelligent techniques. The characteristics of this hierarchical control system and the underlying principles are presented in the following subsections.

A hierarchical structure that incorporates knowledge-based decision making and system management has been successfully applied in various applications. Supervisory control of machinery in industrial automation has successfully demonstrated through experimental studies using a knowledge-based hierarchical control structure, specifically in a fish-processing application [2]. A prototype of variable-geometry robotic manipulator utilizing an intelligent hierarchical control system has been developed for a space-station application and has been studied through both computer simulation and experimentation in the space dynamic and control laboratory [3]. The hierarchical control structure that is proposed here for automation of the lumber drying process is shown in Figure 1-6.

The hierarchical structure has three levels. The lowest level (Level 1) integrates knowledge-based soft control with conventional crisp control algorithms and model identification tools [4]. The intermediate level (Level 2) is the data processing level. Sensory data are abstracted to reflect the process status for use in system monitoring and supervision at the upper level (Level 3). Besides, the system possesses the capability of incorporating information from a multitude of sensors into its knowledge base. This multi-modal sensory information can be easily handled by fuzzy logic techniques for decision making. In particular, knowledge-based sensor fusion may be incorporated [5] as well. Fuzzy inferences have to be defuzzified for physical actions such as direct control and parameter tuning. The top level (Level 3) of the hierarchy, acts as a supervisory controller. This level performs the most intelligent tasks in the system. It consists of a knowledge base made of linguistic fuzzy rules defined by specific membership functions. Data having a low information resolution are interpreted (abstracted) and mapped to the context objects of the knowledge-based for firing of matched rules in generating the fuzzy inference. The hierarchical control system allows

"division of tasks"; specifically, by dividing the complex control process into different layers according to their functionality, it brings about control flexibility and increased efficiency. The research presented in this thesis primarily focuses on the control methodologies of Level 1; in particular, the development of a closed-loop controller based on direct in-wood moisture sensory feedback and the concepts of model identification and intelligent control.
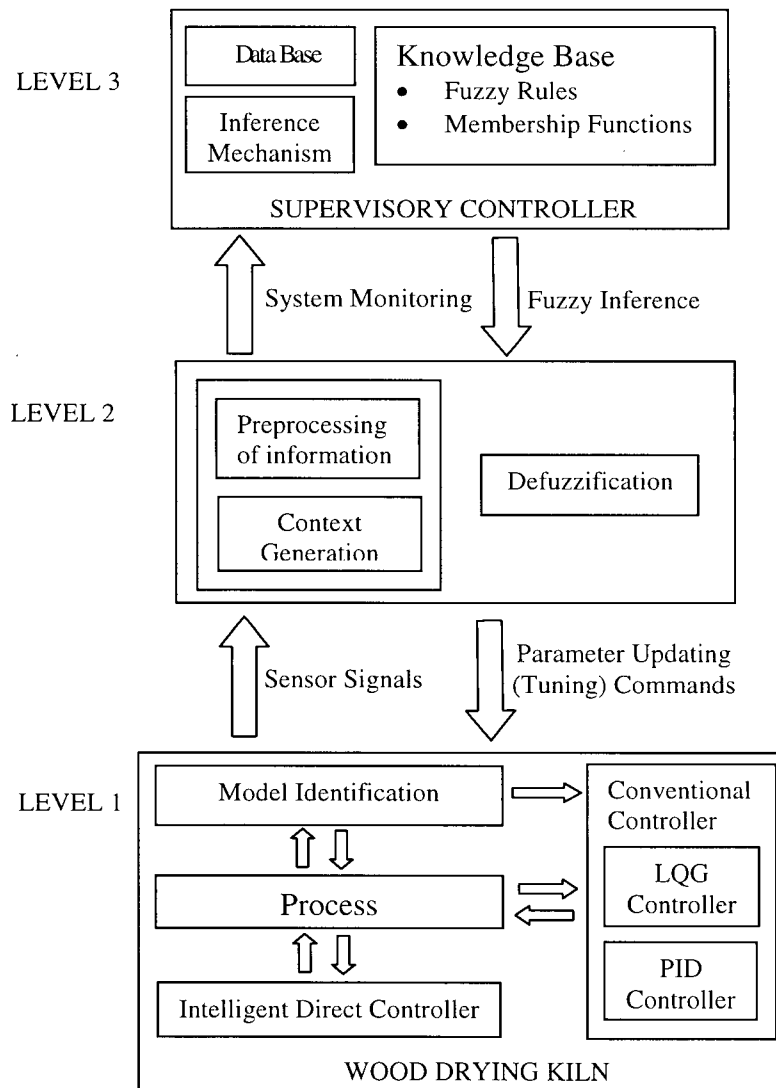
Figure 1-6   A hierarchical control system for a wood drying kiln.

14

1.4.1 Conventional Control

Conventional control refers to those "crisp" or non-fuzzy control methodologies, which typically require a dynamic model of the process. The dynamic model may be explicitly needed as an analytical or computer model described by differential or difference equations. Conventional control has been successfully applied to many applications; however, it can generate unsatisfactory results when the sensory or model information is incomplete and when the complexity of the process is too excessive for it to be handled by a mathematical model, due to extreme nonlinearities and unknowns.

Conventional control uses crisp (or hard) algorithm, and there are several reasons for the practical deficiencies of crisp control algorithms including the following [6]:

- Unknown parameter values
- Changing environment (uncertainty in dynamic interactions and inputs)
- Unpredictable process dynamics (plant uncertainty)
- Inflexible algorithm (system constraints)
- Necessity of complete set of data or information to execute the algorithm
- Process complexity (e.g., excessive nonlinearity)
- Inability to handle "qualitative" or "approximate" information

Conventional model-based control algorithms would fail when system parameters are ambiguous or only partially known, and appropriate estimates have to be made for acceptable operation. Even when the model is accurate, it would not be able to respond to a varying and approximately known environment which the system interacting with. Also, an inflexible (crisp) algorithm is incapable of handling unpredictable process dynamics since the conventional crisp algorithms require a complete set of data to generate proper results. Furthermore, program instructions and data are combined into the same memory of the controller [6]. For example, system failure may result due to an unexpected event of sensing.

1.4.2 Intelligent Control

Intelligent control incorporates human knowledge and expertise into a control system. It makes the operation of a machine or a process "*intelligent*" by making use of knowledge-based soft computing techniques, which include fuzzy logic, neural networks and genetic algorithms.

Intelligent control represents a class of analytical and synthetic control methods that falls beyond the scope of conventional control theory. Fuzzy logic in particular, is characterized by the capability of approximation and approximate reasoning, and is useful in comparison, reasoning, pattern recognition and decision making that are involved in process control. Humans are flexible systems that can adapt to changing and unfamiliar situations, and can gather information in an efficient manner and discard irrelevant details [6]. Humans can also effectively handle vague, incomplete, imprecise and qualitative information in making intelligent decisions [7] and they can learn, infer, perceive, reason, and deduce new useful information and knowledge. In intelligent control it is attempted to use a computer to carry out such actions of a human expert in the domain of control. In particular, soft computing is used for this purpose where techniques of computational intelligence such as fuzzy logic, probability theory, genetic algorithms, and neural networks are synergetically used to mimic human reasoning and decision making [5,8]. Expected capabilities of an intelligent system include the following:

- Dealing with unfamiliar and unexpected situations
- Inference from incomplete information
- Ability to handle qualitative and fuzzy information
- Learning and improvement through learning
- Knowledge acquisition
- Perception including sensory perception
- Use of common sense
- Inductive reasoning
- Pattern recognition

- Innovation.

Intelligent controllers that use fuzzy logic in particular possess the following beneficial characteristics:

- Robustness that comes from the particular techniques of knowledge representation and inference making, which are immune to an extraneous disturbances and noise.
- Fuzzy rules can express in natural linguistic terms a human operator's knowledge and control strategy.
- An explicit model of the process is not needed.
- Knowledge base can be modified and improved during operation, through learning techniques.
- Relatively easy to implement.

An intelligent control system requires techniques of knowledge representation and knowledge processing, which govern reasoning and inference making [9]. Specifically, a *knowledge base* is used to "represent" knowledge, and an *inference mechanism* to "process" knowledge. A model representing the general dynamics of an intelligent system is demonstrated in Figure 1-7.
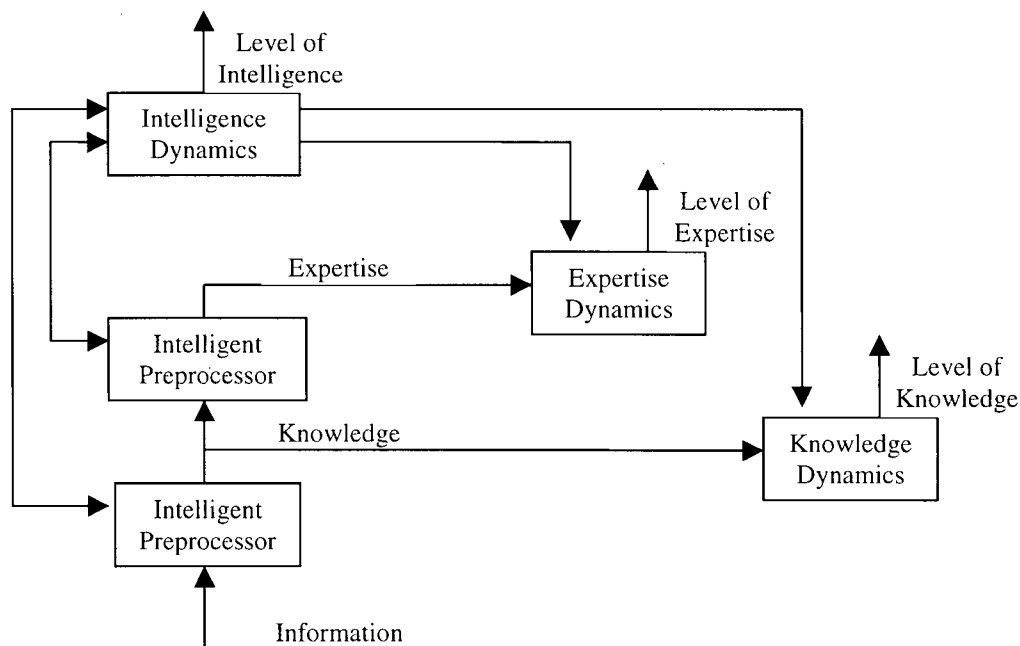
Figure 1-7   A schematic model for the dynamics of an intelligent system.

According to this simplified model, information is converted into knowledge and knowledge into expertise by an intelligent preprocessor. This preprocessing operation requires certain degree of intelligence to perform, and simultaneously intelligence will be enhanced and broadened through the operation. It is therefore represented by a bi-directional line. Besides, knowledge will be gained, and further specialized into expertise through the preprocessing operation. However, knowledge and expertise can be lost or outdated without continuous usage, updating and learning. This characteristic is represented by "Knowledge Dynamics" and "Expertise Dynamics", and the block of "Intelligence Dynamics" allows for variations in the level of intelligence.

1.4.2.1 Knowledge-Based Control Systems

Various sources and forms of knowledge and expertise contribute to the development of the "Knowledge Base" of an intelligent system. This knowledge base in conjunction with current data (context) is used in the reasoning procedures to arrive at inferences. In fuzzy logic-based systems, the so-called "fuzzy reasoning" or "approximate reasoning", is used in the inference-making procedures. The knowledge base is represented by if-then rules of fuzzy descriptors describing both the input (condition) and output (action) variables [6]. For example, "If the moisture error is large and the rate of drying is fast, slightly reduce the power of the heater" is a fuzzy rule with fuzzy descriptors of "large", "fast", and "slightly". These descriptors will be represented by appropriate membership functions, which take values between 0 and 1 for the "grade of membership" (level of possibility of existence).

In knowledge-based decision making in general, inferences I are made by evaluating the sensory information D. New information from sensors or a human interface is matched (operation M) to the knowledge base K typically consisting of if-then rules. Perceptions and inferences are then made by interpreting the new data with respect to the knowledge base, through the inference mechanism known as the "inference engine." Mathematical representation of the above is given by

$$I = M[P(D), K]$$
(1-1)

where $P(.)$ stands for the "preprocessing operator" that converts the context information into a compatible form with K [6]. The resulting series of intelligent inferences can in turn update, refine, and enhance the knowledge base. In the case of fuzzy logic-based systems, K consists of fuzzy rules. Then P represents a "fuzzification" operation and M typically involves a compositional rule of inference [5]. To carry out a crisp action, the inference I needs to be defuzzified, say using the centroid method. The general structure of a knowledge-based system is illustrated in Figure 1-8.
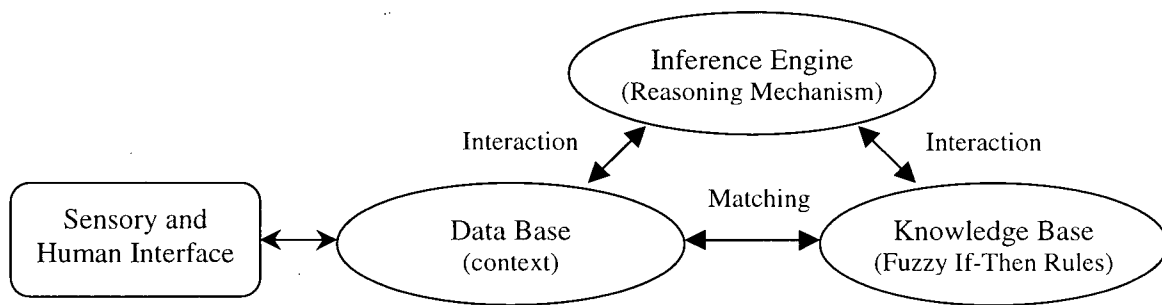
Figure 1-8   The structure of the knowledge-based system.

1.4.2.2 Hierarchical Control

System performance can be improved and enhanced through an integrated hierarchical control system. This control architecture can provide a "division of tasks", where different tasks would be arranged into different levels with different roles in performing various functions of the system. The advantages of such a hierarchical architecture include the following:

- Process efficiency
- Operation flexibility and accuracy
- Supervisory and monitoring capabilities
- Learning and tuning or self-organizing capability.

A generalized model structure for a knowledge-based hierarchical control system is shown in Figure 1-9. The information generated at a lower level in the hierarchy is generally with a higher resolution but with less fuzziness of information [6]. In particular, the degree of information resolution decreases with increased level of the hierarchy, while the fuzziness of information increases with the level of hierarchy. For example, in the control of wood drying, sensory information generated by the low-level sensors contains detail information of temperature readings, relative humidity readings, and moisture content readings of the wood inside the kiln. These sensory data have a high information resolution but with very low fuzziness of information. Since low-level control requires accurate and complete set of data, this information may be employed directly for the purpose of direct low-level control. This information may not be useful, however, at the upper levels where it is required to know the drying quality and process performance for supervisory and monitoring purposes.

$\downarrow \underline{d}_{n+1}$

Functional/Control Knowledge Base

Level n

Sensory/Feedback Filter $\underline{F}_{n,n}$

$\underline{S}_n$

$\underline{F}_{n,n-1}$

$\underline{K}_n$

$\underline{S}_{n-1}$

$\underline{F}_{n,n-2}$

Knowledge-Based Actions $\underline{d}_n$

$\underline{S}_{n-2}$

•

•

•

Sensory Information

$\underline{F}_{n,1}$

$\underline{S}_1$
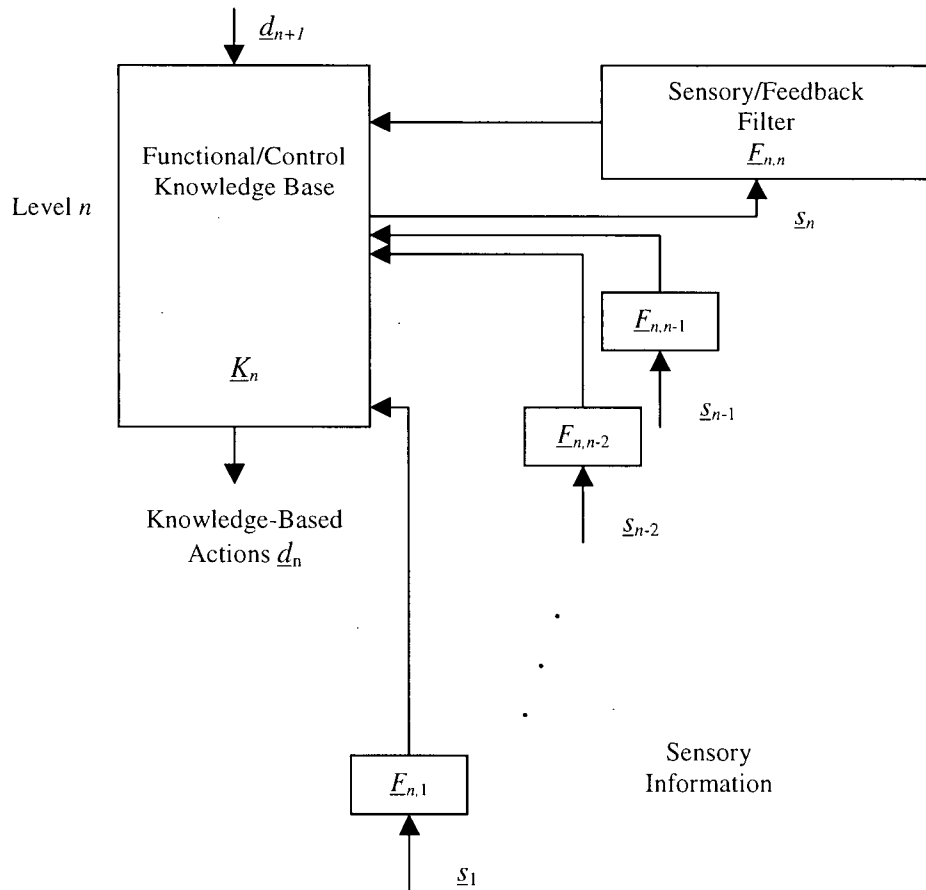
Figure 1-9   A knowledge-based hierarchical control system.

20

During the information processing procedures as indicated in Figure 1-9, the repeated preprocessing of information can be interpreted as a learning process by which the knowledge base is enhanced and updated. The integration of a low-level sensor and a knowledge-based preprocessor in this case may be termed an "intelligent sensor [6]." The inference generation procedure of the knowledge-based hierarchical control system with n levels can be expressed by:

$$d_n = G_n[(F_{n,n} \otimes s_n) \oplus (F_{n,n-1} \otimes s_{n-1}) \oplus (F_{n,n-2} \otimes s_{n-2}) \oplus \ldots \oplus (F_{n,1} \otimes s_1) \oplus d_{n+1} \qquad (1.2)$$

where:

d_i = inference (control actions including reference commands/monitoring) at level i

s_j = sensory information (feedback) from level j

G_n = knowledge system in level n

$F_{n,i}$ = information preprocessor from level i to be used by G_n

$\oplus$ = a generalized combinational operator

$\otimes$ = a generalized transitional operator

1.4.3 Fuzzy Logic Control

Fuzzy logic control is particularly suitable for complex and ill-defined processes where analytical modeling is difficult and the available information is incomplete. A main advantage of fuzzy logic control is its ability to integrate human expertise, experience and knowledge into the rule base, which may contain qualitative, descriptive and linguistic quantities. Consequently neither a precise model nor complete information of the system would be needed. This set of rules forms the knowledge base of the fuzzy control system. A fuzzy logic-based machine combines the advantages of a computer with some of the intelligent characteristics of a human for generating inferences and decisions. For example, fuzzy logic is employed to represent the knowledge of a kiln operator in terms of a set of fuzzy rules. This concerns knowledge representation. A fuzzy action will be triggered by the inference mechanism according to the fuzzy knowledge base, which is determined according to a given set of system observations. This is the task concerning "knowledge processing" [6]. Fuzzy logic control is commonly applied in two

21

architectures, low-level direct fuzzy logic control (DFC) and high-level hierarchical fuzzy logic control (HFC), respectively. These two architectures are shown in Figure 1-10.
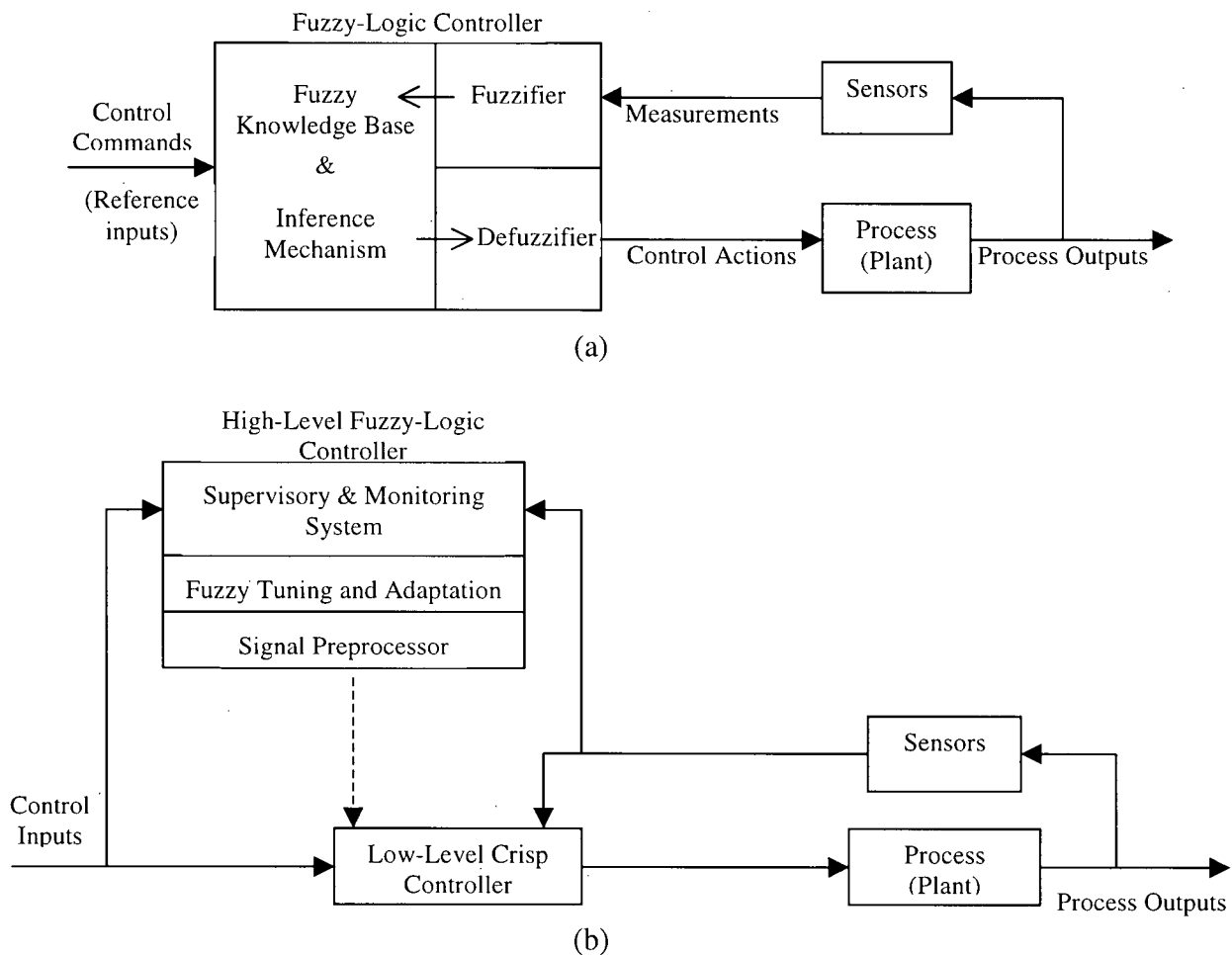
Figure 1-10   Two architectures of fuzzy logic control: (a) direct fuzzy logic control; (b) fuzzy hierarchical control.

In DFC, the sensory information is evaluated against the knowledge base and directly used to generate the control action. In HFC, direct control is carried out by a conventional control scheme, which does not involve fuzzy decision making. An upper level module then evaluates the performance of the system and, if not satisfactory, prescribes corrective action such as controller tuning by employing a fuzzy-logic rule base and a fuzzy inference mechanism.

1.5 Literature Review

In this section, some research work will be outlined related to the development of a fully automated lumber drying control system. In Section 1.5.1, some previous work relevant to the wood drying process will be discussed. One of the key techniques in developing a fuzzy logic controller focuses on fuzzy modeling through the use of fuzzy logic theory and fuzzy sets. Some relevant work will be indicated in Section 1.5.2. Literature on the underlying principles and theory of fuzzy logic and its applications will be explored in Section 1.5.3. Related work on the hierarchical control structure and its application will be outlined in Section 1.5.4, where the significance and applications of intelligent control research will also be highlighted.

1.5.1   Wood Drying Kiln

Some work has been done in the field of lumber drying. Most of the related literature is focused mainly on the modeling of airflow and fluid flow in wood kilns, and the thermodynamic modeling of heat and moisture transfer. Sticker is a wooden strip placed between the courses (layers) of lumber in a kiln load to permit proper air circulation. Basset [10] investigated the relationship between different sticker thicknesses and the average air velocity through the wood stacks. Pang [11] developed a dynamic model to predict the conditions across the stack of softwood inside a kiln. Hua et al. [12] presented a numerical model to simulate the airflow distribution and to solve the flow distribution in a kiln according to its geometry. Tarsiewicz and Leger [13] modeled kiln stacks as heat exchangers, and discussed the model concept and its contribution to control system design. Other major work includes studies of the instrumentation used for measuring wood moisture content (m.c.) and shrinkage development. The concept of utilizing dielectric properties and electrical resistance to measuring wood m.c. was studied by Wengert and Bois [14]. A gravimetric system was developed by Zeleniuc and Ene [15] in which m.c. was measured in terms of the weight lost. Similar work has been done by Little and Moschler [16] in automating kiln drying through a weight-based control system and to establish an optimal drying condition using real time weight loss information.

Canteri and Martin [17] estimated wood quality and shrinkage by laser scanning of surface deformations. This work provides some insight into modeling and understanding of different variables involved in kiln drying.

In wood drying automation, hardly any work is found on closed-loop computer control. Ugolev and Skuratov [18] developed a computer program to determine the optimal drying schedule by simulating the stress-strain condition of wood. A self-tuning closed-loop controller utilizing on-line parameter estimation using the recursive least squares method was developed by Dreiner and Welling [19]. This is relevant to the present research.

1.5.2 Fuzzy Logic and Fuzzy Sets

The concept of fuzzy logic was formalized in 1965 when Zadeh firstly published a paper on the theory of fuzzy sets [20]. This paper presented a radical idea, as it was inconceivable to allow fuzziness or ambiguity in the precision-centred field of engineering, at that time. Later, Zadeh further proposed the idea of fuzzy algorithms which laid the foundation approximate reasoning. In 1973, he published another paper which addressed limitations of preciseness, and referred to a concept as the "principle of incompatibility [21]." This principle states that "when the complexity of a system exceeds a certain level, a precise and meaningful description of the system behavior becomes impossible." Gains published a paper that extensively discussed the rationale behind the necessity of fuzzy logic for the analysis of complex systems and its application to real world problems [22]. The paper also discussed the concept of "possibility" relations in fuzzy logic, which it is different from the probability theory of uncertainty. Japanese researcher Michio Sugeno of the Tokyo Institute of Technology in 1972 followed Zadeh by proposing concepts of fuzzy measure and fuzzy integral, which started the "fuzzy" revolution and the boom of related applications in Japan in the 1980's.

1.5.3 Fuzzy Logic Control and Applications

A turning point for fuzzy logic came in 1974, when the British researcher Ebraham Mamdani of the Queen Mary College of University of London first applied fuzzy logic for the control of a simple steam engine [23]. This was the first industrial application of fuzzy logic theory, and the goal of the particular control problem was to maintain a constant rate in both the engine speed and the outlet pressure. This application was followed by the development of the first fuzzy expert system by Hans Zimmermann, for the evaluation of loan applicants in Germany. Also, the first major industrial application of fuzzy logic was the control of a cement kiln, which was successfully implemented in Denmark in 1980.

Schwartz in 1992 presented a challenging technological application of fuzzy logic in the control of a helicopter, which is a fundamentally unstable system with highly nonlinear dynamics [24]. The flight demonstration programs proceeded smoothly and the fuzzy controller was able to overcome the limitations and constraints of conventional control techniques. This is a good example of application of fuzzy logic, demonstrating its suitability over conventional techniques for a class of problems, since hovering dynamics of a helicopter is a highly nonlinear, and unstable problem with time delay which is greatly influenced by its environment. Another industrial application of fuzzy logic is kiln dryer regulation, where an expert control system is used to optimize the drying process according to the expert experience embedded in the fuzzy rules of the system through learning [25]. Another successful application of fuzzy logic is the automation of an industrial oven line for continuous baking of biscuits for TWIX candies, at MARS Corporation in Germany [26, 27]. This drying process is a nonlinear, time-variant process with changing dynamics, and control variables such as biscuit color and moisture are crucial to the drying results. These two industrial control applications provide justified insights and compromises in the use of fuzzy logic. The present research project of lumber drying, carried out at the National Research Council is an important addition to these previous applications.

Apart from the industrial applications, fuzzy logic is also widely used in a variety of simple every day home appliances, for example, in rice cookers, thermo-pots, washing

machines, microwave ovens, vacuum cleaners, camcoders, word translators, televisions and VCRs, and these implementations were made primarily in Japan during the "fuzzy" revolution. Fuzzy logic fills an important need in modern scientific and technological devices, by allowing the integration and utilization of human knowledge and experience. The utilization and development of fuzzy logic was further spread to systems like elevators, trains, cranes, traffic control and automobiles. For example, Saturn™ has employed fuzzy logic in its automatic transmission downshift mechanism. Mitsubishi Galant™ has applied fuzzy logic in the shift control of an electronically controlled four-speed overdrive automatic transmission.

Fuzzy logic and fuzzy control, because of their soft and flexible algorithms, the integration of human expert knowledge into control laws, and the incorporation of linguistic information into control strategies, have met an important need in the field of automation. The applications of fuzzy logic are further explored in the medical field for patient diagnosis as in breast cancer, software applications like data abstraction and data compression, and in expert systems for legal and business field. Further developments, for example, natural language interfaces would make important advances in the field.

1.5.4 Hierarchical Control and Application

A comprehensive study of hierarchical control is given by Mesarovic, Macho and Takahara [28]. The hierarchy assigns tasks into different levels of a hierarchical structure according to the level of abstraction, level of complexity of decision making, and level of priority of action. The role of fuzzy logic in the management of uncertainty in expert control systems was explored by Zadeh, and a systematic approach for the management of incomplete and imprecise information was developed [29].

De Silva and MacFarlane [30] developed a three-level knowledge-based hierarchical control structure for robotic manipulators. This hierarchy combines the integration of expert knowledge into a knowledge-based soft control scheme, combined with conventional crisp control algorithms. A fuzzy controller consisting of fuzzy if-then rules as its knowledge base is used for servo tuning. The main advantages of this control architecture include its ability to incorporate human implicit knowledge and flexibility in

multi-layered decision making for control. An analytical framework for knowledge-based tuning of a two-level control structure in which a conventional PID controller is tuned utilizing fuzzy logic was studied by de Silva [31]. Computational burden is substantial reduced through the application of the analytical framework. Saridis [32] developed an analytical formulation of the principle of increasing precision with decreasing intelligence, and it constitutes a fundamental principle in hierarchically intelligent control. De Silva [33] presented the relationship between information fuzziness and degree of resolution within the context of a hierarchical control structure, and also developed a criterion for the decoupling of a fuzzy knowledge base. Wickramarachchi [2] successfully implemented a hierarchical control structure on a prototype test-bed of a fish-processing machine in laboratory. The results were found to achieve higher meat recovery rate, and therefore would lead to an increase in the overall yield of the cutting process.

1.6 Research Objectives

The principal objective of the research presented in this thesis is to develop suitable technology for closed-loop automated control of a wood drying process. A particular consideration is given to experimental determination of the behavior of the drying process. Both conventional and fuzzy-logic techniques are used in the kiln control. The practical objectives of the lumber drying industry are the speed of drying, and the quality of dried wood, and the cost of drying. Efficient control is crucial in achieving these objectives. Lumber drying is a very complex process, which depends on many complex and incompletely known factors that are often difficult to control. It is known, however, that the drying quality depends on the following factors:

- Initial condition of the wood
- Drying temperature
- Relative humidity
- Airflow velocity in the environment
- Rate of drying

and they are all interrelated.

In this thesis, the focus is on the first level of a hierarchical control system. In particular, the development of a closed-loop automated lumber drying system utilizing direct fuzzy logic control is addressed. Experimental modeling for investigation of the lumber drying process, development of direct controllers based on the models obtained through system identification, implementation of the techniques into the kiln, and comparison of the performance under conventional and intelligent controllers, through both simulation and experimentation are undertaken.

1.7 Overview of the Thesis

The starting introductory chapter of the thesis presents the underlying background knowledge of lumber drying, conventional and intelligent control, overview of the experimental kiln, objectives of the research, and its motivation. It also provides a review of the relevant literature. The important principles of fuzzy logic are presented in Chapter 2. Chapter 3 details the experimental procedures for data acquisition from the kiln. Chapter 4 mainly concerns system identification and model validation. The controller design and simulation are discussed in Chapter 5. Physical implementation of the controllers and evaluation of the performance are presented in Chapter 6. Chapter 7, which is the final chapter of the thesis, summarizes main contributions of the thesis and experimental results, discusses the system limitations, and suggests improvements and directions for future work.

<center>**Chapter 2**</center>

<center>**FUZZY LOGIC**</center>

In this chapter, the fundamental concepts of fuzzy logic control will be presented in order to provide the necessary background for the developments undertaken in the thesis. The concepts described here are important in the applications of fuzzy logic in control. The main concepts include fuzzy set theory, membership functions, fuzzy relations and reasoning, fuzzy logic operators, and the compositional rule of inference for fuzzy decision making.

2.1 Fuzzy Sets and Membership Functions

Fuzzy logic can be interpreted in terms of fuzzy sets. Fuzzy sets are generalizations of crisp sets to deal with fuzzy, vague, ambiguous concepts. Fuzzy sets handle fuzzy logic just like crisp sets can be used to describe crisp binary logic. As a consequences fuzzy logic is able to represent and process expressions like "a group of *beautiful* ladies" and "they work *close* to downtown", which conventional logic and set theory are unable to handle. Before introducing fuzzy sets and fuzzy logic, next the conventional crisp sets are introduced.

Conventional Boolean Sets

Conventional sets are "crisp sets," and possess crisp boundaries. In other words, an element either belongs to the set or completely excluded from it. The characteristic function X_A of an element x in the universe of discourse X is expressed as:

$$X_A : X \rightarrow \{0, 1\} \tag{2.1}$$

and

$$X_A(x) = \begin{cases} 1 & x \in X. \\ 0 & x \notin X. \end{cases} \tag{2.2}$$

<center>29</center>

where equation (2.2) indicates that if the element x belongs to A, then X_A is 1, and if the element x does not belong to A, then X_A is 0.

Let A and B be the sets of the universe of discourse X. An element x of the universe of discourse that belongs to the set union, intersection, and complement is defined as:

Union

$$A \cup B = \{x \mid x \in A \text{ or } x \in B\} \tag{2.3}$$

Intersection

$$A \cap B = \{x \mid x \in A \text{ and } x \in B\} \tag{2.4}$$

Complement

$$\bar{A} = \{x \mid x \notin A\} \tag{2.5}$$

The Venn diagrams or Euler diagrams of union, intersection, and complement of crisp sets are illustrated in Figure 2-1, (a), (b), and (c), respectively.

(a)   (b)

(c)
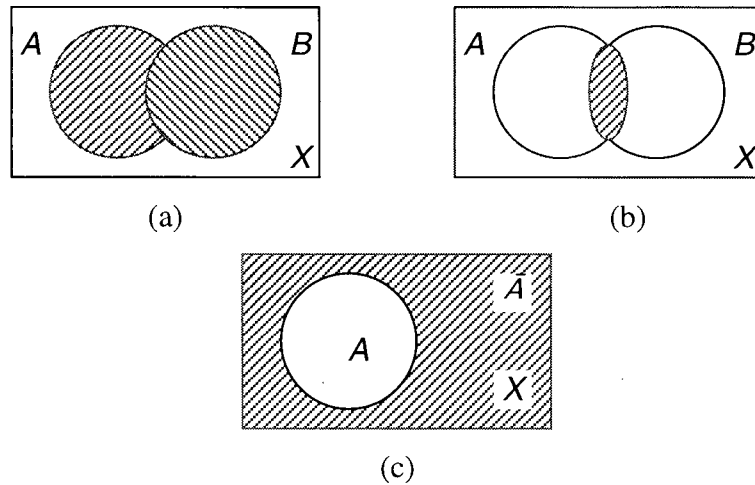
Figure 2-1   The Venn diagrams of: (a) union; (b) intersection; (c) complement.

Fuzzy Sets

Fuzzy logic is an extension of conventional (binary) logic, and analogously, fuzzy set theory is considered as an extension of conventional set theory. A fuzzy set is a collection of elements that has no crisp boundary, and is defined or characterized by a membership

function. Corresponding to the characteristic function of a crisp set, the membership function of a fuzzy set assigns a grade of membership which gives the set membership, except that it can assume any real value between 0 and 1. In particular a value greater than 0 and less than 1 represents a partial membership where the element has a degree of presence inside the set and a complementary presence outside the set. Figure 2.2 (a) shows the Venn diagrams of a crisp set (crisp boundary) and Figure 2.2 (b) shows a fuzzy set (fuzzy boundary).
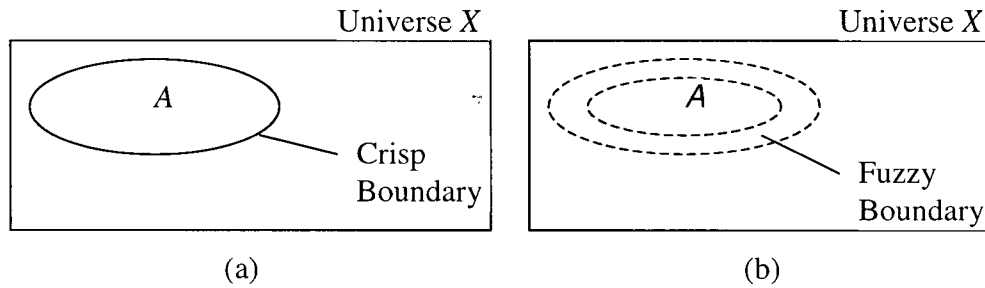
Figure 2-2   The Venn diagrams of: (a) crisp set A; (b) fuzzy set A.

A fuzzy set A in the universe X is defined by a membership function μ_A, which assign a degree of membership in the set, to any element x of the universe of discourse. The membership function μ_A maps the universe of discourse X to the interval of [0, 1], and can be mathematically expressed as

$$\mu_A (x): X \rightarrow [0, 1] \tag{2.6}$$
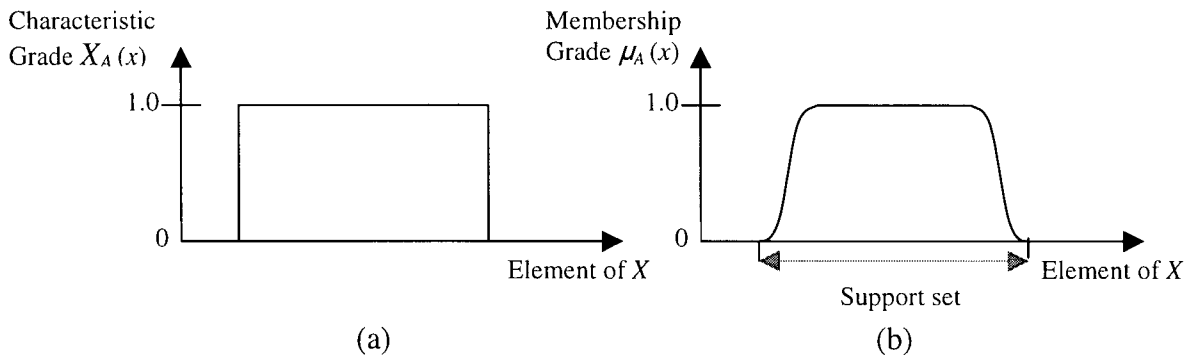
Figure 2-3   Graphical representation of: (a) a crisp set A; (b) a fuzzy set A.

31

A membership value of 1 ($\mu_A(x) = 1$) implies that the corresponding element definitely belongs to (or inside) the fuzzy set A. If the membership value is zero ($\mu_A(x) = 0$), the corresponding element is definitely outside the fuzzy set. The closer the value of $\mu_A(x)$ to 1, the greater the possibility that the corresponding element is inside the set. The graphical representation of the characteristic function of a crisp set and the membership function of a fuzzy set are illustrated in Figure 2-3, (a) and (b), respectively.

According to de Silva [6], a fuzzy set can be completely defined as a universe of discourse and a membership function spanning the universe. The support set of a fuzzy set is the crisp set obtained by omitting the elements of zero grade of membership. Consequently, a fuzzy set is also a subset of its support set. A fuzzy set A with elements x can be symbolically expressed as

$$A = \{(x, \mu_A(x)) \mid x \in X\} \tag{2.7}$$

For a discrete universe of discourse, when each element is paired with its membership grade, it can be symbolically expressed as

$$A = \frac{\mu_A(x_1)}{x_1} + \frac{\mu_A(x_2)}{x_2} + \cdots + \frac{\mu_A(x_i)}{x_i} + \cdots = \sum_{x_j \in X} \frac{\mu_A(x_j)}{x_j} \tag{2.8}$$

If the universe is continuous, an equivalent notation may be given as

$$A = \int_{x \in X} \frac{\mu_A(x)}{x} \tag{2.9}$$

It is important to note that both the series representations given in equations (2.8) and (2.9) are symbolic notations, and in particular there is no mathematical integration in equation (2.9).

Fuzzy sets may also be used for representing fuzzy variables. For example, fuzzy variable of moisture error is defined to have five fuzzy states, namely zero, small, medium, large, and very large (Figure 2-4). Each of these fuzzy states itself is a fuzzy set

with a uniquely defined membership function (Figure 2-5). The fuzzy resolution represents the number of fuzzy states that a fuzzy variable consists of. The fuzzy resolution is 5 in this particular example of moisture error. The fuzzy resolution r_f can also be represented quantitatively as

$$r_f = \frac{w_s}{w_m}$$ (2.10)

where

w_s = width of the support set

w_m = intermodal spacing
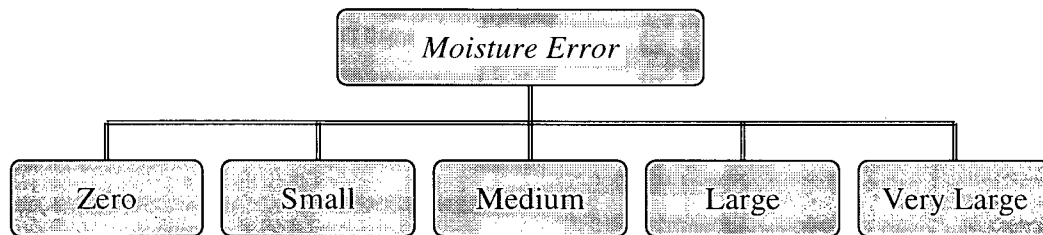
Figure 2-4   An example of fuzzy states: fuzzy variable *moisture error*.
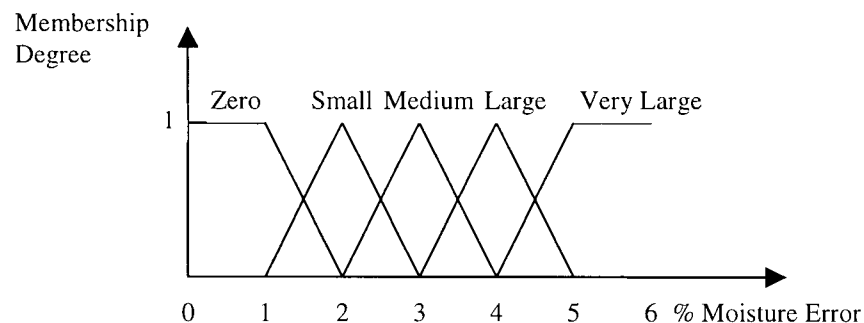
Figure 2-5   An example of membership functions of fuzzy states.

2.2 Fuzzy Operations and Reasoning

In this section, the operations required for the application of fuzzy logic and fuzzy (approximate) reasoning are reviewed. Consider two fuzzy sets A and B defined in the

same universe of discourse. The operations union, intersection, and complement of the fuzzy sets are defined as follows:

Union (OR, ∨)

The union of two fuzzy sets A and B in the same universe X is a fuzzy set in that universe, with membership function given by

$$\mu_{A\vee B}(x) = max\{\mu_A(x), \ \mu_B(x)\} \qquad \forall x \in X \qquad (2.11)$$

Note that the union of fuzzy sets corresponds to the operation "OR" in fuzzy logic.
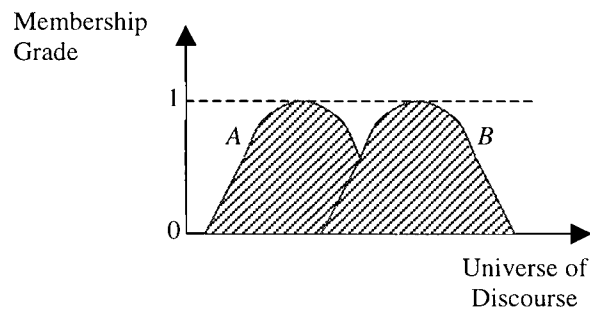
Figure 2-6   Union of fuzzy sets A and B.

Intersection (AND, ∧)

The intersection of two fuzzy sets A and B in the same universe X is a fuzzy set in that universe, with membership function given by

$$\mu_{A\wedge B}(x) = min\{\mu_A(x), \ \mu_B(x)\} \qquad \forall x \in X \qquad (2.12)$$
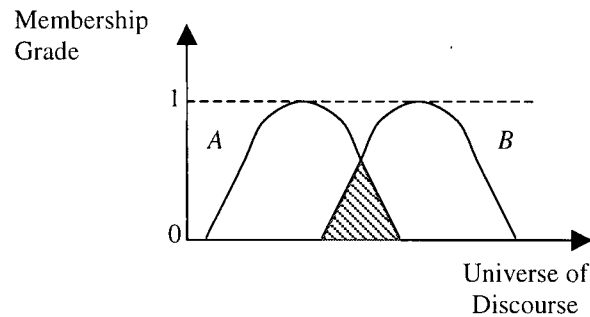
Figure 2-7   Intersection of fuzzy sets A and B.

34

The intersection of fuzzy sets corresponds to the operation "AND" in fuzzy logic.

Complement (NOT)

The complement A' of a fuzzy set A is a fuzzy set in the same universe whose membership function is given by

$$\mu_{A'}(x) = 1 - \mu_A(x) \qquad \text{for all } x \in X \qquad (2.13)$$
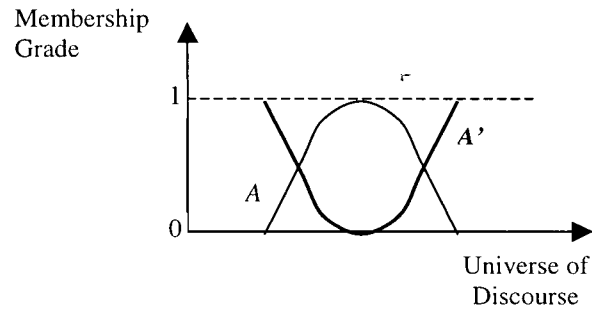
Figure 2-8   Complement of fuzzy set A.

The complement of a fuzzy set corresponds to the operation "NOT" in fuzzy logic.

Cartesian Product

Consider fuzzy sets A_1, A_2,..., A_n defined independently in the single-dimensional universes X_1, X_2,..., X_n, respectively. The Cartesian product $A_1 \times A_2 \times ... \times A_n$ is a fuzzy subset of the Cartesian space $X_1 \times X_2 \times ... \times X_n$, whose membership function is given by

$$\mu_{A1 \times A2 \times ... \times An}(x_1, x_2, ..., x_n) = min\{\mu_{A1}(x_1), \mu_{A2}(x_2), ..., \mu_{An}(x_n)\}$$

$$\forall x_1 \in X_1, \forall x_2 \in X_2, ..., \forall x_n \in X_n \qquad (2.14)$$

Note that the cartesian product corresponds to an "AND" operation.

Fuzzy Relation

Fuzzy relation is given by a fuzzy set in a multidimensional space, and is an extension of the concept of relation in conventional function (crisp set) theory. A fuzzy relation R, in n-dimensional Cartesian product space $X_1 \times X_2 \times \ldots \times X_n$, is a fuzzy set denoted by

$$R_{X1 \times X2 \times \ldots \times Xn} = \{[(x_1, \ldots, x_n), \mu_R(x_1, \ldots, x_n)] | (x_1, \ldots, x_n) \in X_1 \times X_2 \times \ldots \times X_n \} \quad (2.15)$$

or in discrete universe,

$$R = \sum_{X_1 \times X_2 \times \ldots \times X_n} \frac{\mu_R(x_1, x_2, \ldots, x_n)}{(x_1, x_2, \ldots, x_n)} \quad (2.16)$$

if universe is continuous,

$$R = \int_{X_1 \times X_2 \times \ldots \times X_n} \frac{\mu_R(x_1, x_2, \ldots, x_n)}{(x_1, x_2, \ldots, x_n)} \quad (2.17)$$

where μ_R is the membership function of R given as

$$\mu_R : X_1 \times X_2 \times \ldots \times X_n \rightarrow [0, 1] \quad (2.18)$$

In summary, a fuzzy relation is simply given by a membership function expressed in terms of the variables of the particular relation $(x_1, x_2, \ldots, x_n)$. It is important to note that the expressions in equations (2.16) and (2.17) are symbolic shorthand forms of notation, and in particular the integration symbol used in equation (2.17) is not a mathematical integration.

Implication (IF-THEN)

Consider two fuzzy sets A and B in two different universes X and Y, respectively. The fuzzy implication of A implies B (denoted by $A \rightarrow B$) is a fuzzy relation in the Cartesian

product space $X \times Y$. The most commonly used relation for obtaining the membership function of the fuzzy implication is given as

$$\mu_{A \to B}(x,y) = min\{\mu_A(x), \mu_B(y)\} \qquad \forall x \in X, \forall y \in Y \qquad (2.19)$$

Fuzzy (Approximate) Reasoning

Fuzzy reasoning is performed using an inference mechanism (a rule of inference). The knowledge base is expressed as a collection of fuzzy rules in the IF-THEN format, and are called "fuzzy IF-THEN rules." The data (context) which need to be fuzzified first, if crisp, and are matched with the rulebase using the rule of inference, to arrive at a fuzzy inference. The underlying concepts are presented now. In general, fuzzy reasoning can be classified into two categories, known as direct method and indirect method, as indicated in Figure 2-9. It is more common to use direct method in reasoning and inference making. Although indirect methods are technically interesting, they conduct reasoning in the truth-value space and have an unnecessarily complex reasoning mechanism, and are beyond the scope of this study.
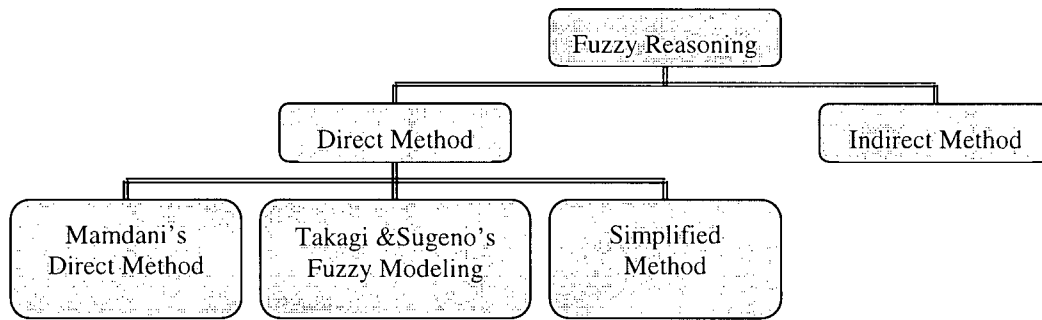
Figure 2-9   Classification of fuzzy reasoning.

The direct method was first proposed by Mamdani in connection with fuzzy logic control, and it has a simple application structure utilizing min- and max- operations [23]. In recent studies of intelligent control, the main focus has been on Mamdani's direct method (MDM). Fuzzy reasoning can be simply summarized by the three steps given below:

- Step 1: Measure the adaptability W of the premise of a rule for a given data value (a *min* operation)
- Step 2: Infer a conclusion using each rule for the adaptability value obtained in Step 1
- Step 3: Obtain the overall conclusion (inference) by aggregating the individual conclusions.

The above steps can be illustrated by an example. Consider two fuzzy rules with two fuzzy condition variables A and B, and one action variable C. This is a two-input-one-output IF-THEN rule, as illustrated by

$$\text{Rule 1:} \quad \text{IF } x \text{ is } A_1 \quad \text{and} \quad y \text{ is } B_1 \quad \text{THEN } z \text{ is } C_1$$
$$\text{Rule 2:} \quad \text{IF } x \text{ is } A_2 \quad \text{and} \quad y \text{ is } B_2 \quad \text{THEN } z \text{ is } C_2 \qquad (2.20)$$

Here, A_1, A_2, B_1, B_2, C_1, and C_2 are all fuzzy sets with individually defined membership functions. Now, suppose the measurement (input to the knowledge-based system) is denoted by (x_0, y_0). The reasoning process for this context is as follows:

Step 1: Measure the adaptability W of each rule for the data point (x_0, y_0), as given by

$$\text{Adaptability of Rule 1: } W_{\text{Rule1}} = \mu_{A1}(x_0) \wedge \mu_{B1}(y_0)$$
$$\text{Adaptability of Rule 2: } W_{\text{Rule2}} = \mu_{A2}(x_0) \wedge \mu_{B2}(y_0)$$

The general representation of the adaptability W_n for n context variables (inputs to the reasoning system) can be written as

$$W_{\text{Rule } j} = \mu_{A1}(x_1) \wedge \ldots \wedge \mu_{An}(x_n) \qquad (2.21)$$

Step 2: Obtain the conclusions of individual rules by applying the adaptability values in Step 1 to the fuzzy sets of the action variables; thus,

$$\text{Conclusion of Rule 1: } \mu_{C1'}(z) = W_1 \wedge \mu_{C1}(z) \qquad \forall z \in Z$$

38

Conclusion of Rule 1: $\mu_{C2'}(z) = W_2 \wedge \mu_{C2}(z)$ $\qquad \forall z \in Z$

Step 3: Aggregate the conclusions of the rules in Step 2 and make the overall inference as follows:

Final conclusion (inference) $\mu_C(z) = \mu_{C1'}(z) \vee \mu_{C2'}(z)$

Aggregation is the process by which the fuzzy sets that represent the outputs of different rules are combined into a single fuzzy set. In general, with m rules, the final inference $\mu_C(z)$ can be written such as

$$\mu_C(z) = \mu_{C1'}(z) \vee \mu_{C2'}(z) \vee \ldots \vee \mu_{Cm'}(z) \qquad (2.22)$$

Basically, the three steps illustrate the crucial ideas of reasoning and decision making in fuzzy logic control. Step 1 corresponds to a "fuzzification" process, where crisp data x_0, y_0, etc. are fuzzified. The final control inference $\mu_C(z)$ itself is a fuzzy set, and typically needs to be "defuzzified" to obtain a crisp control action for process control. This may be accomplished, for example, by picking the centroid z_0 of the membership function $\mu_C(z)$. The three steps can be demonstrated graphically as in Figure 2-10.
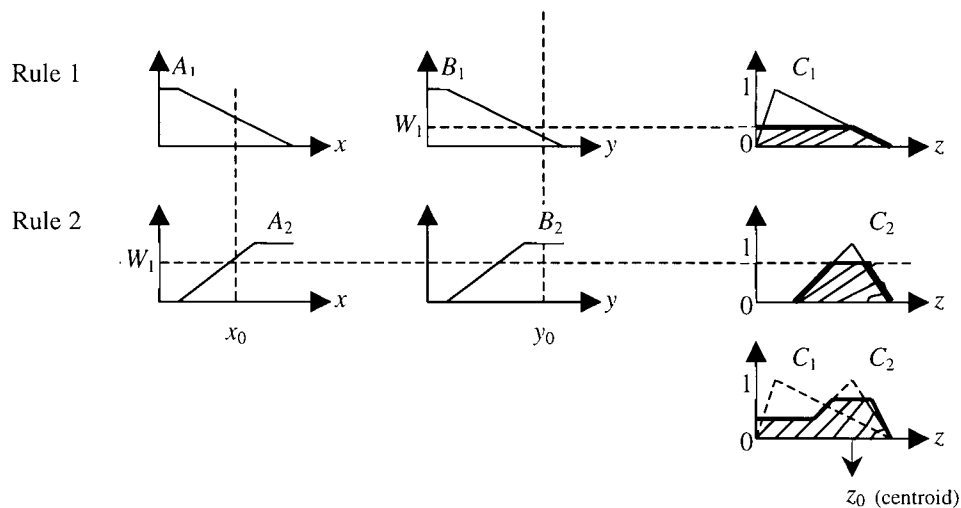
Figure 2-10 An example giving a graphical representation of the reasoning process of MDM.

2.3 Composition and Inference

The concepts of reasoning and decision making used in fuzzy logic can be mathematically formalized. The underlying concepts are introduced now.

Projection

Consider a fuzzy relation as denoted by R in the Cartesian product space $X_1 \times X_2 \times \ldots \times X_n$ and suppose that the n indices are arranged as follows:

$$\{1, 2, \ldots, n\} \rightarrow \{i_1, i_2, \ldots, i_p, j_1, j_2, \ldots, j_q\} \tag{2.23}$$

where $n = p + q$, and i and j denote the newly ordered set of n indices.

The projection of R on to the subspace $X_{i1} \times X_{i2} \times \ldots \times X_{ip}$, which is represented by a fuzzy set P, is denoted by

$$Proj[\mathrm{R}; X_{i1} \times X_{i2} \times \ldots \times X_{ip}]$$

The membership function μ_P of this fuzzy set P is given by

$$\mu_P(x_{i1}, x_{i2}, \cdots, x_{ip}) = \sup_{x_{j1}, x_{j2}, \cdots, x_{jq}} \{\mu_R(x_1, x_2, \cdots, x_n)\} \tag{2.24}$$

The supremum operation is used to deal with continuous independent variables, and *max* operator is used to deal with discrete independent variables.

Cylindrical Extension

Consider the Cartesian product space $X_1 \times X_2 \times \ldots \times X_n$ with the index arrangement as given by

$$\{1, 2, \ldots, n\} \rightarrow \{i_1, i_2, \ldots, i_p, j_1, j_2, \ldots, j_q\}$$

Again, one has $n = p + q$. Also i and j to denote the newly ordered set of n indices. Consider a fuzzy relation R in the subspace $X_{i1} \times X_{i2} \times \ldots \times X_{ip}$, its cylindrical extension $C(R)$ over the entire (n-dimensional) space is given by

$$C(R) = \int\limits_{X_1 \times X_2 \times \cdots \times X_n} \frac{\mu_R(x_{i1}, x_{i2}, \cdots, x_{ip})}{x_1, x_2, \cdots, x_n} \tag{2.25}$$

Join

Consider two fuzzy relations R and S defined in the subspaces $X_1 \times X_2 \times \ldots \times X_p$ and $X_q \times X_{q+1} \times \ldots \times X_n$ respectively, such that R and S together cover the entire n-dimensional space $X_1 \times X_2 \times \ldots \times X_n$. i.e., ($q < p+2$). The join of the fuzzy sets R and S is also a fuzzy set in the $X_1 \times X_2 \times \ldots \times X_n$ space, and is given by

$$Join\ (R,S) = C(R) \wedge C(S) \qquad \text{in} \quad X_1 \times X_2 \times \ldots \times X_n \tag{2.26}$$

Its membership function μ_{Join} is given by

$$\mu_{Join}\ (x_1, x_2, \ldots, x_n) = min\{\mu_{C(R)}(x_1, x_2, \ldots, x_n),\ \mu_{C(S)}(x_1, x_2, \ldots, x_n)\} \tag{2.27}$$

The *min* operation is applied here because of the intersection of the cylindrical extensions of fuzzy sets R and S.

Composition

Consider two fuzzy relations R and S in the subspaces $X_1 \times X_2 \times \ldots \times X_p$ and $X_q \times X_{q+1} \times \ldots \times X_n$ respectively, such that R and S are never disjoint ($q < p+1$). That is, there is at least one common independent variable (one overlapping axis). The composition of R and S is denoted by $R \circ S$ and is given by

$$R \circ S = Proj[Join(R,S);\ X_1, \ldots, X_{q-1}, X_{p+1}, \ldots, X_n] \tag{2.28}$$

It is noted that the projection is performed onto the subspace formed by the disjoint parts of the two subspaces (non-overlapping subspace) of R and S. The operation of *min* applies to *join*, and *sup* applies for *projection*, as clear from equation (2.27) and equation (2.24), respectively. Hence the membership function of the fuzzy set of $R \circ S$ is given by

$$\mu_{(R \circ S)} = sup\{min(\mu_R, \mu_S)\} \tag{2.29}$$

Compositional Rule of Inference

In fuzzy control, the decision-making procedures are done by an inference mechanism or "inference engine," using the compositional rule of inference. Decisions are made according to the fuzzy IF-THEN rules (fuzzy implications) which are embedded in the knowledge base using fuzzy approximate reasoning. An example of such a rule is "IF the moisture error is *large* THEN the temperature of the heater is *very high*." The rule here states that if the moisture error read by the moisture sensor is large, the heater should be left on for a longer time duration in order to provide a higher temperature. Such a description (rule) is a linguistic statement of expert knowledge and experience.

Measurements (data) D which are assumed to be fuzzified are matched with the fuzzy rulebase (knowledge base) R to obtain the fuzzy inference (control action) C. This is done according to the compositional rule of inference which states that:

$$C = D \circ R \tag{2.30}$$

The fuzzy set R is a collection of linguistic rules, which represents the knowledge base of the problem. The context is usually the measured outputs of the process and are crisp quantities, and the control action that drives the process is also typically a crisp quantity. Therefore, process measurements have to be fuzzified and the control action C has to be defuzzified to provide the crisp control value. The membership function of the control action C is obtained according to equation (2.29) as

$$\mu_C = \sup_Y min\,(\mu_D, \mu_R) \tag{2.31}$$

Note that Y represents the space in which the context D is defined. The inference generation procedure given by equation (2.31) is known as the "compositional rule of inference" [34].

2.4 Fuzzy Logic Control

Fuzzy logic control (FLC) uses a set of linguistic rules which are embedded in the knowledge base. The condition and action fuzzy variables in these rules are defined by membership functions, which have to be known. Furthermore, a reasoning (inference making) mechanism is needed for decision making, to generate the control action.

Fuzzy logic control can be defined as a realization of human control strategy, and is particularly suitable or adaptable for complex and ill-defined processes where analytical modeling is difficult. This advantage arises from the fact that FLC does not require a conventional model [6]. Fuzzy logic can be applied in two different architectures, low-level FLC and high-level FLC.

Low-level FLC

Low-level fuzzy logic control has been applied to many applications where the conventional controller is replaced by a direct fuzzy logic controller (DFLC). In the low-level control, the typical variables used as the observation for fuzzy decision making are error e_x, and the rate of change of error $\dot{e}_x$ of the process response. However, direct FLC may fail when the process being controlled has high-bandwidth, which requires very fast and accurate control actions. This drawback arises from the inherent delay and introduced by the reasoning process at the lowest level.

Application of DFLC requires the implementation of a fuzzy control law (knowledge base), fuzzification algorithm, fuzzy inference, and defuzzification procedures for generating control signals for process actuation [6]. These procedures consume a fairly large computation time and therefore introduce delay to the process control action. Besides, error or imprecision can be introduced through sensors since sensory data can be noisy at low-level. Low-level FLC is recommended when some specific conditions are satisfied, as summarized below:

- Required process control bandwidth is sufficiently low (e.g., 1.0 Hz or less)
- Process time constants are relatively large (e.g., 1.0 second or more)
- Process is complex and ill-defined, possessing nonlinearities and time delay.

High-level FLC

It is intuitively more attractive to use fuzzy logic at a higher level, in a hierarchical architecture, where human expertise, experience and knowledge are integrated at upper levels in the hierarchy [30]. Such an arrangement appears to be particularly appropriate in the supervisory control of complex processes where high levels of intelligence would be needed for carrying out upper level tasks. High level FLC has several special features as given below:

- High speed control actions can still be maintained at low level through the utilization of conventional crisp techniques
- Accuracy of the low-level conventional controller can be improved by "intelligent" monitoring, tuning and supervision
- Experience-based monitoring, supervision, and tuning done by control operators, which need not be carried out at as high speeds as what is required for low-level direct control, and can be implemented at an upper level of the hierarchy.

In general, development and operation of fuzzy logic control as described before can be summarized by the following 4 steps of offline design, followed by the 3 steps of real time operation:

Offline
1. Development of a set of linguistic control rules containing fuzzy variables of process outputs (conditions) and control inputs to the process (actions).
2. Generation of a set of membership functions for the process condition and action variables.
3. Application of fuzzy implication to each rule R_i in Step 1, which gives a multi-dimensional membership function μ_{Ri} using the membership functions of Step 2.

4. Combination of the fuzzy relations R_i using fuzzy connectives among rules, and to obtain the membership function μ_R of the overall fuzzy rule base (relation R).

Online

1. Fuzzify the measured process variables as fuzzy singletons.
2. Match the fuzzy measurements obtained in Step 1 with the membership function μ_R of the fuzzy rule base (matching the data to the context), using the compositional rule of inference, and obtain the fuzzy control inference.
3. Defuzzify the control inference (fuzzy) obtained in Step 2 to generate the crisp control value for process actuation through, for instance, the centroid method.

Centroid Defuzzification

Defuzzification is an important process, which converts a fuzzy inference into a crisp control action. In this manner a representative crisp parameter is determined for a given fuzzy set (fuzzy inference) which is represented by a membership function. Defuzzification is commonly performed by employing the *Centroid Method*. Let the membership function of a control inference be denoted by $\mu_C(c)$, with a support set S. Note that, for a fuzzy set A, the support set denoted by S, is a crisp set formed by the collection of all the elements $x_i \in X$ such that $\mu_A(x_i) > 0$. Then, the crisp control action $\hat{c}$ is determined using the centroid method of defuzzification as follows for a continuous universe:

$$\hat{c} = \frac{\int\limits_{c \in S} c\, \mu_C(c)\, dc}{\int\limits_{c \in S} \mu_C(c)\, dc} \tag{2.32}$$

or, in the case of a discrete universe as:

$$\hat{c} = \frac{\sum\limits_{c_i \in S} c_i \mu_C(c_i)}{\sum\limits_{c_i \in S} \mu_C(c_i)} \tag{2.33}$$

45

Alternatively, the control signal at the peak value may be chosen as the defuzzified control action if the membership function of the control inference has only one peak value (*unimodal*). Then the defuzzified control action is given as

$$\hat{c} = c_{max} \ such\ that\ \mu_C(c_{max}) = \max_{c \in S} \mu_C(c) \tag{2.34}$$

If the control membership function has more that one peak (*multimodal*), the defuzzified value for the control action is determined by taking the mean value of this set of peaks, and then by computing the mean value weighted by the corresponding membership grades. Specifically, first determine

$$c_i \ such\ that\ \mu_C(c_i) \ \underline{\underline{\Delta}}\mu_i = \max_{c \in S} \mu_C(c) \quad i = 1, 2, \cdots, p$$

and then compute

$$\hat{c} = \frac{\sum_{i=1}^{p} \mu_i c_i}{\sum_{i=1}^{p} \mu_i} \tag{2.35}$$

Here, p is the total number of peaks (modes) in the membership function. The control action given by the centroid method is known more robust than the one given by the mean of maxima method.

2.5 Hierarchical Control

Hierarchical control systems have been used even prior to the 1970s as a means of organizing and operating large scale and complex systems. The architecture consists of a group of subsystems that are arranged in a hierarchy according to their level of

abstraction, level of complexity of decision making, and the level of priority of action [28]. This is the basis of hierarchical control.

Control tasks are ranked into different levels in the hierarchy according to their functionality. The number of levels within the hierarchy mainly depends on the specific application. In control system applications, the greater the number of levels within the hierarchical system, the more accurate and flexible the control actions. However, there is always a trade off between control accuracy and computational speed. In the following, several aspects of defining the levels of hierarchy are given [6], and the concept is presented graphically in Figure 2-11.

Considerations of the level of hierarchy:

- nature of the tasks
- information resolution
- fuzziness of information
- control bandwidth
- event duration (cycle time of process action).

Tasks with different functionalities are ranked into different levels of the hierarchy for performing specific assignments. The information resolution at the lowest level is relatively high since low-level crisp controllers, in particular, require fast and accurate information at high bandwidth. This information resolution decreases with the level of hierarchy since tasks performed at higher level require more "intelligence", and therefore detail information will not be needed. Similarly, the degree of fuzziness is very low at the lowest level and increases with the level of hierarchy. The reason for that is a high degree of fuzziness can be tolerated at high levels of the hierarchy, while even a slight fuzziness at the lowest level can lead to errors and inaccurate control. The control bandwidth decreases with the level of hierarchy since tasks at the higher levels will involve operations such as preprocessing, system monitoring, quality assessment and grading, or parameter tuning, which require more time. Similarly, the event duration increases with the level of the hierarchical system since information abstraction and interpretation are

more prominent at upper levels, compared to direct processing that would be needed at lower levels. Also, the required cycle time of processing will be longer due to the more "intelligent" operations that are required at higher levels.
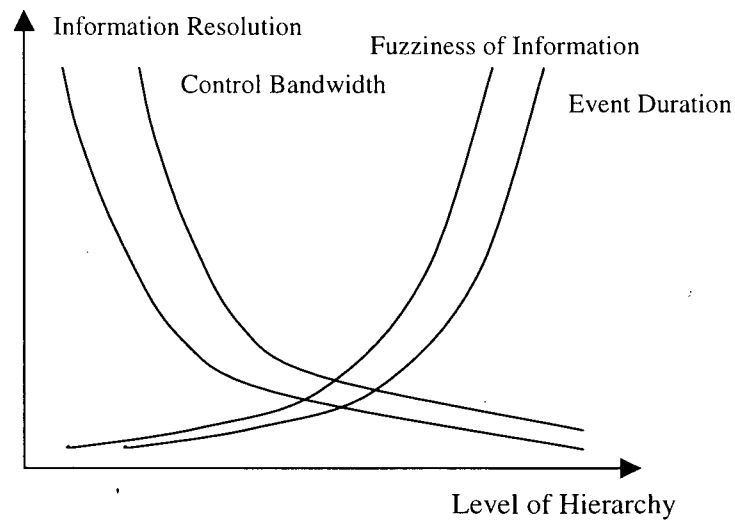
Figure 2-11   Qualitative relationships of information resolution, fuzziness of information, control bandwidth and event duration with the level of hierarchy.

With the background material presented in Chapters 1 and 2, it is now possible to address the problem of controlling an industrial kiln for wood drying. Chapter 3 will present the experimental development and data acquisition, which are necessary for model identification in direct conventional control.

Chapter 3

EXPERIMENTAL DEVELOPMENT

A good understanding of the process dynamics of the kiln system is important to kiln control. This is particularly true when using conventional techniques for control. In the present research both conventional and knowledge-based techniques are studied for kiln control. In view of this, and in view of the complexity of the kiln dynamics, experimental modeling rather than analytical modeling is undertaken. Experiments have to be properly planned and conducted in data acquisition for experimental modeling, which is also known as model identification. In this chapter, details of the performed experiments are described. Considerations include the system constraints, and experimental curves for both external computer control and internal heater control of temperature, moisture content, and relative humidity.

3.1 System Constraints

The experimental kiln setup has two constraints. First, the filament of the heater itself should not be heated above a temperature of 350 °C, which is the factory limit. Second, throughout the experiments, the highest temperature used to dry the wood pieces should not exceed 85 °C, to ensure proper quality of the dried wood.

3.2 Experiment Description

In the first stage of this research project, nine experiments were carried out to investigate the kiln behavior. The experimental results are presented in sections 3.3.1 and 3.3.2. Section 3.3.1 presents six experiments (Experiments #1 through #6) with the control input signal generated and provided by the host computer. Each experiment is performed under one particular constant fan speed and one particular heater input duration, while the kiln is loaded with eight pieces of wet wood. Section 3.3.2 presents three experiments

(Experiments #7 through #9) where internal heater control that comes with the manufacturer, is used. Here, the heater input is not controlled by the host computer, but by its internal Proportional plus Integral (PI) control hardware. The heater is set to either on or off position according to the upper and lower limit settings. The details of each experiment are given below:

Experiment #1
- Fan speed set at 500 RPM
- Heater kept on throughout its maximum duration (8 minutes)

Experiment #2
- Fan speed set at 500 RPM
- Heater kept on for half its maximum duration (4 minutes)

Experiment #3
- Fan speed set at 750 RPM
- Heater kept on throughout its maximum duration (8 minutes)

Experiment #4
- Fan speed set at 750 RPM
- Heater kept on for half its maximum duration (4 minutes)

Experiment #5
- Fan speed set at 1000 RPM
- Heater kept on throughout its maximum duration (8 minutes)

Experiment #6
- Fan speed at 1000 RPM
- Heater kept on for half its maximum duration (4 minutes)

Experiment #7

- Upper temperature limit is set at 100°C, and the lower limit set at 98°C
- Fan speed at 1000 RPM
- Heater is turned on when temperature drops below the lower temperature setting
- Heater is turned off when temperature exceeds the upper temperature setting

Experiment #8 (Same experimental setup as experiment #7 but with different initial conditions)

- Upper temperature limit is set at 100°C, and the lower limit set at 98°C
- Fan speed is set at 1000 RPM
- Heater is turned on when the temperature drops below the lower temperature setting
- Heater is turned off when the temperature exceeds the upper temperature setting

Experiment #9

- Upper temperature limit is set at 100°C, and lower limit set at 98°C
- Fan speed is set at 750 RPM
- Heater is turned on when temperature drops below the lower temperature setting
- Heater is turned off when temperature exceeds the upper temperature setting.

3.3 Experimental Curves and Results

The following two subsections present the experimental curves of the collected data for temperature, moisture content, and relative humidity responses. For each experiment, the temperature readings from each thermocouple (a total of 12 thermocouples), the moisture content readings from each pair of wood moisture content sensors (a total of 8 pairs), and the relative humidity readings from the relative humidity sensors (a total of 2 relative humidity sensors) are plotted and presented.

3.3.1 External computer control of input

In external control of kiln input, the computer sends out a control signal to switch on or off the heater. Table 3.1 gives the data files for experiments 1 through 6. The subsections that follow present the temperature, moisture content and relative humidity curves corresponding to the collected experimental data.

Table 3.1   Data files of the experiments.

EXPERIMENTS	DATA FILE
Experiment #1	Pretest_500w.txt
Experiment #2	Exp5.txt
Experiment #3	Pretest_750w.txt
Experiment #4	Exp7.txt
Experiment #5	Pretest_1kw.txt
Experiment #6	Exp9.txt

3.3.1.1 Temperature curves

The temperature distribution curve is plotted for different zones of the kiln. The wood drying kiln setup has been divided into four zones according to the locations of the thermocouples. They are named zone 1, zone 2, zone 3, and zone 4.

Experiment #1

- Fan speed set at 500 RPM

- Heater on for 8 minutes
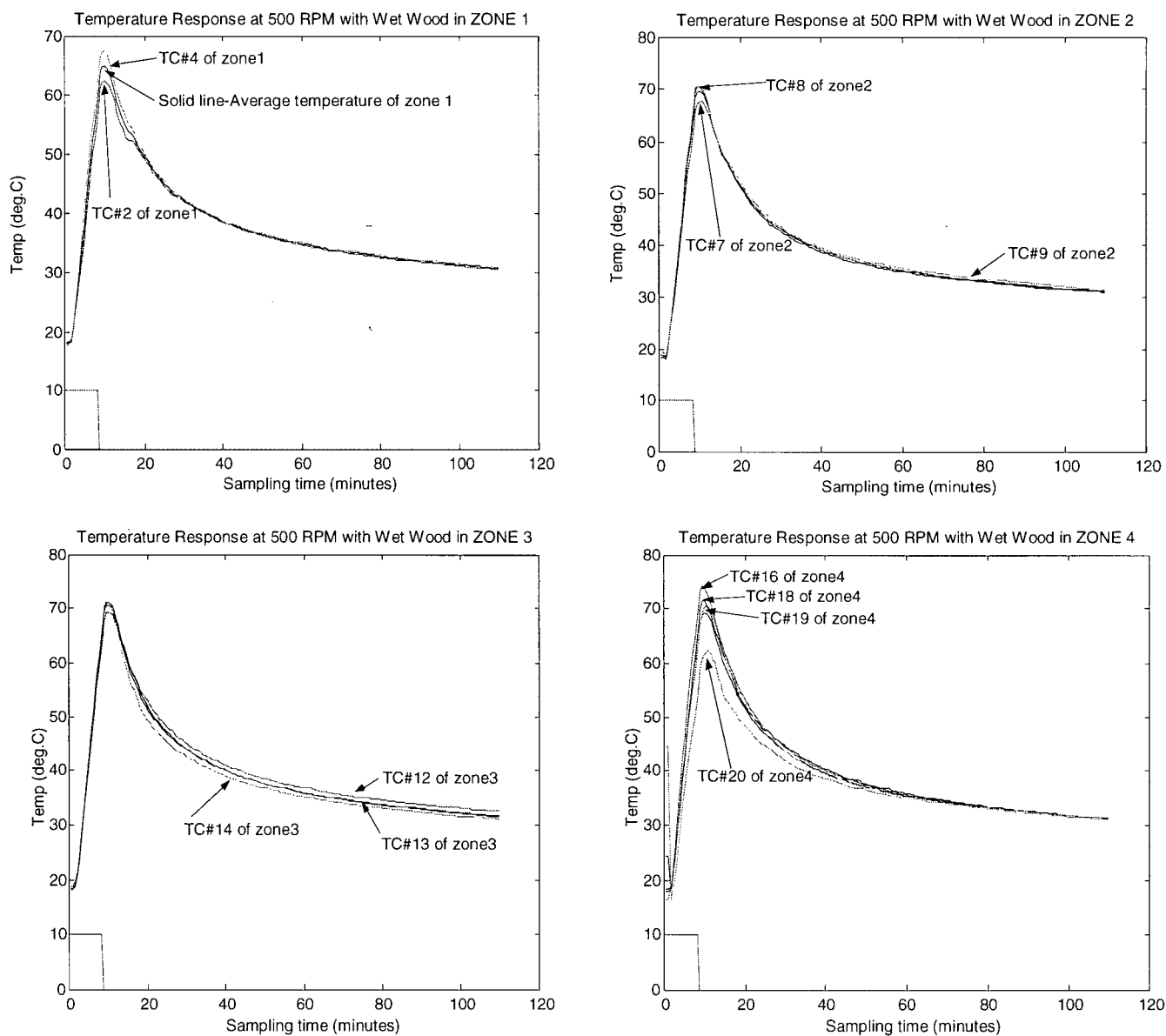
Figure 3-1   Temperature curves of experiment #1 for different zones in the kiln.

Experiment #2

- Fan speed set at 500 RPM

- Heater on for 4 minutes

Figure 3-2   Temperature curves of experiment #2 for different zones in the kiln.

Experiment #3

- Fan speed set at 750 RPM
- Heater on for 8 minutes

Figure 3-3   Temperature curves of experiment #3 for different zones in the kiln.

Experiment #4

- Fan speed set at 750 RPM
- Heater on for 4 minutes

Temperature Response at 750 RPM, Heater ON 4 min, with Wet Wood in ZONE 1

TC#4 of zone1
Solid line-average temp of zone1
TC#2 of zone1

Temperature Response at 750 RPM, Heater ON 4 min, with Wet Wood in ZONE 2
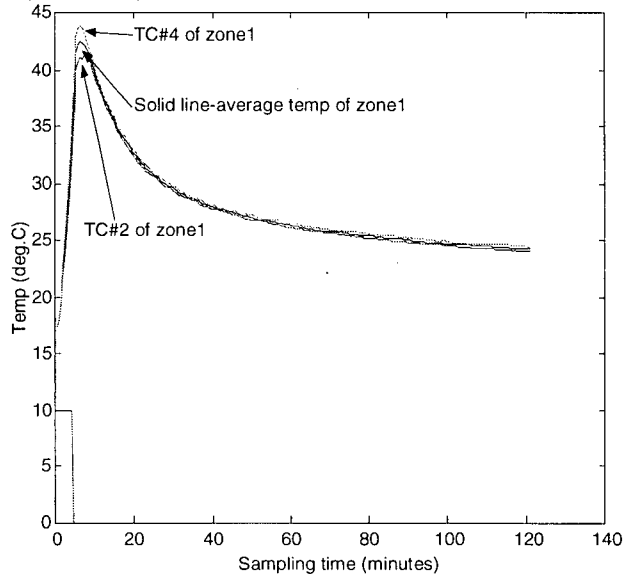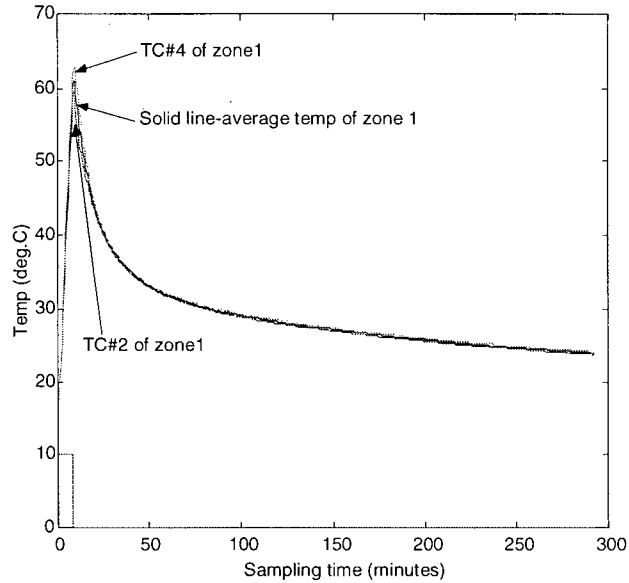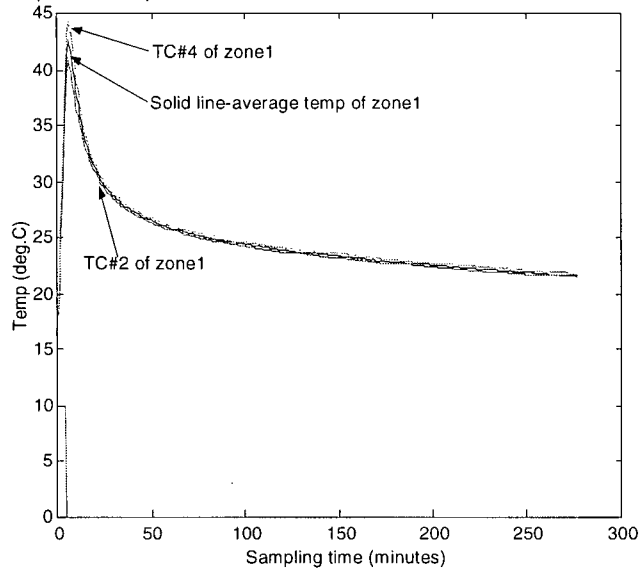
TC#9 of zone2
TC#8 of zone2
TC#7 of zone2

Temperature Response at 750 RPM, Heater ON 4 min, with Wet Wood in ZONE 3
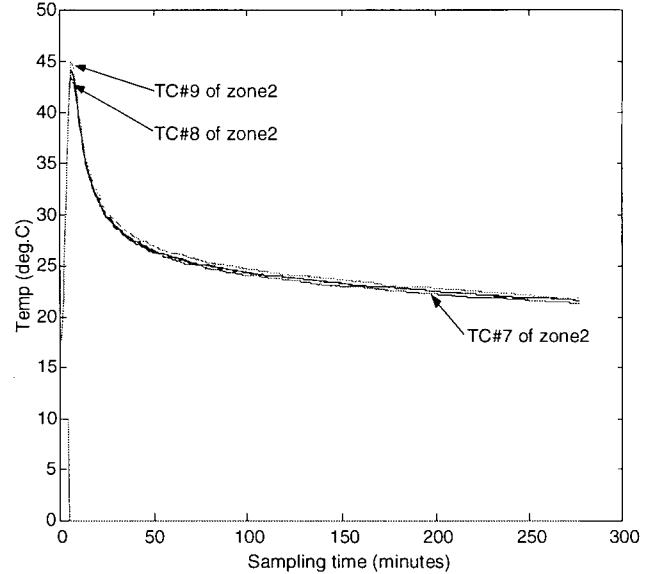
TC#13 of zone3
TC#12 of zone3
TC#14 of zone3

Temperature Response at 750 RPM, Heater ON 4 min, with Wet Wood in ZONE 4
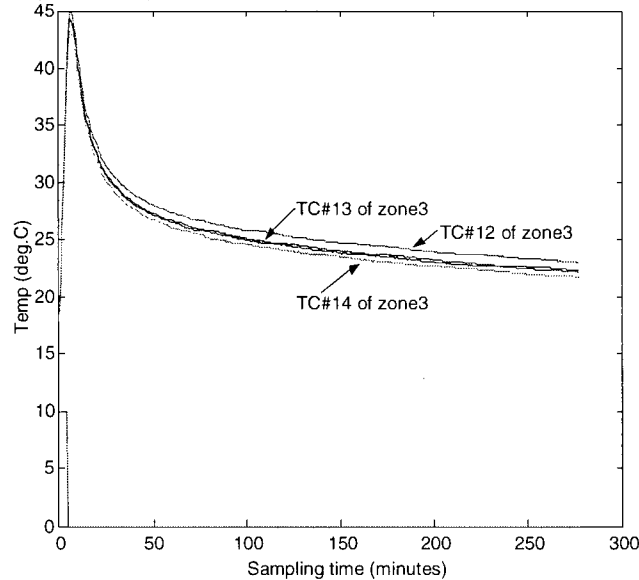
TC#16 of zone4
TC#19 of zone4
TC#18 of zone4
TC#20 of zone4
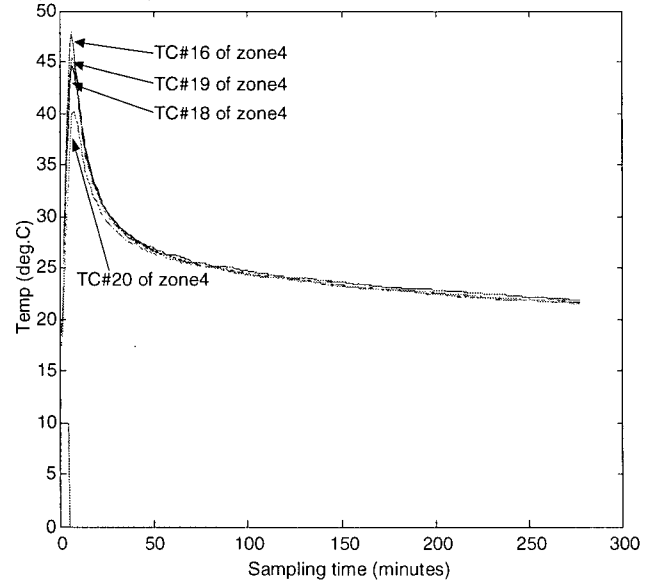
Figure 3-4   Temperature curves of experiment #4 for different zones in the kiln.
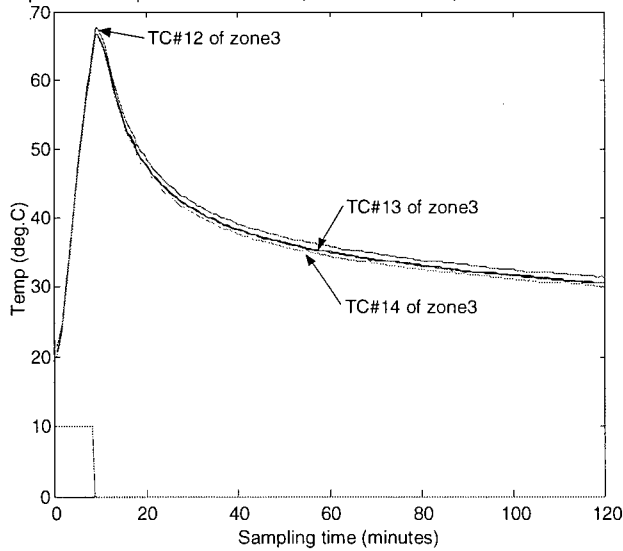
Experiment #5

- Fan speed set at 1000 RPM
- Heater on for 8 minutes
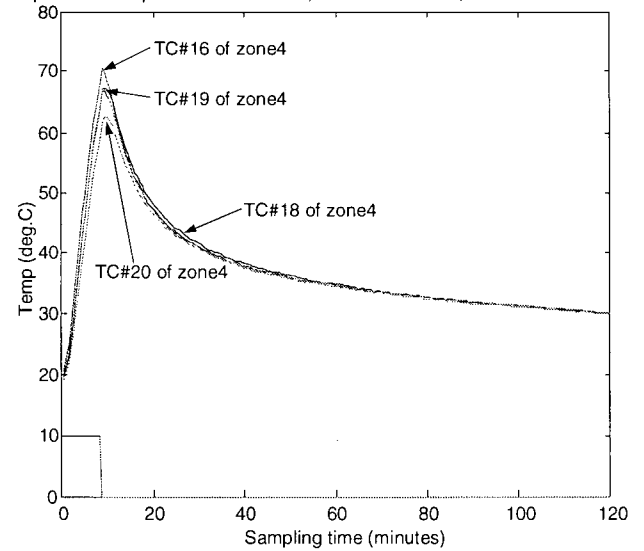
Figure 3-5   Temperature curves of experiment #5 for different zones in the kiln.
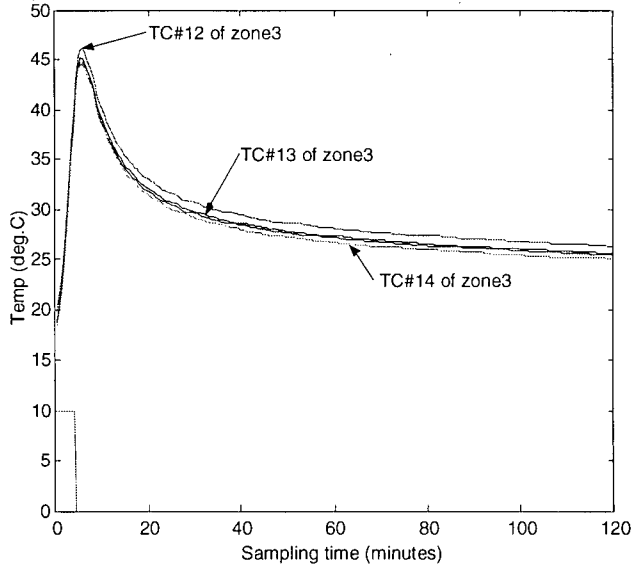
Experiment #6

- Fan speed set at 1000 RPM
- Heater on for 4 minutes
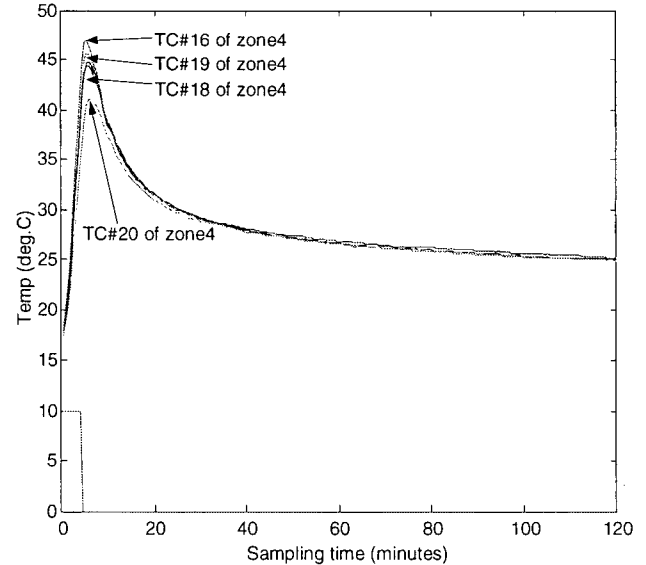
Figure 3-6   Temperature curves of experiment #6 for different zones in the kiln.

In section 3.3.1.1., the temperature curves for various zones at different fan speeds and heating durations are illustrated. It is noted that the zones have very similar temperature distribution curves. When the heater is on, temperature rises rapidly in each zone. The temperature drops with some time delay when heater is turned off. By examining the collected data files, the following conclusions are drawn:

For a fan speed of 500 RPM, with the heater kept on for 8 minutes, the highest temperature reached by the kiln load is about 69°C. After the heater is turned off, there is a time delay of about 2 minutes before the temperature begins to drop. At the same fan speed, when the heater is on only for 4 minutes, the highest temperature reached is about 44°C. Time delay is about 2.8 minutes.

For a fan speed of 750 RPM, with the heater kept on for 8 minutes, the highest temperature reached is about 64°C. When the heater is turned off, there is a time delay of about 1.6 minutes. At the same fan speed, when the heater is on for half the duration 4 minutes, the highest temperature reached is about 44°C with a time delay of 2 minutes.

For a fan speed of 1000 RPM, with the heater kept on for 8 minutes, the highest temperature reached by the kiln is approximately 66°C. The time delay after the heater is shut off is about 1.3 minutes. For the same fan speed, with the heater kept on for 4 minutes, the highest temperature reached is about 44°C, with a time delay of 1.6 minutes. Results of the temperature distribution curves of the six experiments are summarized in Table 3-2.

Table 3-2   Summary of the temperature data.

Fan Speed	Highest Temperature Reached	Time Delay	% Reduction in Time Delay
500 RPM	69 °C (8 minutes heater ON)	2 minutes	500 RPM as reference
500 RPM	**44 °C (4 minutes heater ON)**	**2.8 minutes**	**500 RPM as reference**
750 RPM	64 °C (8 minutes heater ON)	1.6 minutes	20 %
750 RPM	**44 °C (4 minutes heater ON)**	**2.0 minutes**	**28.6 %**
1000 RPM	66 °C (8 minutes heater ON)	1.3 minutes	35 %
1000 RPM	**44 °C (4 minutes heater ON)**	**1.6 minutes**	**42.9 %**

In conclusion, for a heater on duration of 8 minutes, different fan speeds have an effect on peak temperature. Highest average temperature reached from each zone drops from 69°C to 66°C when the fan speed is increased from 500 RPM to 1000 RPM. In fluid dynamics, this can be explained by the heat transfer coefficient curve. The heat transfer coefficient is a function of the Reynolds number, and the fan speed is directly proportional to the Reynolds number. Therefore, a different fan speed will have a different heat transfer coefficient curve. However, the curves are quite close to each other in the beginning. This explains why the decrease in the peak temperature is not that drastic (only 5 % reduction) in a heater on duration of 8 minutes. Another reason may be the poor air circulation in the kiln setup. On the other hand, for a heater on duration of 4 minutes, a change in the fan speed does not have any effect on the average peak temperature reached within each zone. A shorter time duration corresponds to the bottom part of the heat transfer coefficient curve at the start, in which different curves are very close to each other. Therefore, there is hardly any change in temperature, and this chance may not be observable. Time delay after the heater is shut off, decreases for increasing fan speed. A higher fan speed provides a better cooling effect, and hence the temperature drops quicker. A note has to be made here in comparing the delay time for each individual fan speed setting. At the same fan speed setting, the delay time for a heater on duration of 4 minutes is found to be larger in all cases. Wood drying is a complex process, and many variables are involved. One of the reasons for this scenario is that the temperature would not yet be evenly distributed throughout the kiln in 4 minutes. Warm air tries to move from a high temperature zone to a low temperature zone by convection. Besides, a temperature distribution curve is based on the diffusion equation in fluid mechanics, and consists of 3 different stages:

1. Rising stage

2. Steady state

3. Descending stage.

For an 8 minute duration, temperature may already be in the steady state and therefore takes less time to go to the descending stage, which corresponds to a temperature drop. Also, the temperature distribution within the kiln is more even and the effect of diffusion is greatly reduced. For the case of 4 minutes duration, even though the heater is shut off,

the temperature would not response very quickly due to the diffusion effect, and it takes a longer time for the temperature to move from the rising stage to the steady state, and then to the descending stage. Therefore, it takes a longer time for the temperature to drop in a shorter heater-on duration. From these experiments, it is observed that a higher fan speed (e.g., 1000 RPM) can greatly reduce the time delay, compared to a low fan speed settings (500 and 600 RPM). It also makes smaller the deviation between different heater-on duration for the same fan speed setting.

3.3.1.2 Moisture content curves

The moisture content distribution curves are plotted using the sensors located on the wood pieces as shown in Figure 3-7. Note that eight pairs of moisture content sensors are used, and each pair is tapped into one piece of wood at an arbitrary location.
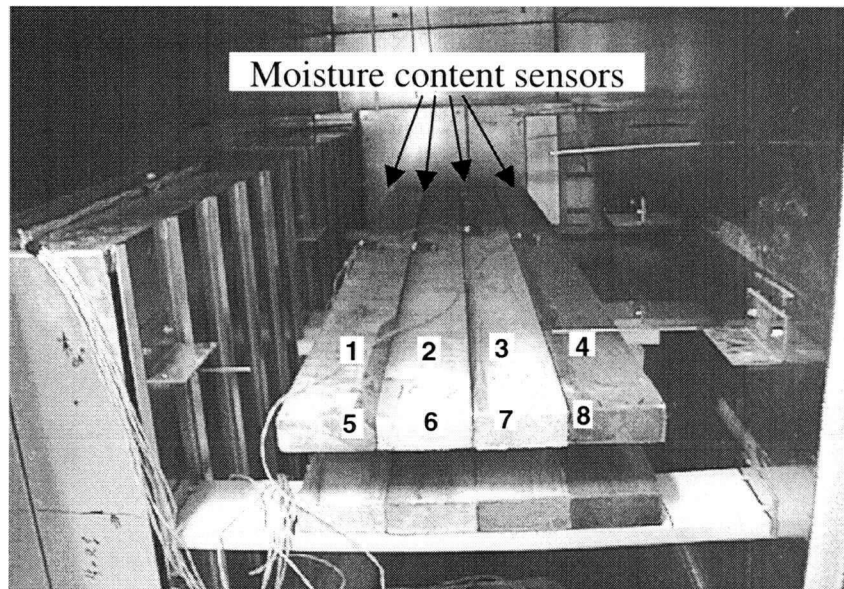
Figure 3-7   Locations of the moisture content sensors inside the kiln.

Experiment #1 (data file pretest_500w.txt)

Fan speed set at 500 RPM, and Heater kept on for 8 minutes
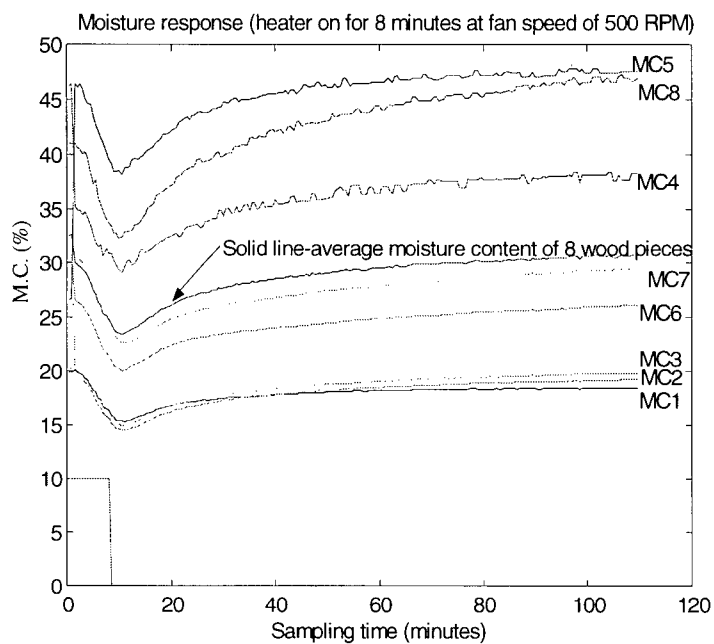
Figure 3-8   Moisture content curves of experiment #1.

Experiment #2

Fan speed set at 500 RPM, and Heater kept on for 4 minutes
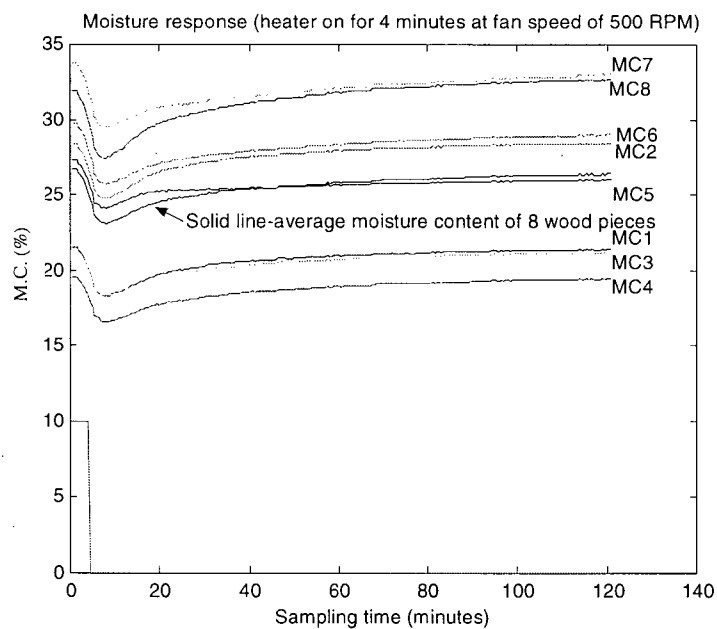
Figure 3-9   Moisture content curves of experiment #2.

Experiment #3

Fan speed set at 750 RPM, and Heater kept on for 8 minutes

Moisture response (heater on for 8 minutes at fan speed of 750 RPM)
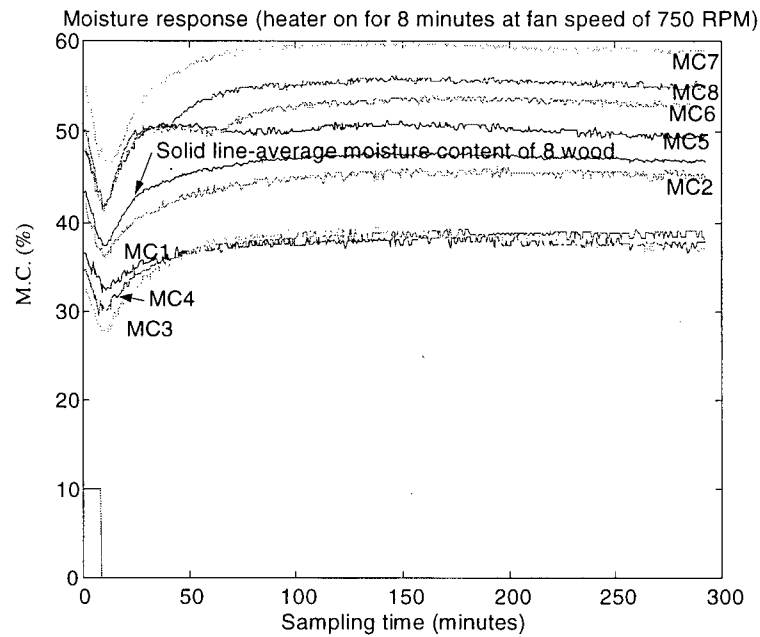
Figure 3-10   Moisture content curves of experiment #3.

Experiment #4

Fan speed set at 750 RPM, and Heater kept on for 4 minutes

Moisture response (heater on for 4 minutes at fan speed of 750 RPM)
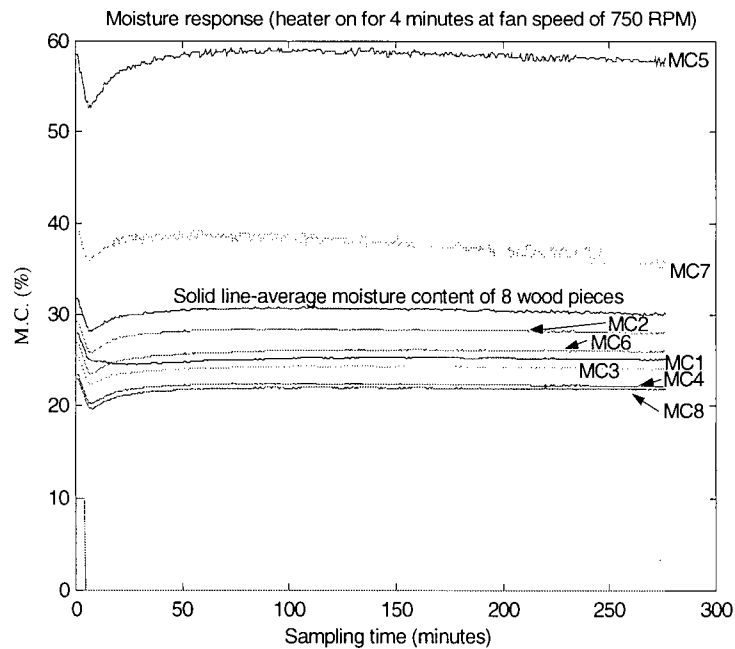
Figure 3-11   Moisture content curves of experiment #4.

Experiment #5

Fan speed set at 1000 RPM, and Heater kept on for 8 minutes
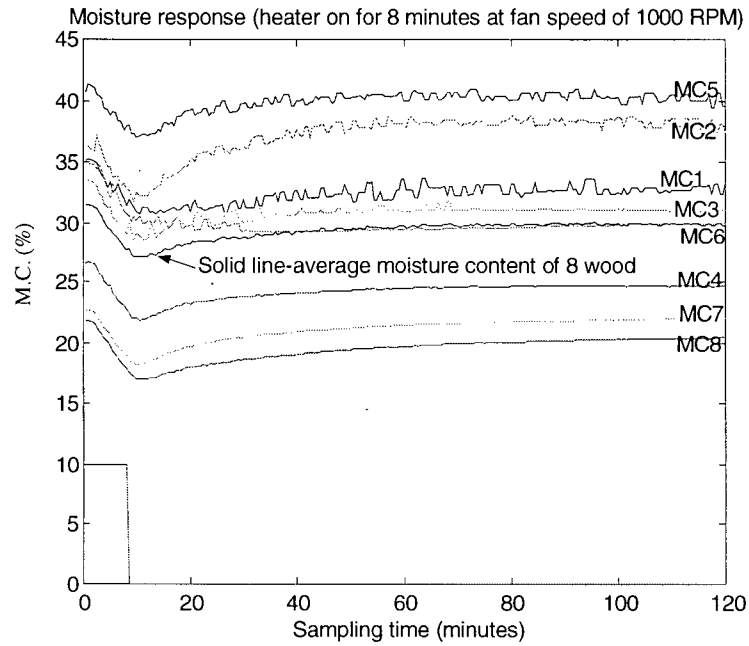
Figure 3-12   Moisture content curves of experiment #5.

Experiment #6

Fan speed set at 1000 RPM, and Heater kept on for 4 minutes
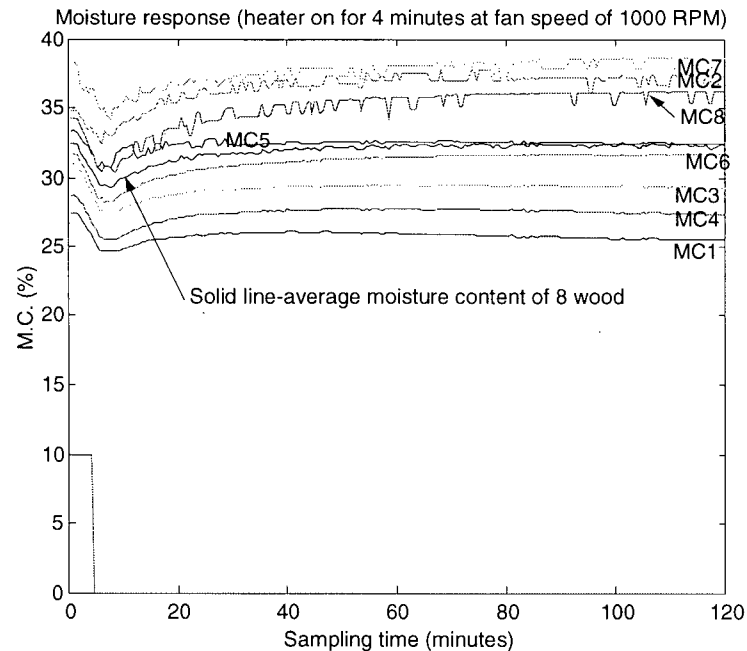
Figure 3-13   Moisture content curves of experiment #6.

In Section 3.3.1.2., the moisture content curves of the 8 pieces of wood are presented. It is noted that the moisture content distribution curves are quite similar in the different experiments. Slight initial increase of moisture content in the data that is shown, for example, in Figure 3-12 may be due to such reason as sensor delay, initial build up of moisture in wood, and the initial diffusion of moisture from other regions of the wood interior to the sensing points. The moisture content of each wood piece rapidly drops when the heater is on. When the heater is turned off, the moisture continues to drop with a time delay, and then increases slowly to a steady level. By examining each data files, the following conclusions can be drawn:

At a fan speed of 500 RPM and with the heater kept on for 8 minutes, the time delay of the moisture content response is 2.6 minutes. For the same fan speed setting, but with heater kept on only for 4 minutes, time delay is greater (3.5 minutes).

At a fan speed of 750 RPM and with the heater kept on for 8 minutes, the time delay is 2.8 minutes. For the same fan speed setting but with heater kept on only for 4 minutes, the time delay becomes 3.3 minutes.

At a fan speed of 1000 RPM and with the heater kept on for 8 minutes, the time delay is 1.9 minutes. For the same fan speed setting, but the heater kept on only for 4 minutes, the time delay becomes 2.6 minutes. The results are summarized in Table 3-3.

Table 3-3   Summary of the moisture content response characteristics.

Fan Speed in RPM	Time Delay of the Moisture Content in minutes
500 RPM (Heater on 8 mins.)	2.6
500 RPM (Heater on 4 mins.)	**3.5**
750 RPM (Heater on 8 mins.)	2.8
750 RPM (Heater on 4 mins.)	**3.3**
1000 RPM (Heater on 8 mins.)	1.9
1000 RPM (Heater on 4 mins.)	**2.6**

In conclusion, increasing the fan speed from 500 RPM to 750 RPM does not result in a significant improvement in the time delay. However, further increase of the fan speed to 1000 RPM reduces the time delay by 27% and 26% for the cases of heater on time of 8

minutes and 4 minutes, respectively (with reference to the condition with a fan speed of 500 RPM). Fan speeds of 1000 RPM or more are suggested for reducing the time delay, as clear from the experimental results. The reasons for the increase of moisture content after the heater is shut off are summarized below:

1. Poor air circulation   2. Condensation   3. Diffusion

When air circulation is poor inside the kiln, it is difficult to efficiently remove the evaporated moisture out of the kiln. Then a large quantity of moisture will remain inside the kiln, which will create a high concentration of moisture. When the heater is turned off, the inside temperature of the kiln drops and the wood pieces will gain back moisture through condensation, as well as through diffusion. This will result in increasing the moisture content of the wood pieces after the heater is turned off.

It is important to note that the time delay when the heater on duration is 4 minutes larger than that when the heater on duration is 8 minutes. The reason for this is the larger moisture concentration gradient that is developed during the shorter heater on period. In the case where the heater on duration is 8 minutes, the surface of a wood piece assumes almost the same temperature as the surrounding air inside the kiln. A moisture gradient may still develop within the inner and the surface regions of the wood. Moisture will continue to loose due to this moisture gradient. When the heater on duration is shorter, the surface temperature of a wood piece and the surrounding air may not reach equilibrium, and a steeper moisture concentration gradient will develop. As a result, moisture from a wood piece will continue to move from regions of high moisture concentration to those of low moisture concentration, thereby increasing the delay time.

3.3.1.3 Relative humidity curves

The relative humidity distribution curves are plotted using sensors at two locations RH#1 and RH#2, as shown in Figure 1-5. RH#1 is located in the right side of the kiln between zone 1 and zone 2. RH#2 is located inside the plenum between zone 2 and zone 3, which essentially measures the relative humidity of the air inside the plenum.

Experiment #1 (data file pretest_500w.txt)

- Fan speed = 500 RPM

- Heater on duration = 8 minutes

Relative humidity response (heater on duration is 8 minutes at a fan speed of 500 RPM)
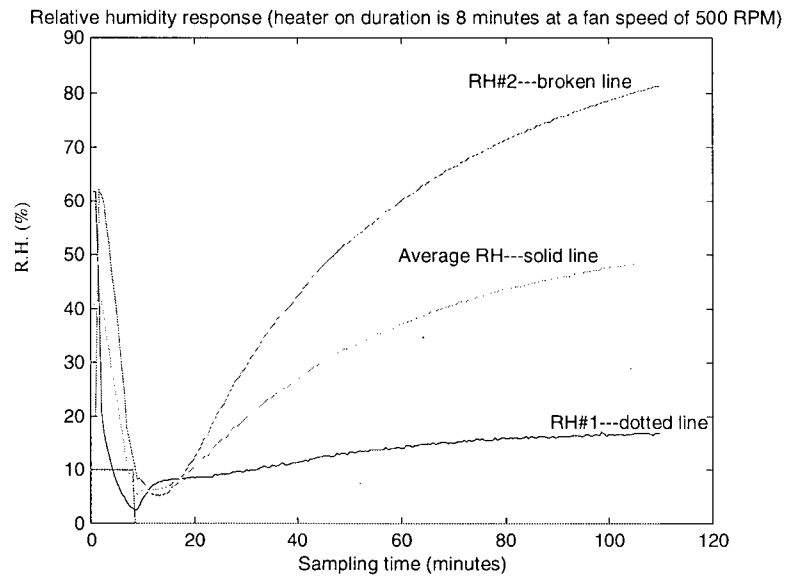
Figure 3-14   Relative humidity curves of experiment #1.

Experiment #2 (data file exp5.txt)

- Fan speed = 500 RPM

- Heater on duration = 4 minutes

Relative humidity response (heater on duration is 4 minutes at a fan speed of 500 RPM)
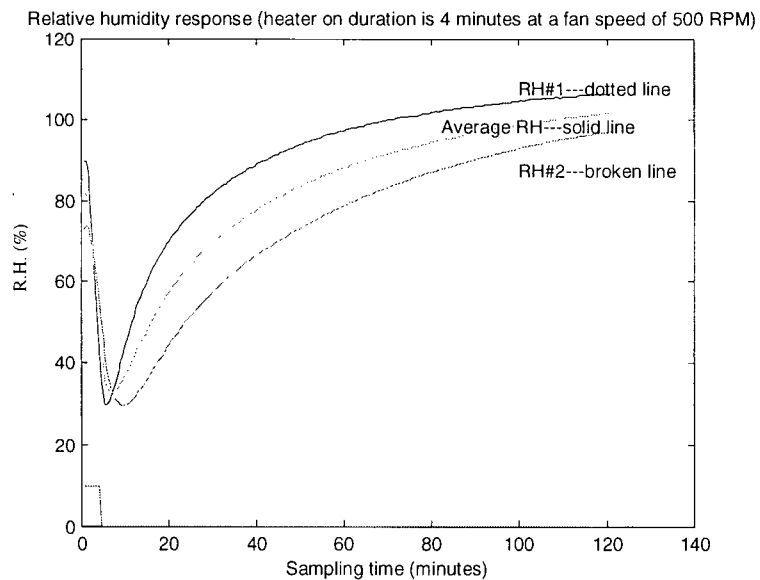
Figure 3-15   Relative humidity curves of experiment #2.

67

Experiment #3

- Fan speed = 750 RPM

- Heater on duration = 8 minutes

Relative humidity response (heater on duration is 8 minutes at a fan speed of 750 RPM)
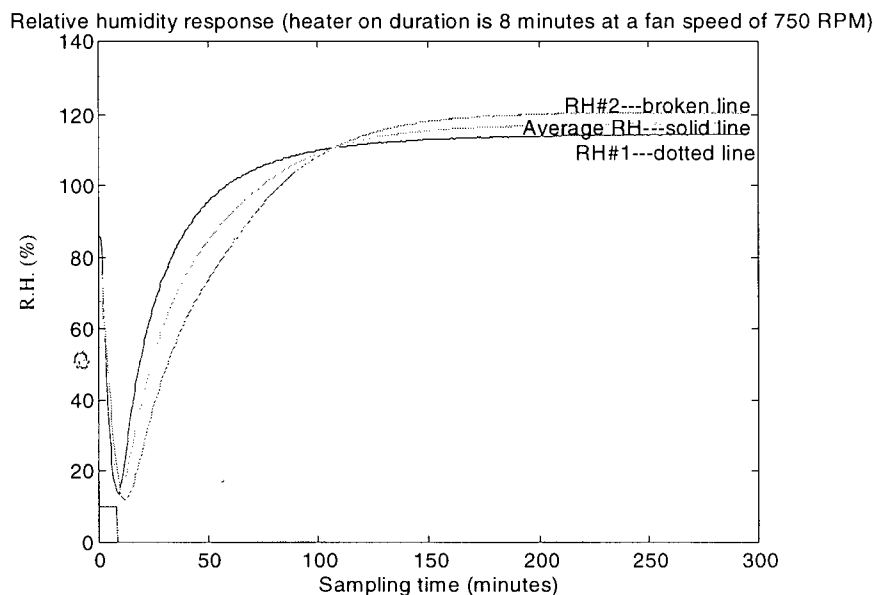
Figure 3-16   Relative humidity curves of experiment #3.

Experiment #4 (data file exp7.txt)

- Fan speed = 750 RPM

- Heater on duration = 4 minutes

Relative humidity response (heater on duration is 4 minutes at a fan speed of 750 RPM)
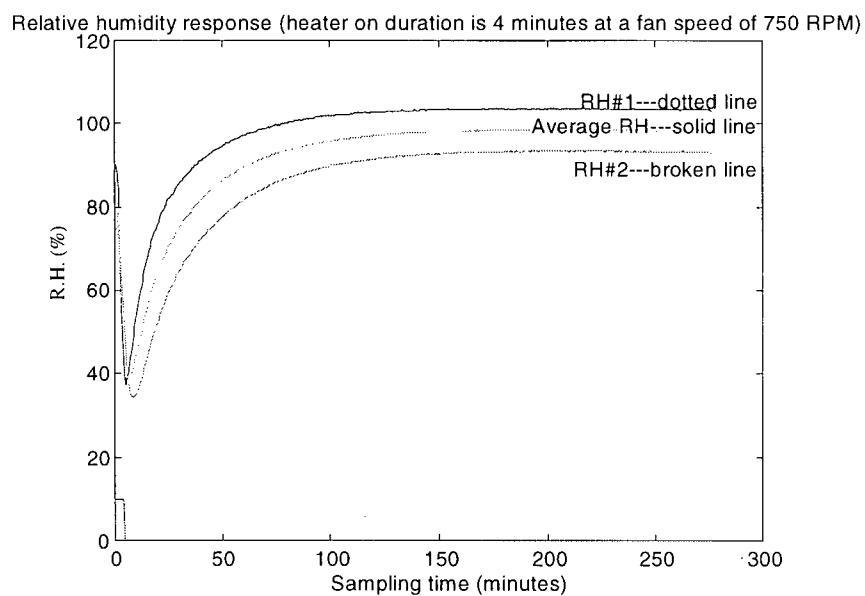
Figure 3-17   Relative humidity curves of experiment #4.

Experiment #5

- Fan speed = 1000 RPM

- Heater on duration = 8 minutes
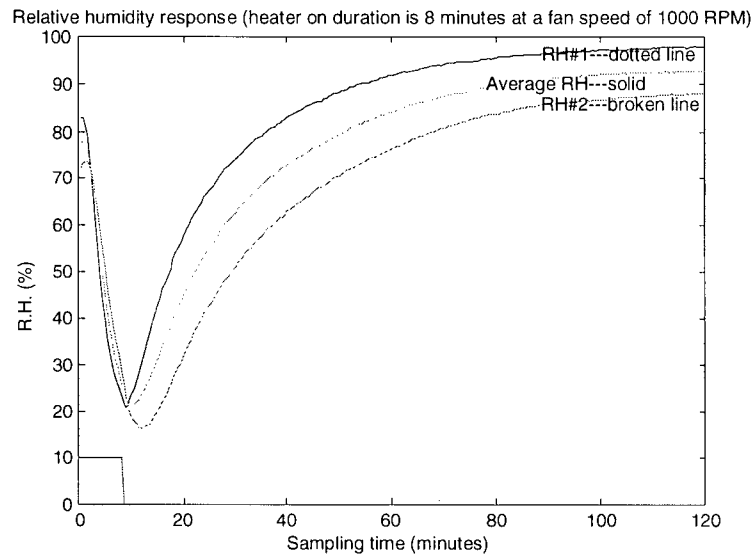
Figure 3-18   Relative humidity curves of experiment #5.

Experiment #6 (data file exp9.txt)

- Fan speed = 1000 RPM

- Heater on duration = 4 minutes
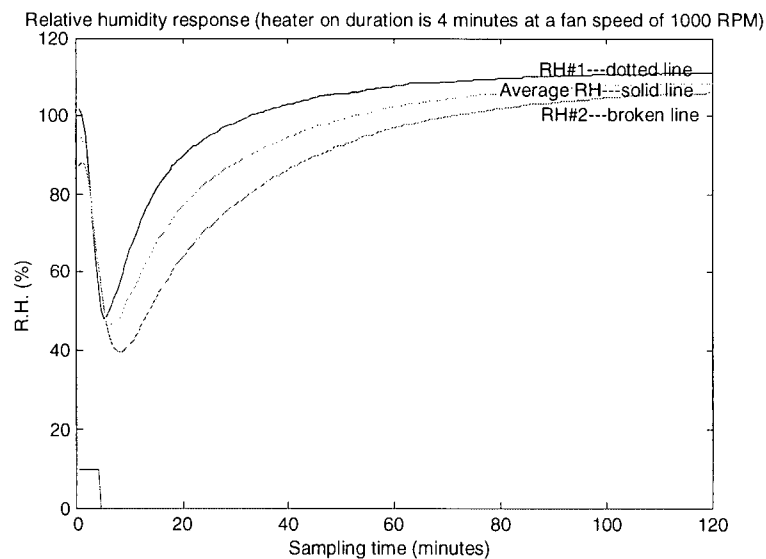
Figure 3-19   Relative humidity curves of experiment #6.

69

Experimental results of the relative humidity distribution measure are presented in section 3.3.1.3.. When the heater is on, the relative humidity inside the kiln drops rapidly, since the quantity of moisture at saturation is larger at higher temperature. From the experiment results, it is clear that the fan speed has an effect on the relative humidity inside the kiln. For a fan speed of 500 RPM, the relative humidity inside the kiln drops almost to zero when the heater is turned on for a long duration. When the fan speed increases to 750 RPM, the relative humidity drop decreases. For a fan speed of 1000 RPM, the relative humidity inside the kiln is the highest among the three cases of fan speed. If the relative humidity is too low inside the kiln, a greater moisture gradient will be generated between the wood and the kiln interior and moisture will be evaporated from the wood at a faster rate. This will develop stresses on the wood piece, and as a result the wood quality will deteriorate. In conclusion, higher fan speed is recommended for wood drying in the present setup in order to retain a higher relative humidity level within the kiln, as well as to avoid excessive stress development inside the wood piece.

3.3.2 Internal heater control

With internal heater control, the host computer will not be responsible for generating a control signal to switch on and off the heater. The heater itself will be turned on or off according to the upper and lower limit settings of temperature. The heater controller contains an internal proportional integral (PI) control unit, and a thermostat inserted between the heater filaments. The upper limit of temperature is set at 100°C, while the lower limit is set at 98°C, for experiments 7, 8, and 9. At the start, the heater is kept on as long as the temperature read by the thermostat does not exceed the upper limit. Then the heater is turned off, when the internal thermostat reads a temperature greater than 100°C, and will be back on again when the temperature drops below the lower temperature limit of 98°C. This section presents the temperature, moisture content, and relative humidity experimental data that are collected.

Table 3-4   Files for the temperature response data.

EXPERIMENTS	DATA FILE
Experiment #7	Test1.txt
Experiment #8	Test2.txt
Experiment #9	Test3.txt

3.3.2.1 Temperature curves

Data files for the temperature response information obtained in the present set of experiments are given in Table 3-4. The temperature distribution curves are plotted below for different zones inside the kiln. The interior of the kiln has been divided up into four zones, according to the locations of the thermocouples. They are named zone 1, zone 2, zone 3, and zone 4.

Experiment #7

- Upper temperature limit = 100°C, lower limit = 98°C

- Fan speed = 1000 RPM

- Heater on when temperature drops below the lower temperature setting

- Heater off when temperature exceeds the upper temperature setting
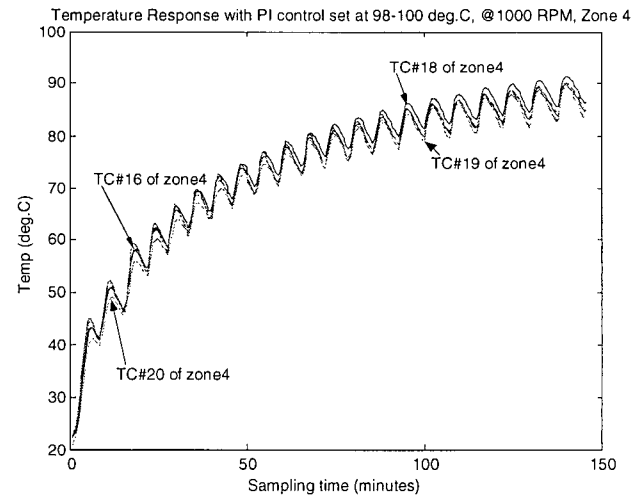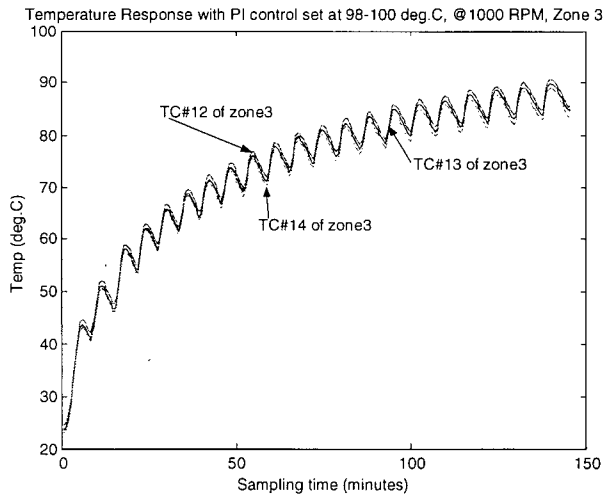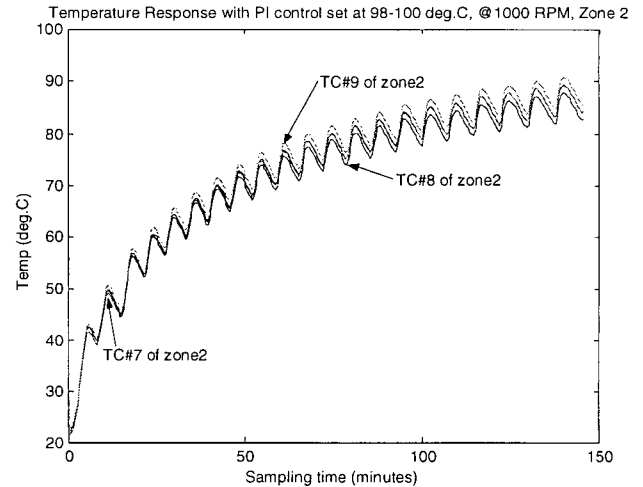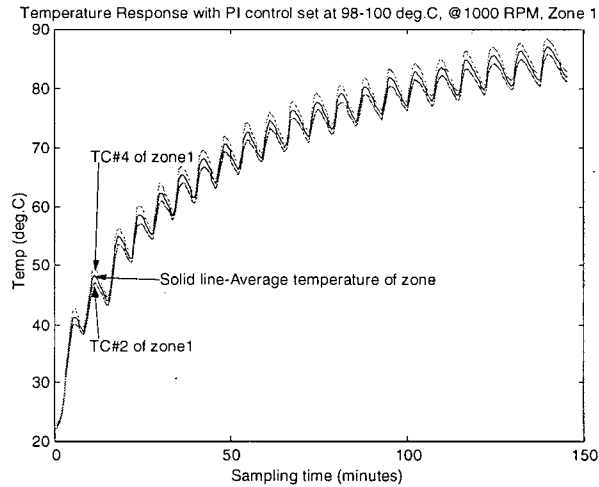
Figure 3-20   Temperature curves of experiment #7 for different zones of the kiln interior.

<u>Experiment #8 (Same setup as experiment #7 but with a different initial condition)</u>

- Upper temperature limit =100°C, lower limit = 98°C

- Fan speed = 1000 RPM

- Heater on when temperature drops below the lower temperature setting

- Heater off when temperature exceeds the upper temperature setting
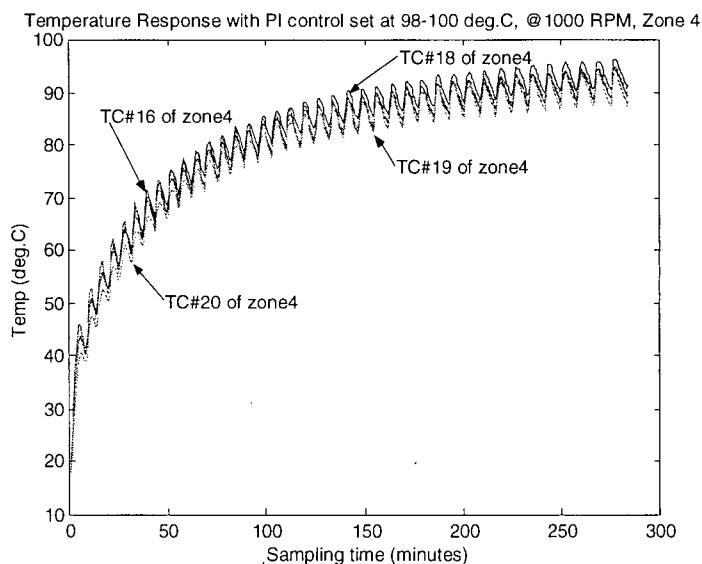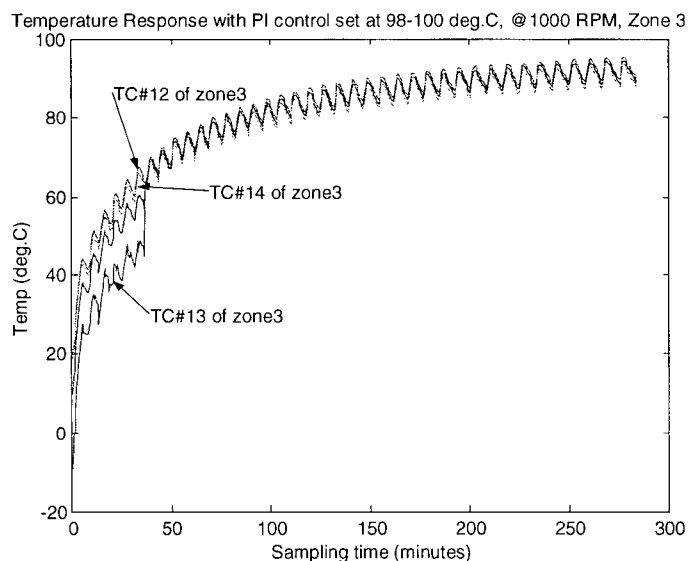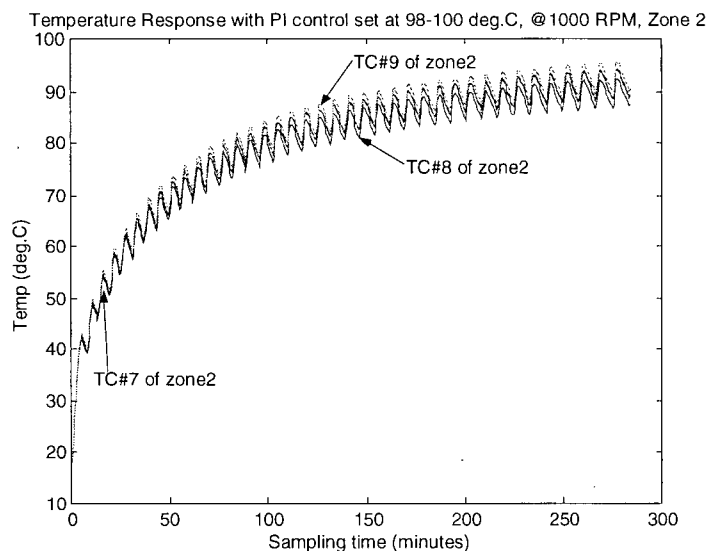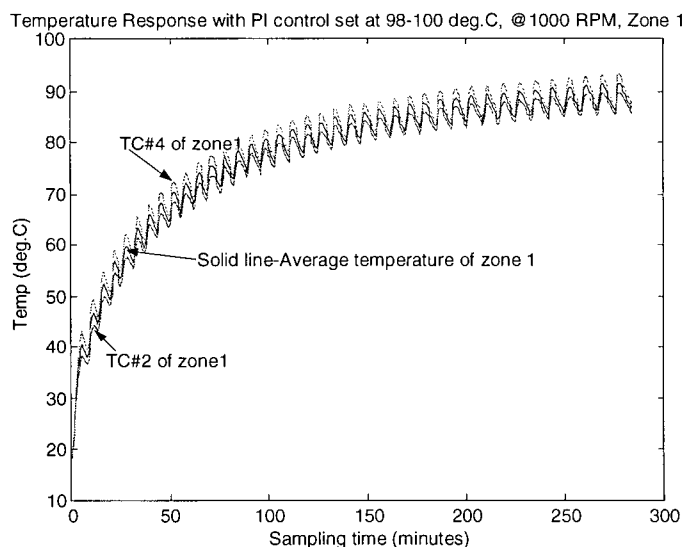
Figure 3-21   Temperature curves of experiment #8 for different zones of the kiln interior.

Experiment #9

- Upper temperature limit = 100°C, lower limit = 98°C

- Fan speed = 750 RPM

- Heater on when temperature drops below the lower temperature setting

- Heater off when temperature exceeds the upper temperature setting
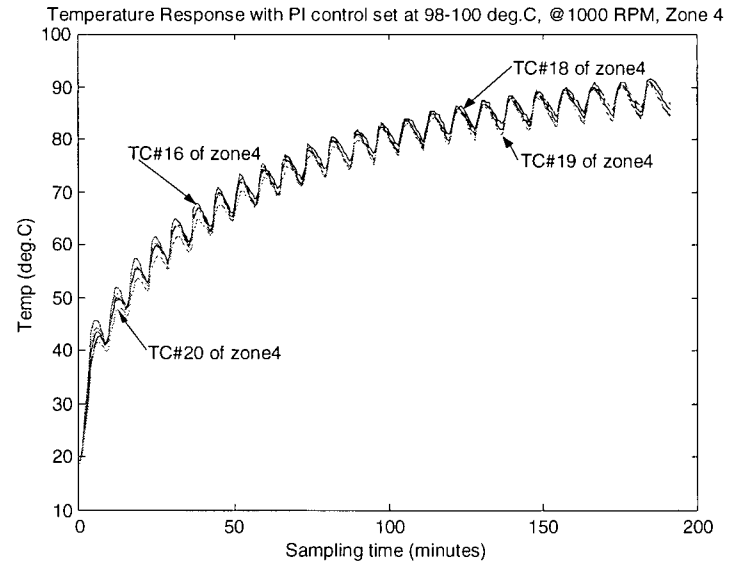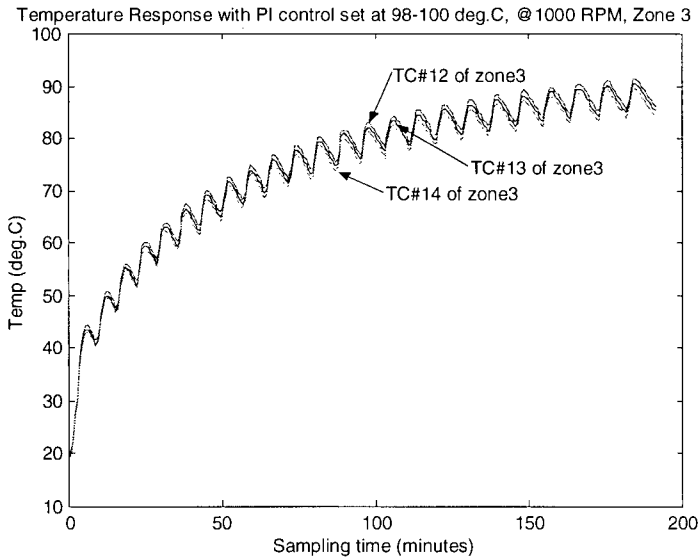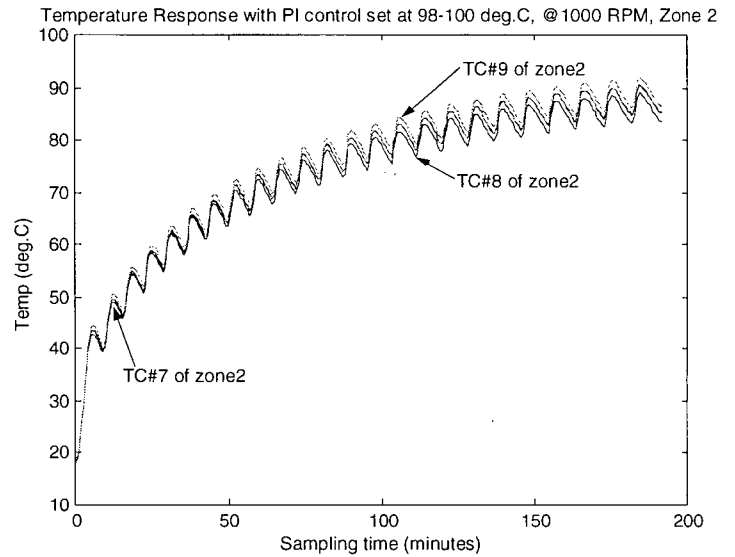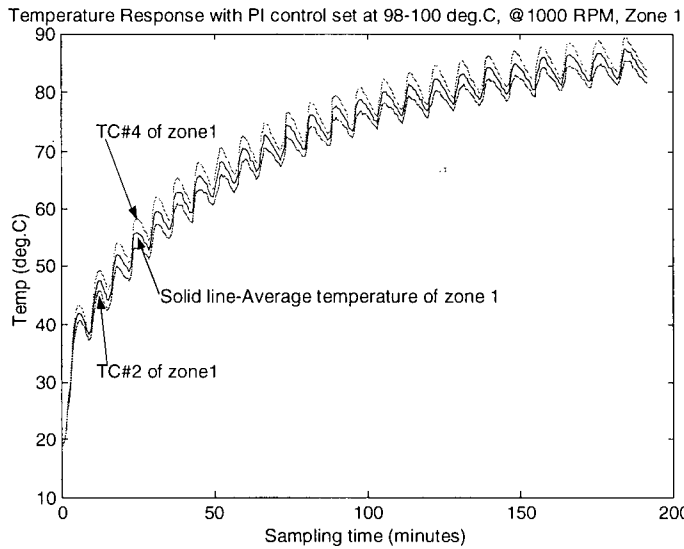
Figure 3-22   Temperature curves of experiment #9 for different zones of the kiln
interior.

3.3.2.2 Moisture content curves

The moisture content distribution curves are plotted below exactly the same way as in Section 3.3.1.2, but with the internal heater PI controller activated.

Experiment #7

- Upper temperature limit = 100°C, lower limit = 98°C

- Fan speed = 1000 RPM

- Heater on when temperature drops below the lower temperature setting

- Heater off when temperature exceeds the upper temperature setting

The associated curve is shown in Figure 3-23.
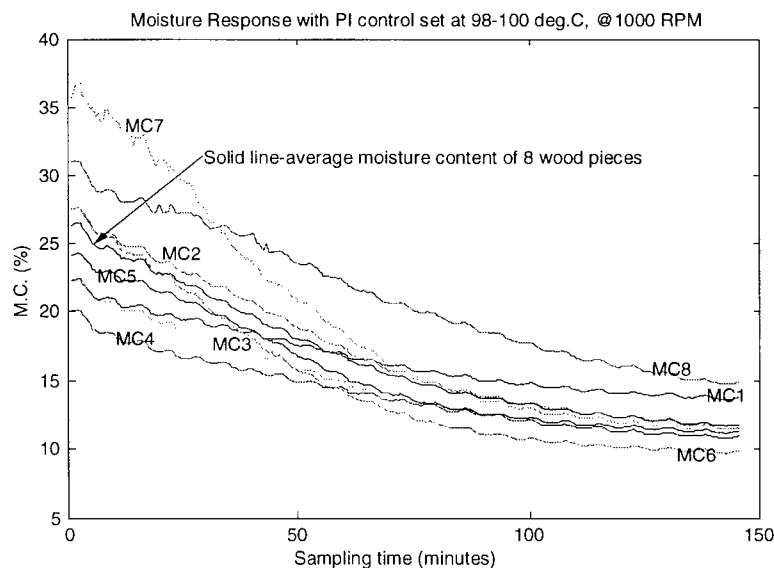
Figure 3-23   Moisture content curves of experiment #7.

Experiment #8 (Same setup as experiment #7 but with a different initial condition)

- Upper temperature limit = 100°C, lower limit = 98°C

- Fan speed = 1000 RPM

- Heater on when temperature drops below the lower temperature setting

- Heater off when temperature exceeds the upper temperature setting

The associated curve is shown in Figure 3-24.
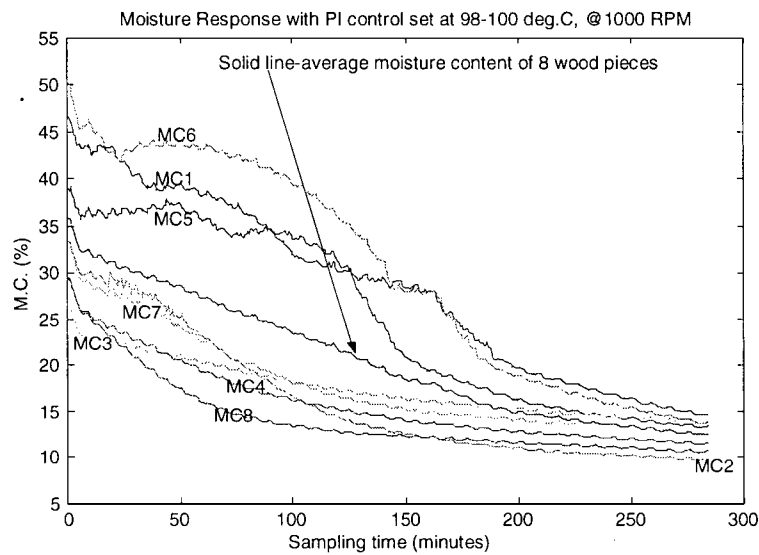
Figure 3-24   Moisture content curves of experiment #8.

Experiment #9

- Upper temperature limit = 100°C, lower limit = 98°C

- Fan speed = 750 RPM

- Heater on when temperature drops below the lower temperature setting

- Heater off when temperature exceeds the upper temperature setting

The associated curve is shown in Figure 3-25.
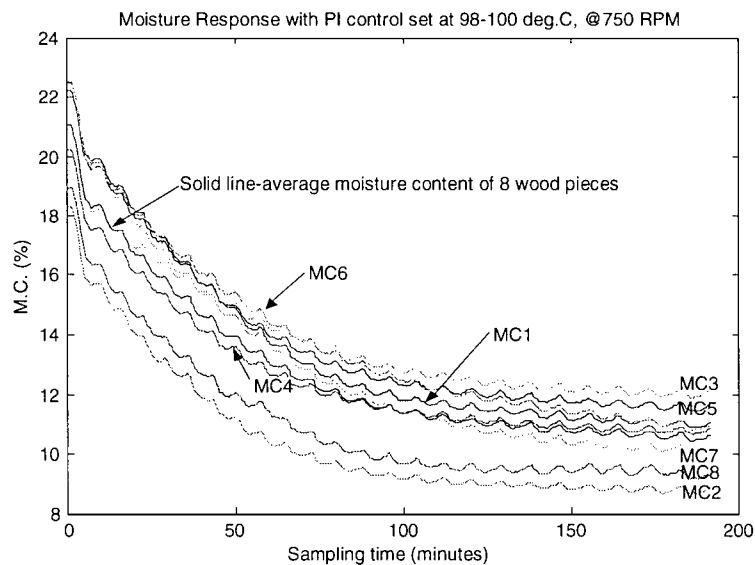
Figure 3-25   Moisture content curves of experiment #9.

3.3.2.3 Relative humidity curves

The relative humidity distribution curves are plotted below using the sensors RH#1 and RH#2. The sensor RH#1 is located at the right side of the kiln between zone 1 and zone 2. The sensor RH#2 is located inside the plenum between zone 2 and zone 3, and it essentially measures the relative humidity of air inside the plenum.

Experiment #7

- Upper temperature limit = 100°C, lower limit = 98°C

- Fan speed = 1000 RPM

- Heater on when temperature drops below the lower temperature setting

- Heater off when temperature exceeds the upper temperature setting

The corresponding curve is shown in Figure 3-26.

Moisture Response with PI control set at 98-100 deg.C, @1000 RPM
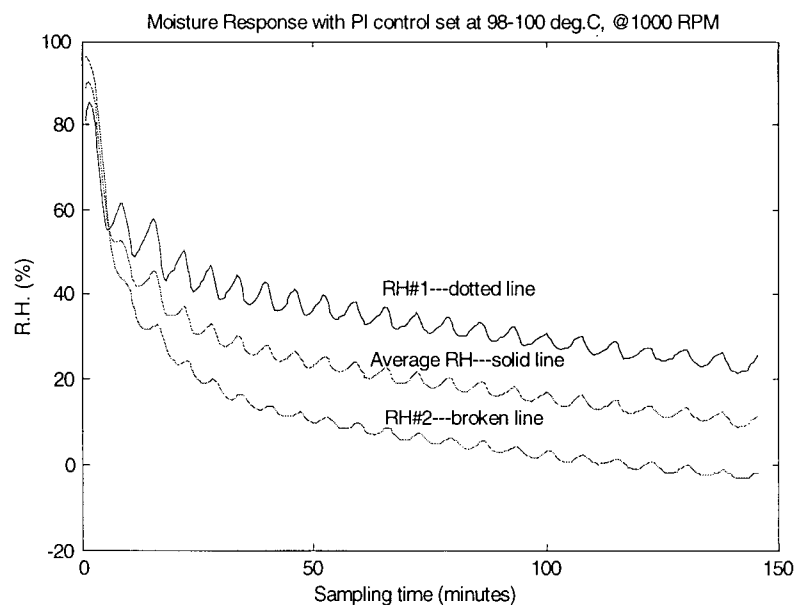
Figure 3-26   Relative humidity curves of experiment #7.

77

Experiment #8 (Same setup as experiment #7 but with a different initial condition)

- Upper temperature limit = 100°C, lower limit = 98°C

- Fan speed = 1000 RPM

- Heater on when temperature drops below the lower temperature setting

- Heater off when temperature exceeds the upper temperature setting

The corresponding curve is shown in Figure 3-27.
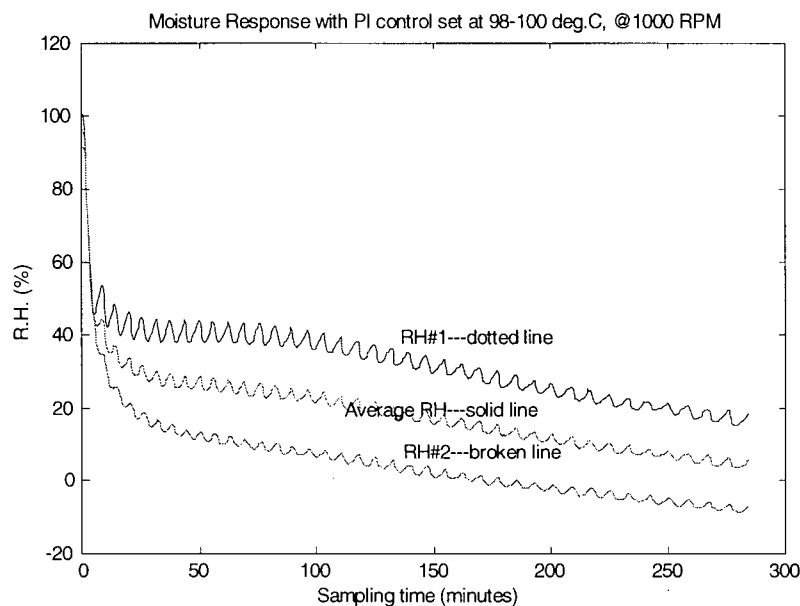
Figure 3-27   Relative humidity curves of experiment #8.

Experiment #9

- Upper temperature limit = 100°C, lower limit = 98°C

- Fan speed = 750 RPM

- Heater on when temperature drops below the lower temperature setting

- Heater off when temperature exceeds the upper temperature setting

The corresponding curve is shown in Figure 3-28.
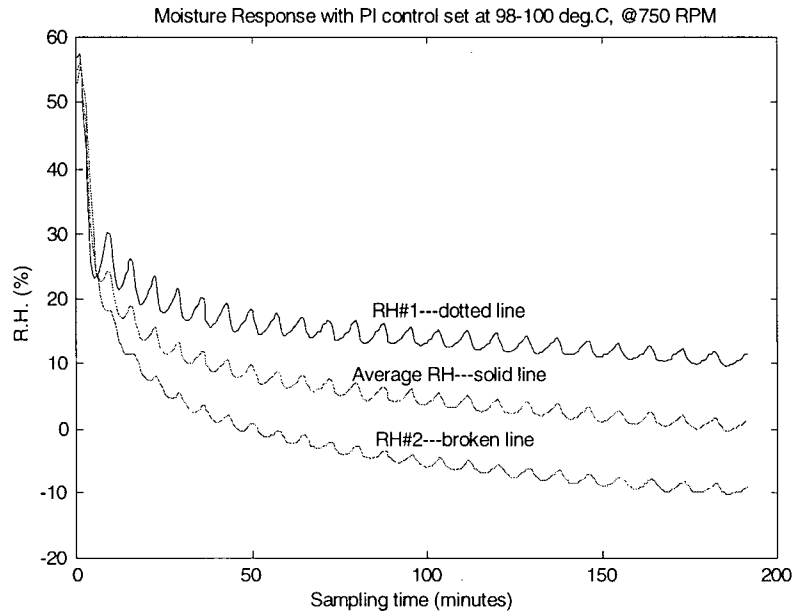
Figure 3-28   Relative humidity curves of experiment #9.

For internal heater control, the temperature curves of experiments 7, 8 and 9 show similar responses. Experiments 7 and 8 are carried out at the same fan speed of 1000 RPM, but with different initial conditions. Their temperature response curves have the same shape. For experiment 9, again the shape of response curve is the same even though the fan speed is changed to 750 RPM. In all cases, the temperature response curve rises when the heater is on, and drops with a time delay when the heater is off. The curves are exactly the same as those given in section 3.3.1.1, but it just repeats itself as the heater is switched on and off. The moisture content curves in experiments 7, 8 and 9 have the same distribution as in Section 3.3.1.2, but with a repetition of the curve due to the subsequent heater on and off actions of the PI controller. The moisture content of the wood pieces drops when the heater is on, and begins to increase when the heater is turned off. The relative humidity drops again when the heater is turned on, and begins to rise when the heater is turned off. The curves for all these experiments have the same response as those in Section 3.3.1.3, except for the repetition according to the heater on and off sequence.

With the experimental data acquired and presented in this chapter, the model identification can be carried out for the kiln system. The details of this procedure are given next, in Chapter 4.

Chapter 4

SYSTEM IDENTIFICATION

Experimental modeling concerns determination of a suitable model for a process through experimental data. In view of the complexity of the physical processes that take place within a wood drying kiln, analytical modeling is quite difficult. Even if an analytical model is formulated with adequate detail, its use in control will be questionable in view of the associated complexity. Consequently, it is undertaken here to develop an experimental model for the kiln. The steps include determination of a model structure, estimation of the model parameters using experimental data, and finally validation of the model. These steps collectively are termed model identification. This chapter presents a model identification for the wood drying kiln. The kiln process is considered as a black box and the input/output data collected as in Chapter 3, which contain the dynamic information of the system is used for system identification. The parameters are estimated for different model orders. In model validation, the model outputs are compared with the real experimental outputs for the same inputs. The dynamic model is assumed to be a set of single-input-single-output (SISO) processes with no time delay, and accordingly the outputs are assumed to be uncoupled.

4.1 Introduction

On-line determination of process parameters is an essential part of performing system identification. The key steps of system identification are:

1. Selection of the model structure (system order)
2. On-line data acquisition procedure or experiment design
3. Parameter estimation
4. Validation of the model.

System (model) identification is performed using input and output (external) measurements. A white noise input signal (in the form of a pulse-width-modulated or PWM signal) is applied to the kiln so that all the dynamic modes of the system are excited. By making use of the collected input/output (I/O) data, which contain the dynamic information for controlling the system, appropriate input/output models for various processes of the kiln system are established. The associated model parameters are estimated so that they will represent the best fit to the data, in the sense of least squared error.

The general system equation is written in the form of an auto regression moving average (ARMA) model as

$$y(k)+a_1y(k-1)+\ldots+a_ny(k-n)=b_1u(k-1)+b_2u(k-2)+\ldots+b_mu(k-m)+e(k) \tag{4.1}$$

where u is the system input, y is the system output, e is the measurement noise, and $n \geq m$ for any order (n) of the system. Equation (4.1) can be rewritten in the z-domain as

$$\frac{Y(z)}{U(z)} = \frac{b_1 z^{-1} + b_2 z^{-2} + \ldots + b_m z^{-m}}{1 + a_1 z^{-1} + \ldots + a_n z^{-n}} \tag{4.2}$$

For a second order ARMA model, the system equation is given by

$$y(k)+a_1y(k-1)+a_2y(k-2)=b_1u(k-1)+b_2u(k-2)+e(k) \tag{4.3}$$

where the output $y(k)$ may represent the average temperature reading, the average moisture content reading, or the average relative humidity reading; while the input $u(k)$ represents the heater input in Section 4.2.1, and it further represents the heater input for the first sub-system or the average temperature input for the second sub-system in Section 4.4; and $e(k)$ is the estimation error. Equation (4.3) is rewritten in the z-domain as (with $e(k) = 0$)

$$Y(z)+a_1z^{-1}Y(z)+a_2z^{-2}Y(z)=b_1z^{-1}U(z)+b_2z^{-2}U(z) \tag{4.4}$$

82

which corresponds to the z-domain transfer function

$$Y(z) = \frac{b_1 z^{-1} + b_2 z^{-2}}{1 + a_1 z^{-1} + a_2 z^{-2}} U(z) \tag{4.5}$$

giving the realization

$$Y(z) = \frac{B(z)}{A(z)} U(z) \tag{4.6}$$

where the numerator polynomial $B(z) = b_1 z + b_2$

and the denominator polynomial $A(z) = z^2 + a_1 z + a_2$

Now define the states x_1 and x_2 such that

$$\begin{aligned} x_1(k) &= f(k) \\ x_2(k) &= f(k+1) \end{aligned} \tag{4.7}$$

where $f(k)$ is defined according to

$$F(z) = \frac{U(z)}{A(z)} \tag{4.8}$$

Consequently, we have

$$U(z) = F(z)A(z) = F(z)[\, z^2 + a_1 z + a_2 \,] \tag{4.9}$$

or,

$$\begin{aligned} u(k) &= f(k+2) + a_1 f(k+1) + a_2 f(k) \\ u(k) &= x_2(k+1) + a_1 x_2(k) + a_2 x_1(k) \end{aligned} \tag{i}$$

and

$$Y(z) = F(z)B(z) = F(z)[b_1 z + b_2] \tag{4.10}$$

or, $$y(k) = b_1 f(k+1) + b_2 f(k) \tag{ii}$$

Rearrange (i):

$$x_2(k+1) = -a_2 x_1(k) - a_1 x_2(k) + u(k) \tag{4.11}$$

From (ii):

$$y(k)=b_1x_2(k)+b_2x_1(k) \tag{4.12}$$

In the matrix form then, the state space model is given in the controllable canonical form as

$$\begin{bmatrix} x_1(k+1) \\ x_2(k+1) \end{bmatrix} = \begin{bmatrix} 0 & 1 \\ -a_2 & -a_1 \end{bmatrix}\begin{bmatrix} x_1(k) \\ x_2(k) \end{bmatrix} + \begin{bmatrix} 0 \\ 1 \end{bmatrix}u(k)$$

$$y(k) = \begin{bmatrix} b_2 & b_1 \end{bmatrix}\begin{bmatrix} x_1(k) \\ x_2(k) \end{bmatrix} \tag{4.13}$$

Assume that N measurements are taken, and with $N=n+m$. Equation (4.1) is rewritten as

$$y(k)= -a_1y(k-1)-\ldots-a_ny(k-n)+b_1u(k-1)+b_2u(k-2)+\ldots+b_mu(k-m)+e(k) \tag{4.14}$$

Rearrange (4.14):

$$y(k) = [-y(k-1)\cdots -y(k-n) \quad u(k-1)\cdots u(k-m)]\begin{bmatrix} a_1 \\ \vdots \\ a_n \\ b_1 \\ \vdots \\ b_m \end{bmatrix} + e(k) \tag{4.15}$$

Equation (4.15) can be presented in a general form

$$y(k) = \phi_k\theta + e(k) \tag{4.16}$$

where ϕ_k is a row vector of $1{\times}N$, θ is a column vector of $N{\times}1$. The basic least squares estimator is given as

$$Y(N) = \Phi_N\theta + e(N) \tag{4.17}$$

in which $Y(N)$ is a column vector of $N{\times}1$, Φ_N is a square matrix of $N{\times}N$, and $e(N)$ is a column vector of $N{\times}1$, as given below:

$$y(N) = \begin{bmatrix} y(1) \\ y(2) \\ \vdots \\ y(k) \\ \vdots \\ y(N) \end{bmatrix} \; ; \quad \Phi_N = \begin{bmatrix} \phi_1 \\ \phi_2 \\ \vdots \\ \phi_k \\ \vdots \\ \phi_N \end{bmatrix} \; ; \quad e(N) = \begin{bmatrix} e(0) \\ e(1) \\ \vdots \\ e(k) \\ \vdots \\ e(N-1) \end{bmatrix} \qquad (4.18)$$

Thus, the recursive least squares estimator for N measurements (with $e(N)=0$) is given as

$$\hat{\theta}(N) = \hat{\theta}(N-1) + K_N[y(N) - \hat{y}(N)] \qquad (4.19)$$

where $\hat{\theta}(N)$ is the estimate of θ based on N measurements

$\hat{\theta}(N-1)$ is the estimate of θ based on N-1 measurements

K_N is the *Gain* matrix of $N{\times}1$, P_N is the computational square matrix of $N{\times}N$, $y(N)$ is the actual system output, and $\hat{y}(N)$ is the system output estimate based on N measurements, and is computed by the following equations:

$$\hat{y}(N) = \phi_N \hat{\theta}(N-1)$$
$$K_N = P_{N-1}\phi_N^T (I + \phi_N P_N \phi_N^T)^{-1}$$
$$P_N = (I - K_N \phi_N)P_{N-1}$$

with the following initial conditions:

1. $\hat{\theta}(0) = 0$
2. $P_0 = \alpha I$

where the parameter α is very large, reflecting very low confidence in the initial estimate. Equation (4.19) which provides parameter estimate updating has the clear physical interpretation of

[*new parameter estimate*] = [*old parameter estimate*] + *gain * estimation error*

For the sub-system models, ϕ is defined as

$$\phi_k = [-y(k\text{-}1) \quad -y(k\text{-}2) \quad u(k\text{-}1) \quad u(k\text{-}2)]$$

By implementing this algorithm in MATLAB, the parameters of the system models are estimated using real time input/output kiln data.

4.2 Parameter Estimation

In this section, the parameter estimation of the single input single output (SISO) models for the temperature, moisture content and relative humidity are presented. In section 4.2.1, control signal to turn on or off the heater is generated by the PC. Parameters are estimated to fit the relationship between the heater input signal and each output variable. In section 4.2.2, the control signal to switch on or off the heater is not provided by the P.C., and instead generated by the internal PI controller of the heater. Parameters estimated in this section are used to establish a system order that can reasonably represent the process.

4.2.1   External computer input control

In the acquisition of data for this section, the input control signal for switching on or off the heater is generated by the PC. The output response is then collected for parameter estimation. The following subsections will present the parameter estimation results for a particular system order of a model, assumed to be single-input-single-output, which generates the temperature model, moisture content model and the relative humidity model.

4.2.1.1 Second order, SISO temperature model

Model identification results for the temperature response are presented now. The model structure is a second order single-input-single-output (SISO) one. The model input is the

control signal for switching on and off the heater. Estimated parameter values are given below.

Experiment #1

- Fan speed = 500 RPM, Heater kept on for 8 minutes
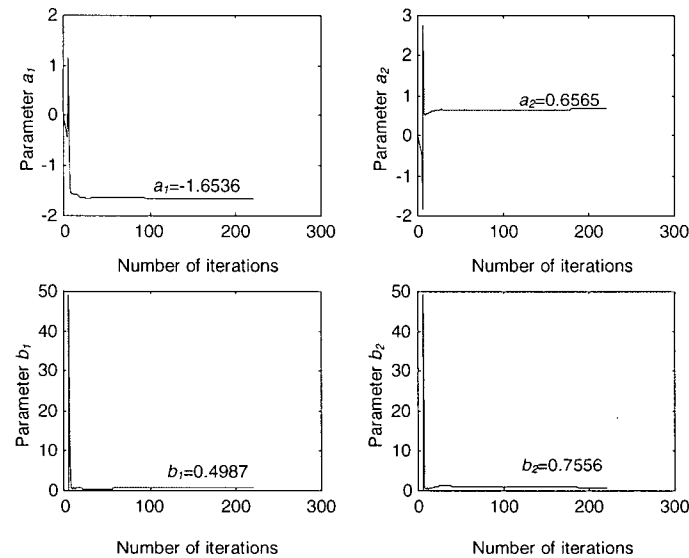
Figure 4-1   Parameter estimation in experiment #1 (500 RPM with heater ON for 8 minutes).

Experiment #2

- Fan speed = 500 RPM, Heater kept on for 4 minutes
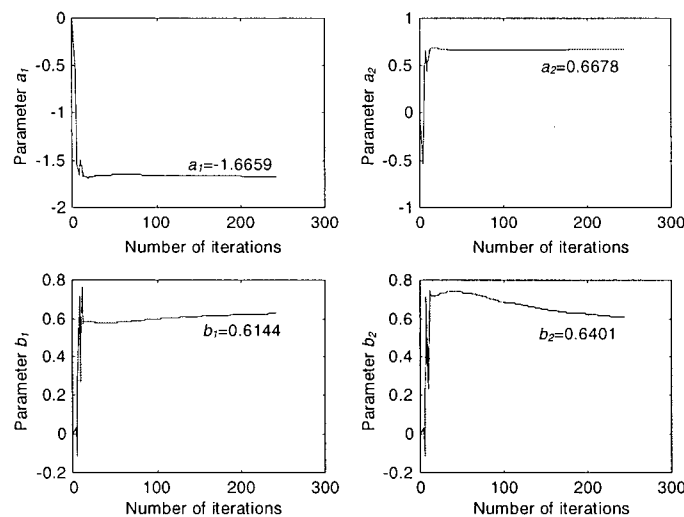
Figure 4-2   Parameter estimation in experiment #2 (500 RPM with heater ON for 4 minutes).

Experiment #3

- Fan speed = 750 RPM, Heater kept on for 8 minutes
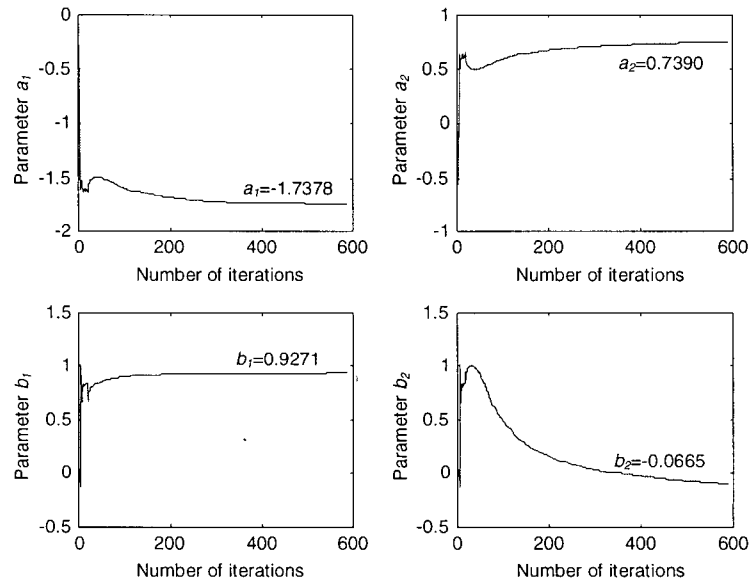
Figure 4-3   Parameter estimation in experiment #3 (750 RPM with heater ON for 8 minutes).

Experiment #4

- Fan speed = 750 RPM, Heater kept on for 4 minutes
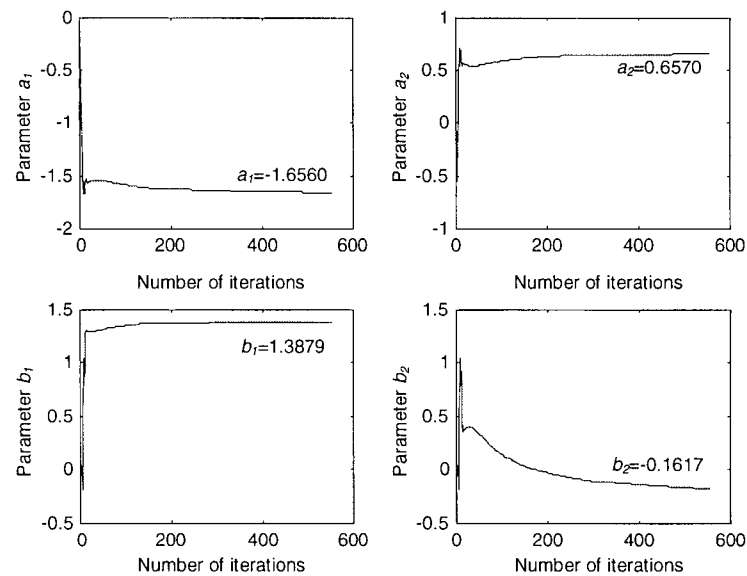
Figure 4-4   Parameter estimation in experiment #4 (750 RPM with heater ON for 4 minutes).

Experiment #5 (data file pretest_1kw.txt)

- Fan speed = 1000 RPM, Heater kept on for 8 minutes
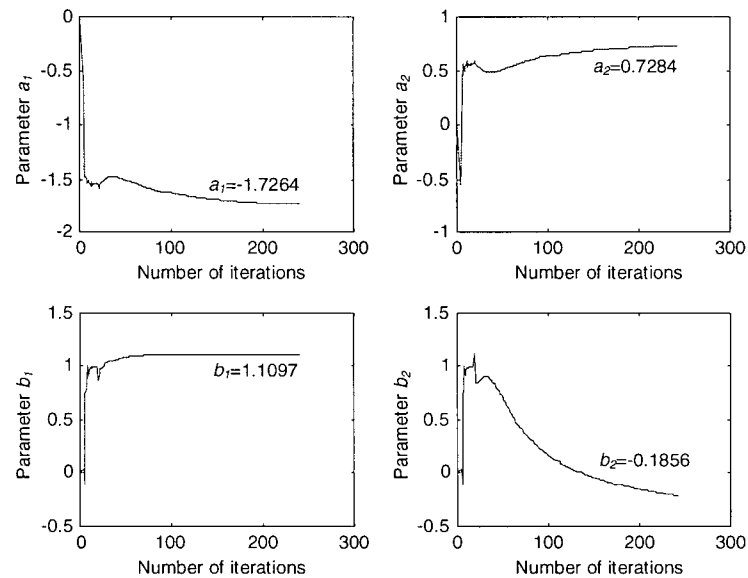
Figure 4-5   Parameter estimation in experiment #5 (1000 RPM with heater ON for 8 minutes).

Experiment #6

- Fan speed = 1000 RPM, Heater kept on for 4 minutes
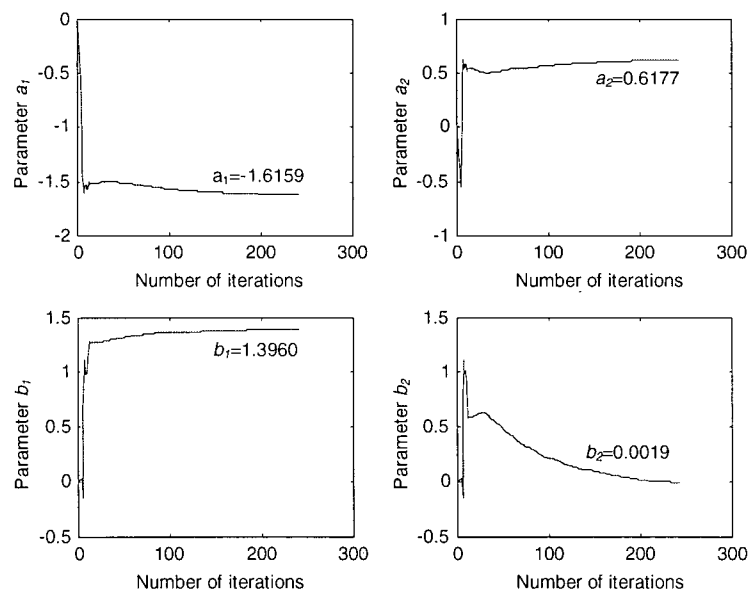
Figure 4-6   Parameter estimation in experiment #6 (1000 RPM with heater ON for 4 minutes).

The parameter estimation results for the second order SISO temperature model are summarized in Table 4-1.

Table 4-1   Estimated parameters of the second order SISO temperature model.

Test Conditions	Estimated Parameters			
	a_1	a_2	b_1	b_2
500 RPM, heater ON 8 minutes	-1.6536	0.6565	0.4987	0.7556
500 RPM, heater ON 4 minutes	-1.6659	0.6678	0.6144	0.6401
750 RPM, heater ON 8 minutes	-1.7378	0.7390	0.9271	-0.0665
750 RPM, heater ON 4 minutes	-1.6560	0.6570	1.3879	-0.1617
1000 RPM, heater ON 8 minutes	-1.7264	0.7284	1.1097	-0.1856
1000 RPM, heater ON 4 minutes	-1.6159	0.6177	1.3960	0.0019

The estimation results show consistency in parameters a_1 and a_2. However, the parameters b_1 and b_2 do not show consistency. This is primarily due to the differences in initial condition and fan speed. For a fan speed of 500 rpm, the estimated parameters a_1 and a_2 for 8 minute and 4 minute heater inputs are very close to each other. For a fan speed of 750 rpm, the difference between the estimated a parameters tends to widen, for the two cases of heat input. The deviation worsens for the fan speed of 1000 rpm.

In conclusion, the level of nonlinearity seems to be low at lower fan speeds; for example, 500 rpm. Deviations in the estimated parameter values for both 8 minute and 4 minute heater inputs become larger at higher fan speed. This means the process nonlinearity is high with respect to the fan speed, but it is not as severe with respect to the heater input.

4.2.1.2 SISO moisture content model

In this section, second, third and fourth order moisture content models are used for parameter estimation and to investigate the convergence of the estimated parameters.

4.2.1.2.1 Second order moisture content model

Model identification results for the moisture content response are presented here. The model structure is a second order SISO one. The model input is the control signal for switching on and off the heater, and estimated parameter values are given below.

Experiment #1 (data file pretest_500w.txt)

- Fan speed = 500 RPM, Heater kept on for 8 minutes
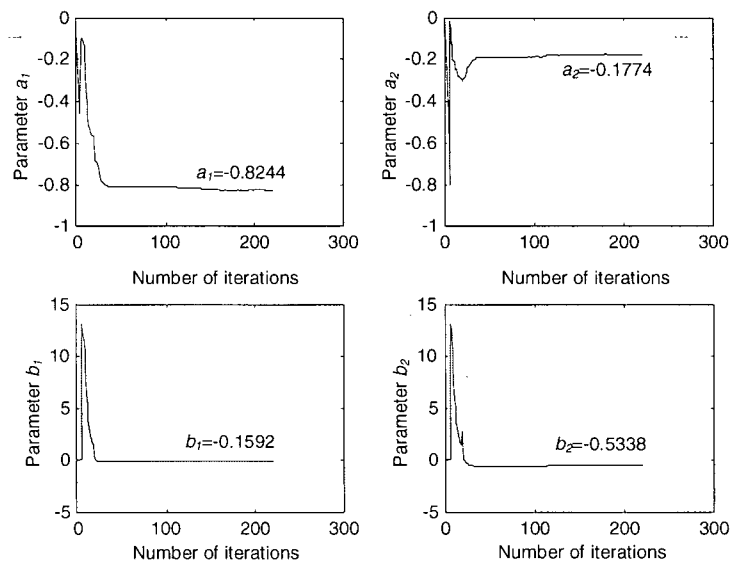
Figure 4-7   Parameter estimation in experiment #1 (500 RPM with heater ON for 8 minutes).

Experiment #2 (data file exp5.txt)

- Fan speed = 500 RPM, Heater kept on for 4 minutes
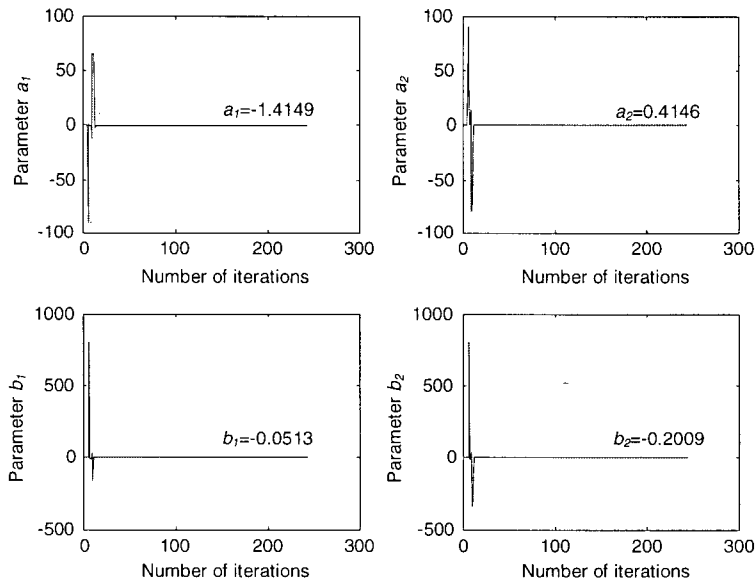
Figure 4-8   Parameter estimation in experiment #2 (500 RPM with heater ON for 4 minutes).

Experiment #3 (data file pretest_750w.txt)

- Fan speed = 750 RPM, Heater kept on for 8 minutes
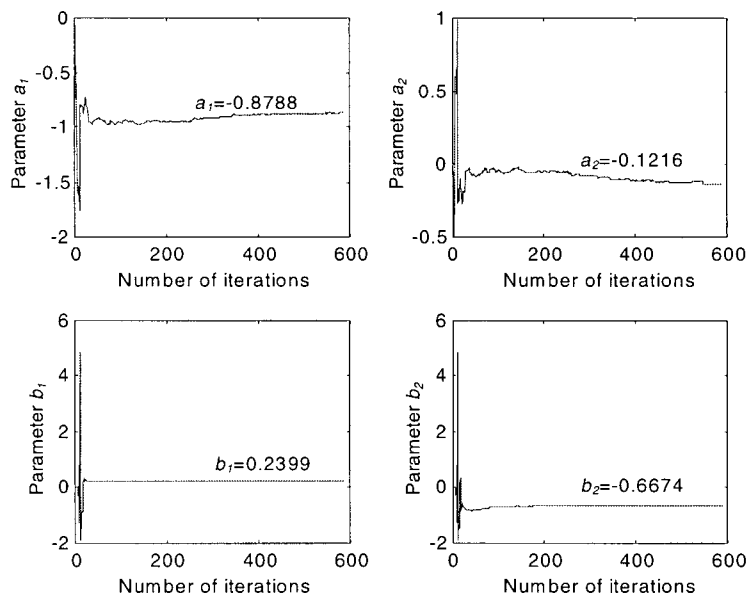
Figure 4-9   Parameter estimation in experiment #3 (750 RPM with heater ON for 8 minutes).

Experiment #4 (data file exp7.txt)

- Fan speed = 750 RPM, Heater kept on for 4 minutes
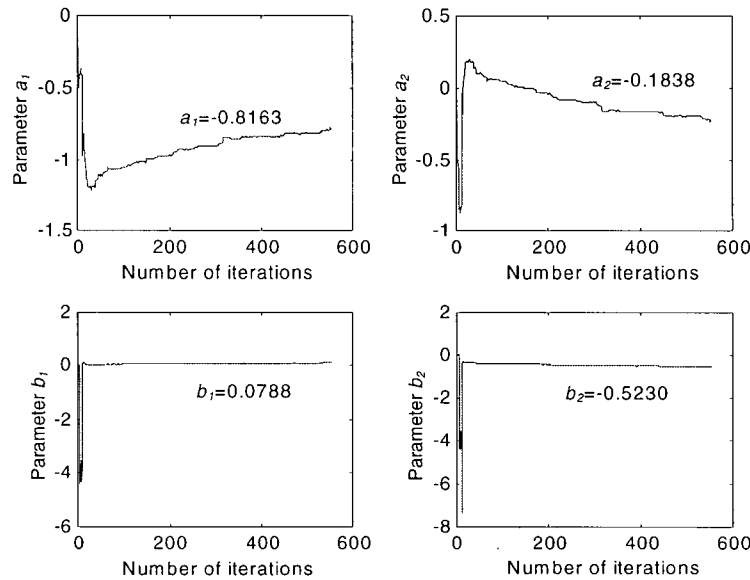
Figure 4-10   Parameter estimation in experiment #4 (750 RPM with heater ON for 4 minutes).

Experiment #5 (data file pretest_1kw.txt)

- Fan speed = 1000 RPM, Heater kept on for 8 minutes
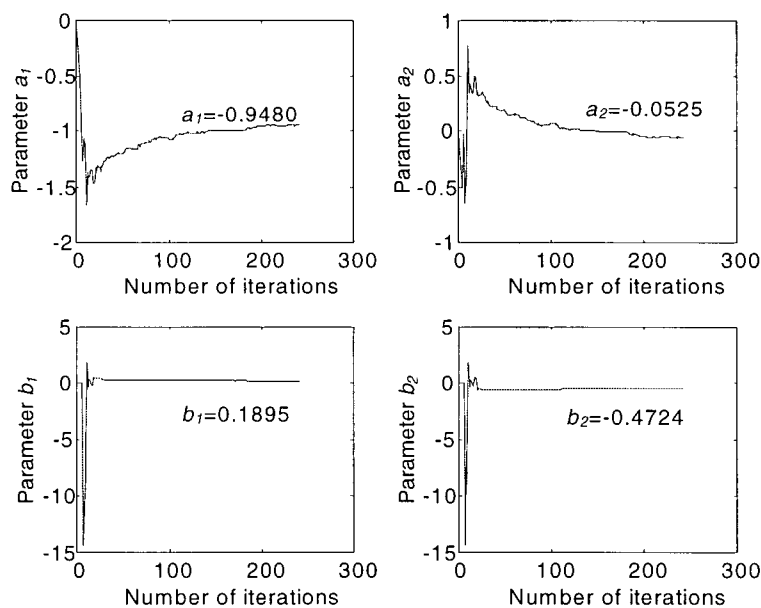
Figure 4-11   Parameter estimation in experiment #5 (1000 RPM with heater ON for 8 minutes).

<u>Experiment #6 (data file exp9.txt)</u>

- Fan speed = 1000 RPM, Heater kept on for 4 minutes
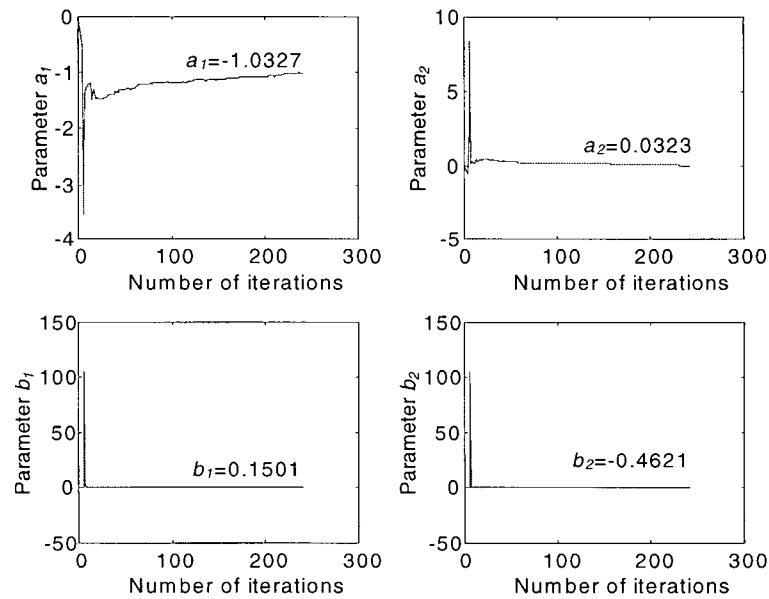
Figure 4-12   Parameter estimation in experiment #6 (1000 RPM with heater ON for 4 minutes).

The parameter estimation results for the second order SISO moisture content model are summarized in Table 4-2.

Table 4-2   Estimated parameters of the second order SISO moisture content model.

Test Conditions	Estimated Parameters			
	a_1	a_2	b_1	b_2
500 RPM, heater ON 8 minutes	-0.8244	-0.1774	-0.1592	-0.5338
500 RPM, heater ON 4 minutes	-1.4149	0.4146	-0.0513	-0.2009
750 RPM, heater ON 8 minutes	-0.8788	-0.1216	0.2399	-0.6674
750 RPM, heater ON 4 minutes	-0.8163	-0.1838	0.0788	-0.5230
1000 RPM, heater ON 8 minutes	-0.9480	-0.0525	0.1895	-0.4724
1000 RPM, heater ON 4 minutes	-1.0327	0.0323	0.1501	-0.4621

For the moisture content model, the estimated results do not show consistency in both parameters a and b. This may be due to reasons such as process nonlinearity, inadequate

94

model order and coupling effects of the process variables. The estimated parameter a_1 appears to be most consistent, while the estimated parameter a_2 exhibits significant variation and even change of sign. This is not a satisfactory outcome. Next, a higher order (third order) SISO model is used for the moisture content model to estimate the model parameters.

4.2.1.2.2   Third order moisture content model

Model identification results for the moisture content response of a third order SISO model are presented now. The model input is again the control signal for switching on and off the heater. Estimated parameter values are given below.

Experiment #1 (data file pretest_500w.txt)

- Fan speed = 500 RPM, Heater kept on for 8 minutes

Figure 4-13   Parameter estimation in experiment #1 (500 RPM with heater ON for 8 minutes).

Experiment #2 (data file exp5.txt)

- Fan speed = 500 RPM, Heater kept on for 4 minutes

Figure 4-14   Parameter estimation in experiment #2 (500 RPM with heater ON for 4 minutes).

Experiment #3 (data file pretest_750w.txt)

- Fan speed = 750 RPM, Heater kept on for 8 minutes
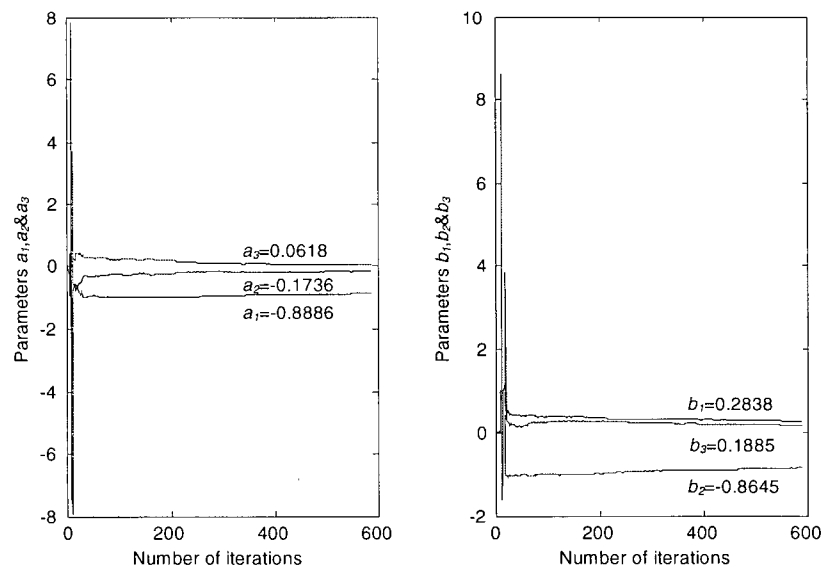
Figure 4-15   Parameter estimation in experiment #3 (750 RPM with heater ON for 8 minutes).

Experiment #4 (data file exp7.txt)

- Fan speed = 750 RPM, Heater kept on for 4 minutes

Figure 4-16   Parameter estimation in experiment #4 (750 RPM with heater ON for 4 minutes).

Experiment #5 (data file pretest_1kw.txt)

- Fan speed = 1000 RPM, Heater kept on for 8 minutes

Figure 4-17   Parameter estimation in experiment #5 (1000 RPM with heater ON for 8 minutes).

Experiment #6 (data file exp9.txt)

- Fan speed = 1000 RPM, Heater kept on for 4 minutes

Figure 4-18   Parameter estimation in experiment #6 (1000 RPM with heater ON for 4 minutes).

The parameter estimation results for the third order SISO moisture content model are summarized in Table 4-3.

Table 4-3   Parameter estimation results of the third order SISO moisture content model.

Test Conditions	a_1	a_2	a_3	b_1	b_2	b_3
500 RPM, ON 8 minutes	-0.9788	0.0322	-0.0551	-0.0019	-0.1972	-0.2923
500 RPM, ON 4 minutes	-1.0555	-0.2860	0.3411	-0.0180	0.1233	-0.3835
750 RPM, ON 8 minutes	-0.8886	-0.1736	0.0618	0.2838	-0.8645	0.1885
750 RPM, ON 4 minutes	-0.7682	-0.1651	-0.0668	0.0795	-0.3632	-0.2153
1000 RPM, ON 8 minutes	-1.8670	-0.1174	0.9846	1.3837	-0.4126	0.1205
1000 RPM, ON 4 minutes	-0.9130	0.0631	-0.1506	0.1185	-0.0544	-0.4857

For parameter estimation of the moisture content model, it is noticed again that there is no consistency in the results for both parameters a and b even though the system order

98

has been increased to three. By comparing the estimated parameters for the second and the third order SISO moisture content models, it can be concluded that the second order model is better than the third order model. Also, a significant nonlinearity is observed with respect to the fan speed than for the heating input, in both cases.

In conclusion, the nonlinearity in the moisture content model is higher in general, than in the temperature model. For the second order moisture model, there is a sign change in a_2 for the first and last pair of experiments (fan speeds of 500 and 1000 rpm). For the third order moisture model, there is a sign change in both parameters a_2 and a_3. This could be attributed to model error, experimental error, or computational error. In view of this, the first and the last pair of experiments are repeated to further investigate the sign change of a_2.

4.2.1.2.3 Repeated experiments

Eight experiments are conducted in this section for checking the sign change in the model parameters at fan speeds of 500 rpm and 1000 rpm. Four experiments are repeated for checking the sign changes in the second order moisture content model, while the remaining four experiments are repeated for investigating the sign changes in the third order moisture content model. First consider the second order model. The results are given below.

Repeated experiments for the second order moisture content model

The data file used for the repeated experiments #1 to #4 are summarized in Table 4-4.

Table 4-4   Data files of the repeated experiments for the second order moisture content model.

Experiment Number	Data file	Fan speed (RPM) / Heater duration (mins)
Repeated experiment #1	redo_500w.txt	500 / 8
Repeated experiment #2	redo_exp5.txt	500 / 4
Repeated experiment #3	redo_1kw.txt	1000 / 8
Repeated experiment #4	redo_exp9.txt	1000 / 4

Repeated Experiment #1 for 2nd Order Moisture Content Model (data file redo_500w.txt)

- Initial moisture content is below 18%, average m.c. is around 15%

- Fan speed = 500 RPM, Heater kept on for 8 minutes
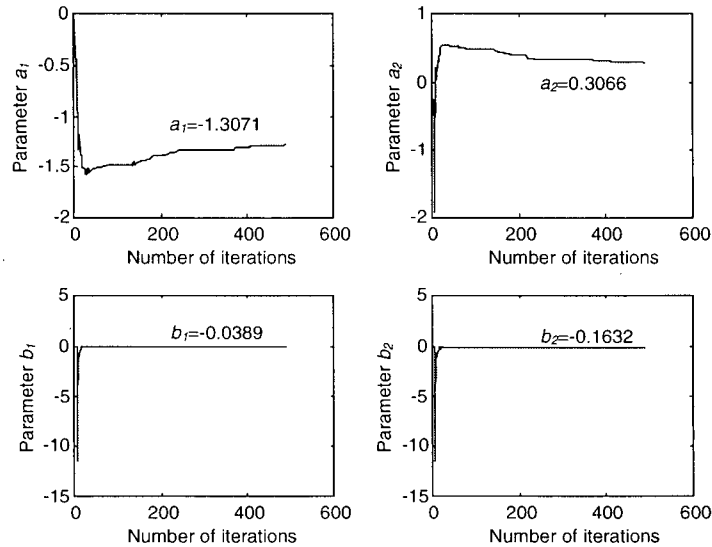
Figure 4-19   Parameter estimation in repeated experiment #1 (500 RPM with heater ON for 8 minutes).

Repeated Experiment #2 for 2nd Order Moisture Content Model (data file redo_exp5.txt)

- Initial moisture content condition is almost the same as in experiment #1

- Fan speed = 500 RPM, Heater kept on for 4 minutes
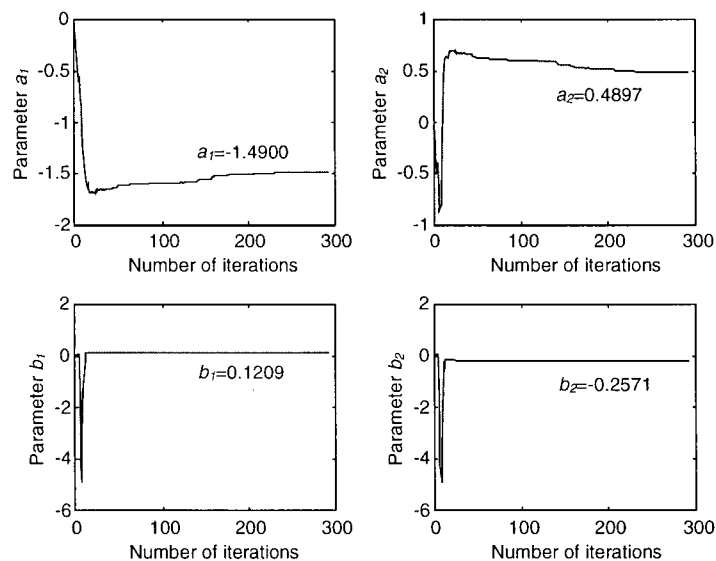
Figure 4-20   Parameter estimation in repeated experiment #2 (500 RPM with heater ON for 4 minutes).

Repeated Experiment #3 for 2nd Order Moisture Content Model (data file redo_1kw.txt)

- Initial moisture content condition is below 16%, average m.c. is around 13%

- Fan speed = 1000 RPM, Heater kept on for 8 minutes
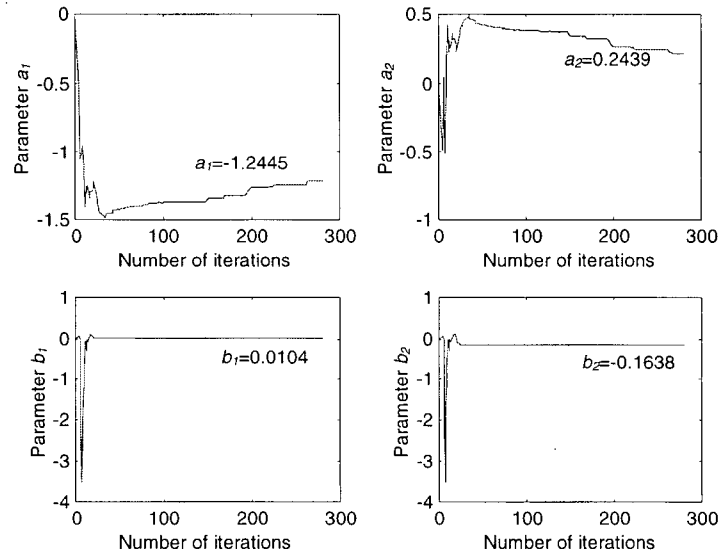
Figure 4-21   Parameter estimation in repeated experiment #3 (1000 RPM with heater ON for 8 minutes).

Repeated Experiment #4 for 2nd Order Moisture Content Model (data file redo_exp9.txt)

- Initial moisture content condition is below 15%, average m.c. is around 12.5%

- Fan speed = 1000 RPM, Heater kept on for 4 minutes
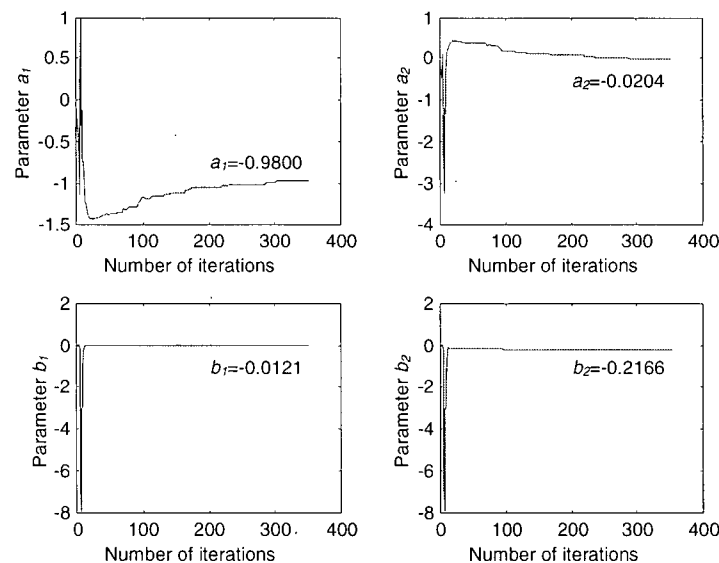
Figure 4-22   Parameter estimation in repeated experiment #4 (1000 RPM with heater ON for 4 minutes).

Parameters estimated from the four repeated experiments of the 2nd order SISO moisture content model, as given above, are recorded to further investigate for the sign change in parameter a_2. Results of the previous experiments and the repeated experiments are summarized in Table 4-5.

Table 4-5   Estimated parameters from the two sets of experiments (2nd order model), for moisture content.

Test Conditions (Data file)	Estimated Parameters			
	a_1	a_2	b_1	b_2
500 RPM, ON 8 minutes (data file pretest_500w.txt)	-0.8244	-0.1774	-0.1592	-0.5338
500 RPM, ON 4 minutes (data file exp5.txt)	-1.4149	0.4146	-0.0513	-0.2009
1000 RPM, ON 8 minutes (data file pretest_1kw.txt)	-0.9480	-0.0525	0.1895	-0.4724
1000 RPM, ON 4 minutes (data file exp9.txt)	-1.0327	0.0323	0.1501	-0.4621
500 RPM, ON 8 minutes (data file redo_500w.txt)	-1.3071	0.3066	-0.0389	-0.1632
500 RPM, ON 4 minutes (data file redo_exp5.txt)	-1.4900	0.4897	0.1209	-0.2571
1000 RPM, ON 8 minutes (data file redo_1kw.txt)	-1.2445	0.2439	0.0104	-0.1638
1000 RPM, ON 4 minutes (data file redo_exp9.txt)	-0.9800	-0.0204	-0.0121	-0.2166

As clear from Table 4-5, the estimated values of a_1 in the repeated experiments are found to be more stable and consistent, but as before there exist variations at different fan speed. There is also a sign change in the estimated values of the parameter a_2. In conclusion, the moisture model deviates too much during the drying process. This can be caused by the complex physical changes that take place during the wood drying process including structural changes of wood, and the complexity of fluid dynamics and heat transfer, and also experimental and computational errors.

Next the four experiments are repeated to further investigate the third order model. These four repeated experiments are performed using the same wood species, and almost the same initial moisture content conditions. The moisture content in these repeated experiments is all below 20%, and the average m.c. of the 8 pieces of lumber is around 15%. The results from these repeated experiments for the third order model are given below.

Repeated experiments for estimation of the third order moisture content model

The data file used for the repeated experiments #5 to #8 are summarized in Table 4-6.

Table 4-6   Data files of the repeated experiments for the third order moisture content
                 model.

Experiments Number	Data file	Fan speed (RPM) / Heating duration (mins)
Repeated experiment #5	redo_500w.txt	500 / 8
Repeated experiment #6	redo_exp5.txt	500 / 4
Repeated experiment #7	redo_1kw.txt	1000 / 8
Repeated experiment #8	redo_exp9.txt	1000 / 4

Repeated Experiment #5 for 3rd Order Moisture Content Model (data file redo_500w.txt)

- Initial moisture content is below 18%; Average m.c. is approximately 15%

- Fan speed = 500 RPM, Heater kept on for 8 minutes
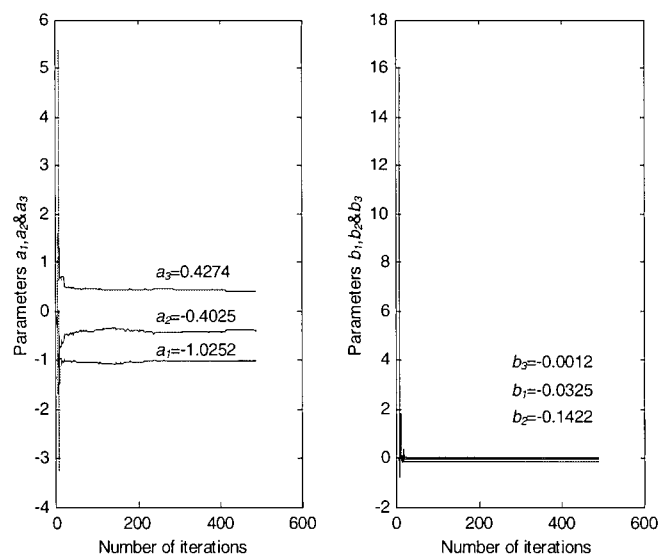
Figure 4-23   Parameter estimation in repeated experiment #5 (500 RPM with heater
                 ON for 8 minutes).

Repeated Experiment #6 for 3rd Order Moisture Content Model (data file redo_exp5.txt)

- Initial moisture content is similar to that in repeated experiment #5

- Fan speed = 500 RPM, Heater kept on for 4 minutes
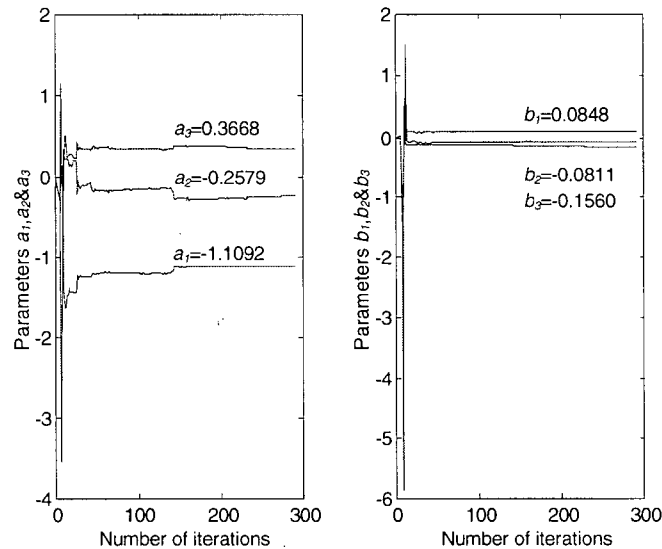
Figure 4-24   Parameter estimation in repeated experiment #6 (500 RPM with heater ON for 4 minutes).

Repeated Experiment #7 for 3rd Order Moisture Content Model (data file redo_1kw.txt)

- Initial moisture content is below 16%; Average m.c. is approximately 13%

- Fan speed = 1000 RPM, Heater kept on for 8 minutes
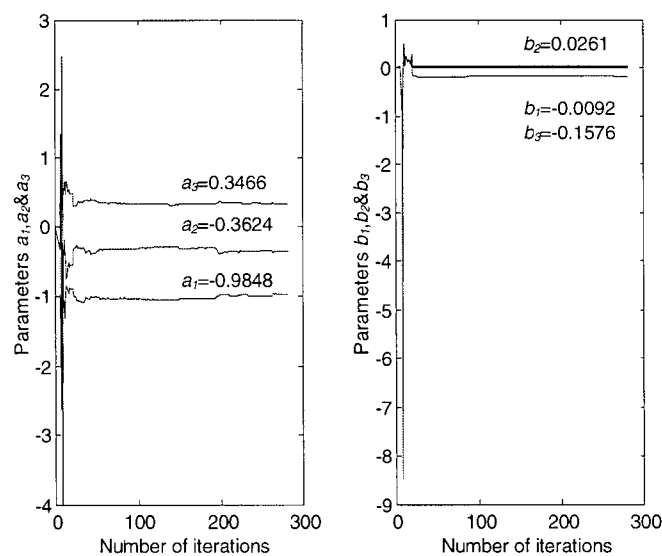
Figure 4-25   Parameter estimation in repeated experiment #7 (1000 RPM with heater ON for 8 minutes).

Repeated Experiment #8 for 3rd Order Moisture Content Model (data file redo_exp9.txt)

- Initial moisture content is below 15%; Average m.c. is approximately 12.5%

- Fan speed = 1000 RPM, Heater kept on for 4 minutes
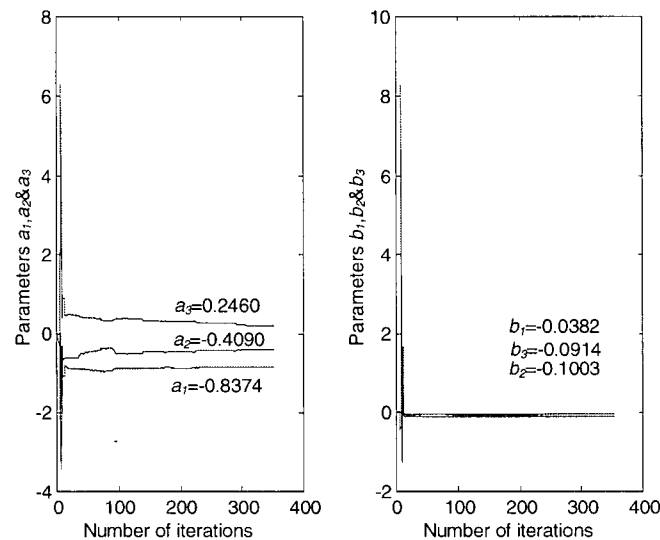
Figure 4-26   Parameter estimation in repeated experiment #8 (1000 RPM with heater ON for 4 minutes).

The estimated parameters for the third order SISO moisture content model for both sets of experiments are summarized in Table 4-7. Parameters estimated for a_1, a_2 and a_3 in the previous experiments do not show consistency in both the value and the sign. In all the previous experiments, different wood pieces are used at different fan speeds, and the average moisture content is approximately 30%. The same wood pieces are used for the four repeated experiments, but the average moisture content is around 15%. Parameters estimated for a_1, a_2 and a_3 in the repeated experiments show consistency in both the value and the sign. This shows that different initial moisture contents in the wood pieces do affect model parameters. Furthermore, the nature of the wood pieces themselves affect model parameters. In particular, even though the same wood specie is used, different wood grain orientations that result from the way the wood is cut would affect the drying process.

Table 4-7 Estimated parameters from the two sets of experiments (3rd order model).

Test Conditions (Data file)	Estimated Parameters					
	a_1	a_2	a_3	b_1	b_2	b_3
500 RPM, ON 8 minutes (data file pretest_500w.txt)	-0.9788	0.0322	-0.0551	-0.0019	-0.1972	-0.2923
500 RPM, ON 4 minutes (data file exp5.txt)	-1.0555	-0.2860	0.3411	-0.0180	0.1233	-0.3835
1000 RPM, ON 8 minutes (data file pretest_1kw.txt)	-1.8670	-0.1174	0.9846	1.3837	-0.4126	0.1205
1000 RPM, ON 4 minutes (data file exp9.txt)	-0.9130	0.0631	-0.1506	0.1185	-0.0544	-0.4857
500 RPM, ON 8 minutes (data file redo_500w.txt)	-1.0252	-0.4025	0.4274	-0.0325	-0.1422	-0.0012
500 RPM, ON 4 minutes (data file redo_exp5.txt)	-1.1092	-0.2579	0.3668	0.0848	-0.0811	-0.1560
1000 RPM, ON 8 minutes (data file redo_1kw.txt)	-0.9848	-0.3624	0.3466	-0.0092	0.0261	-0.1576
1000 RPM, ON 4 minutes (data file redo_exp9.txt)	-0.8374	-0.4090	0.2460	-0.0382	-0.1003	-0.0914

4.2.1.2.4 Fourth order moisture content model

In this section, the moisture content model is further enhanced to fourth order, and examined. Four cases are investigated at a fan speed of 1000 rpm since high fan speeds are known to provide good results in the wood drying process. The data files are summarized in Table 4-8. The results from the parameter estimation procedure are presented next.

Table 4-8 Data files for the fourth order moisture content model.

Experiments Number	Data file	Fan speed (RPM) / Heater duration (mins)
Experiment #5	pretest_1kw.txt	1000 / 8
Experiment #6	exp9.txt	1000 / 4
Repeated experiment #3	redo_1kw.txt	1000 / 8
Repeated experiment #4	redo_exp9.txt	1000 / 4

Experiment #5

Data file: pretest_1kw.txt; Heater kept on for 8 minutes; Fan speed = 1000 RPM
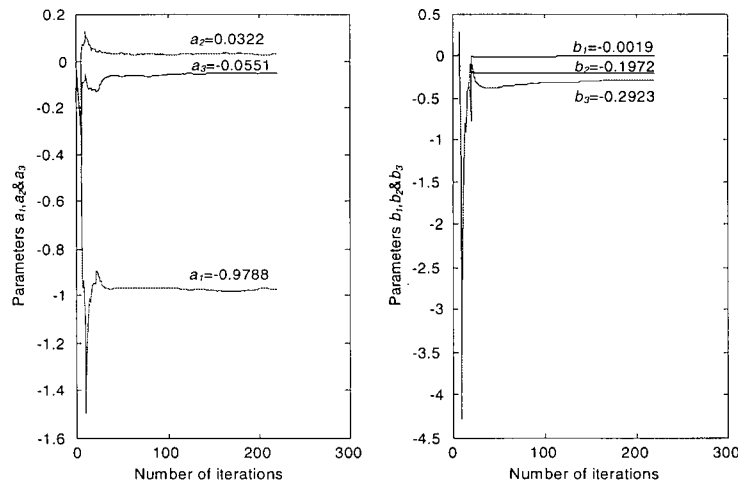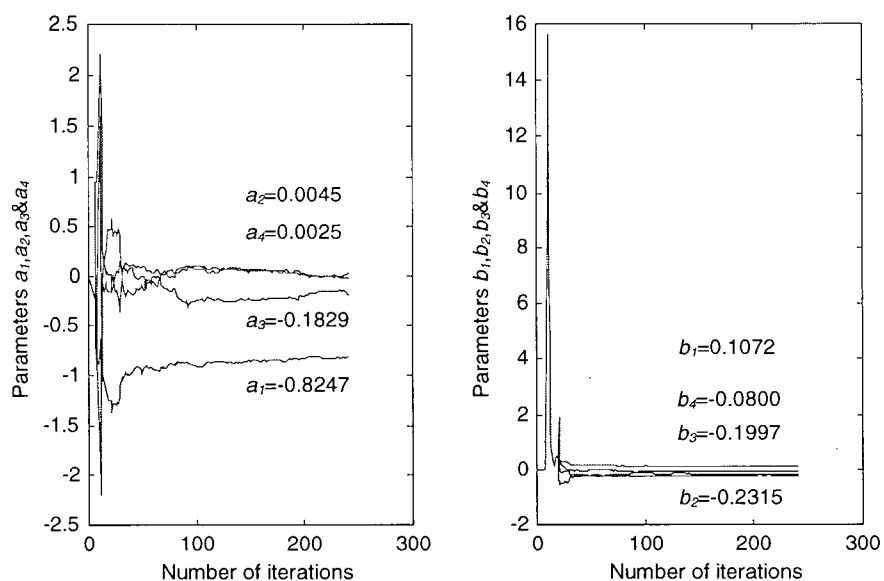

Figure 4-27   Parameter estimation in experiment #5 (1000 RPM with heater ON for 8 minutes).

Experiment #6

Data file: exp9.txt; Heater kept on for 4 minutes; Fan speed = 1000 RPM
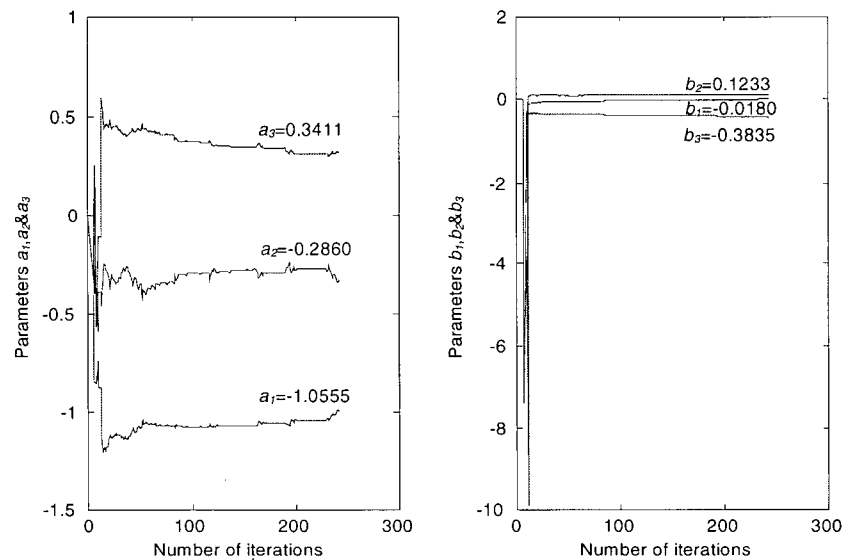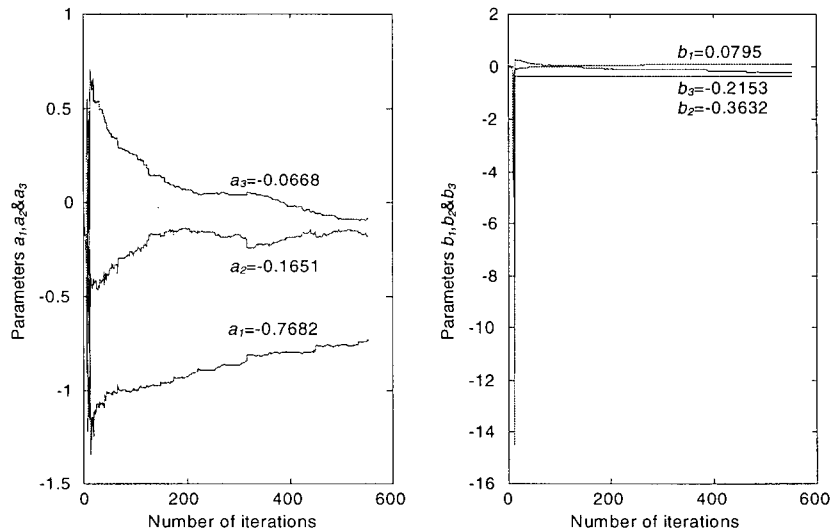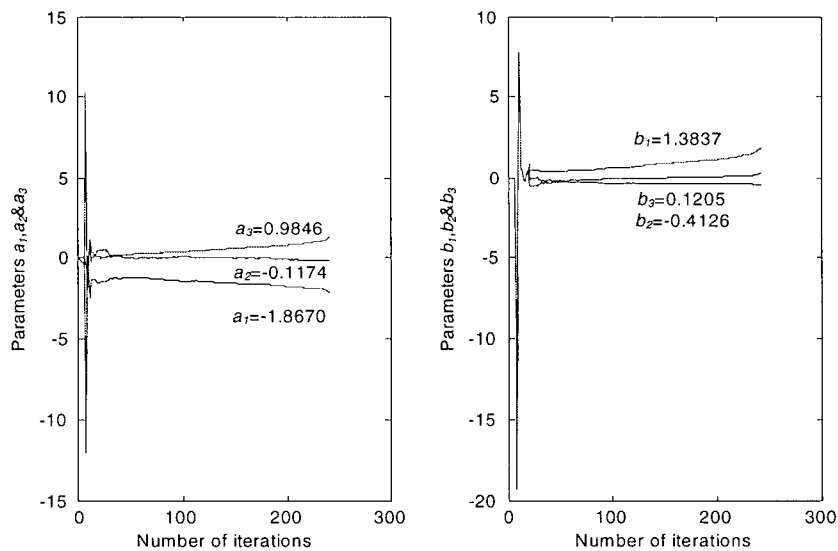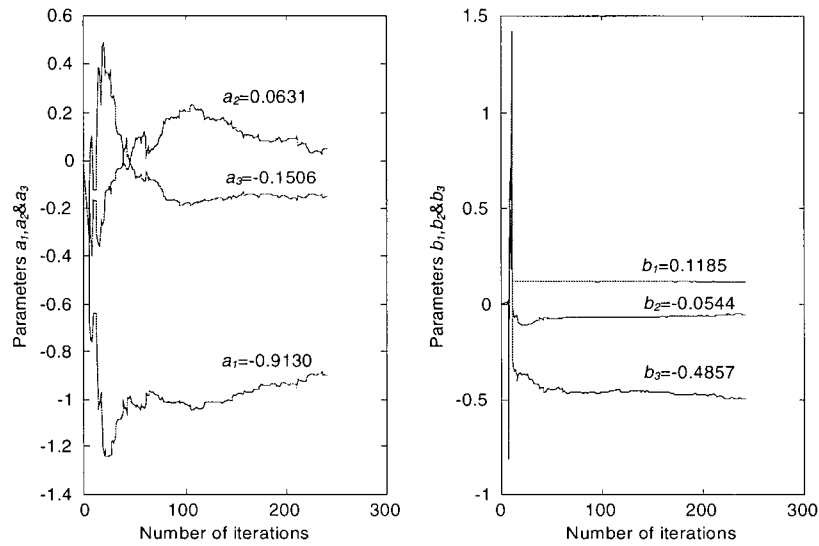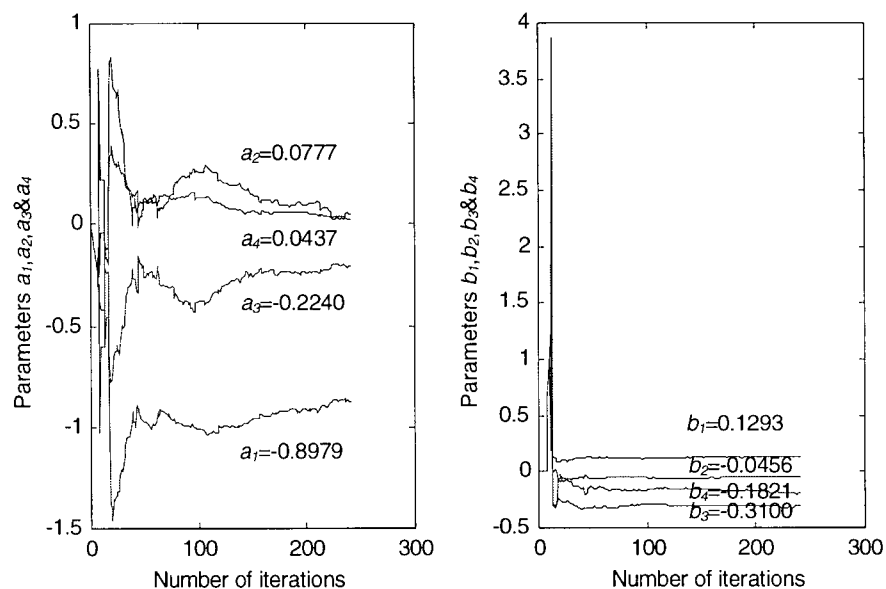

Figure 4-28   Parameter estimation in experiment #6 (1000 RPM with heater ON for 4 minutes).

Repeated Experiment #3

Data file: redo_1kw.txt; Heater kept on for 8 minutes; Fan speed = 1000 RPM
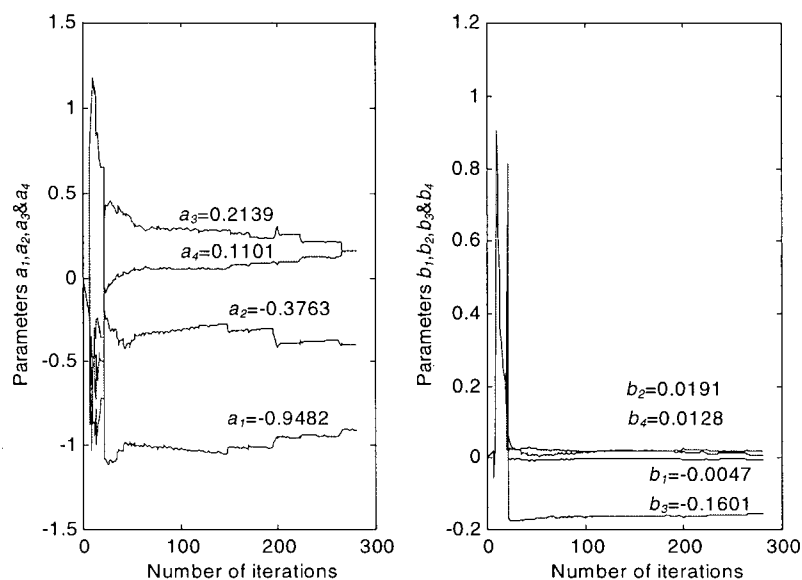
Figure 4-29   Parameter estimation in repeated experiment #3 (1000 RPM with heater ON for 8 minutes).

Repeated Experiment #4

Data file: redo_exp9.txt; Heater kept on for 4 minutes; Fan speed = 1000 RPM
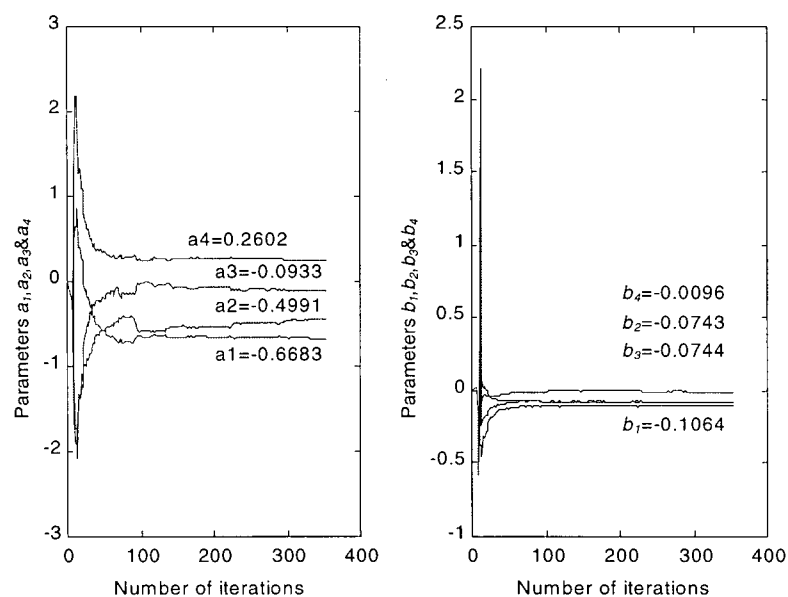
Figure 4-30   Parameter estimation in repeated experiment #4 (1000 RPM with heater ON for 4 minutes).

The parameter estimation results from the 4 experiments performed at a fan speed of 1000 RPM are presented in Table 4-9.

Table 4-9   Parameter estimation results for the fourth order SISO moisture content model.

Experiment	Estimated Parameters							
	a_1	a_2	a_3	a_4	b_1	b_2	b_3	b_4
Experiment #5	-0.8247	0.0045	-0.1829	0.0025	0.1072	-0.2315	-0.1997	-0.0800
Experiment #6	-0.8979	0.0777	-0.2240	0.0437	0.1293	-0.0456	-0.3100	-0.1821
Repeated Experiment #3	-0.9482	-0.3763	0.2139	0.1101	-0.0047	0.0191	-0.1601	0.0128
Repeated Experiment #4	-0.6683	-0.4991	-0.0933	0.2602	-0.1064	-0.0743	-0.0744	-0.0096

The results again do not show consistency in both value and sign. Estimated values of a and b do not converge. This indicates that the moisture content model is nonlinear, and a higher model order may not improve the results. What particular model structure is appropriate will be considered under model validation.

4.2.1.3 Second order, SISO relative humidity model

Now, the model identification results for the relative humidity response is given. A second order single-input-single-output (SISO) model structure is used. The model input is the control signal for switching on and off the heater. The estimated parameters are given below.

Experiment #1 (data file pretest_500w.txt)

- Fan speed = 500 RPM; Heater kept on for 8 minutes
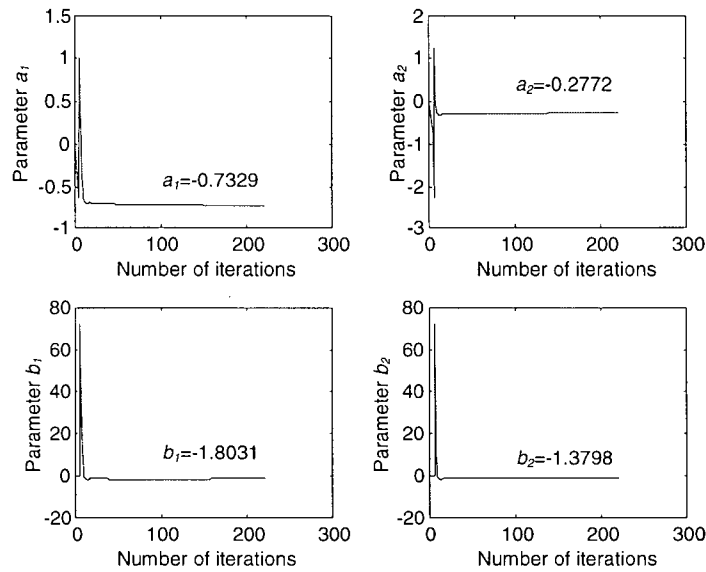
Figure 4-31   Parameter estimation in experiment #1 (500 RPM with heater ON for 8 minutes).

Experiment #2 (data file exp5.txt)

- Fan speed = 500 RPM; Heater kept on for 4 minutes
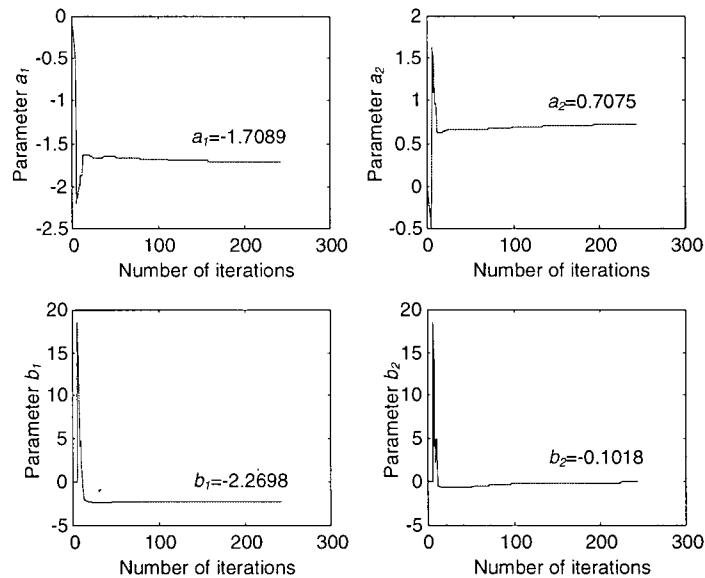
Figure 4-32   Parameter estimation in experiment #2 (500 RPM with heater ON for 4 minutes).

110

Experiment #3 (data file pretest_750w.txt)

- Fan speed = 750 RPM; Heater kept on for 8 minutes
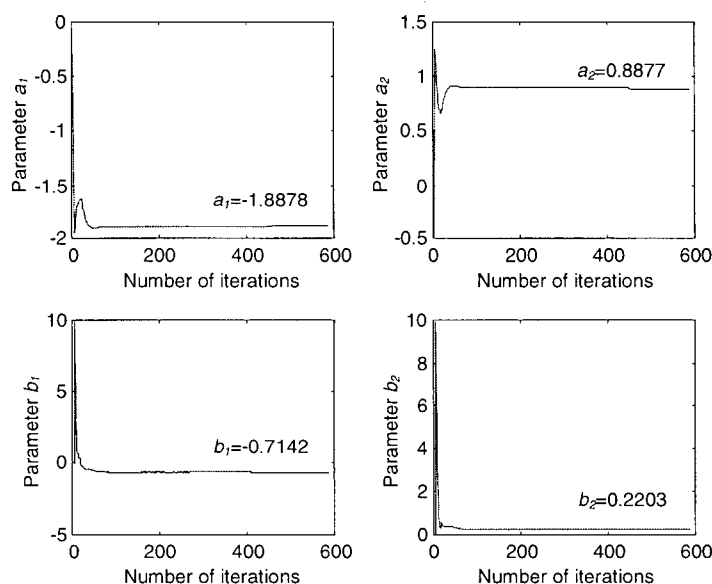
Figure 4-33   Parameter estimation in experiment #3 (750 RPM with heater ON for 8 minutes).

Experiment #4 (data file exp7.txt)

- Fan speed = 750 RPM; Heater kept on for 4 minutes
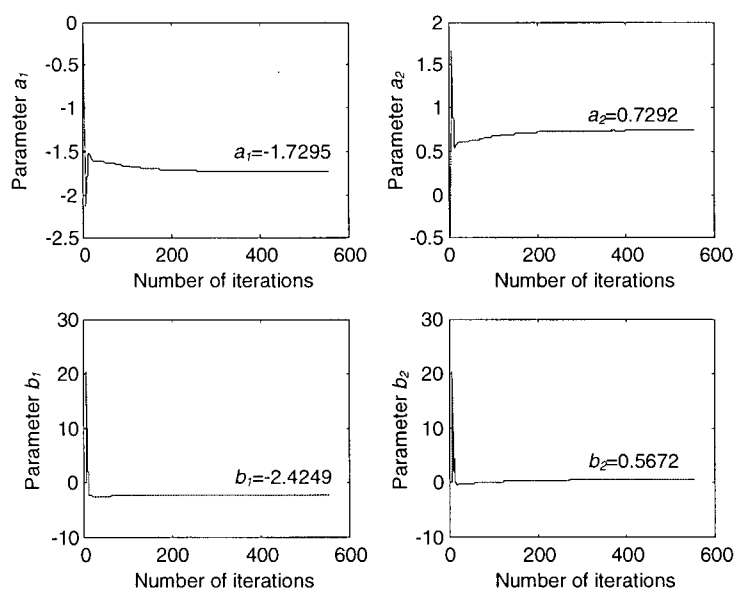
Figure 4-34   Parameter estimation in experiment #4 (750 RPM with heater ON for 4 minutes).

Experiment #5 (data file pretest_1kw.txt)

- Fan speed = 1000 RPM; Heater kept on for 8 minutes
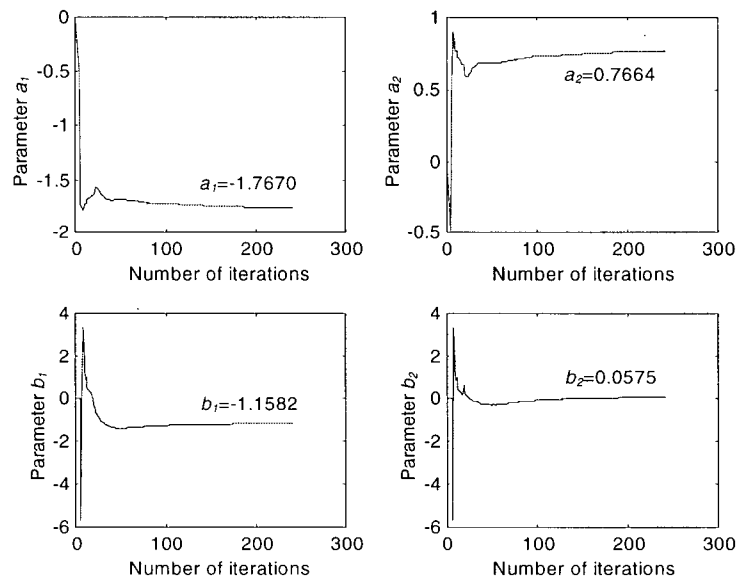
Figure 4-35   Parameter estimation in experiment #5 (1000 RPM with heater ON for 8 minutes).

Experiment #6 (data file exp9.txt)

- Fan speed = 1000 RPM; Heater kept on for 4 minutes
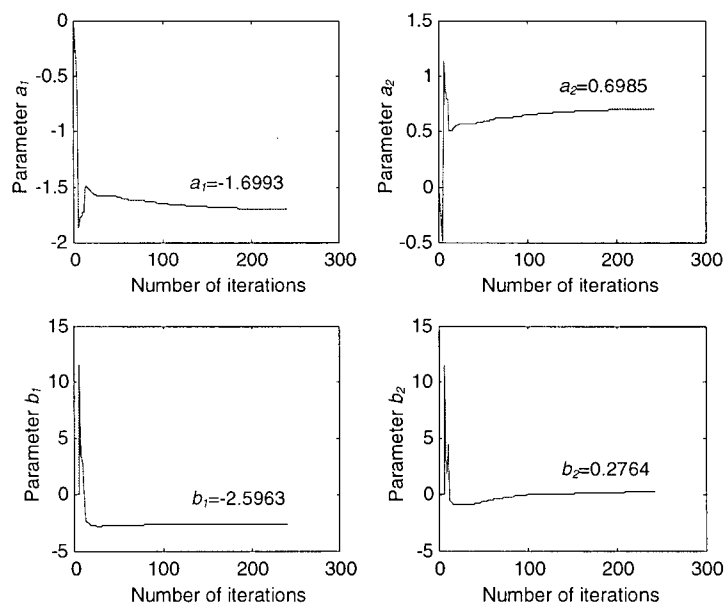
Figure 4-36   Parameter estimation in experiment #6 (1000 RPM with heater ON for 4 minutes).

112

The parameter estimation results for the second order SISO relative humidity model are summarized in Table 4-10.

Table 4-10   Estimated parameters for the second order SISO relative humidity model.

Test Conditions	Estimated Parameters			
	a_1	a_2	b_1	b_2
500 RPM, ON 8 minutes	-0.7329	-0.2772	-1.8031	-1.3798
500 RPM, ON 4 minutes	-1.7089	0.7075	-2.2698	-0.1018
750 RPM, ON 8 minutes	-1.8878	0.8877	-0.7142	0.2203
750 RPM, ON 4 minutes	-1.7295	0.7292	-2.4249	0.5672
1000 RPM, ON 8 minutes	-1.7670	0.7664	-1.1582	0.0575
1000 RPM, ON 4 minutes	-1.6993	0.6985	-2.5963	0.2764

From the results, for the parameter estimation of the second order SISO relative humidity model, it is seen that the parameters a_1 and a_2 show good consistency, except for the first test condition (500 rpm, 8 minutes). Accordingly, the parameter estimation results in first data set are ignored, and the relative humidity model is taken to be second order.

From the results presented in Section 4.2.1, it is seen that the experimental temperature model developed using the estimated parameters, is found to have the best consistency and hence the lowest nonlinearity. By examining the estimated parameters a_1 and a_2, it is noted that the results are reasonably consistent. Larger deviations in the parameter values occur at higher fan speeds, however, indicating that the nonlinearity increases with fan speed. The relative humidity results exhibit moderate nonlinearity. The nonlinearity seems to be higher at lower fan speeds, since in this case there is larger deviation in the parameter values, and furthermore there is a sign change in the parameter a_2.

In concluding the section, the parameter estimation results for different models used in this section are summarized as follows:

1. Temperature Model

The parameters estimated for the 2nd order SISO temperature model show consistency in both parameters a_1 and a_2. With reasonable accuracy, the temperature model can be represented as a second order SISO model. In this case, nonlinearity appears to be negligible, compared to the results for the other models.

2. Moisture Content Model

The parameters estimated for the second order SISO moisture content model do not show consistency in both value and sign. Therefore, 4 experiments are repeated to investigate the sign change in parameters, in particular. From the results it is clear that there is still no consistency in both value and sign. This implies that the process dynamics continue to alter during the drying process. Parameter a_1 appears to be more stable, but both the value and the sign continue to change in parameter a_2. No improvement is found in the parameter estimation through the use of the third order moisture model in two sets of experiments (called, "previous" and "repeated"). There is no sufficient convergence in all estimated parameters, but a_1 still appears to be more stable since it exhibits no sign change. For parameters a_2 and a_3, both sign and the value continue to change. When the model structure is further increased to fourth order, the results of parameter estimation still do not show sufficient consistency in both value and sign. Also, there is no convergence in the parameters a and b. Moisture content model exhibits the highest nonlinearity among the three models. This can be observed in both sets of experiments, as exhibited through the level of inconsistency of estimated parameters. Model parameters are affected by the initial moisture content and nature of the wood pieces. Even though the same wood species is used in the experiments, the way they are cut have an effect in their grain orientation. Grain orientation has an effect on the rate of moisture evaporation from wood. Furthermore, the relative humidity and the temperature inside the kiln also have an effect on the moisture content of wood. Therefore, the drying process is complex and rather coupled, and the nonlinearity is found to be particularly high for the moisture content model.

3. Relative Humidity Model

The parameter estimation results for the second order SISO relative humidity model show adequate consistency in both value and sign. The nonlinearity appears to decrease with increase in fan speed, an observation that is made in view of the fact that the estimated values tend to be closer to each other at higher fan speeds. The nonlinearity in the relative humidity process is found to be somewhat higher than in the temperature process, but is considered a moderate nonlinearity.

4.2.2 Internal heater control

In internal heater control, the control input is regulated by the internal PI controller of the heater. Parameters are estimated to investigate the possibility of a linear relationship between the output temperature response and the output moisture content behavior, under the heater PI control. Upper and lower limits of the PI control are set at 100°C and 98°C. The heater on off states will be controlled according to the two bounds. Three experiments are performed, denoted as experiment #7, 8 and 9. The data files obtained from the experiments are listed in Table 4-11.

Table 4-11   Data files used in the parameter estimation of internal heater control.

Experiment	Data file	Fan speed in RPM
Experiment #7	test1.txt	1000
Experiment #8	test2.txt	1000
Experiment #9	test3.txt	750

4.2.2.1 Temperature and moisture content model

Now the results of parameter estimation for the moisture content model, with temperature as input, are given. A second order linear model is used.

115

Experiment #7 (Data file test1.txt)

- Upper temperature limit = 100°C; lower limit = 98°C

- Fan speed = 1000 RPM

- Heater on when temperature drops below the lower temperature setting

- Heater off when temperature exceeds the upper temperature setting

The results are shown in Figure 4-37.
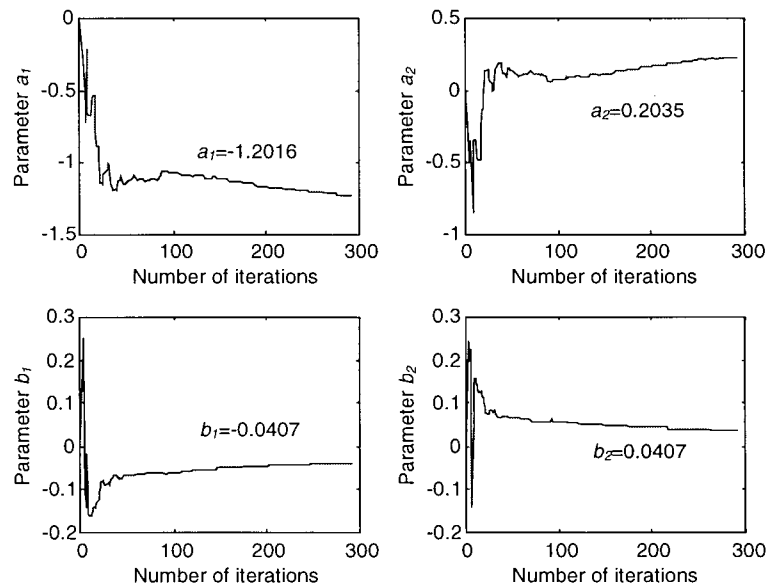
Figure 4-37   Parameter estimation in experiment #7 (1000 RPM with internal heater control).

Experiment #8 (Same experimental set up as experiment #7 but with a different initial moisture content condition; Data file test2.txt)

- Upper temperature limit = 100°C; lower limit = 98°C

- Fan speed = 1000 RPM

- Heater on when temperature drops below the lower temperature setting

- Heater off when temperature exceeds the upper temperature setting

   The results are shown in Figure 4-38.
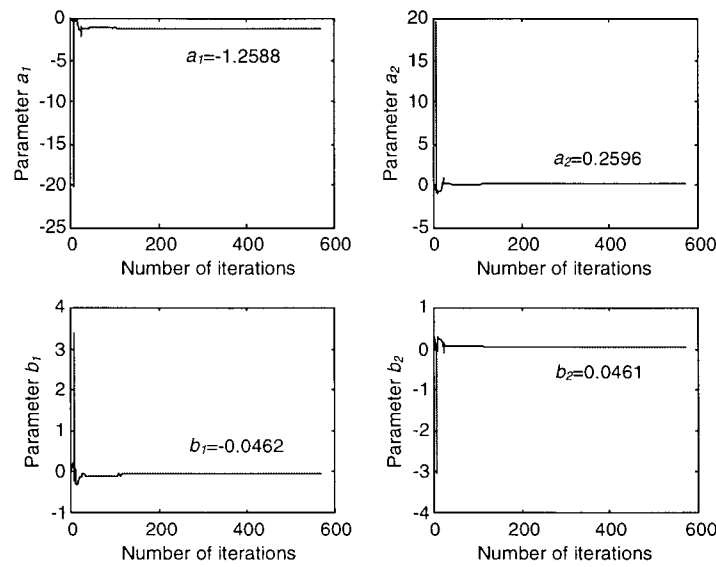
Figure 4-38   Parameter estimation in experiment #8 (1000 RPM with internal heater control).

Experiment #9 (Data file test3.txt)

- Upper temperature limit = 100°C; lower limit = 98°C
- Fan speed = 750 RPM
- Heater on when temperature drops below the lower temperature setting
- Heater off when temperature exceeds the upper temperature setting

  The results are shown in Figure 4-39.
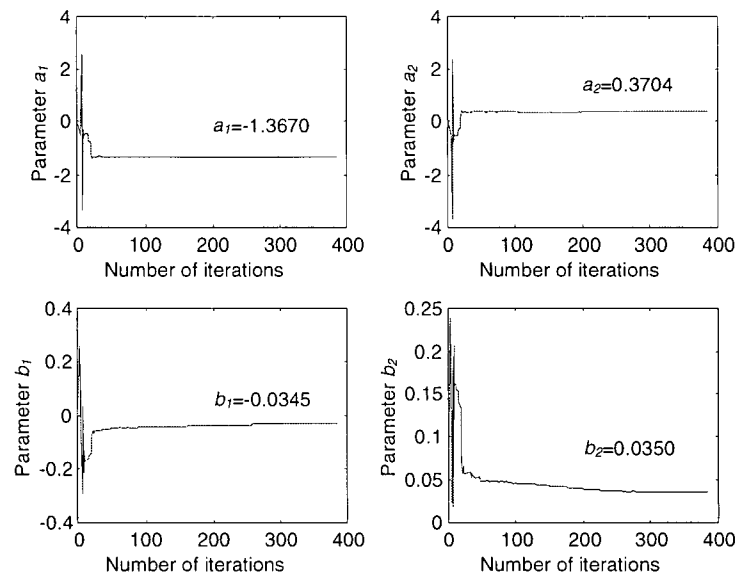
Figure 4-39   Parameter estimation in experiment #9 (750 RPM with internal heater control).

The parameter estimation results for the 2nd order SISO temperature-to-moisture-content relation model, using internal heater control input signal, are summarized in Table 4-12.

Table 4-12   Estimated parameters of the second order temperature to moisture content model.

Experiment Number and Fan Speed	Estimated Parameters			
	a_1	a_2	b_1	b_2
Experiment #7 @ 1000 RPM	-1.2016	-0.2035	-0.0407	0.0407
Experiment #8 @ 1000 RPM	-1.2588	0.2596	-0.0462	0.0461
Experiment #9 @ 750 RPM	-1.3670	0.3704	-0.0345	0.0350

4.3 Model Validation

The accuracy of an identified model is judged on the basis of the closeness of the model response to the actual process response when the same input is applied to both the model and the physical process. This is the basis of model validation that is employed here. In Section 4.2, parameters were estimated from the experimental input output data, which were used to develop SISO state space models of the second, third and fourth order, for moisture content response. Control input to the heater, was used as the input signal in model identification. Now the same input signal is applied to the developed state space model, and the model response is determined. This is then compared with the actual experimental response of the physical kiln. The accuracy of the identified model is represented using "squared error." The main steps are: (1) compute the second and third order model parameters using the same set of input-output data, (2) determine the value of the squared error between the actual data and the model response for each of the two models, (3) compute the mean squared error according to equation (4-20) and the standard deviation of error.

118

$$Mean \ squared \ error = \frac{1}{T} \int_0^T (squared \ error) \, dt \qquad (4.20)$$

Note that the models have been identified at fan speeds of 500, 750 and 1000 rpm. A similar procedure is adopted in the model validation of the fourth order moisture content model at fan speed of 1000 rpm. The estimated parameters used in this section are taken from Section 4.2, and are summarized in Tables 4-13, 4-14 and 4-15.

For validation of the second and third order moisture content models, ten sets of curves are plotted, to show the actual experimental response, the second order model response, and the third order model response, according to the estimated parameters listed in Tables 4-13 and 4-14, respectively. Model accuracy is compared on the basis of the squared error values between actual experimental response and the model response. Root mean squared (rms) error values and standard deviations for the same period of time response, are given in Table 4-16. Validation of the fourth order moisture model is presented separately, using the 4 sets of estimated results given in Table 4-15. Four sets of curves are plotted that include the squared error between the actual response and the model response, for a fan speed of 1000 rpm. The mean squared error is computed according to equation (4-20) as before, for the same duration of time response.

Table 4-13   Estimated parameters for the second order moisture content model.

Test Conditions (Experiment number, data file)	Estimated Parameters			
	a_1	a_2	b_1	b_2
500 RPM, ON 8 minutes (Experiment #1, pretest_500w.txt)	-0.8244	-0.1774	-0.1592	-0.5338
500 RPM, ON 4 minutes (Experiment #2, exp5.txt)	-1.4149	0.4146	-0.0513	-0.2009
500 RPM, ON 8 minutes (Repeated Experiment #1, redo_500w.txt)	-1.3071	0.3066	-0.0389	-0.1632
500 RPM, ON 4 minutes (Repeated Experiment #2, redo_exp5.txt)	-1.4900	0.4897	0.1209	-0.2571
750 RPM, ON 8 minutes (Experiment #3, pretest_750w.txt)	-0.8788	-0.1216	0.2399	-0.6674
750 RPM, ON 4 minutes (Experiment #4, exp7.txt)	-0.8163	-0.1838	0.0788	-0.5230
1000 RPM, ON 8 minutes (Experiment #5, pretest_1kw.txt)	-0.9480	-0.0525	0.1895	-0.4724
1000 RPM, ON 4 minutes (Experiment #6, exp9.txt)	-1.0327	0.0323	0.1501	-0.4621
1000 RPM, ON 8 minutes (Repeated Experiment #3, redo_1kw.txt)	-1.2445	0.2439	0.0104	-0.1638
1000 RPM, ON 4 minutes (Repeated Experiment #4, redo_exp9.txt)	-0.9800	-0.0204	-0.0121	-0.2166

Table 4-14   Estimated parameters for the third order moisture content model.

Test Conditions (Experiment Number)	Estimated Parameters					
	a_1	a_2	a_3	b_1	b_2	b_3
500 RPM, ON 8 minutes Experiment #1	-0.9788	0.0322	-0.0551	-0.0019	-0.1972	-0.2923
500 RPM, ON 4 minutes Experiment #2	-1.0555	-0.2860	0.3411	-0.0180	0.1233	-0.3835
500 RPM, ON 8 minutes Repeated Experiment #1	-1.0252	-0.4025	0.4274	-0.0325	-0.1422	-0.0012
500 RPM, ON 4 minutes Repeated Experiment #2	-1.1092	-0.2579	0.3668	0.0848	-0.0811	-0.1560
750 RPM, ON 8 minutes Experiment #3	-0.8886	-0.1736	0.0618	0.2838	-0.8645	0.1885
750 RPM, ON 4 minutes Experiment #4	-0.7682	-0.1651	-0.0668	0.0795	-0.3632	-0.2153
1000 RPM, ON 8 minutes Experiment #5	-1.8670	-0.1174	0.9846	1.3837	-0.4126	0.1205
1000 RPM, ON 4 minutes Experiment #6	-0.9130	0.0631	-0.1506	0.1185	-0.0544	-0.4857
1000 RPM, ON 8 minutes Repeated Experiment #3	-0.9848	-0.3624	0.3466	-0.0092	0.0261	-0.1576
1000 RPM, ON 4 minutes Repeated Experiment #4	-0.8374	-0.4090	0.2460	-0.0382	-0.1003	-0.0914

Table 4-15   Estimated parameters for the fourth order moisture content model.

Experiment	Estimated Parameters							
	a_1	a_2	a_3	a_4	b_1	b_2	b_3	b_4
Experiment #5	-0.8247	0.0045	-0.1829	0.0025	0.1072	-0.2315	-0.1997	-0.0800
Experiment #6	-0.8979	0.0777	-0.2240	0.0437	0.1293	-0.0456	-0.3100	-0.1821
Repeated Experiment #3	-0.9482	-0.3763	0.2139	0.1101	-0.0047	0.0191	-0.1601	0.0128
Repeated Experiment #4	-0.6683	-0.4991	-0.0933	0.2602	-0.1064	-0.0743	-0.0744	-0.0096

4.3.1 Validation of the second and third order moisture content models

Ten sets of curves are plotted for the actual response of the kiln (experimental data), and the responses of the second order and the third order model, using the same sets of input-output data files. The "squared error" curves for the two models are also shown.

Experiment #1

Data file: pretest_500w.txt; Heater kept on for 8 minutes; Fan speed = 500 RPM
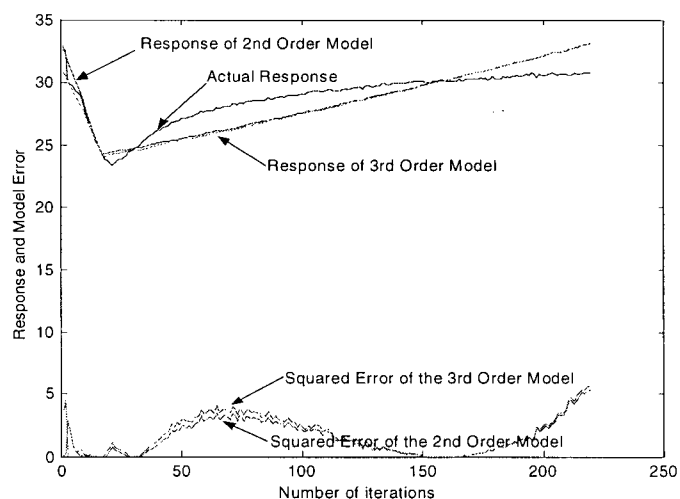
Figure 4-40   Validation of the moisture content model of experiment #1.

Experiment #2

Data file: exp5.txt; Heater kept on for 4 minutes; Fan speed = 500 RPM
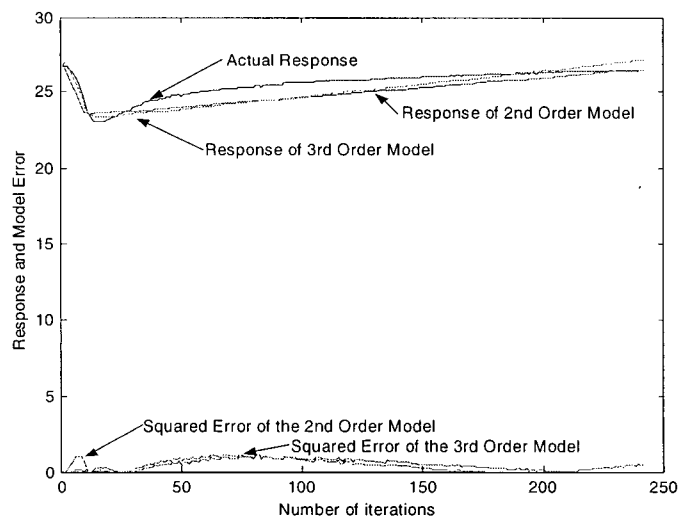
Figure 4-41   Validation of the moisture content model of experiment #2.

Repeated Experiment #1

Data file: redo_500w.txt; Heater kept on for 8 minutes; Fan speed = 500 RPM
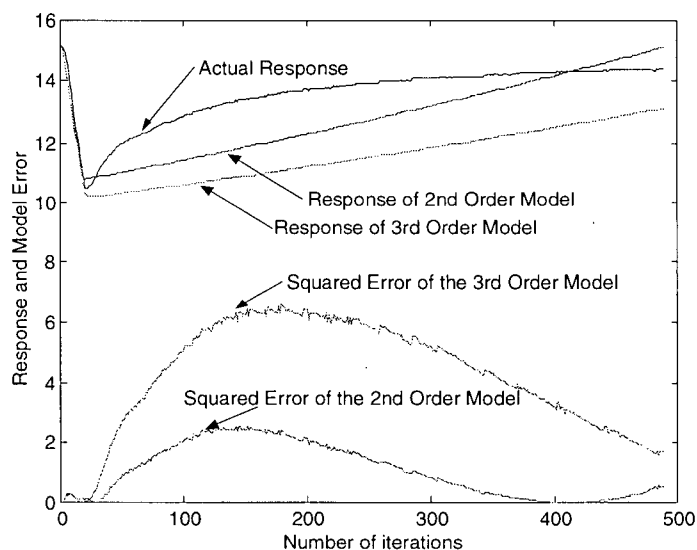
Figure 4-42   Validation of the moisture content model of repeated experiment #1.

Repeated Experiment #2

Data file: redo_exp5.txt; Heater kept on for 4 minutes; Fan speed = 500 RPM
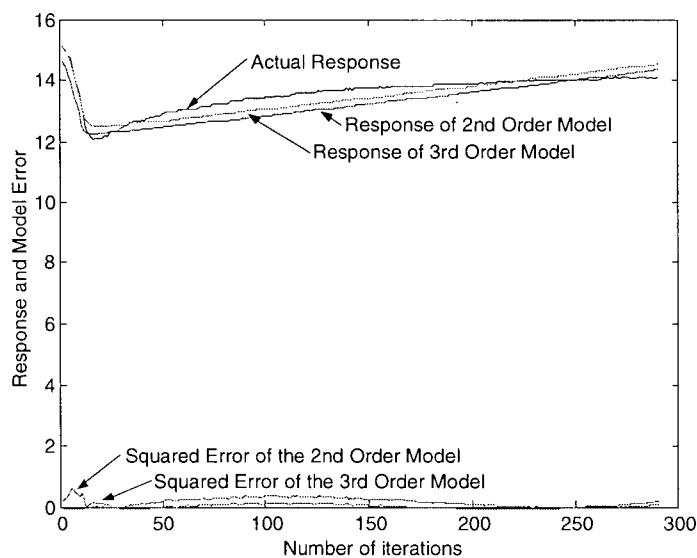
Figure 4-43   Validation of the moisture content model of repeated experiment #2.

Experiment #3

Data file: pretest_750w.txt; Heater kept on for 8 minutes; Fan speed = 750 RPM
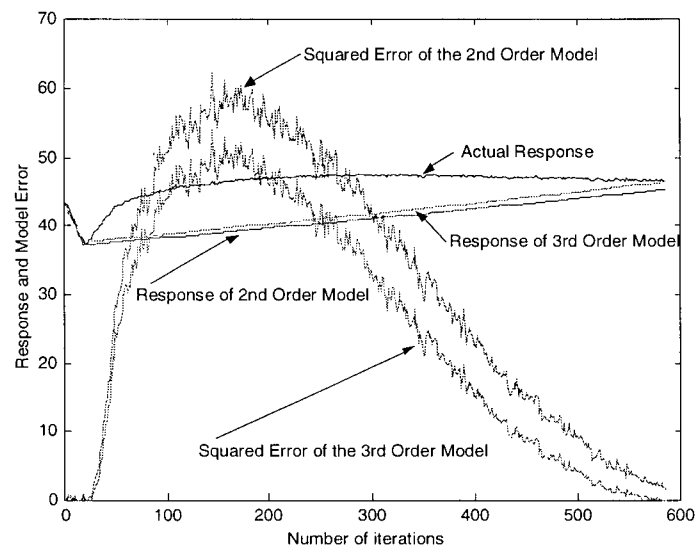
Figure 4-44   Validation of the moisture content model of experiment #3.

Experiment #4

Data file: exp7.txt; Heater kept on for 4 minutes; Fan speed = 750 RPM
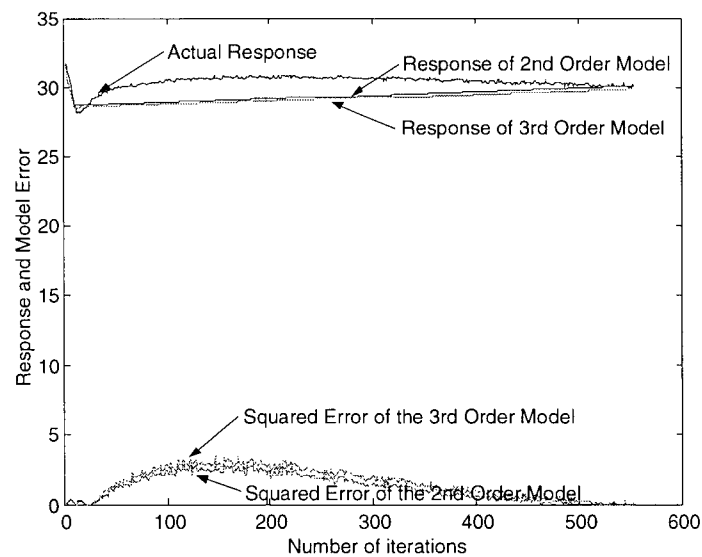
Figure 4-45   Validation of the moisture content model of experiment #4.

Experiment #5

Data file: pretest_1kw.txt; Heater kept on for 8 minutes; Fan speed = 1000 RPM
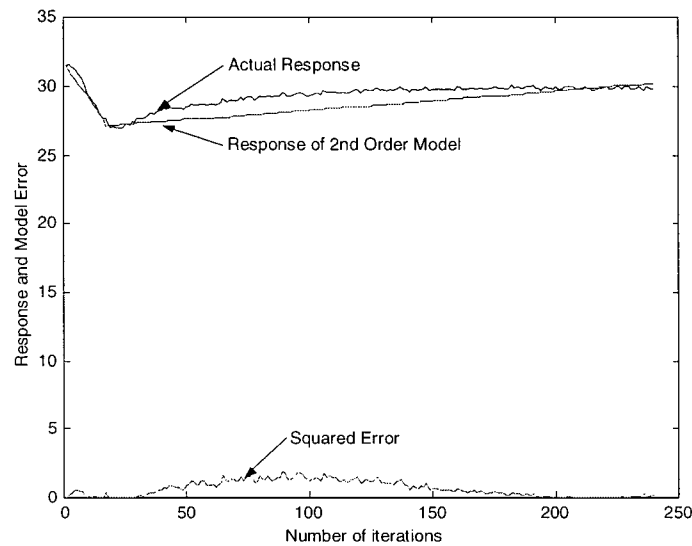
Figure 4-46   Validation of the moisture content model of experiment #5.

Experiment #6

Data file: exp9.txt; Heater kept on for 4 minutes; Fan speed = 1000 RPM
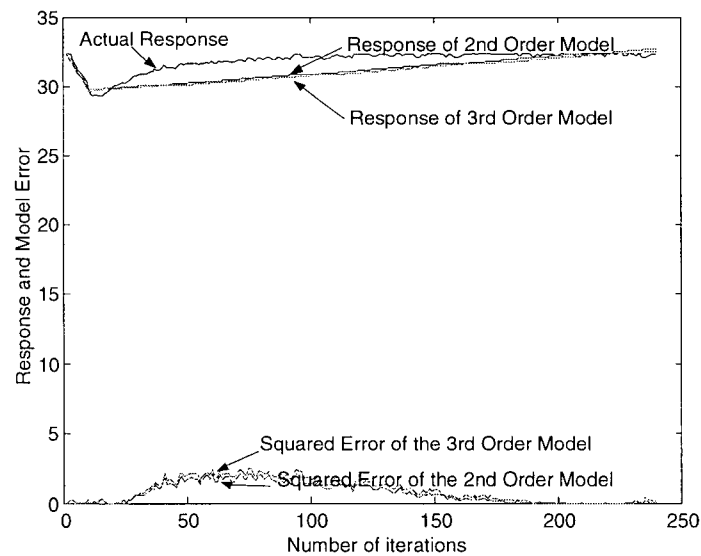
Figure 4-47   Validation of the moisture content model of experiment #6.

Repeated Experiment #3

Data file: redo_1kw.txt; Heater kept on for 8 minutes; Fan speed = 1000 RPM
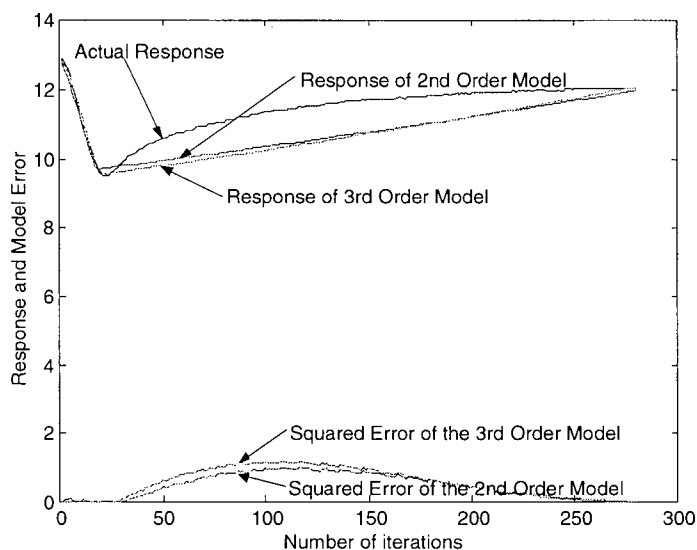
Figure 4-48   Validation of the moisture content model of repeated experiment #3.

Repeated Experiment #4

Data file: redo_exp9.txt; Heater kept on for 4 minutes; Fan speed = 1000 RPM
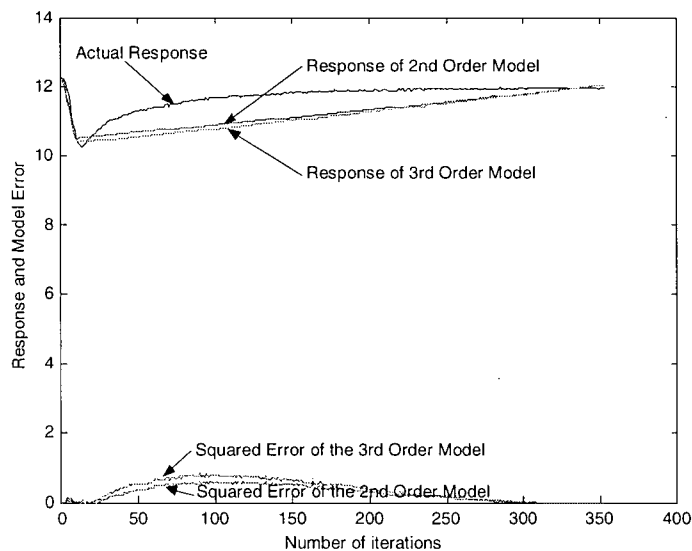
Figure 4-49   Validation of the moisture content model of repeated experiment #4.

The root mean squared (rms) error and the standard deviation of error (std. error) for each of the ten experiments are given in Table 4-16. Based on these results of model validation, for both the second order and the third order models, it is seen the estimated models are not uniformly satisfactory. The squared error between the actual experimental response and the model response appears to be very large in several cases. In experiment #1, model response closely follows the actual response in the descending region. However, this is not the case in both the rising region and the steady region. A similar behavior is seen in all ten experiments. Worst cases are the repeated experiment #1, and the experiments #3 and #5. In both repeated experiment #1 and experiment #3, the estimated squared error is the largest among the others. In particular, the results from experiment #3 should be discarded. In experiment #5, the third order moisture model does not show satisfactory results as the model response does not follow the actual response at all. Both rms and std. error have to be considered in picking the best experimental model. In this sense, the third order model obtained from the Repeated Experiment #2 appears to provide the best results.

Table 4-16   Error values for the moisture content model.

Experiment	2nd Order Model		3rd Order Model	
	rms error	std. Error	rms error	std. Error
Experiment #1	1.2371	1.2004	1.3121	1.2388
Experiment #2	0.6823	0.3997	0.6493	0.5264
Repeated Experiment #1	1.0203	0.6774	2.0564	0.5627
Repeated Experiment #2	0.4126	0.2673	0.2750	0.2597
Experiment #3	5.5788	2.1780	4.9682	2.2832
Experiment #4	1.1113	0.5350	1.2505	0.5188
Experiment #5	0.8018	0.4907	Nil	Nil
Experiment #6	0.8661	0.5853	0.9542	0.5807
Repeated Experiment #3	0.6927	0.3315	0.7462	0.3860
Repeated Experiment #4	0.5214	0.2780	0.5946	0.3102

In the next section, model validation for the fourth order moisture model will be investigated using four sets of experimental data, obtained at a fan speed of 1000 rpm.

4.3.2   Validation of the fourth order moisture content model

In this section model validation is performed using four sets of experimental data, for the fourth order moisture content model. The results are compared on the basis of the squared error between the model response and the actual experimental response of the kiln.

Experiment #5

Data file: pretest_1kw.txt; Heater kept on for 8 minutes; Fan speed = 1000 RPM
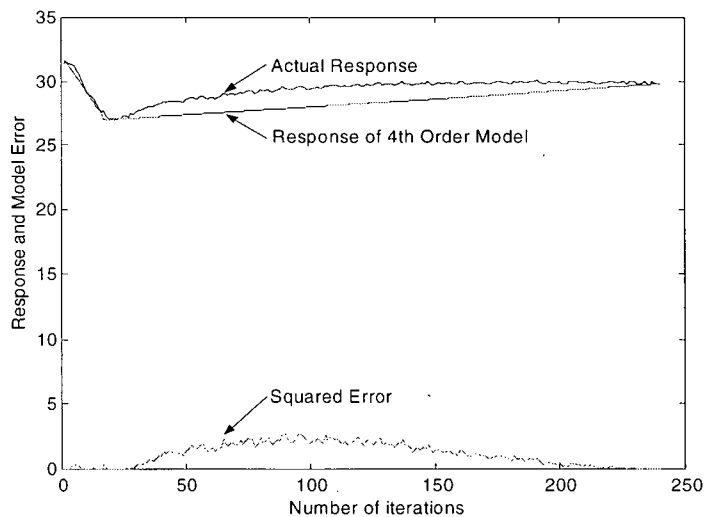
Figure 4-50   Validation of the 4th order moisture content model of experiment #5.

Experiment #6

Data file: exp9.txt; Heater kept on for 4 minutes; Fan speed = 1000 RPM
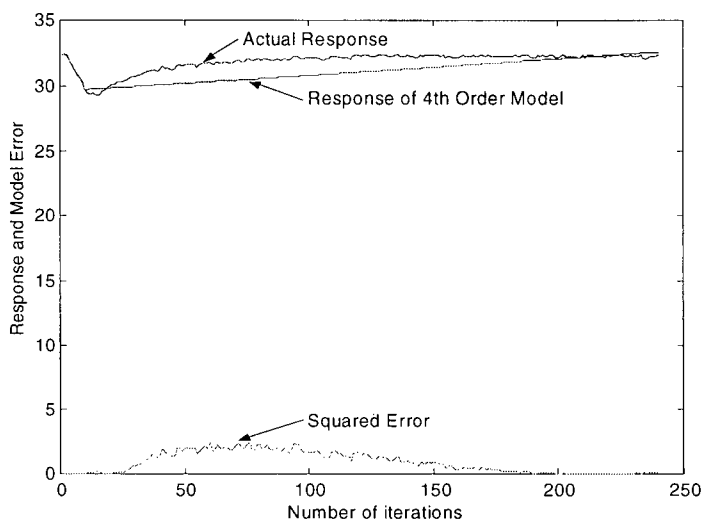
Figure 4-51   Validation of the 4th order moisture content model of experiment #6.

Repeated Experiment #3

Data file: redo_1kw.txt; Heater kept on for 8 minutes; Fan speed = 1000 RPM
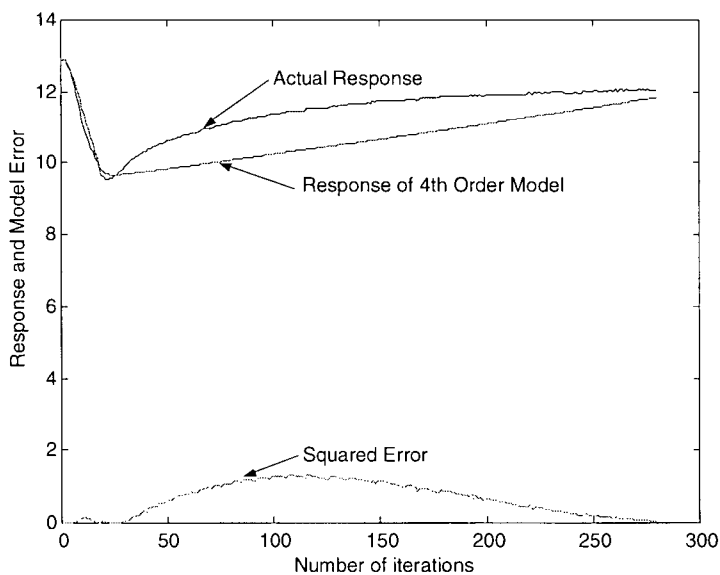
Figure 4-52   Validation of the 4th order moisture content model of repeated experiment #3.

Repeated Experiment #4

Data file: redo_exp9.txt; Heater kept on for 4 minutes; Fan speed = 1000 RPM
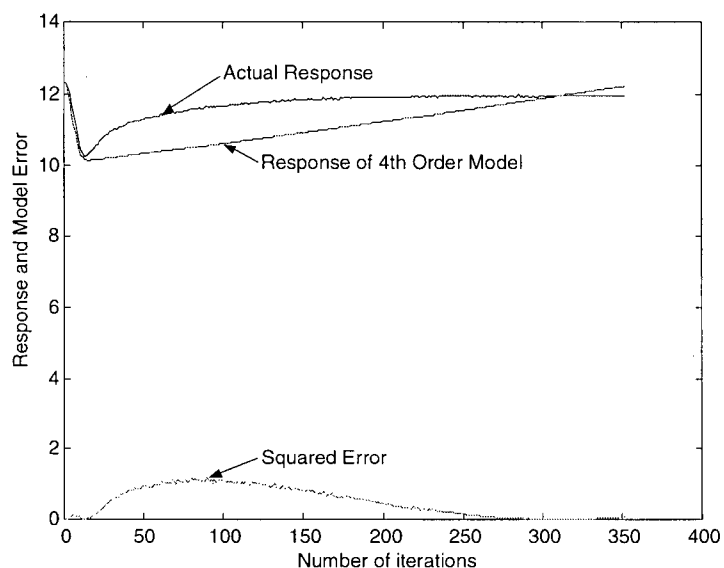
Figure 4-53   Validation of the 4th order moisture content model of repeated experiment #4.

The root mean squared (rms) error and the standard deviation of error (std. error) for the fourth order moisture content model determined from the four sets of data are given in Table 4-17.

Table 4-17   Error values for the fourth order moisture content model.

Experiment	Model Error	
	rms error	std. error
Experiment #5	1.0634	0.4892
Experiment #6	0.9337	0.5852
Repeated Experiment #3	0.8184	0.3947
Repeated Experiment #4	0.6968	0.4035

From the results it is seen that the fourth order moisture content model does not provide any improvement over the lower order models. The calculated root mean squared

error and the standard deviation of error between the actual response and the model response are almost the same as those for the second and the third order models.

Since the experimental model for moisture content has been developed directly using the heater control signal as the input and the moisture content measurements as the output data, some internal dynamics of the process could be missed in the moisture model. Therefore, an alternative approach will be utilized next to develop the moisture content model, where the model is separated into two sub models. This approach will be shown in the next section.

4.4 Experiment Model for Moisture Content Using External Computer Control of Input

Instead of developing the moisture content model directly, as done in the approach presented thus far, an alternative approach would be to consider the moisture model as two separate sub models as shown in the block diagram of Figure 4-55, in comparison with Figure 4-54.

Input u_h → Overall Moisture Content Model → Response y_m
(Heater control signal) (Moisture content)
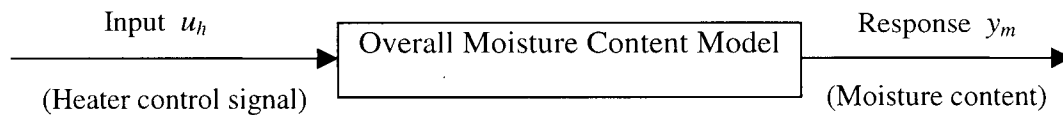
Figure 4-54   Block diagram of the first approach of model identification.

Input u_h → [KILN: Heat-Temp Model → Intermediate Response y_t (Temperature) → Temp-Moist Model] → Response y_m
(Heater control signal) (Moisture content)
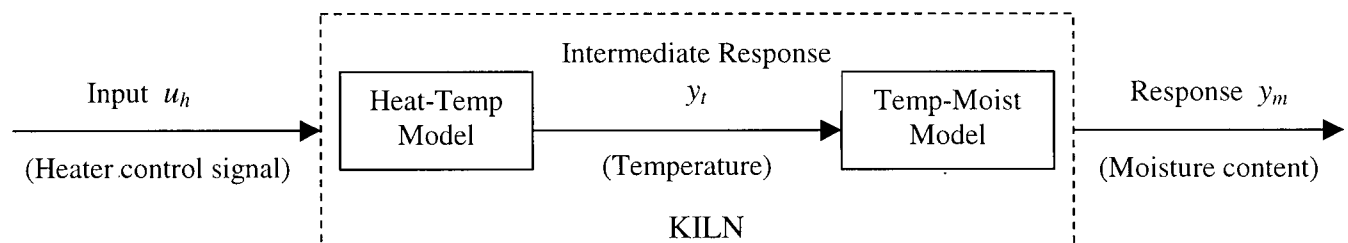
Figure 4-55   Block diagram of the second approach of model identification.

The system is represented by two sub-systems; namely, the *heat-temperature* model and the *temperature-moisture* model, as shown in Figure 5-55 where

u_h = control signal to the heater (ON/OFF)

y_t = temperature response (output of the heat-temperature model)

y_m = moisture response (output of the temperature-moisture model)

Each of the two sub models is taken to be a single input single output (SISO) system. The fan speed is set at a fixed and high value throughout the experiment. The input to the heat-temperature (first) sub-system is the heater on/off signal, while the output is the thermocouple reading (temperature). For the temperature-moisture (second) sub-system, the input is the temperature as read by the thermocouple and the output is the moisture content as read by the associated sensor attached to the wood pieces in the kiln.

In the following section, the temperature-moisture relation of the sub model approach will be identified, which will include the parameter estimation and the model validation of both the second and third order model structures. The corresponding sub model is shown in Figure 4-56.

Input y_t → Temp-Moist Model → Response y_m

(Kiln Temperature) (Moisture Content of Wood)
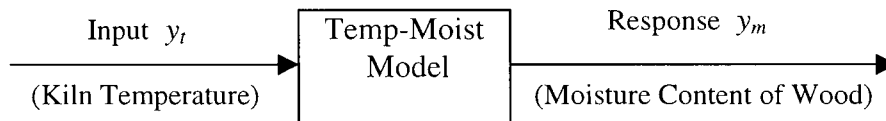
Figure 4-56   The experimental modeling of the temperature-moisture content sub model.

where y_t is the temperature response of the kiln and y_m is the moisture response of the wood pieces in the kiln. Subsequently, the heat-temperature sub model will be identified, which will include parameter estimation and model validation.

4.4.1 Parameter estimation of the temperature-moisture content relation

In the following sub sections, the second and third order single-input-single-output (SISO) *temperature-moisture content* models are investigated, under a constant fan speed of 1000 rpm, using second order and third order model structures.

4.4.1.1 Second order, SISO temperature-moisture content model

Now the results from parameter estimation for the second order sub model of moisture content, with kiln temperature as the input, are presented.

Experiment #5

Data file: pretest_1kw.txt; Heater kept on for 8 minutes; Fan speed = 1000 RPM
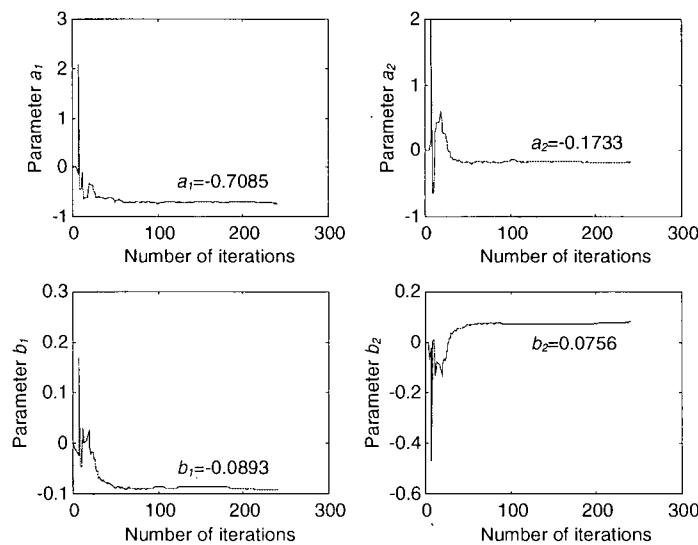
Figure 4-57   Parameter estimation in experiment #5 for the 2nd order temp-moist model (1000 RPM with heater ON for 8 minutes).

133

Experiment #6

Data file: exp9.txt; Heater kept on for 4 minutes; Fan speed = 1000 RPM
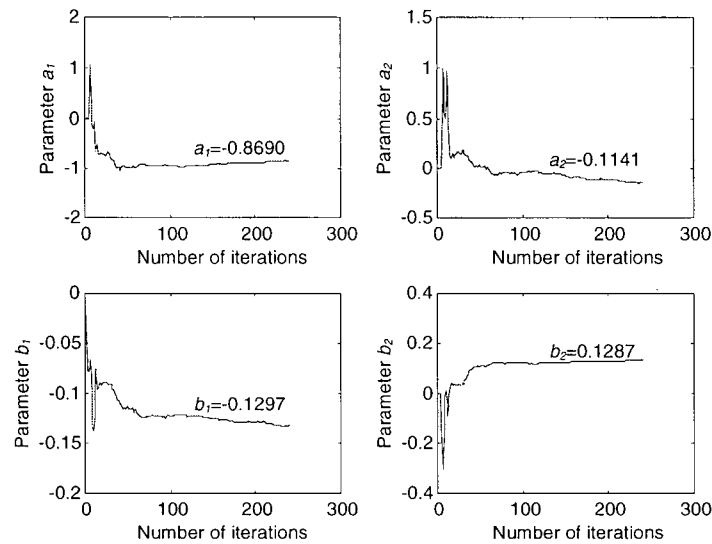
Figure 4-58   Parameter estimation in experiment #6 for the 2nd order temp-moist model (1000 RPM with heater ON for 4 minutes).

Repeated Experiment #3

Data file: redo_1kw.txt; Heater kept on for 8 minutes; Fan speed = 1000 RPM
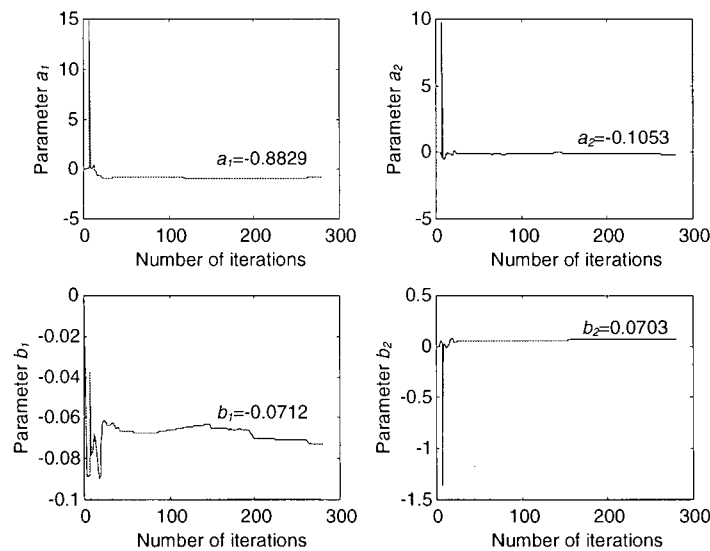
Figure 4-59   Parameter estimation in repeated experiment #3 for the 2nd order temp-moist model (1000 RPM with heater ON for 8 minutes).

Repeated Experiment #4

Data file: redo_exp9.txt; Heater kept on for 4 minutes; Fan speed = 1000 RPM
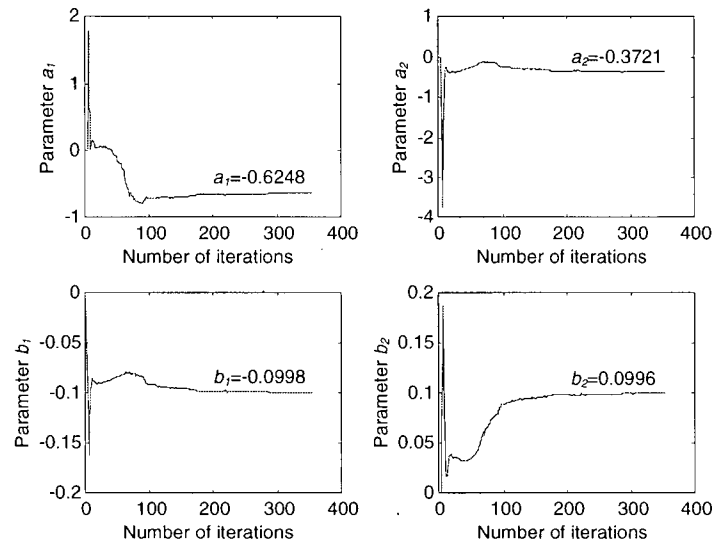
Figure 4-60   Parameter estimation in repeated experiment #4 for the 2nd order temp-moist model (1000 RPM with heater ON for 4 minutes).

The estimated parameters for the second order SISO sub model for temperature to moisture content are given in Table 4-18.

Table 4-18   Estimated parameters of the 2nd order temperature-moisture content model.

Test Conditions (Experiment number, data file)	Estimated Parameters			
	a_1	a_2	b_1	b_2
1000 RPM, ON 8 minutes (Experiment #5, pretest_1kw.txt)	-0.7085	-0.1733	-0.0893	0.0756
1000 RPM, ON 4 minutes (Experiment #6, exp9.txt)	-0.8690	-0.1141	-0.1297	0.1287
1000 RPM, ON 8 minutes (Repeated Experiment #3, redo_1kw.txt)	-0.8829	-0.1053	-0.0712	0.0703
1000 RPM, ON 4 minutes (Repeated Experiment #4, redo_exp9.txt)	-0.6248	-0.3721	-0.0998	0.0996
Average Estimated Parameter (ignoring repeated expt.#4 data)	-0.8201	-0.1309	-0.0967	0.0915

From this table it is noticed that the parameters estimated for the second order SISO temperature-moisture model show consistency in both the value and the sign. The average value of the estimated parameters is computed, after ignoring the data of repeated experiment #4 since the estimated parameters of a are significantly different from the estimated parameters from the first three experiments.

4.4.1.2 Third order, SISO temperature-moisture content model

Now the results from the parameter estimation for the third order sub model of moisture content, with kiln temperature as the input, are presented.

Experiment #5

Data file: pretest_1kw.txt; Heater kept on for 8 minutes; Fan speed = 1000 RPM
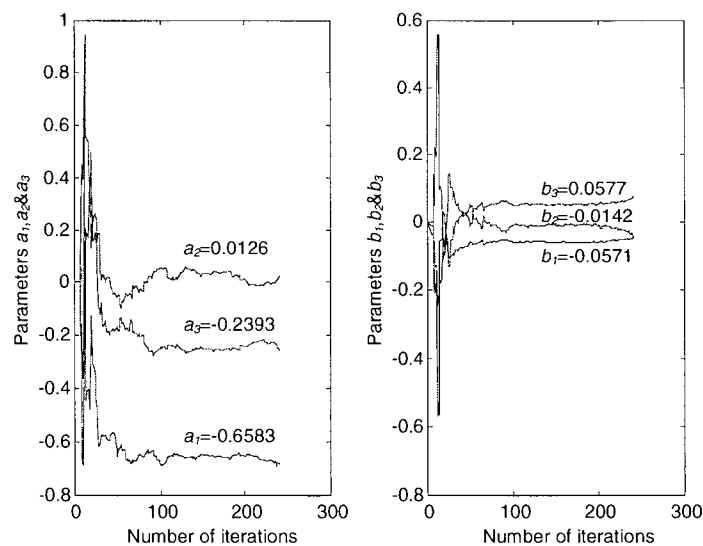
Figure 4-61   Parameter estimation in experiment #5 for the 3rd order temp-moist model (1000 RPM with heater ON for 8 minutes).

Experiment #6

Data file: exp9.txt; Heater kept on for 4 minutes; Fan speed = 1000 RPM
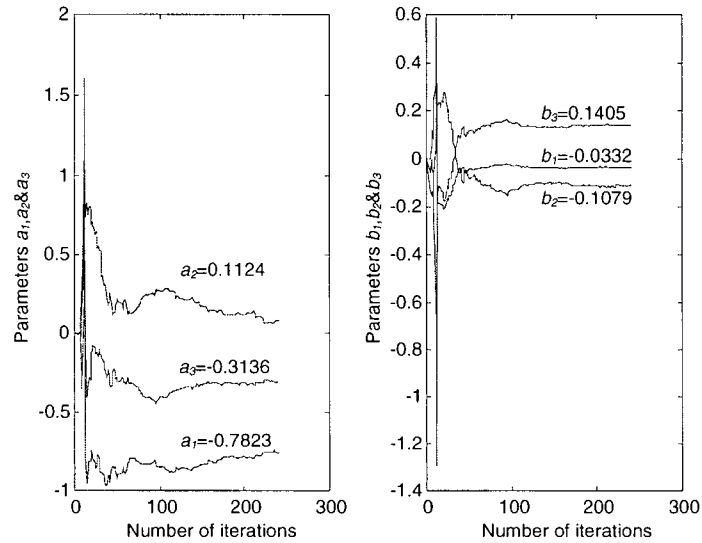
Figure 4-62   Parameter estimation in experiment #6 for the 3rd order temp-moist model (1000 RPM with heater ON for 4 minutes).

Repeated Experiment #3

Data file: redo_1kw.txt; Heater kept on for 8 minutes; Fan speed = 1000 RPM
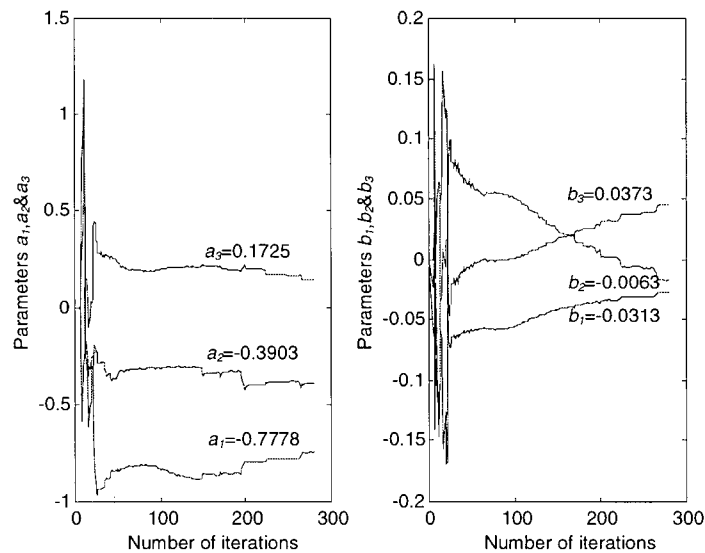
Figure 4-63   Parameter estimation in repeated experiment #3 for the 3rd order temp-moist model (1000 RPM with heater ON for 8 minutes).

Repeated Experiment #4

Data file: redo_exp9.txt; Heater kept on for 4 minutes; Fan speed = 1000 RPM
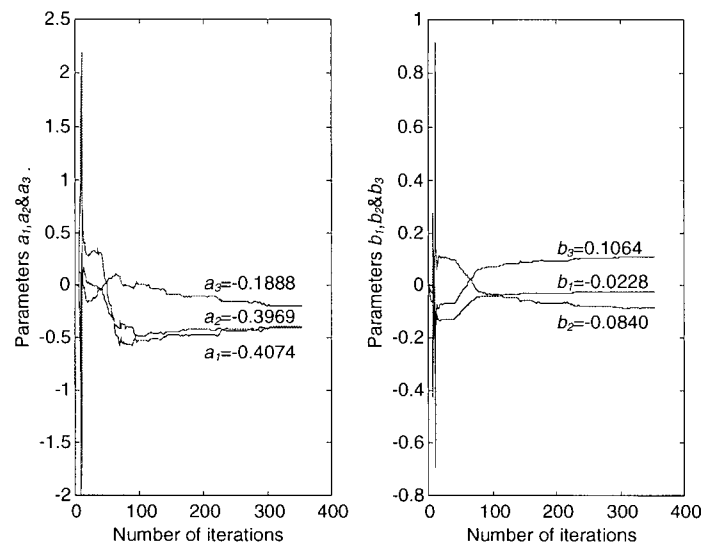
Figure 4-64   Parameter estimation in repeated experiment #4 for the 3rd order temp-moist model (1000 RPM with heater ON for 4 minutes).

The estimated parameters for the third order model structure of the temperature-moisture content sub model are summarized in Table 4-19.

Table 4-19   Estimated parameters of the 3rd order temperature-moisture content model.

Test Conditions (Experiment Number)	Estimated Parameters					
	a_1	a_2	a_3	b_1	b_2	b_3
1000 RPM, ON 8 minutes Experiment #5	-0.6583	0.0126	-0.2393	-0.0571	-0.0142	0.0577
1000 RPM, ON 4 minutes Experiment #6	-0.7823	0.1124	-0.3136	-0.0332	-0.1079	0.1405
1000 RPM, ON 8 minutes Repeated Experiment #3	-0.7778	-0.3903	0.1725	-0.0313	-0.0063	0.0373
1000 RPM, ON 4 minutes Repeated Experiment #4	-0.4074	-0.3969	-0.1888	-0.0228	-0.0840	0.1064

138

It is clear from these results that for the third order SISO temperature-moisture model, there is no consistency in both value and sign of the estimated parameters in a. The estimated parameters in a_1, b_1, b_2 and b_3 show consistency in sign but still do not show sufficient consistency in value. The values of the estimated parameters for the third order SISO temperature-moisture content model do not seem to converge properly.

4.4.2 Parameter estimation for the 2nd order heat-temperature relation

This section presents results of parameter estimation for the *heat-temperature* sub model. Four experiments are presented at a fan speed of 1000 rpm. The parameters are estimated using a second order model structure.

Experiment #5

Data file: pretest_1kw.txt; Heater kept on for 8 minutes; Fan speed = 1000 RPM
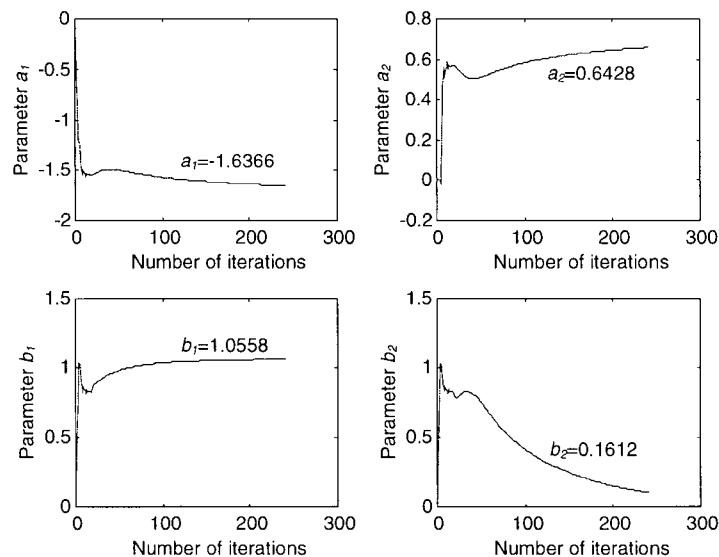
Figure 4-65   Parameter estimation in experiment #5 for the 2nd order heat-temp model (1000 RPM with heater ON for 8 minutes).

139

Experiment #6

Data file: exp9.txt; Heater kept on for 4 minutes; Fan speed = 1000 RPM
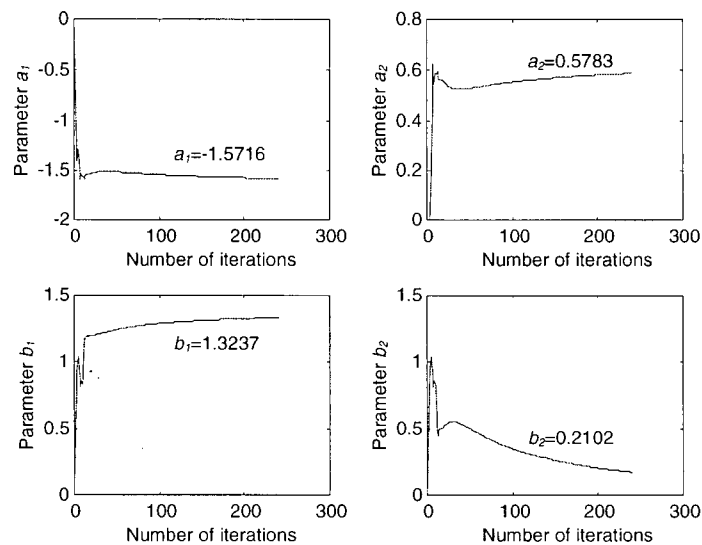
Figure 4-66   Parameter estimation in experiment #6 for the 2nd order heat-temp model (1000 RPM with heater ON for 4 minutes).

Repeated Experiment #3

Data file: redo_1kw.txt; Heater kept on for 8 minutes; Fan speed = 1000 RPM
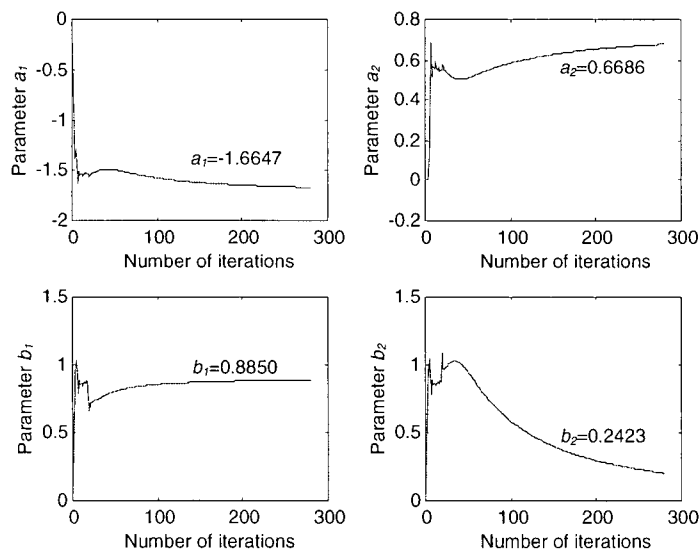
Figure 4-67   Parameter estimation in repeated experiment #3 for the 2nd order heat-temp model (1000 RPM with heater ON for 8 minutes).

Repeated Experiment #4

Data file: redo_exp9.txt; Heater kept on for 4 minutes; Fan speed = 1000 RPM
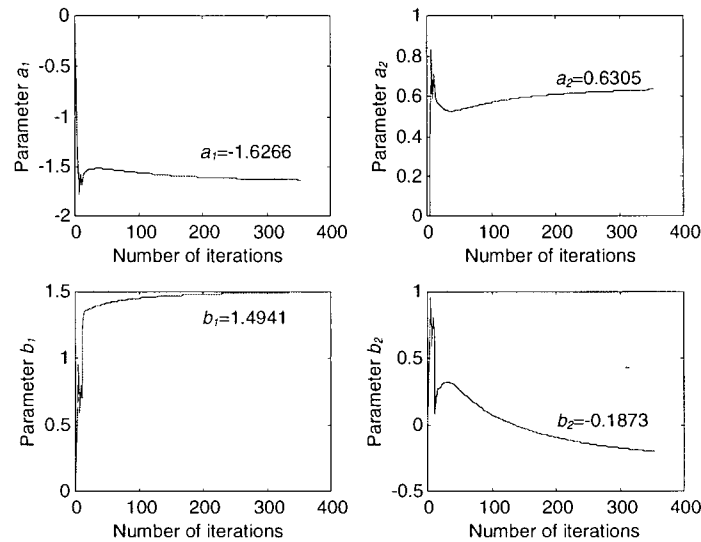
Figure 4-68   Parameter estimation in repeated experiment #4 for the 2nd order
heat-temp model (1000 RPM with heater ON for 4 minutes).

The estimated parameters of the second order SISO heat-temperature sub model for all four sets of experiments are summarized in Table 4-20. The average values of the estimated parameters from the experiments are also given in the table, after ignoring the set of estimated parameters from the repeated experiment #4, due to the sign inconsistency of this experiment.

Table 4-20   Estimated parameters of the second order heat-temperature model.

Experiment Number, Data File	Estimated Parameters			
	a_1	a_2	b_1	b_2
Experiment #5, pretest_1kw.txt	-1.6366	0.6428	1.0558	0.1612
Experiment #6, exp9.txt	-1.5716	0.5783	1.3237	0.2102
Experiment #3, redo_1kw.txt	-1.6647	0.6686	0.8850	0.2423
Experiment #4, redo_exp9.txt	-1.6266	0.6305	1.4941	-0.1873
Average Estimated Parameter (ignoring repeated expt.#4)	-1.6243	0.6299	1.0882	0.2046

The estimated parameters of the 2nd order SISO temperature model show consistency in both value and sign. The estimated values in the repeated experiment #4 are consistent, except for the estimated value of the parameter for b_2, which has a sign change. This may be due to process nonlinearities and experimental error. In view of this, the average values of the estimated parameters are computed without including the data of the repeated experiment #4.

4.4.3 Validation of the SISO temperature-moisture content model

In this section, actual kiln response and the model response are plotted for both second order and third order temperature-moisture content models, using the same set of data files used in parameter estimation. Input to the model structure is the average temperature profile. Both the second and the third order model structures are validated for all cases including experiments #5 and #6, and repeated experiments #3 and #4 using the data files pretest_1kw, exp9.txt, redo_1kw and redo_exp9 as listed in Table 4-21.

Table 4-21   Data files used for validation of the temperature-moisture content model.

Experiments	Data file
Experiment #5	Pretest_1kw.txt
Experiment #6	Exp9.txt
Repeated Experiment #3	Redo_1kw.txt
Repeated Experiment #4	Redo_exp9.txt

4.4.3.1 Validation of the second order temperature-moisture content model

Validation of the 2nd order temperature-moisture model using average temperature readings as input data and average moisture readings as output data is presented here. Four experiments are investigated under a fan speed of 1000 rpm. The actual kiln response, the model response, and the estimated squared error are all presented in each figure below.

142

Experiment #5

Data file: pretest_1kw.txt; Heater kept on for 8 minutes; Fan speed = 1000 RPM
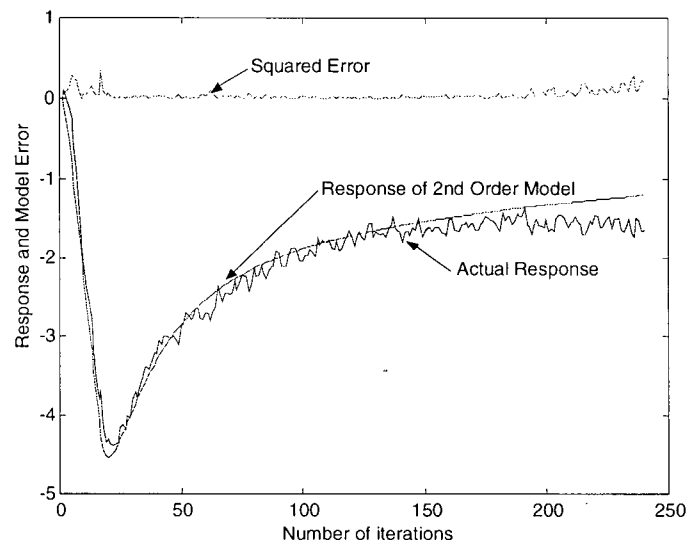
Figure 4-69   Validation of the 2nd order temp-moist model of experiment #5.

Experiment #6

Data file: exp9.txt; Heater kept on for 4 minutes; Fan speed = 1000 RPM
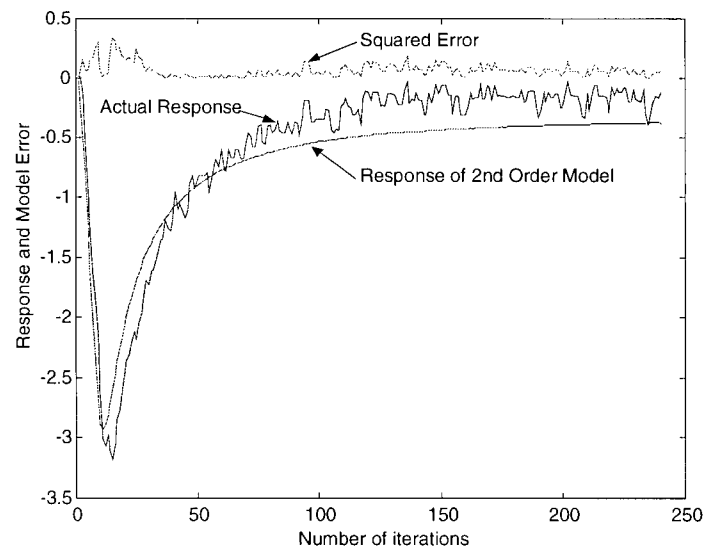
Figure 4-70   Validation of the 2nd order temp-moist model of experiment #6.

Repeated Experiment #3

Data file: redo_1kw.txt; Heater kept on for 8 minutes; Fan speed = 1000 RPM
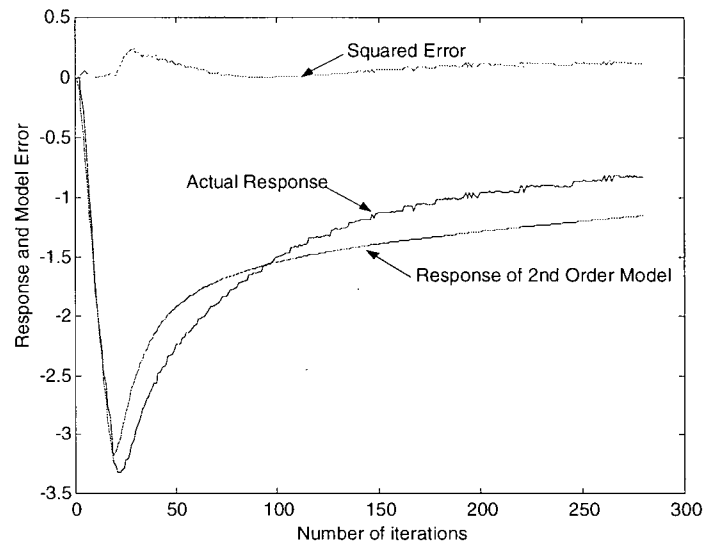
Figure 4-71   Validation of the 2nd order temp-moist model of repeated experiment #3.

Repeated Experiment #4

Data file: redo_exp9.txt; Heater kept on for 4 minutes; Fan speed = 1000 RPM
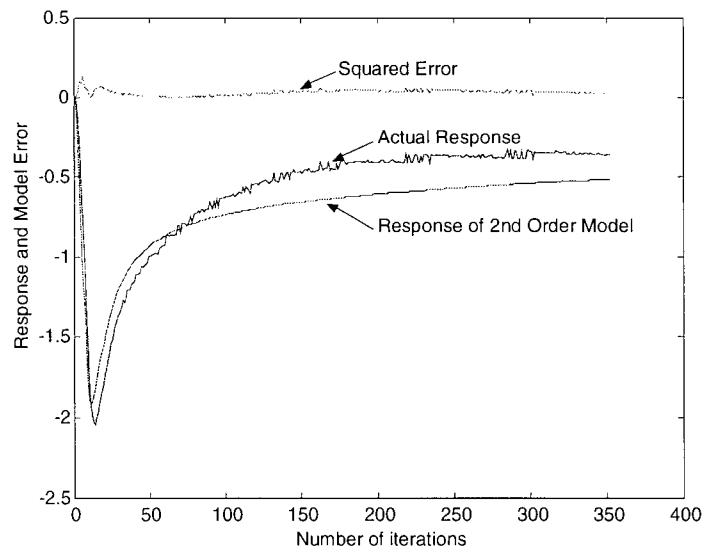
Figure 4-72   Validation of the 2nd order temp-moist model of repeated experiment #4.

4.4.3.2 Validation of the third order temperature-moisture content model

In this section, the same set of experimental data as for the second order model is used to validate the third order temperature-moisture content model. The actual kiln response, model response, and the squared error of the two responses are plotted in each figure below.

Experiment #5

Data file: pretest_1kw.txt; Heater kept on for 8 minutes; Fan speed = 1000 RPM
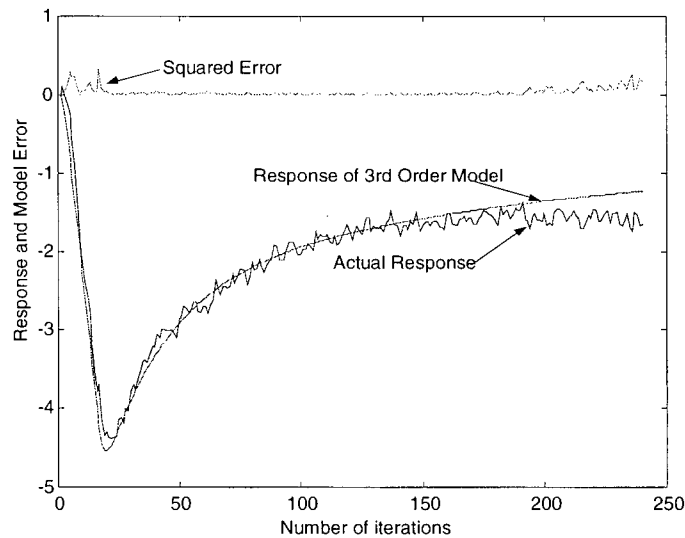
Figure 4-73   Validation of the 3rd order temp-moist model of experiment #5.

Experiment #6

Data file: exp9.txt; Heater kept on for 4 minutes; Fan speed = 1000 RPM
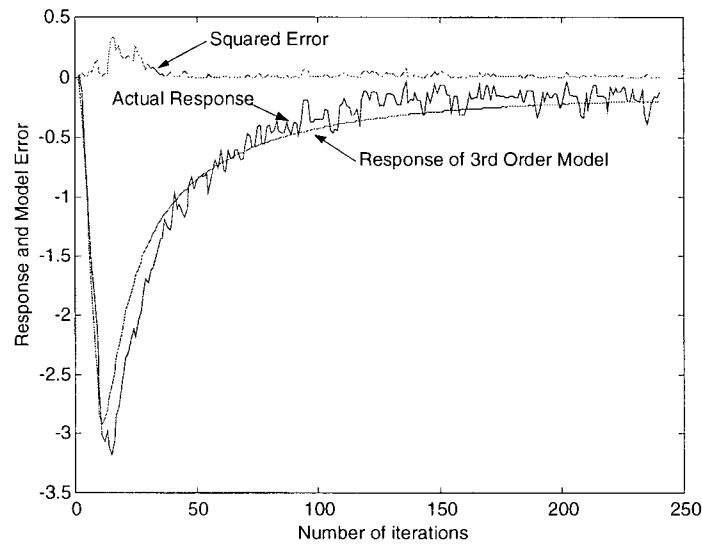
Figure 4-74   Validation of the 3rd order temp-moist model of experiment #6.

Repeated Experiment #3

Data file: redo_1kw.txt; Heater kept on for 8 minutes; Fan speed = 1000 RPM
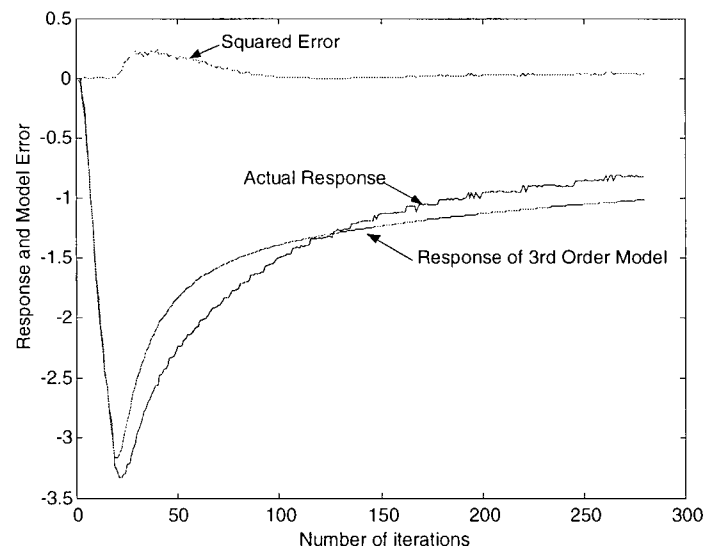
Figure 4-75   Validation of the 3rd order temp-moist model of repeated experiment #3.

Repeated Experiment #4

Data file: redo_exp9.txt; Heater kept on for 4 minutes; Fan speed = 1000 RPM
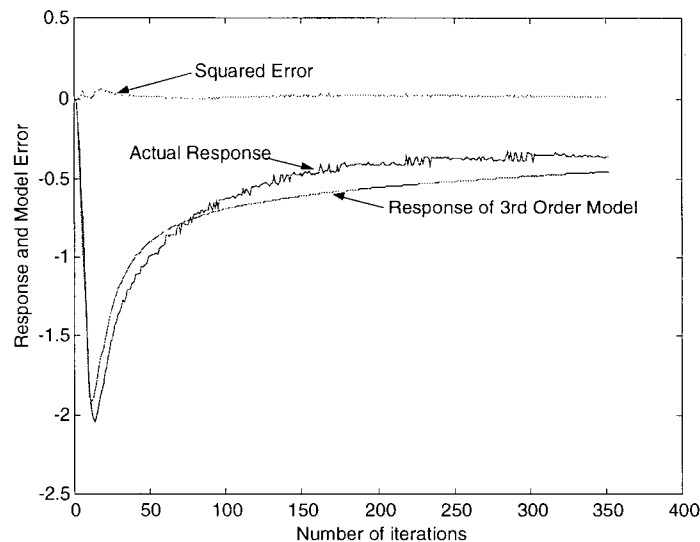
Figure 4-76   Validation of the 3rd order temp-moist model of repeated experiment #4.

From the results of model validation, it is noted that the results for the second order model structure of the temperature-moisture content relation are similar to those for the third order model structure. However, when the system order is increased from two to three, the performance does not improve. The root mean squared (rms) error and the standard deviation of error (std. error) for each of the four experiments are given in Table 4-22. The squared error between the actual experimental response and the model response for the second order model is small. However, this is not the case for the third order model. Worst cases are the experiment #5 and #6, and the repeated experiment #3. In both experiments #5 and #6, the estimated squared error is much larger than all the values estimated for the second order model. In repeated experiment #3, the estimated squared error is the largest among the others. In particular, the results from repeated experiment #3 should be discarded. Even though the std. error seems to be very small for the third order temperature-moisture content model estimated from experiments #5 and #6, these results do not give the least rms error. Both rms and std. error have to be considered in picking the best experimental model. In this sense, the second order temperature-moisture content model appears to provide the best results. Furthermore, the

147

parameters estimated for the second order SISO temperature-moisture model shows consistency in both sign and value, while the parameters estimated for the third order model do not show any consistency. Therefore, the second order model structure is more appropriate in representing the temperature-moisture content relation.

Table 4-22   Error values for the temperature-moisture content model.

Experiment	2nd Order Model		3rd Order Model	
	rms error	std. Error	rms error	std. Error
Experiment #5	0.6810	0.3009	1.3976	0.2785
Experiment #6	0.2084	0.2066	1.3296	0.3617
Repeated Experiment #3	0.4800	0.2109	2.4224	1.3760
Repeated Experiment #4	0.1844	0.1242	0.8364	0.2141

In the next section, the average value of the estimated parameters from experiments #5 and #6, and the repeated experiments #3 and #4 will be used as the parameter entries for the state space model. This average model will be used to validate with the actual kiln response in the four sets of experiments, and also in the two sets of internal heater control experiments, (experiments #7 and #8) using the data files test1 and test2.

4.4.3.3 Validation of the second order average model for temperature-moisture content

This section validates the second order *temperature-moisture* model for experiments #5 and #6, and the repeated experiments #3 and #4, using the average of estimated parameters. The squared error between the actual kiln response and the model response, together with the actual and model responses are all plotted in each figure below. The parameters used in the model validation in this section are given in Table 4-23.

Table 4-23   Estimated average parameters of the 2nd order temp-moist model.

2nd Order SISO Temp-Moist Model using Average Estimated Parameters	a_1	a_2	b_1	b_2
Model Validation Parameters	-0.8201	-0.1309	-0.0967	0.0915

Experiment #5

Data file: pretest_1kw.txt; Heater kept on for 8 minutes; Fan speed = 1000 RPM
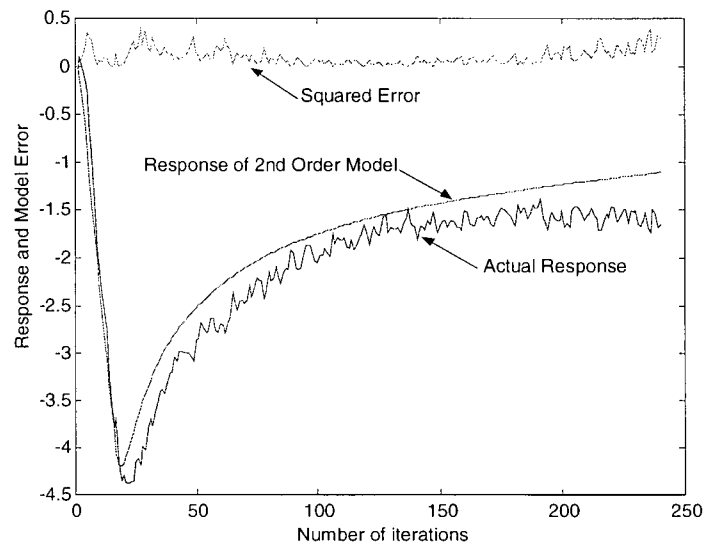
Figure 4-77   Validation of the 2nd order temp-moist model of experiment #5 using average estimated parameters.

Experiment #6

Data file: exp9.txt; Heater kept on for 4 minutes; Fan speed = 1000 RPM
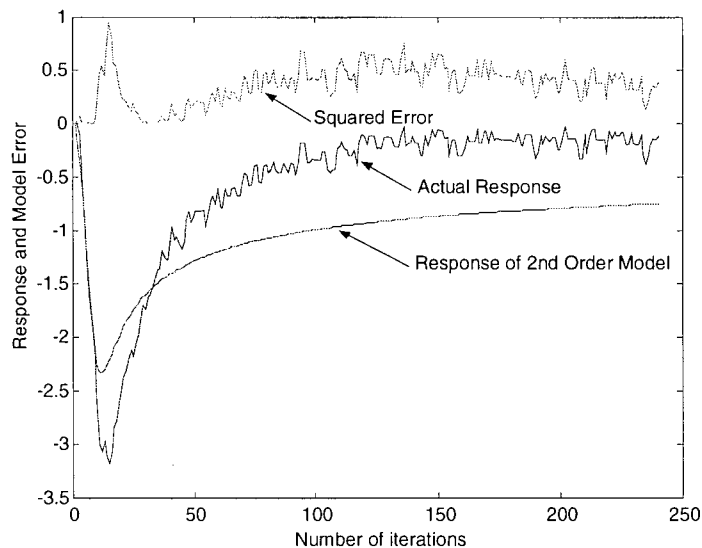
Figure 4-78   Validation of the 2nd order temp-moist model of experiment #6 using average estimated parameters.

Repeated Experiment #3

Data file: redo_1kw.txt; Heater kept on for 8 minutes; Fan speed = 1000 RPM
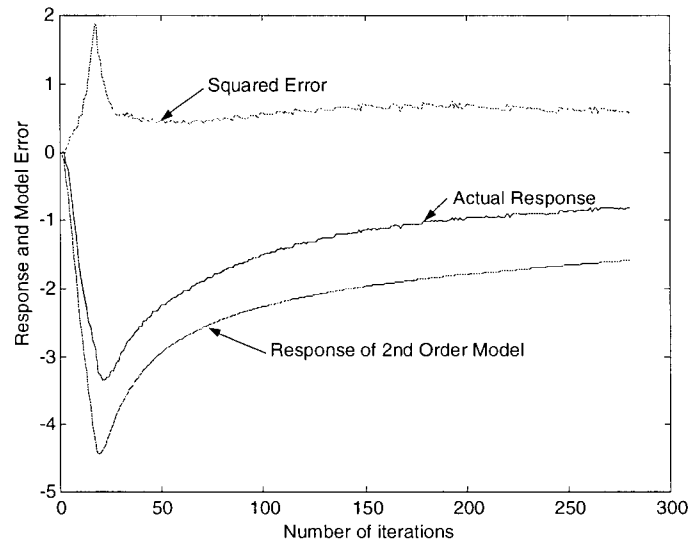
Figure 4-79   Validation of the 2nd order temp-moist model of repeated
                     experiment #3 using average estimated parameters.

Repeated Experiment #4

Data file: redo_exp9.txt; Heater kept on for 4 minutes; Fan speed = 1000 RPM
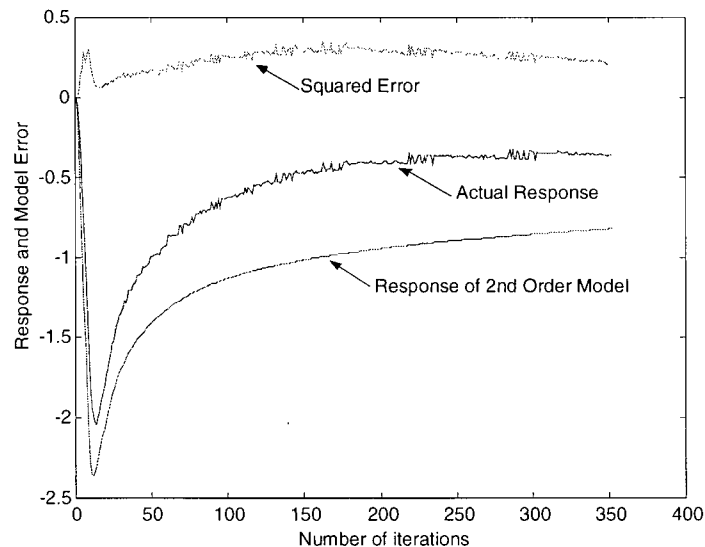
Figure 4-80   Validation of the 2nd order temp-moist model of repeated
                     experiment #4 using average estimated parameters.

Note the results obtained using average parameters estimated from experiments utilizing external heater control signal generated by the PC. The model response appears to match the actual kiln response for the first 50 iterations (25 minutes). After that the model response does not follow the actual response, and therefore the squared error increases significantly after 100 iterations, (approximately one hour). This can be accounted for by the changing dynamics of the drying process, which includes the change of microscopic wood structure and interactions between heat transfer and moisture evaporation. The root mean squared (rms) error and the standard deviation of error (std. error) for each of the four experiments are given in Table 4-24. Based on these results of model validation for the second order *temperature-moisture* model using the average of estimated parameters, it is seen the estimated models are not uniformly satisfactory. In experiment #5, model response closely follows the actual response in the descending region. However, this is not the case in both the rising region and the steady region. A similar behavior is seen in all four experiments. Worst case is the experiment #6, and the estimated squared error is the largest among the others. The squared error between the actual experimental response and the model response appears to be very large in all cases. Even though the std. error seems to be the least in experiment #5 and repeated experiment #4, the results do not give the least rms error.

Table 4-24   Error values for the temperature-moisture content model using internal heater control data file.

Experiment	2nd Order Model	
	rms error	std. Error
Experiment #5	0.8664	0.2133
Experiment #6	2.6260	1.7743
Repeated Experiment #3	2.2762	0.8301
Repeated Experiment #4	0.9638	0.2375

4.4.3.4 Validation of the second order temperature-moisture content model using internal heater control data file

This section summarizes the model validation of experiments #7 and #8 that have been carried out using internal heater control signal as the input signal to the system. The actual kiln response, model response, and the squared error of the two responses are plotted in each figure below.

Experiment #7

- Upper temperature limit = 100°C; lower limit = 98°C

- Fan speed = 1000 RPM

- Heater on when temperature drops below the lower temperature setting

- Heater off when temperature exceeds the upper temperature setting
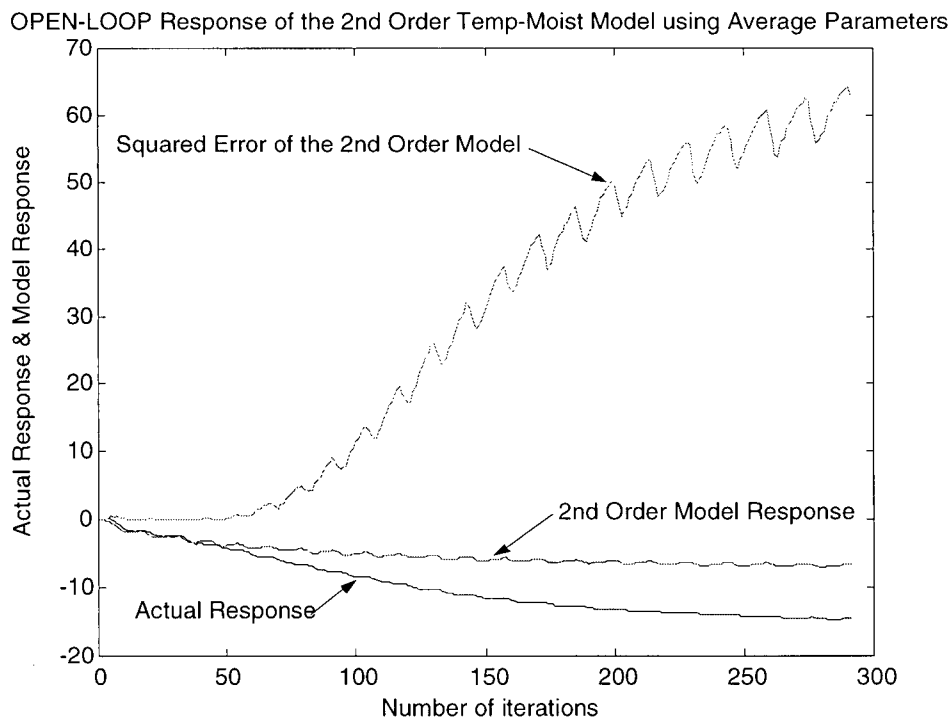
Figure 4-81   Validation of the 2nd order temp-moist model of experiment #7 using internal heater control input signal.

Experiment #8 (Same as experiment #7 but with different initial experimental condition)

- Upper temperature limit = 100°C; lower limit = 98°C

- Fan speed = 1000 RPM

OPEN-LOOP Response of the 2nd Order Temp-Moist Model using Average Parameters
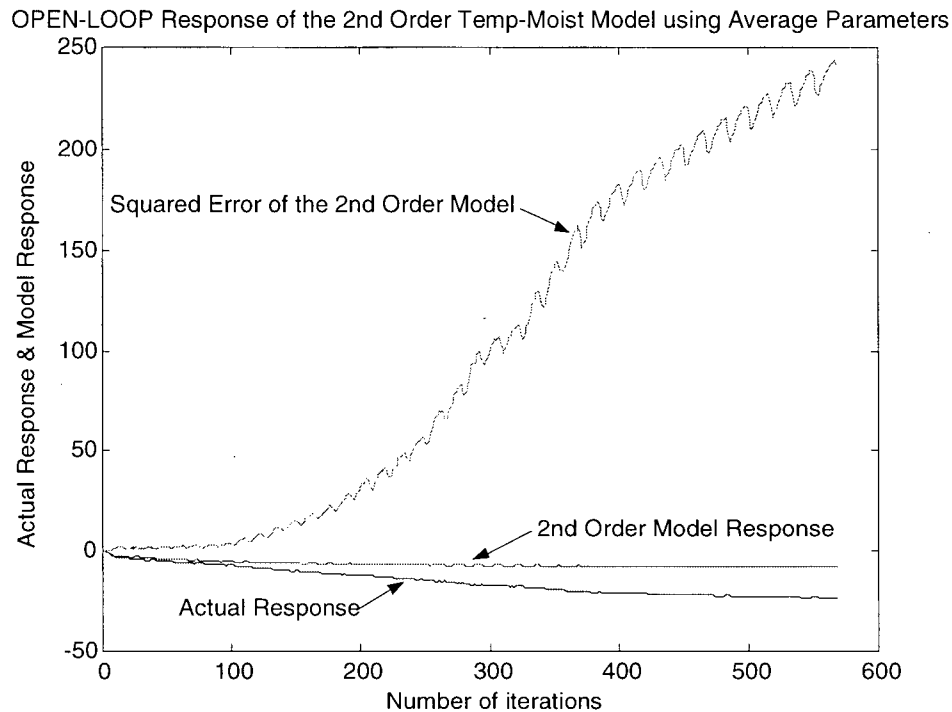
Figure 4-82   Validation of the 2nd order temp-moist model of experiment #8 using internal heater control input signal.

From the simulation result of experiments 7 and 8, it is noticed that the squared error between the model response and the actual response increases drastically, as before, after 100 iterations (one hour). This indicates that the model structure is not adequate as the process is time varying, and hence the model response no longer follows the actual response.

153

4.4.4 Validation of the 2nd order SISO heat-temperature model

This section presents the model validation of the second order SISO *heat-temperature* model, using average estimated parameters. The temperature model used in this section for model validation is based on the average value of the estimated parameters computed from the previous set of experiments. The corresponding model parameters are given in Table 4-25.

Table 4-25   Estimated average parameters of the second order SISO heat-temperature model.

Model Parameters	a_1	a_2	b_1	b_2
Parameter Values	-1.6243	0.6299	1.0882	0.2046

Experiment #5

Data file: pretest_1kw.txt; Heater kept on for 8 minutes; Fan speed = 1000 RPM
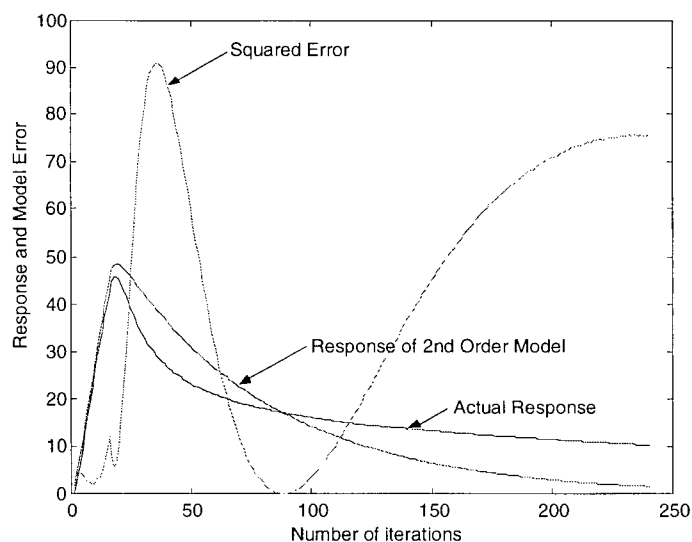
Figure 4-83   Validation of the 2nd order heat-temp model of experiment #5 using average estimated parameters.

Experiment #6

Data file: exp9.txt; Heater kept on for 4 minutes; Fan speed = 1000 RPM
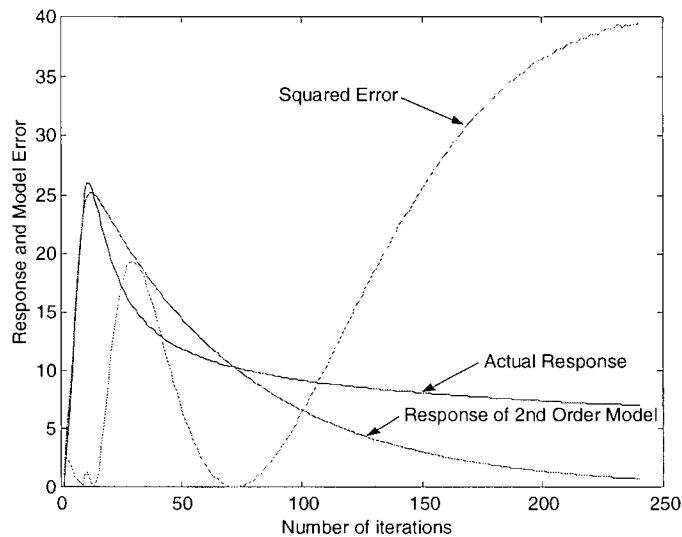
Figure 4-84   Validation of the 2nd order heat-temp model of experiment #6 using average estimated parameters.

Repeated Experiment #3

Data file: redo_1kw.txt; Heater kept on for 8 minutes; Fan speed = 1000 RPM
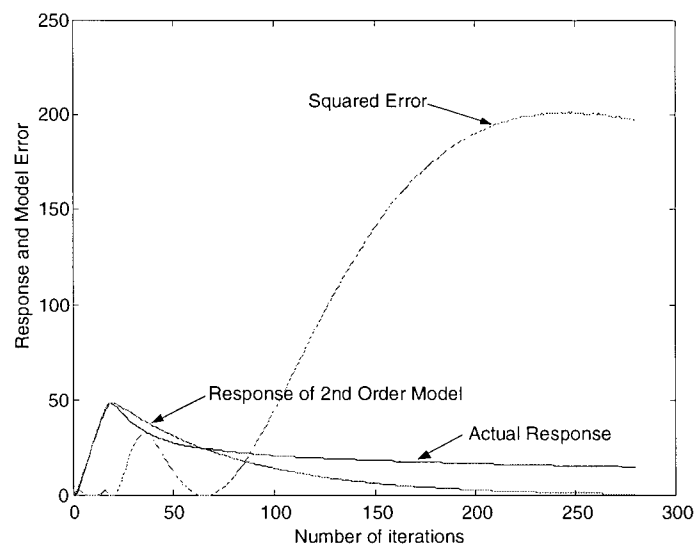
Figure 4-85   Validation of the 2nd order heat-temp model of repeated experiment #3 using average estimated parameters.

155

Data file: redo_exp9.txt; Heater kept on for 4 minutes; Fan speed = 1000 RPM
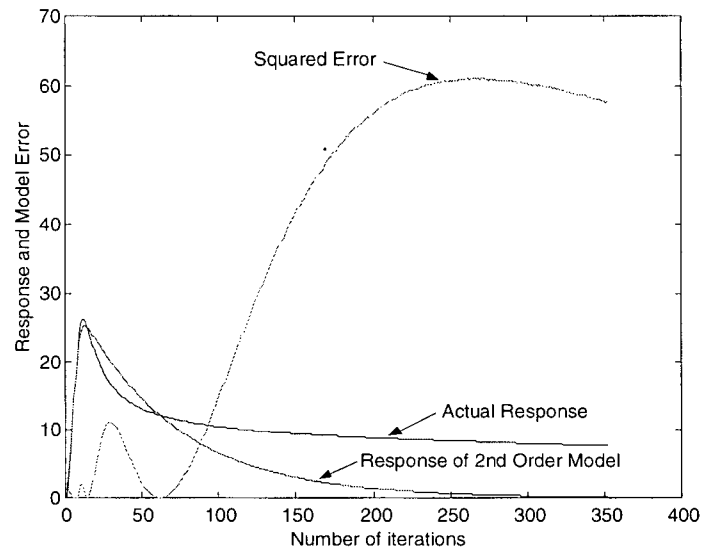
Figure 4-86   Validation of the 2nd order heat-temp model of repeated
experiment #4 using average estimated parameters.

The root mean squared (rms) error and the standard deviation of error (std. Error) for each of the four experiments are given in Table 4-26. Both the squared error and the standard deviation of error between the actual experimental response and the model response appear to be very large in all cases. Response of the temperature model that uses a second order SISO structure basically follows the shape of the actual response of the kiln. The rising portions of the two responses coincide almost exactly, and then deviate from each other after about 70 iterations (approximately 35 minutes). The model response ends with a zero value in all cases since the model is assumed to be linear, and zero initial conditions are assumed. The actual response is always higher than the model response since the system starts at room temperature. The temperature of the actual kiln does not go to zero, and it returns to the room temperature after the heater is shut off.

Table 4-26   Error values for the heat-temperature model.

Experiment	2nd Order Model	
	rms error	std. Error
Experiment #5	0.8664	0.2133
Experiment #6	2.6260	1.7743
Repeated Experiment #3	2.2762	0.8301
Repeated Experiment #4	0.9638	0.2375

4.5 Model Index

In this section, a model index (*M.I.*) is defined as the ratio of the root mean square (rms) value of the error between the actual kiln response and the estimated model response. Assume a sequence of control inputs $\{u(1), u(2) \dots , u(N-1), u(N)\}$ that are applied to the system. The corresponding sequence of actual response values of the system $\{y(1), y(2), \dots , y(N-1), y(N)\}$ and the sequence of model outputs $\{\hat{y}(1), \hat{y}(2), \dots , \hat{y}(N-1), \hat{y}(N)\}$ are determined. The sequence of estimation error values $\{e(1), e(2), \dots , e(N-1), e(N)\}$, is then determined, and the squared error values are computed according to

$$e^2_{(i)} = (y_{(i)} - \hat{y}_{(i)})^2 \tag{4.21}$$

Then, the mean square error is given by

$$\bar{e}^2_{(i)} = \frac{e^2_{(i)}}{N} \tag{4.22}$$

The root mean square (rms) value of estimation error, *RMS$_{error}$*, is given by

$$RMS_{error} = \sqrt{\frac{(e_{(1)} + e_{(2)} + \dots + e_{(N-1)} + e_{(N)})^2}{N}} \tag{4.23}$$

157

Similarly, the root mean square value of actual response, $RMS_{actual\ response}$, is given by

$$RMS_{actual\ response} = \sqrt{\frac{(y_{(1)} + y_{(2)} + ... + y_{(N-1)} + y_{(N)})^2}{N}} \qquad (4.24)$$

The model index ($M.I.$) is defined as

$$M.I. = \frac{RMS_{error}}{RMS_{actual\ response}} \times 100\% \qquad (4.25)$$

It should be clear that the model index is an indication of how well the model represents the actual system. The model index is computed as a percentage. The larger the value of M.I. the larger the estimation error between the actual response and the model response. The model index values for the six experiments of the section on model validation (Sections 4.4.3.1., 4.4.3.2., 4.4.3.3., 4.4.3.4., and 4.4.4.) are given in Tables 4-27 through 4-31.

Table 4-27   Model Index values for the second order SISO temperature-moisture model (External heater control).

Experiment Number	Data File	Model Index
Experiment #5	pretest_1kw.txt	8.98%
Experiment #6	exp9.txt	27.58%
Repeated Experiment #3	redo_1kw.txt	17.70%
Repeated Experiment #4	redo_exp9.txt	24.53%

Table 4-28   Model Index values for the third order SISO temperature-moisture model (External heater control).

Experiment Number	Data File	Model Index
Experiment #5	pretest_1kw.txt	8.13%
Experiment #6	exp9.txt	18.49%
Repeated Experiment #3	redo_1kw.txt	14.05%
Repeated Experiment #4	redo_exp9.txt	18.14%

158

Table 4-29   Model Index values for the second order SISO temperature-moisture model using average estimated parameters (External heater control).

Experiment Number	Data File	Model Index
Experiment #5	Ave. estimated parameters	14.45%
Experiment #6	Ave. estimated parameters	66.46%
Repeated Experiment #3	Ave. estimated parameters	50.23%
Repeated Experiment #4	Ave. estimated parameters	69.90%

Table 4-30   Model Index values for the second order SISO temperature-moisture model (Internal heater control).

Experiment Number	Data File	Model Index
Experiment #7	test1.txt	50.39%
Experiment #8	test2.txt	60.36%

Table 4-31   Model Index values for the second order SISO heat-temperature model using average estimated parameters (External heater control).

Experiment Number (data file)	Data File	Model Index
Experiment #5 (pretest_1kw.txt)	Ave. estimated parameters	33.81%
Experiment #6 (exp9.txt)	Ave. estimated parameters	40.06%
Repeated Experiment #3 (redo_1kw.txt)	Ave. estimated parameters	46.88%
Repeated Experiment #4 (redo_exp9.txt)	Ave. estimated parameters	56.84%

4.5.1   Discussion of the model index results

By comparing the model index values of the second and the third order temperature-moisture model, using the same data file, it is noted that the model index is found to improve when system order increases. Since there is no consistency in both the value and the sign of the estimated parameters for the third order model, average estimated parameters are computed based on the estimated parameters of the second order model. Due to reasons of model nonlinearity, it is seen that the model index doubles when the average parameters are used. For the 2nd order temperature model using average estimated parameters, model index is found to vary from 30% to 60%. This variation is

accounted for by the variation of the microstructure of the wood, particular since different wood pieces are used in the experiments.

It may be concluded that the wood drying process may be represented more appropriately by separating the entire process into two sub-systems, namely the *heat-temperature* model and the *temperature-moisture* model. Also, the drying process is found to have some time delay, and the process is clearly nonlinear. Due to the inconsistency in the higher order estimated parameters and the high values of the computed model index values, it appears that model-based conventional control is inadequate for proper control of an industrial lumber drying kiln. Model-free intelligent control using fuzzy logic appears to be more desirable in view of these observations. This aspect is addressed in Chapter 5.

Chapter 5

` CONTROLLER DEVELOPMENT AND SIMULATION

5.1   Introduction

This chapter presents the two closed-loop controllers that have been developed for the wood-drying kiln. The controllers use direct moisture feedback from wood pieces. Both conventional and intelligent control methodologies are incorporated into the system. The performance of the controllers is compared and evaluated, using computer simulations. Both controllers are designed to operate at an operating temperature below 85 °C, in order to ensure satisfactory quality of dried wood. In the following sections, design details of the controllers are elaborated. The simulations performed in this section assume zero initial conditions. The room temperature is assumed to be 25 °C, with respect to which the temperature readings are given. For example, temperature reading of 60 °C corresponds to an actual temperature of 85 °C.

5.2   Conventional PID Control System

First a double loop proportional-integral-derivative (PID) control system is developed to provide feedback control for the wood-drying kiln. The control system consists of a *Moisture PID* controller (M-PID) in the outer loop, and a *Temperature PID* controller (T-PID) in the inner loop, with a *pulse-width-modulated* (PWM) heater controller. The block diagram of the PID control system is illustrated in Figure 5-1.

The physical kiln system may be separated to two main processes as the heat-temperature process and the temperature-moisture process. Analogously, then, the model of the kiln system is also divided into two sub-systems, as mentioned in Chapter 4; specifically, the *heat-temperature* model and the *temperature-moisture* model. This representation is shown in Figure 5-1. Converged, average parameters obtained from the

parameter estimation procedure are used in the models that build up the kiln model. The proportional gain (K_p), integral gain (K_i), and derivative gain (K_d) for both M-PID and T-PID are selected using the Ziegler-Nichols technique [34] and is presented in Table 5-1.
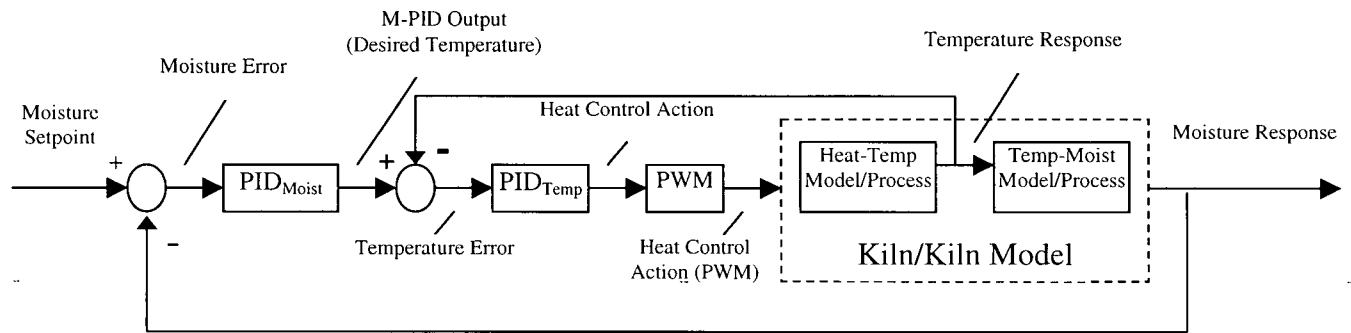
Figure 5-1   Block diagram of the PID control system.

Figure 5-2 gives an elaborate block diagram showing the details of the overall system, which is used for simulation in MATLAB Simulink. The Temp-Control subsystem represents the heat-temperature model, which consists of the second order ARMA model (with average parameter values obtained from parameter estimation in Chapter 4), and the PWM heater controller. The latter controller is further broken down for illustration. Similarly, the temperature-moisture model is represented by the second order ARMA model as shown in the figure. The transfer function representing the second order ARMA models of the heat-temperature process and the temperature-moisture process for the simulation, respectively, are given by

$$\frac{Y(z)}{U(z)} = \frac{1.0882\, z^{-1} + 0.2046\, z^{-2}}{1 - 1.6243\, z^{-1} + 0.6299\, z^{-2}} \tag{5.1}$$

$$\frac{Y(z)}{U(z)} = \frac{-0.0967\, z^{-1} + 0.0915\, z^{-2}}{1 - 0.8201\, z^{-1} - 0.1309\, z^{-2}} \tag{5.2}$$
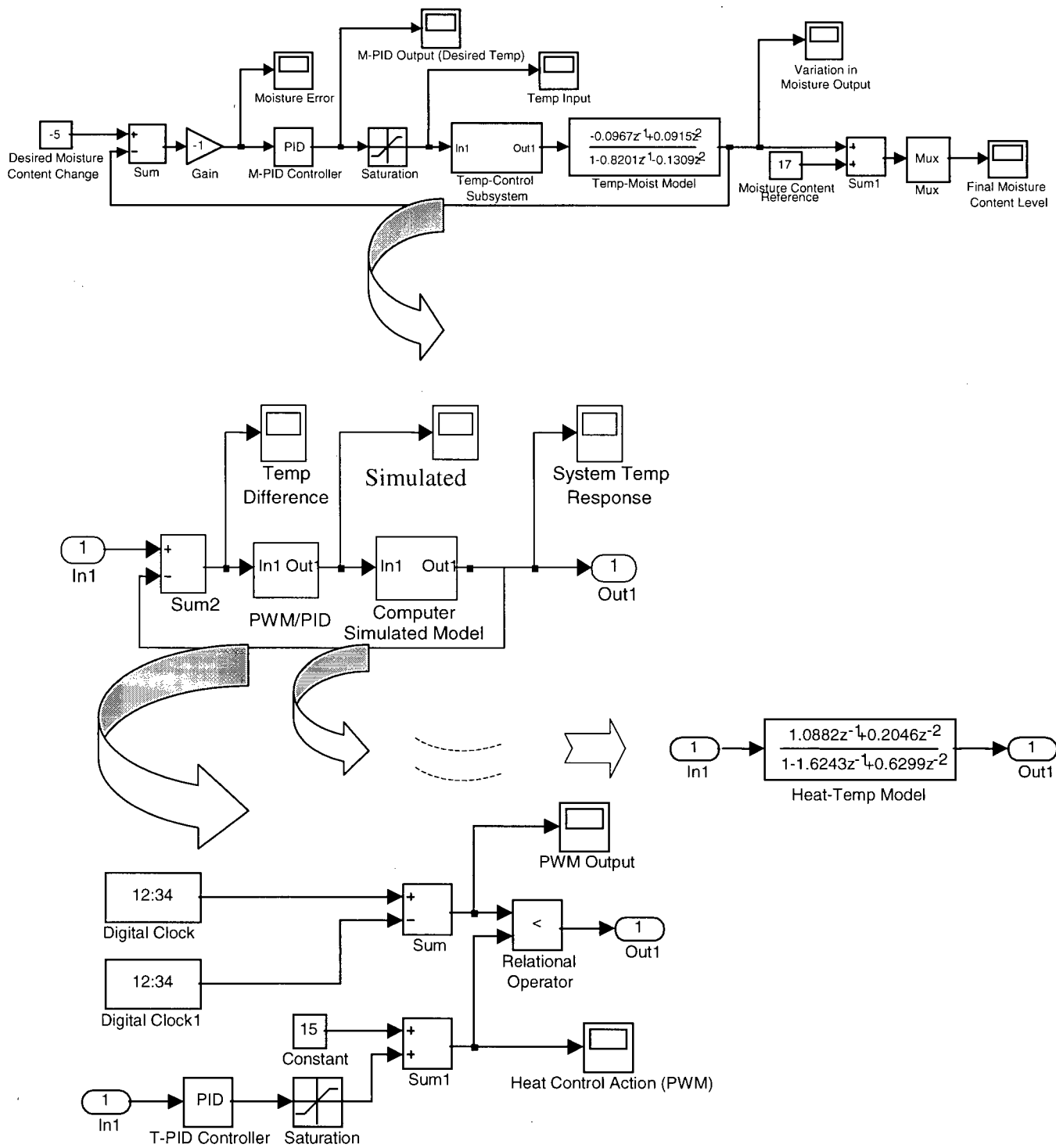
Figure 5-2   The elaborate block diagram of the PID control system.

163

Table 5-1   PID controller gains.

Controller	Proportional Gain (K_p)	Integral Gain (K_i)	Derivative Gain (K_d)
M-PID	95	0.003	0.01
T-PID	20	0.005	0.60

The moisture error is calculated from the difference between the moisture setpoint and the actual average moisture response from the sensor for wood moisture content. The moisture error is then corrected by the Moisture-PID controller, and the M-PID output which has a physical meaning of desired temperature, is then compared with the actual average temperature response as measured by thermocouples. The temperature error is then corrected by the inner T-PID controller. The resulting heat control action which is pulse-width-modulated (PWM) is used to control the heater on duration within each sampling time interval. Typical simulation results of the PID control system are presented in the next section. All computer simulations are run for two hours, using a sampling time of 30 seconds. The control system is aimed at reducing the moisture content by 3% and 5%, in the cases shown in Figures 5-3 and 5-4, respectively.

5.2.1   PID simulation results

Both the moisture response and the moisture error are computed during the entire drying simulation. The M-PID output which depends on the error between the moisture setpoint and the actual moisture response, is computed and has a physical meaning of the desired temperature. Also, the temperature response is computed as the output of the Heat-Temperature model, and the pulse-width-modulated heat control action is computed as the output of the PWM module, which depends on the T-PID output. Figure 5-3 shows the simulation results for the case of a desired reduction of the moisture content by 3%.

From the results of this case, it is evident that the PID controller is capable of bringing down the wood moisture content from 17% to 14%, as desired, with a maximum error of 0.6%. Saturation (at 300 °C) occurs in the desired output temperature as generated by the M-PID at the very beginning of the simulation.
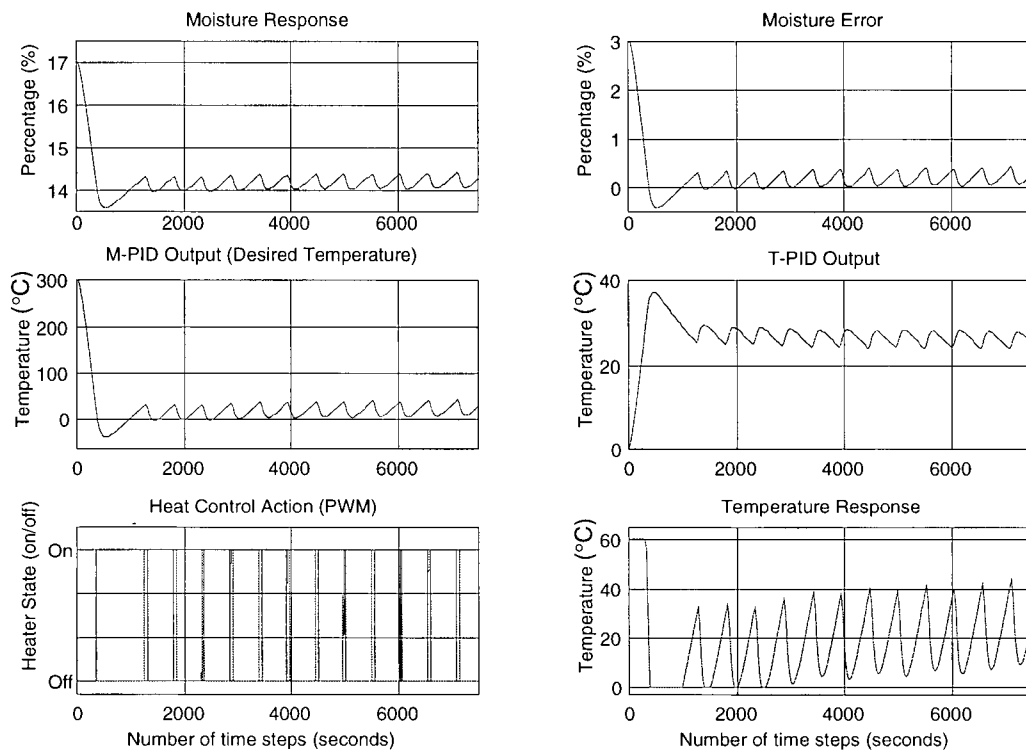
Figure 5-3   Simulation results from the PID control system for a desired reduction of
moisture by 3%.
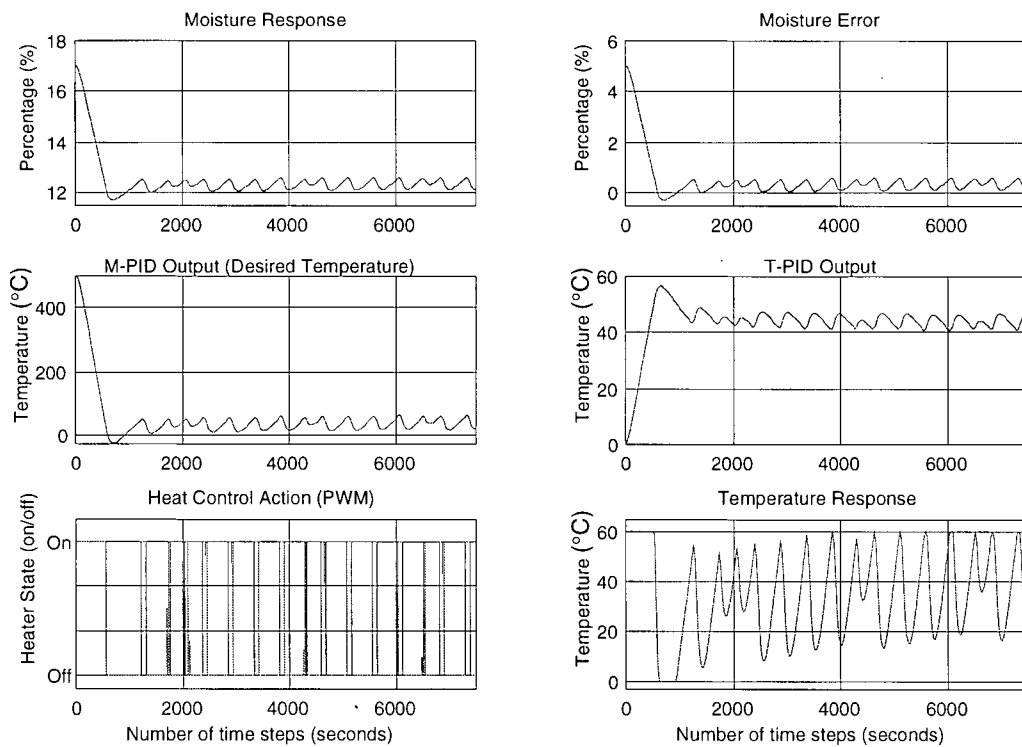
Figure 5-4   Simulation results from the PID control system for a desired reduction of
moisture by 5%.

The desired temperature is then maintained at an average value of 52 °C for the rest of the simulation, as clear from Figure 5-3. The PWM heat control action is recorded. The heat control action from the T-PID shows reasonably satisfactory result. The simulation results for a desired 5% reduction of moisture is shown in Figure 5-4. In this case, the PID controller is capable of removing moisture from 17% to 12%, with a maximum error of 0.6%. Saturation occurs at the M-PID output for the desired temperature of 500 °C, which is higher than the saturation value in removing 3% of moisture, which is justified since more energy is required to remove the extra moisture. The rest of the simulation is maintained at an average desired temperature of 70 °C. The PWM control action for the heater is also recorded.

5.3   Fuzzy Logic Control System

Now, the use of direct fuzzy logic control in the kiln system is demonstrated through computer simulation. The fuzzy logic control system that has been developed in the present work consists of a *Fuzzy Moisture* controller in the outer loop for correcting the moisture error, and a *Temperature PID* (T-PID) in the inner loop with pulse-width-modulated (PWM) heater control as before. The block diagram of the fuzzy control system is basically the same as the PID control system, except that the *Moisture PID* (M-PID) is replaced by the *Fuzzy Moisture* controller, and is presented in Figure 5-5.
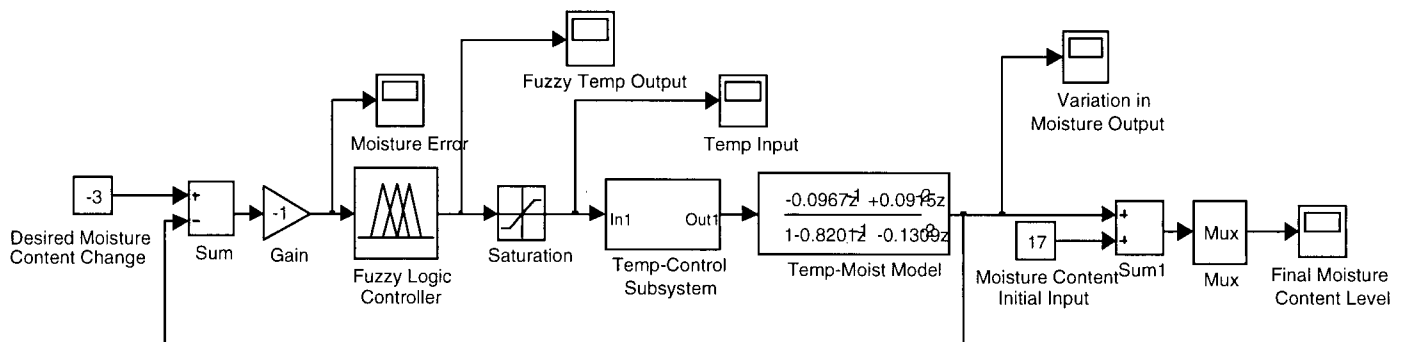
Figure 5-5   The simulation block diagram (Simulink) of the fuzzy-logic moisture control system.

The input to the *Fuzzy Moisture* controller is the moisture error, which is defined as the difference between the moisture content setpoint and the actual moisture content of the wood as measured by the in-wood moisture content sensors. The output of the *Fuzzy Moisture* controller is the desired temperature of the kiln. The moisture error is given by

$$Moisture\ Error\ (e_{moisture}) = Moisture\ Setpoint - Actual\ Moisture\ Content \qquad (5.3)$$

5.3.1 Membership Functions

A crucial step in the development of a fuzzy logic controller is the proper selection of membership functions for both input (condition) and output (action) variables in the rulebase. A common practice in establishing a membership function for a particular fuzzy set is to first discretize the universe of discourse, and then assigns a degree of membership to each value in the universe. Triangular and trapezoidal shapes are commonly used.

In the present thesis, a triangular shape membership function with a peak grade of unity for the most representative value of the fuzzy quantity, is chosen for the input variables. Both triangular and trapezoidal functions are chosen as the membership function of the output variables. The membership functions for both input and output variables are shown in Figure 5-6.

The fuzzy variable representing the moisture error is defined to have five fuzzy states with the corresponding membership functions denoting the input variables. The five states are: negative small (NS), zero (ZR), positive small (PS), positive medium (PM) and positive large (PL). The fuzzy variable of the control inference, which is the desired kiln temperature is also assigned a resolution of 5. These fuzzy states of the action variable are defined as very low (VL), low (L), medium (M), high (H) and very high (VH), with associated membership functions chosen as discussed before.

167
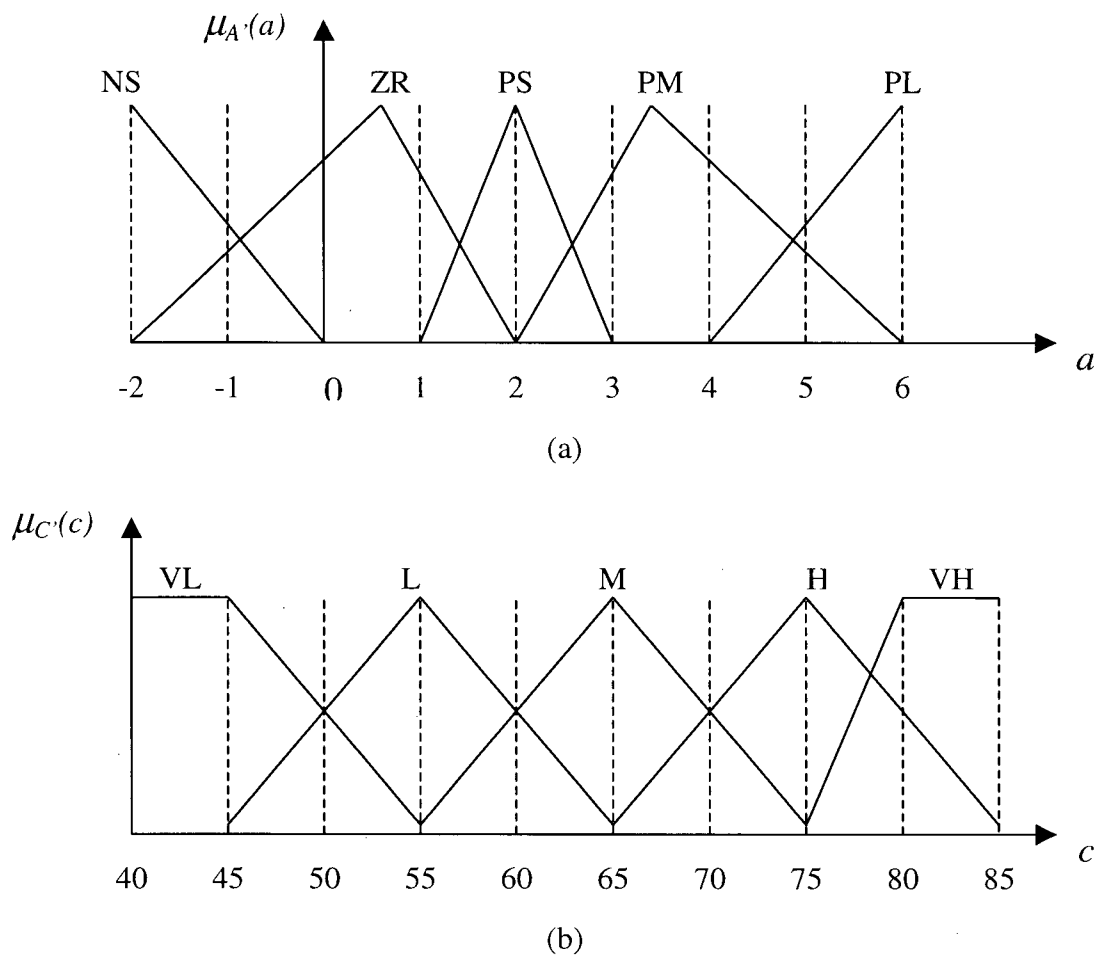
Figure 5-6   Membership functions of: (a) input (condition) variables; (b) output (action) variables.

5.3.2 Fuzzy rulebase

In general, a rule in a fuzzy knowledge base of direct fuzzy control, is a relation of the form:

$$\text{IF } A_i \text{ THEN } C_i \tag{5.4}$$

where, A_i is a fuzzy quantity representing process measurement; in the present situation it represents wood moisture error, and C_i is a fuzzy quantity representing a control action;

here it represents a change in reference temperature. The compositional rule of inference is given by

$$\mu_{C'}(c) = \sup_{a} \min \left[\mu_{A'}(a), \mu_R(a,c) \right] \tag{5.5}$$

where $\mu_{C'}$ is the membership function of the control inference, and $\mu_{A'}$ and μ_R are the membership functions of fuzzy set A' and fuzzy relation R, respectively. Note that R represents the control rulebase. The final crisp control inference is obtained through defuzzification of the fuzzy inference C' using the centroid method.

The support set S of a fuzzy set A is the crisp set formed by the collection of all elements $x_i \in X$, such that $\mu_A(x_i) > 0$. Let the membership function of a control inference be given by $\mu_C(c)$, with a support set S. The crisp control action $\hat{c}$, using the centroid method, is determined by, in the discrete case,

$$\hat{c} = \frac{\displaystyle\sum_{c_i \in S} c_i \mu_C(c_i)}{\displaystyle\sum_{c_i \in S} \mu_C(c_i)} \tag{5.6}$$

The moisture error (crisp) obtained from the moisture setpoint and the actual wood moisture sensor measurements is first fuzzified in order to apply the compositional rule of inference by equation (5-5). The resulting control inference (C') is defuzzified to provide the crisp control action ($\hat{c}$) using equation (5-6).

The rule base of the *Fuzzy Moisture* controller consists of five rules that are of the form given by (5-4), and is summarized below:

	IF *moisture* is *NS*	THEN *temperature* is *VL*
or	IF *moisture* is *ZR*	THEN *temperature* is *L*
or	IF *moisture* is *PS*	THEN *temperature* is *M*
or	IF *moisture* is *PM*	THEN *temperature* is *H*
or	IF *moisture* is *PL*	THEN *temperature* is *VH*

Through implementation of the linguistic rules and membership functions, a direct fuzzy logic controller for moisture control is developed. The simulation results of the fuzzy logic control system, implemented using MATLAB Simulink, is presented in the next section.

5.3.3 Simulation results

The fuzzy logic controller is developed by implementing the rule base with the corresponding membership functions of the fuzzy variables in MATLAB using the Fuzzy Toolbox. The simulation block diagram used in MATLAB Simulink, for computer simulation of the developed fuzzy logic control system, is shown in Figure 5-5. The block diagram of the fuzzy control system is similar to that of the PID control system, except that the M-PID controller is replaced by the fuzzy logic controller, for moisture control. Simulations for the desired removal of 3% and 5% of moisture are performed.

The moisture error is calculated as before and is corrected by the fuzzy logic controller to provide the desired output temperature. Similarly, the temperature error is corrected by the inner T-PID controller, which provides a heat control action as a pulse-width-modulated (PWM) signal. It was found that the fuzzy logic controller is able to dry the wood from a moisture content of 17% down to 14% with a maximum deviation of 0.3%, which is only half the error resulted from the PID controller. Simulations were run for two hours, and no saturation was found to occur during the entire simulation period. The average desired operating temperature is approximately 50 °C and the average value of the percentage duty cycle of the PWM heater controller is less than 15%, compared with a 50% duty cycle for the PID controller. This shows a distinct improvement due to the fuzzy logic control system, where a conventional PID controller is integrated with intelligent control. Figure 5-7 shows the simulation results for the fuzzy logic control system in removing 3% of moisture.
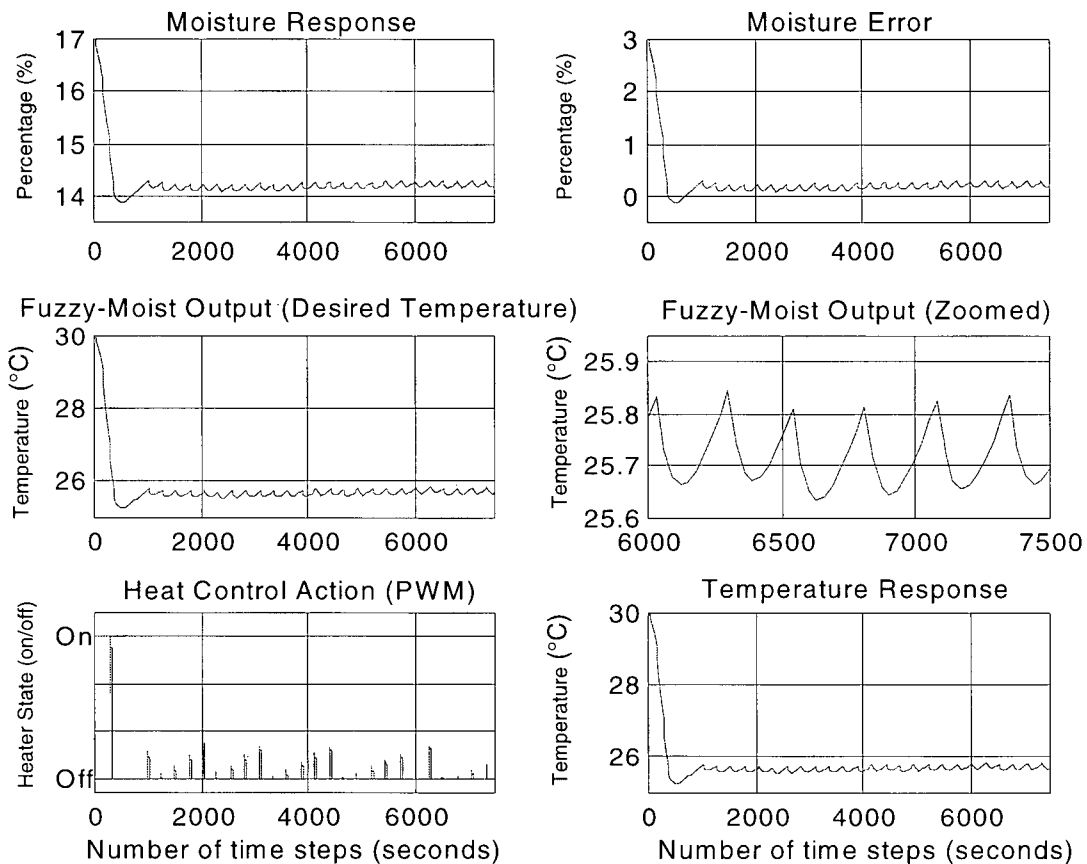
Figure 5-7   Simulation results from the Fuzzy + PID control system for the desired reduction of moisture by 3%.

Similarly, the simulation results for the removal of 5% of moisture is given in Figure 5-8. The fuzzy control system was found to be capable of removing the moisture content from 17% to 12% with a maximum error of 0.3%, which is again only half of the error resulted from the PID control system. Saturation did not occur throughout the simulation. The average value of the pulse-width-modulated heater control is less than 30% duty cycle. The average desired temperature is 70 °C for the entire simulated drying process. In this case, the required energy (PWM duty cycle) and the desired temperature are higher than those for the 3% moisture removal since a larger quantity of moisture was removed.
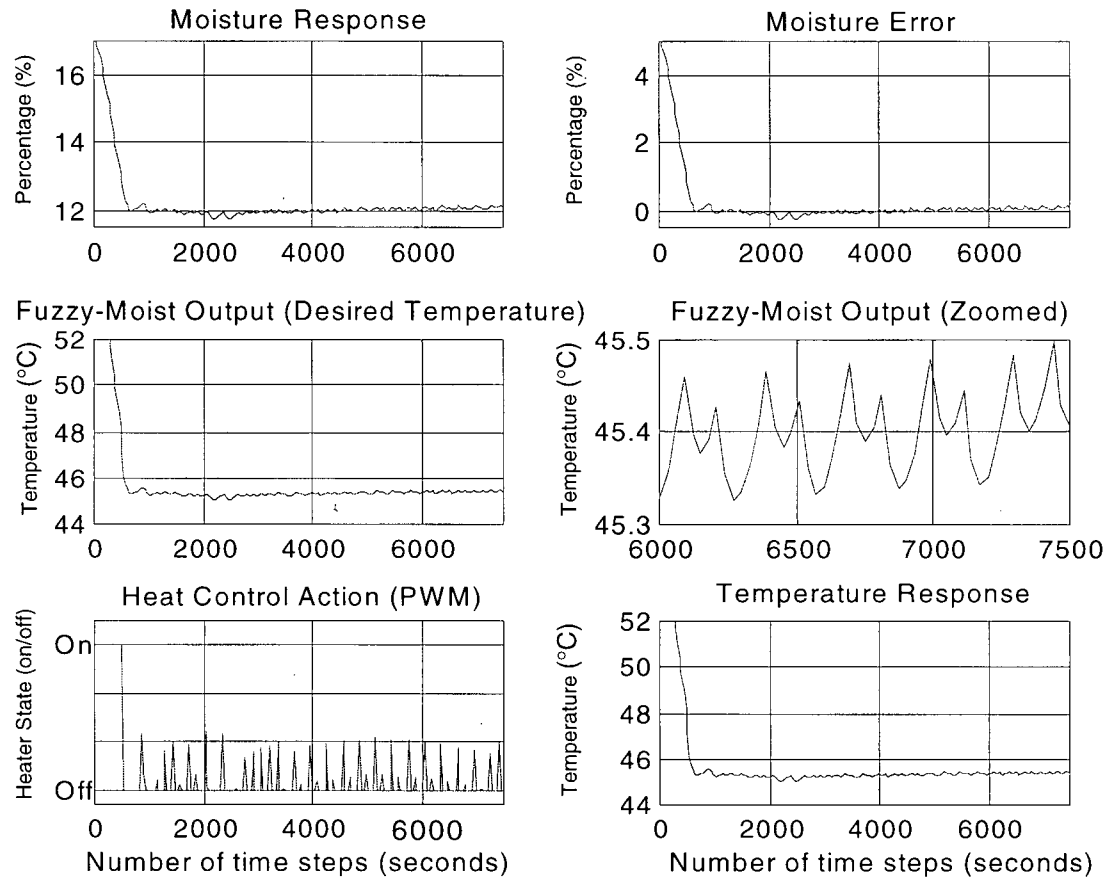
Figure 5-8   Simulation results from the Fuzzy + PID control system for the desired
reduction of moisture by 5%.

5.4   Discussion

From the simulation results it was found that the Fuzzy + PID control system gives
superior results compared to the conventional PID control system. This can be attributed
to the flexibility of the fuzzy logic controller and the use of a control knowledge base that
is specific to the particular process, which can provide better performance in complex
processes.

In both 3% and 5% moisture removal simulations, the fuzzy logic control system was
found to reduce the error of the final moisture setpoint to half that from PID control, and
at the same time resulted in significant reduction in the PWM duty cycle. This
improvement can lead to considerable economic benefits in the wood drying industry.

This is particularly true since two critical factors in determining the success of wood drying are the quality of dried wood and the duration of the wood drying process. An improvement of either one of these two factors can lead to substantial benefits in the wood drying industry. In Chapter 6, the two controllers will be implemented in the prototype kiln and experiments will be performed to compare with the simulation results.

Chapter 6

CONTROLLER IMPLEMENTATION AND EXPERIMENTATION

The two controllers developed in the present work are implemented on the prototype kiln system at the National Research Council. This chapter presents on-line experimental studies of the controllers using the prototype system. The experimental results are presented and the controller performance is investigated.

6.1 On-line PID Control System

Conventional PID Control System

The double loop proportional-integral-derivative controller developed in this work, was as employed in Chapter 5 for the purpose of computer simulation studies. The same controller is implemented on-line in the prototype wood drying kiln. The gains for both the *Moisture PID* (M-PID) in the outer loop and the *Temperature PID* (T-PID) in the inner loop are identical to the gains being used in the simulations, and is given in Table 6-1.

Table 6-1   Gains used in the conventional PID controllers.

Controller	Proportional Gain (K_p)	Integral Gain (K_i)	Derivative Gain (K_d)
M-PID	95	0.003	0.01
T-PID	20	0.005	0.60

The experimental results using the conventional PID control system in desired removal of 3% of moisture in wood is presented in Figure 7-1. The heater (on) duration within each sampling time, the pulse-width-modulated (PWM) duty cycle, the average kiln temperature, and the average moisture of wood pieces are all recorded and presented. It is seen from the experimental results that the controller is capable of reducing the moisture

174

level from 16.6% to 13.9% (the average moisture level) with a maximum error of ±0.4%. The average operating temperature throughout the entire experiment is found to be approximately 56 °C, and over-drying below the desired moisture setpoint can occur during the drying process.
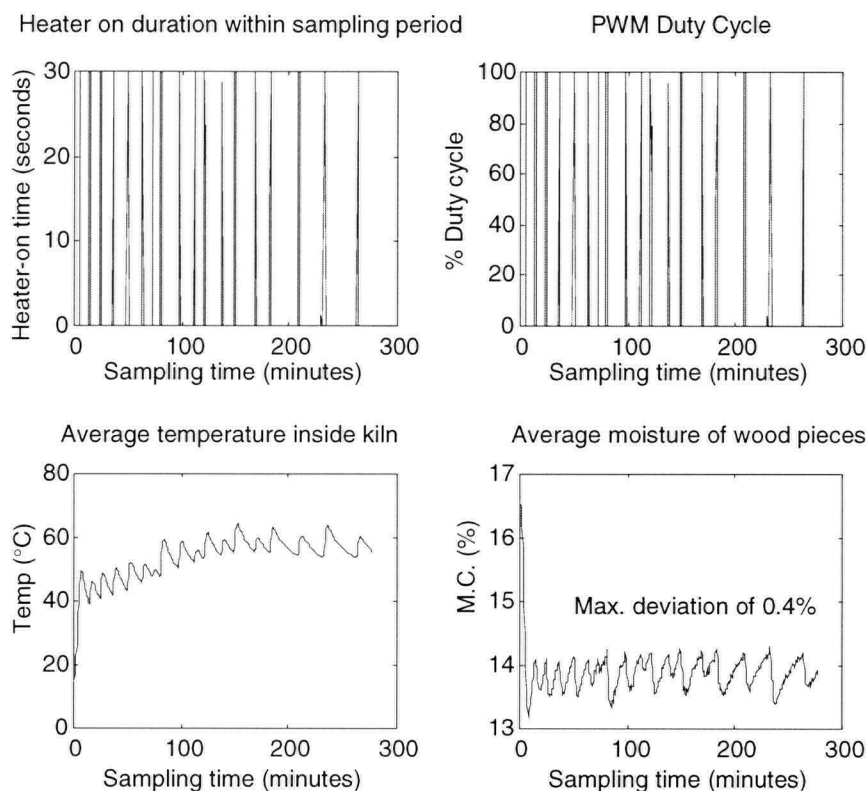
Figure 6-1   Experimental results with the conventional PID control system in desired reduction of the moisture level by 3%.

Similarly, the experimental results for the desired removal of 5% of moisture from the wood are presented in Figure 6-2. Again, the controller is capable of reducing the average moisture level from 22.9% to 18.2%, with a maximum error of   ±0.4%. The average value of the desired operating temperature is approximately 50 °C. Since in the case of 5% moisture removal, the initial temperature is approximately 80 °C compared with the initial temperature of 50°C in the 3% moisture removal case, it is clear that more energy is required to remove the excess moisture in the former case. The PWM duty cycle and

the heater-on duration within each sampling period are also recorded and presented in Figure 6-2. Some over-drying can still be found, since the moisture level drops below the setpoint.
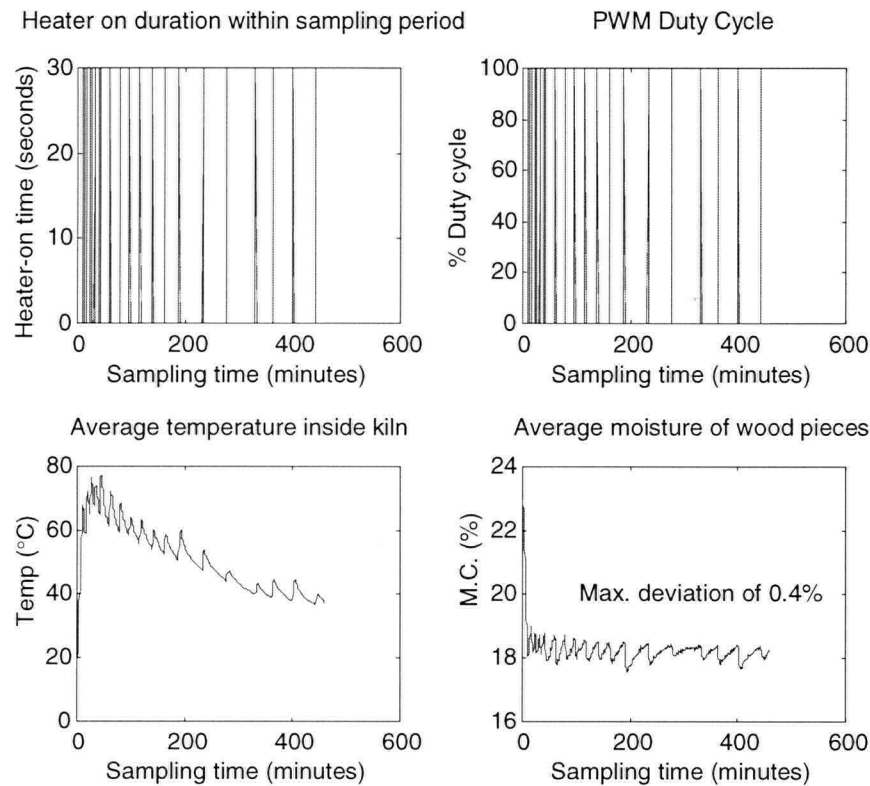
Figure 6-2   Experimental results with the conventional PID control system in desired reduction of the moisture level by 5%.

Tuned Conventional PID Control System

Several experiments are performed using different gains for both M-PID and T-PID in the conventional PID control system. The gains obtained from simulations are tuned using the Ziegler-Nichols technique [35] in order to achieve the best on-line performance. Experimental results from different runs do not show large variations in terms of performance. The best results were obtained using the gains given in Table 6-2 for both M-PID and T-PID.

Table 6-2   Gains used in the tuned PID controllers.

Controller	Proportional gain (K_p)	Integral gain (K_i)	Derivative gain (K_d)
M-PID	100	0.001	0.01
T-PID	20	0.005	0.80

The experimental results in the desired removal of 3% of moisture from wood show good results as presented in Figure 6-3. In a 7 hour run, the controller is able to bring down the moisture level from 17.5% to 14.8%, with a maximum error of ±0.3%. The overall desired operating temperature is maintained at approximately 50 °C. The PWM duty cycle remains almost the same as the previous case without tuning. The effect of over-drying is greatly reduced, and happens only in the beginning of the drying process.

For the moisture removal of 5%, experimental results were obtained from an extensive run. In this experiment, the system was set to run for 23 hours. Again, good results were achieved, as presented in Figure 6-4. The controller was found to be capable of reducing the moisture from 16.9% to 12.3%, with a maximum error of ±0.4%.
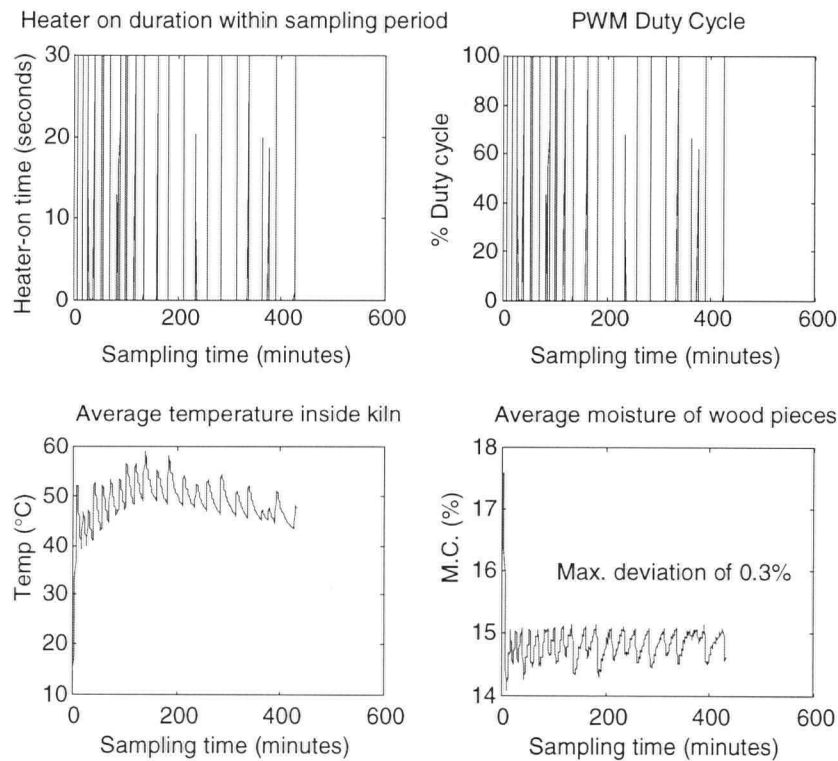
Figure 6-3   Experimental results with the tuned conventional PID control system for a desired reduction of the moisture level by 3%.
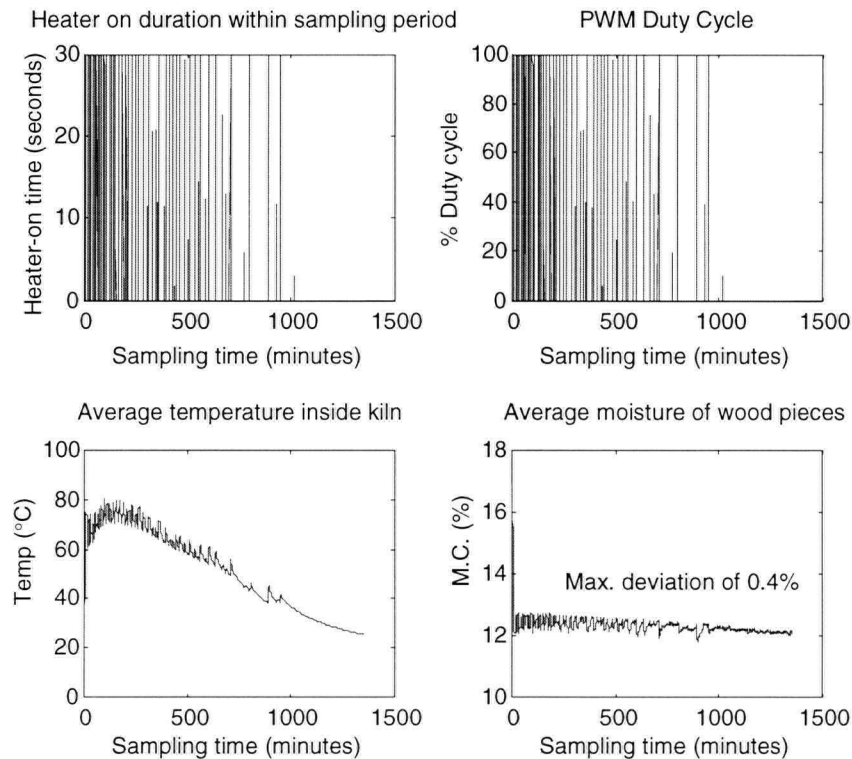
Figure 6-4   Experimental results with the tuned conventional PID control system for a desired reduction of the moisture level by 5%.

The desired operating temperature was found to be approximately 51 °C throughout the experiment, and the PWM duty cycle remained more or less the same, but with more activity at the start of the experiment. In this experiment, the heater was turned off after 17 hours, and then the moisture content settled at a steady level of 12%, with a maximum error of only ±0.1%. The over-drying effect was not found to occur in this experiment.

6.2 Experiments with Fuzzy Logic Control System

In this section, the Fuzzy-plus-PID control system developed in the present work and studied in Chapter 5 using computer simulation, is implemented in the prototype kiln system on-line for the investigation of controller performance. Also, the fuzzy logic controller for moisture control is tuned on-line in order to achieve improved performance. The experimental results are presented in the following subsections. The gains for the PID temperature controller are kept the same as those that give the best performance

results previously in the conventional PID control system. ($K_p = 20$, $K_i = 0.005$, $K_d = 0.80$)

6.2.1 Initial fuzzy logic control system

The controller developed for simulation study is implemented in the prototype kiln system at the National Research Council. The *Fuzzy Moisture* controller consists of 5 rules. The condition variables of the fuzzy input (moisture error) are defined as negative small (NS), zero (ZR), positive small (PS), positive medium (PM), and positive large (PL). The design of the fuzzy condition variable of NS allows some degree of over-drying to occur in order to compensate for poor ventilation of the kiln set up. The experimental results for the desired removal of moisture by 3% and 5%, are shown in figures 6-5 and 6-6, respectively.

Experimental results

It is noticed from the results of Figure 6-5 that the fuzzy control system is capable of reducing the moisture content from 13.7% down to 11% (approximately 3%) with a deviation of ±0.2%. The desired operating temperature is maintained at approximately 45 °C, but with a PWM duty cycle of less than 20%. It is seen that there is no occurrence of over-drying during the entire drying experiment.

In the experiment where the desired reduction of the moisture content was 5%, the controller was incapable of removing 5% of moisture during the drying process. Instead, the moisture content was reduced from 15.2% to 12.1%, which corresponds to a moisture reduction of only 3.1%. Although the operating temperature was maintained at 50 °C and the PWM duty cycle was increased, the performance of the initial fuzzy control system was found to be inadequate.
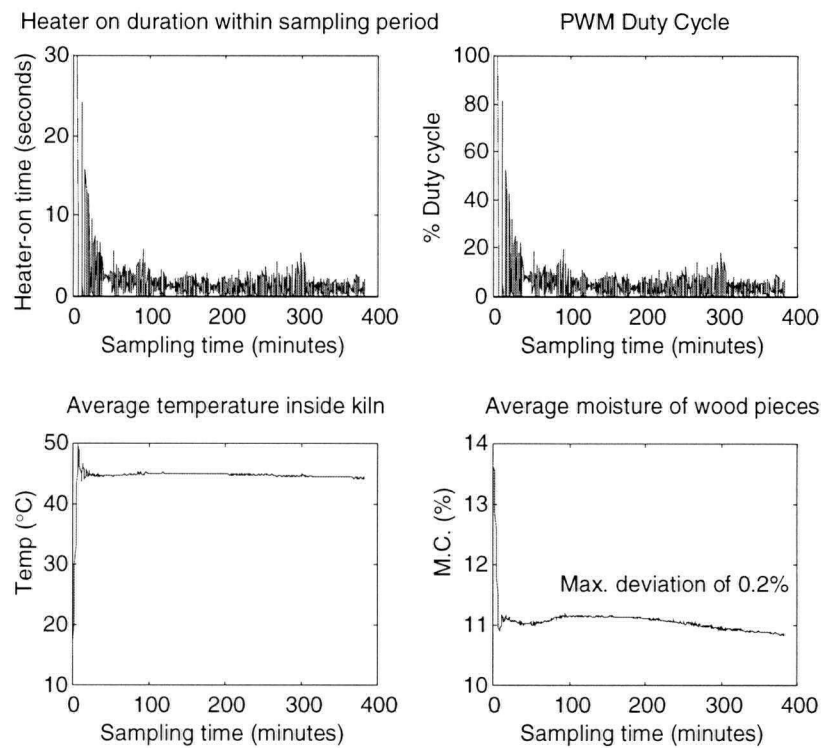
Figure 6-5   Experimental results using the fuzzy logic control system (initial version) for a desired reduction of the moisture content by 3%.
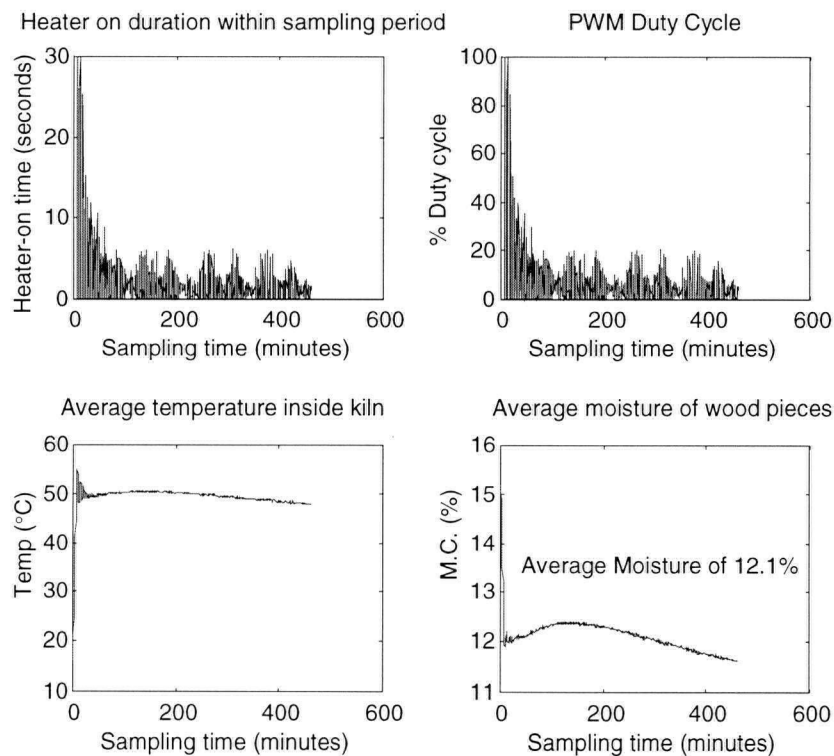
Figure 6-6   Experimental results using the fuzzy logic control system (initial version) for a desired reduction of the moisture content by 5%.

6.3 Modified Fuzzy Logic Control System

In this section, the fuzzy logic controller for moisture control is tuned according to the experimental results. Changes are made to adjustments of the condition variables, action variables, and fuzzy gains. The rule base of the *Fuzzy Moisture* controller still consists of 5 rules. The following subsections summarize the changes made to the initial version of the fuzzy controller. The experimental results obtained from the modified fuzzy controllers are presented. Two modified versions are presented.

6.3.1　Modified fuzzy controller Version 1

Since the controller is inadequate to provide sufficient output for the removal of 5% of moisture, some modifications have to be made to it. In particular, it is clear that the gain of the fuzzy control action variable has to be increased. The following modifications are implemented to tune the fuzzy controller:

- Range of the condition variable is changed from [-2→6 %] to [0→6 %].
- Range of the action variable is changed from [40→85 °C] to [40→110 °C]
- Individual fuzzy states of the condition (input) variable are modified, but still retaining 5 fuzzy states, as follows: Zero (ZR), Positive Small (PS), Positive Median (PM), Positive Large (PL), and Extremely Large (EL). Note that the fuzzy state of Negative Small (NS) is removed, and the new state of Extremely Large (EL) is added. The fuzzy states of the action (output) variable are retained.

Note that instead of allowing 2% of over-drying, now the lower limit of the input fuzzy gain is modified to zero. Furthermore, the upper bound of the output fuzzy gain is altered to 110 °C in order to provide a larger output control signal. The membership functions of the modified input states, and the output states are shown in Figure 6-7.
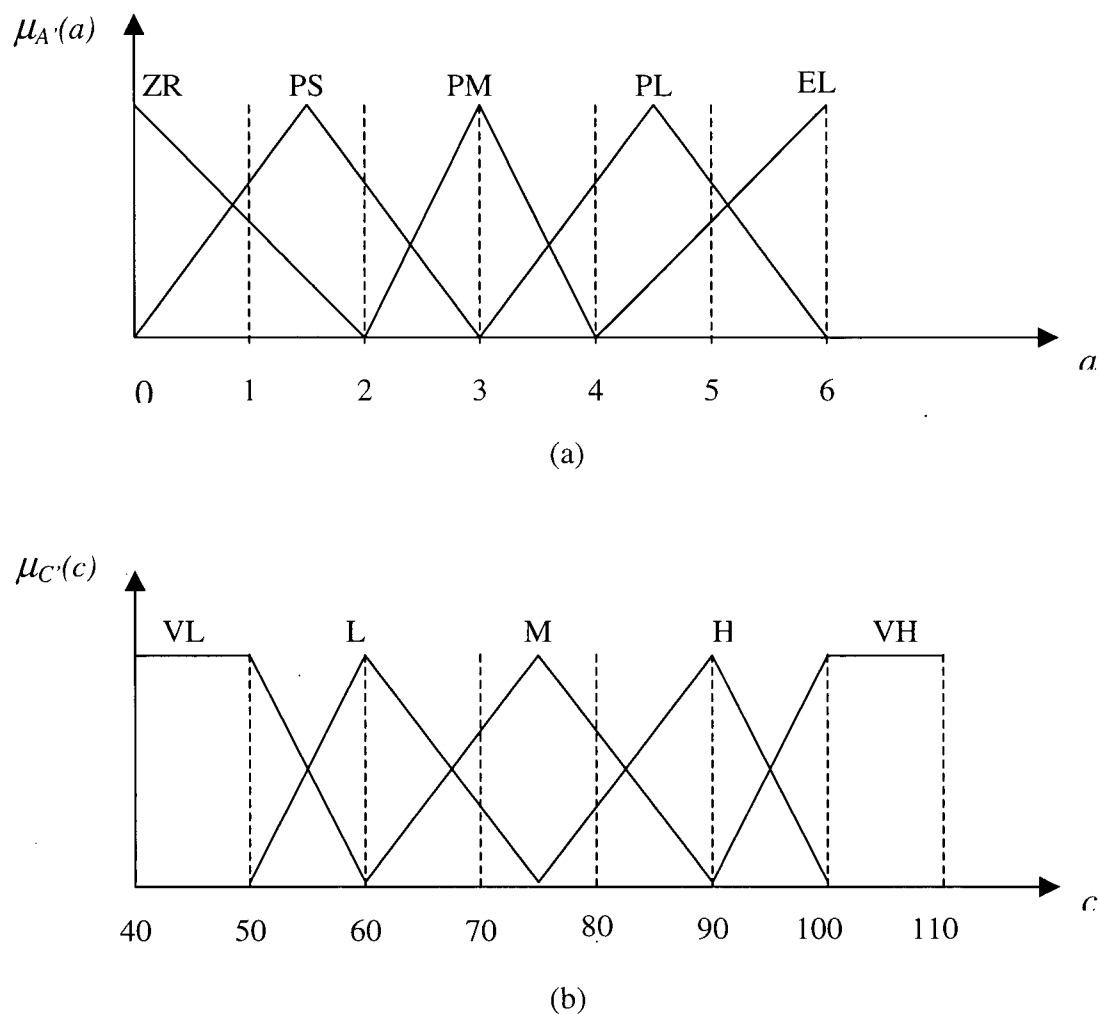
Figure 6-7   Modified membership functions of: (a) input states; (b) output states.

The modified rule base of the *Fuzzy Moisture* controller consists of the following 5 rules:

	IF *moisture error* is *ZR*	THEN *temperature* is *VL*
or	IF *moisture error* is *PS*	THEN *temperature* is *L*
or	IF *moisture error* is *PM*	THEN *temperature* is *M*
or	IF *moisture error* is *PL*	THEN *temperature* is *H*
or	IF *moisture error* is *EL*	THEN *temperature* is *VH*

The experimental results of the modified fuzzy controller Version 1 are shown in Figure 6-8.

Figure 6-8   Experimental results for the modified fuzzy PID control system Version 1 for desired reduction of the moisture content by 5%.

From the results, it is observed that the controller output has increased. The average value of the PWM duty cycle is maintained above 20%, and the average operating temperature is maintained at 60 °C. In this test, even though the desired reduction of moisture content is 5%, the controller was only able to take away 4.1% of moisture from an initial average moisture content of 14.2% down to 10.1%. Therefore, the fuzzy PID requires further tuning to provide sufficient output to achieve the desired performance.

6.3.2   Modified fuzzy controller Version 2

Now, instead of modifying the fuzzy states of the input and output variables, a scale factor is added to different ranges of the fuzzy states. The shapes of the membership

functions and the number of rules in the rule base remain the same. The range of the fuzzy input (condition) states is divided into four zones as: [0→2], [2→3], [3→4], and [4→6].

Direct fuzzy logic control of moisture

Consider the schematic diagram of the control system as shown in Figure 6-9. The measured process variable is the moisture content of the wood pieces inside the kiln, which is provided by the moisture content sensors. The moisture error, e_m, (Moisture setpoint – Actual m.c.) is computed and communicated to the fuzzy moisture controller, and the controller in return determines the operating temperature (C) that should be maintained to eliminate the error.
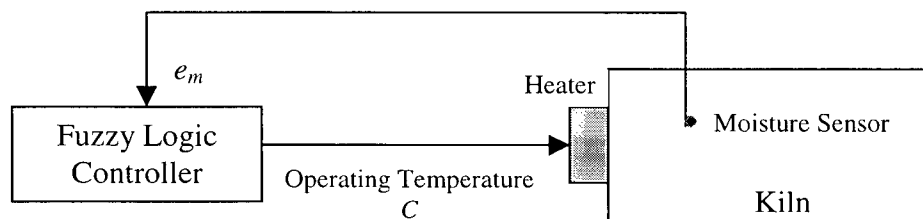
Figure 6-9   Direct fuzzy moisture control system of a drying kiln.

The fuzzy rule base of the moisture controller is presented graphically in Figure 6-10. Each fuzzy rule will fire a condition fuzzy grade according to the measured moisture error. These membership grades of the fuzzy states in the five rules are then determined. (This is a *min* operation, but in the present rulebase there is only one condition variable, and hence combined condition membership grade is in fact the read membership grade from the moisture error membership function.) This membership grade will be used to clip the corresponding membership function of the control action C, and the resulting "clipped" membership functions of C for all five rules are then superimposed (a *max* operation) to obtain the control inference C'. This result is a fuzzy set, and the final control action $\hat{C}$ for generating the required operating temperature is obtained through defuzzification using the centroid method. In this modification, the following scale factors are added to the range of the process action (output) variable:

- Scale factor of 1.15 is assigned to range [0→2].

- Scale factor of 1.20 is assigned to range [3→4].

- Scale factor of 1.25 is assigned to range [4→6].

Condition   Action

Rule 1:

Rule 2:

Rule 3:

Rule 4:

Rule 5:
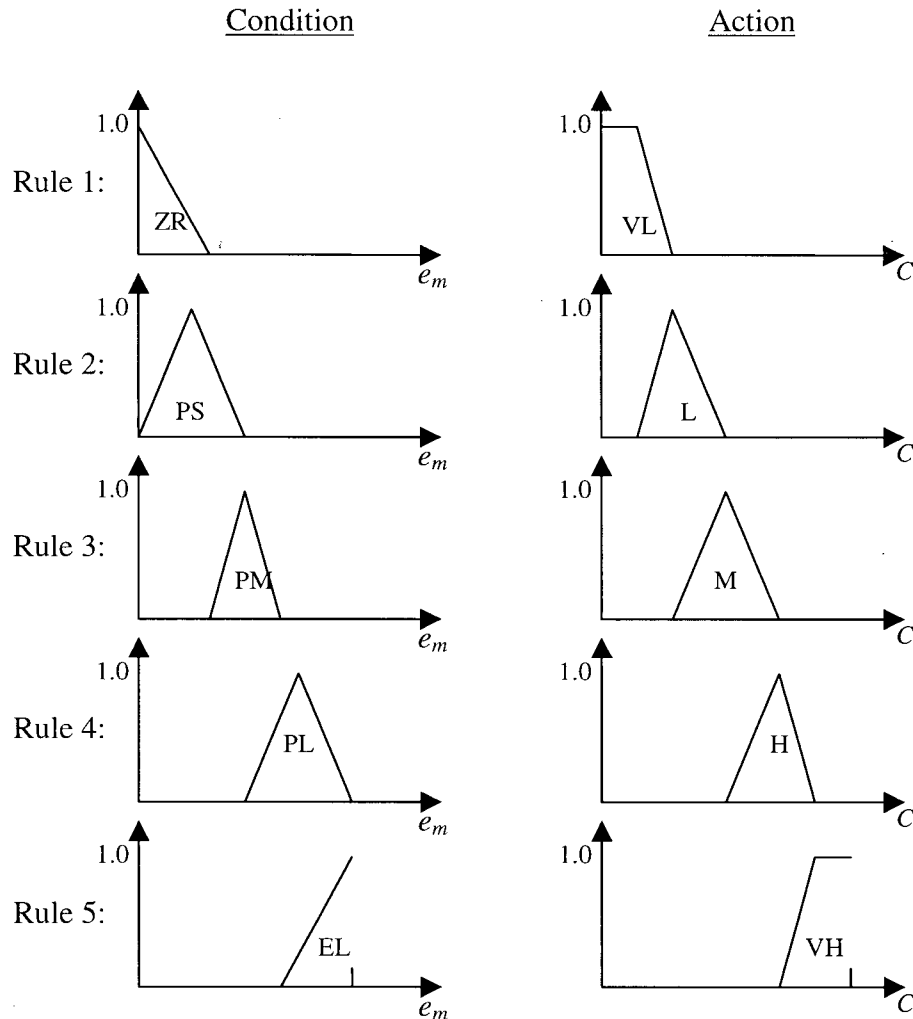
Figure 6-10   The fuzzy rule base of the moisture controller.

Experimental results

The experimental results using the modified fuzzy controller Version 2 for desired removal 3% of moisture is presented in Figure 6-11. The controller is able to bring the moisture level down from an initial value of 15.7% to 12.5%, with a maximum error of ±0.3%. The average operating temperature is maintained at approximately 45 °C, and a

maximum temperature of approximately 60 °C in the beginning. The PWM duty cycle is recorded and presented as well. Figure 6-12 shows the experimental results in a desired removal 5% of moisture. It is seen that the modified controller is capable of reducing the moisture content from an initial value of 21.7% down to 16.3 % with a maximum error of ±0.3%. Note that this moisture error turns out to be less than ±0.1% after a 5 hour run. The average operating temperature is maintained at approximately 37 °C, with the highest temperature occuring in the beginning of the drying, at approximately 67 °C. The PWM duty cycle is found to be off after 4 hours of operation. Both tests were run for about 11 hours.
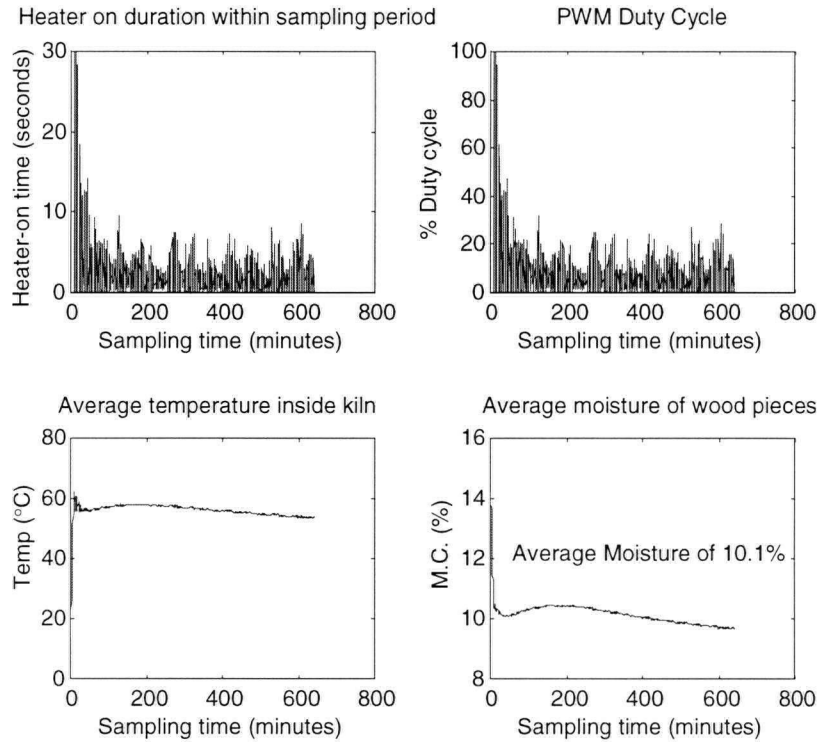
Figure 6-11   Experimental results for the modified fuzzy PID control system Version 2, for a desired reduction of the moisture content by 3%.

Figure 6-12   Experimental results for the modified fuzzy PID control system Version 2, for a desired reduction of the moisture content by 5%.

6.3.3   Modified fuzzy controller Version 3

The modifications to the fuzzy PID control system, as presented in the previous section (modified Version 2) already shows good drying results. Now a further modification is incorporated anticipating still better performance. Specially, the scale factors that were added to the four different ranges of the fuzzy action (output) variable is further tuned to determine whether further improvement in performance would be possible. The adjustments in the modified Version 3 are summarized below:

- Scale factor of the 1st range [0→2] is increased from 1.15 to 1.25.
- Scale factor of 1.20 is assigned to the 2nd range [2→3].
- Scale factor of 1.20 is assigned to the 3rd range [3→4] (remains unchanged).
- Scale factor of 1.25 is assigned to the 4th range [4→6] (remains unchanged).

The shape of the membership functions for both input (condition) and output (action) variables remains unchanged. The number of rules in the rule base also remains unchanged.

Experimental results

First experiment is performed to investigate the controller performance in a desired removal 3% of moisture. The results of this test are shown in Figure 6-13.
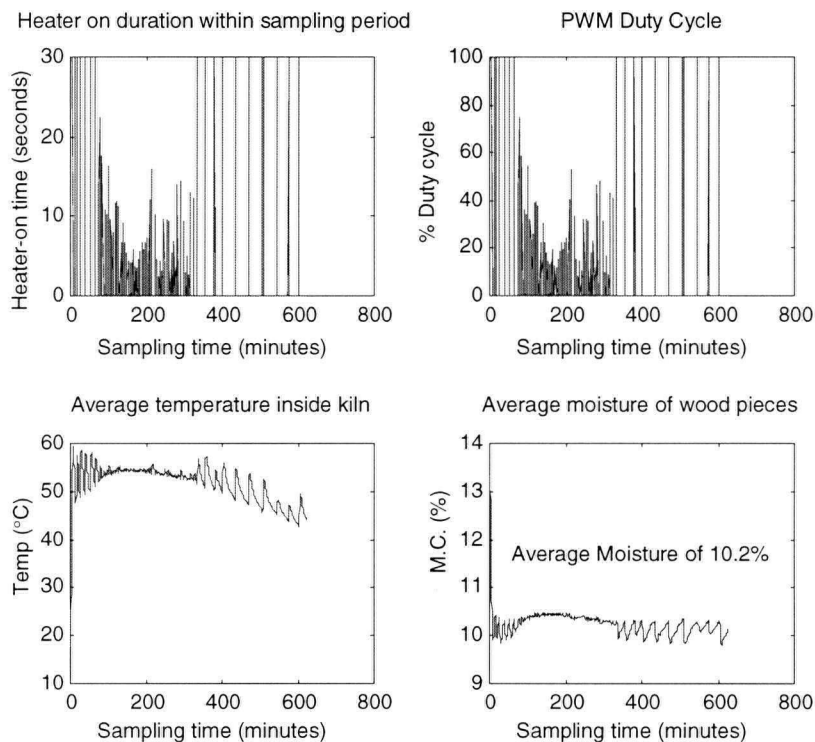
Figure 6-13   Experimental results for the modified fuzzy PID control system Version 3 for desired reduction of the moisture content by 3%.

In this experiment, the modified fuzzy controller is capable of performing the desired removal of 3% of moisture, by bringing the moisture level down from an initial value of 13.3% to 10.2%, with a maximum error of ±0.3%. The average desired operating temperature is maintained at 51.5 °C, with a maximum operating temperature of 60 °C, in the beginning of the drying process. The PWM duty cycle is recorded and presented as well.

Two more tests are performed to investigate the controller performance in a desired removal of 5% of moisture, in order to further confirm the controller performance. The first test is run for approximately 23 hours (a long test run). The final average moisture level is found to settle at 11.4% in this case. The controller is capable of reducing the moisture content from 16.4% down to 11.4%, which exactly corresponds to the desired setpoint input to the controller interface, with a maximum deviation of error of ±0.2% throughout the experiment. Also, the desired operating temperature is maintained at approximately 46 °C. The PWM duty cycle is recorded and presented. The experimental results are presented in Figure 6-14.
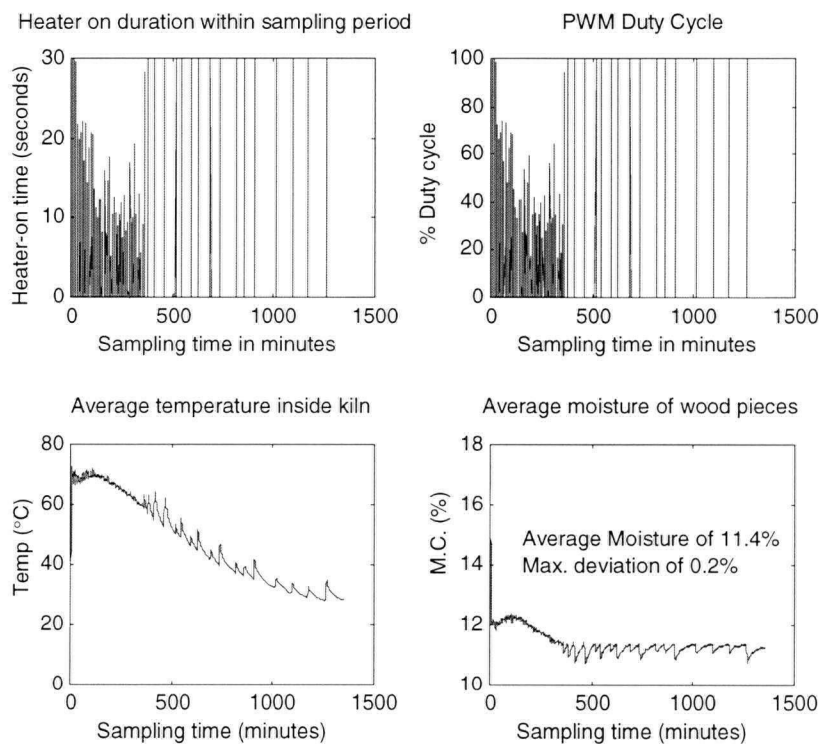
Figure 6-14   Experimental results with the modified fuzzy PID control system Version 3 for a long test run, in a desired reduction of the moisture level by 5%.

Similarly, the second test is carried out to investigate the controller performance in a desired removal of 5% of moisture. This experiment is run for approximately 10 hours. It is observed that the controller system again gives satisfactory results. An initial moisture content of 18.7% is brought down to an average value of 13.6%, which is very close to the ideal result, with a maximum error of just ±0.1%. The desired operating temperature

is maintained at approximately 42 °C for the entire drying process, and the heater is found to be off after 200 minutes, except for a very short on period. The corresponding PWM duty cycle is recorded and presented. The experimental results for this test is presented in Figure 6-15.
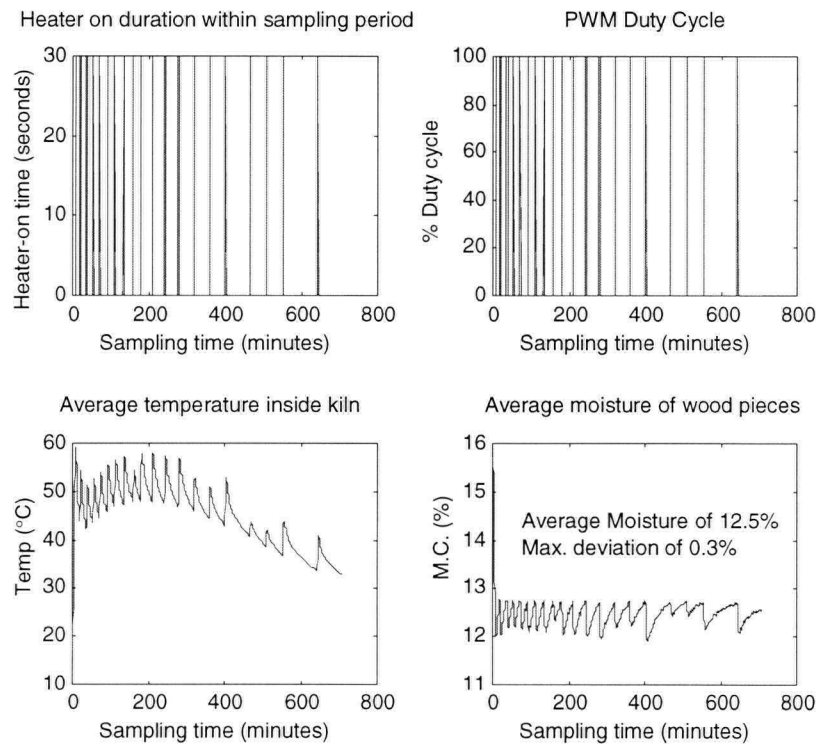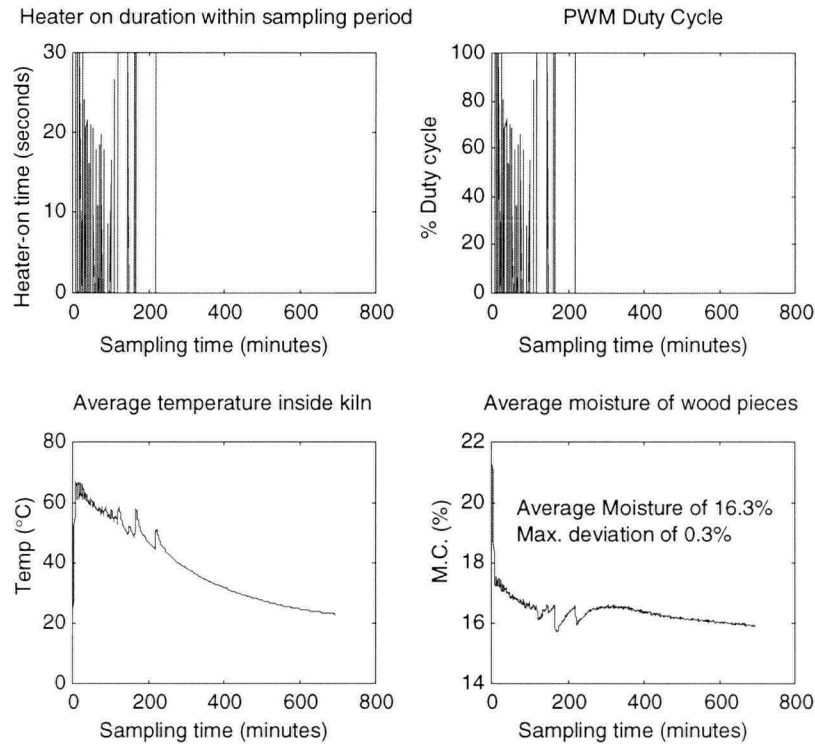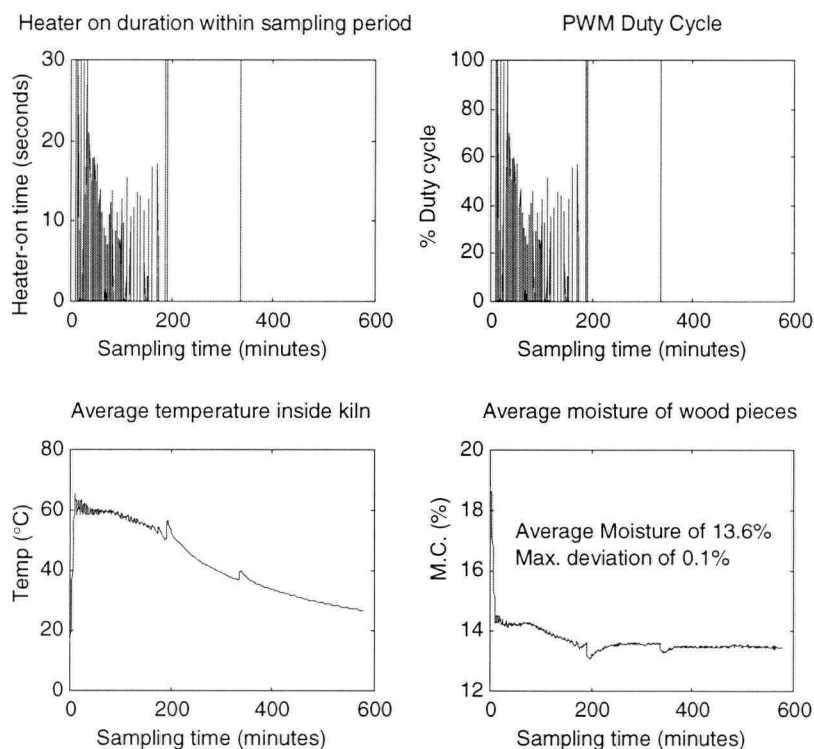

Figure 6-15   Experimental results for the modified fuzzy PID control system Version 3, in a desired reduction of the moisture content by 5%.

6.4 Experimental Summary

This chapter presented the implementation of both a conventional PID control system (a double-loop PID control system) and an integrated intelligent controller together with conventional PID controller (a fuzzy plus PID control system) in a prototype kiln system for wood drying.

With the PID control system, on-line experimental results were obtained and compared with the simulation results. On-line results satisfactorily matched the simulations, except that some level of tuning was required to achieve better results. All test runs were able to

achieve the drying specification of a desired reduction in the moisture content of wood by either 3% or 5%. In each case, the controller was able to dry the wood according to the input moisture set point with a maximum deviation error of ±0.3% to ±0.4%. Experiments with different control gains showed almost exactly the same drying response and had a very similar pattern, except that the final moisture error was different. The best results that the PID controller could achieve corresponded to an error of ±0.3%. The average value of the desired operating temperature throughout each experiment was found to be approximately 52 °C.

For the fuzzy PID control system, on-line experimental results matched quite well with the simulation results, in the desired removal of 3% of moisture. For the desired removal of 5% of the moisture, the controller was incapable of providing sufficient control output for achieving the objective. Consequently, modifications were done to the fuzzy controller in order to meet the drying specification. The experimental results in all test runs showed good drying performance with an average deviation error of ±0.3%, and even less than ±0.1% in some tests. The average value of the desired operating temperature throughout each test run was found to be approximately 46 °C, and the heater-on duration was found to operate with a different PWM duty cycle ranging from 5% to 100% of the full duty cycle.

In a conclusion, on-line experimental results were presented and compared with the simulation results for both conventional and fuzzy PID control schemes. Both control schemes showed promising results, and sometimes the PID control system showed drying result as good as those from the fuzzy logic control system. The final drying results under similar conditions could have different drying responses for the two control systems, since different wood pieces were used in each experiment. In view of the variation of the microscopic structure of the wood pieces used in the experiment, even though the same species (spruce) was used, different results could be obtained under identical experimental conditions. By examining the test runs as a whole, in general, it can be concluded that the fuzzy logic controller performed better than the PID controller with regard to the final moisture error and energy consumption. The fuzzy logic controller generally could produce better drying results together with a smaller final moisture deviation error. In some tests with the fuzzy controller, wood pieces could be dried to

exactly the same condition as specified by the moisture setpoint, with less than ±0.1% error, which the PID controller was unable to achieve. Besides, the fuzzy logic controller only required an average temperature of 46 °C compared to 52 °C for the PID controller. It follows that the PWM duty cycle for operation was lower for the fuzzy control system compared to the PID control system. Also, the range of operation for the PWM duty cycle was wider for the fuzzy control system. All these improvements in performance that result from the fuzzy logic control system may be credited to the fact that human experience and control episodic knowledge can be integrated into the control system through the use of a fuzzy-logic knowledge base.

Chapter 7

CONCLUDING REMARKS

This thesis investigated the control of industrial wood drying kilns. The physics of wood drying was examined. Existing procedures of kiln control were discussed and shortcoming of these techniques were pointed out. Conventional PID control and the integration of intelligent control with conventional PID control for a wood drying kiln were investigated through the development of a closed-loop moisture feedback control system. Extensive experiments were carried out using a prototype wood drying kiln, for understanding the practical drying process and for system identification. System models were identified by estimating the model parameters and validating the model order. These experimental models were used for simulation studies. Once reasonable models were established in this manner, both conventional PID and fuzzy logic PID controllers were developed and implemented in computer simulations. Then both control systems were implemented in the downscaled prototype wood-drying kiln in laboratory. The controllers performance was investigated through extensive on-line experimentation. Both conventional PID and fuzzy-PID control systems produced good results, while generally the fuzzy-PID control system performed better.

7.1 Problems Associated With the Physical Setup

Throughout the experiments, some phenomena and problems were observed relating to the physical setup of the wood drying kiln. These problems are summarized below:

- Poor air circulation
- Insufficient fan speed
- Allocation of sensors
- Limited removal of moisture.

The ventilation system of the physical setup is poor since there is only one small circular vent at the top of the kiln for air circulation. When a large batch of wood pieces was loaded into the kiln for drying, say 20 pieces, it took a very long time to dry the wood to a desired level, and a large quantity of moisture was found to be trapped at the bottom of the kiln interior.

The fan motor is capable of generating fan speeds up to 3000 rpm; however, the maximum speed that the fan can be operated trouble-free is about 1000 rpm. Throughout the experiments, this constraint on the operating speed of the fan was observed. Problems would arise when this limit is exceeded; for example, since the metal surface of the kiln is not quite rigid, unacceptable vibrations would occur between the mounting of the fan shaft and the metal surface.

Primary objectives of wood drying control are to reduce the drying time, which will save energy while increasing the production rate, and to ensure good quality of dried wood. In this thesis, controllers were developed and performance was evaluated in terms of energy consumption (drying duration, heater-on time, and duty cycle) as well. Unfortunately, the quality of dried wood is not directly measurable and is difficult to control in the present experimental system. Throughout the experiments, quality of dried wood was assured by limiting the drying temperature to a maximum value of 85 °C, and the drying time was kept below 3 hours. In order to develop a control scheme for quality, one must consider relative humidity which is one of the crucial control factors. The relative humidity sensors that are being used in the existing kiln were unable to provide highly reliable and useful information due to the misallocation of the sensors. Two relative humidity sensors were recently installed in the system, one on each side of the kiln. One of them had been placed too close to the heater and the other one had been placed inside the plenum where the relative humidity was quite low. Therefore, the sensors read a very high value at the start of the experiment, and then reached a very low reading (almost zero or negative value) once the heater was kept on for 15 minutes.

Another phenomenon that was found in relation to the setup was that the system could not remove more than 6% of moisture from the wood. This could be attributed to the poor ventilation in the system, and consequently moisture would build up inside the kiln during the drying process. The moisture that is evaporated from the wood pieces would

be greatly suppressed due to the saturated moisture in the surrounding air caused by the poor air circulation of the system. Two experiments were run to verify this scenario. The first experiment was run to observe the moisture content response by setting the operating temperature at 80 °C and maintaining this temperature throughout the entire experiment using PID temperature control. The moisture dropped from an initial moisture content of 19% to 13.3%, and accordingly 5.7% of moisture was removed at the beginning of the run. The moisture then started to build up and reached a peak moisture level of 17.6% even though the operating temperature was still maintained at 80 °C. It finally settled at 16% after a 7 hour run. Similarly, a second experiment was performed under the same operating conditions, but started with a lower level of initial moisture content. Again, the moisture content dropped from 12.5% to 7.3%, whereby 5.2% of the moisture was removed at the start of the experiment. The moisture level then increased to 7.8% and finally settled at 6.5% in a long test run of approximately 10 hours. The results of the moisture response under the constant temperature condition of 80 °C are presented in Figure 7-1.

(a)   (b)
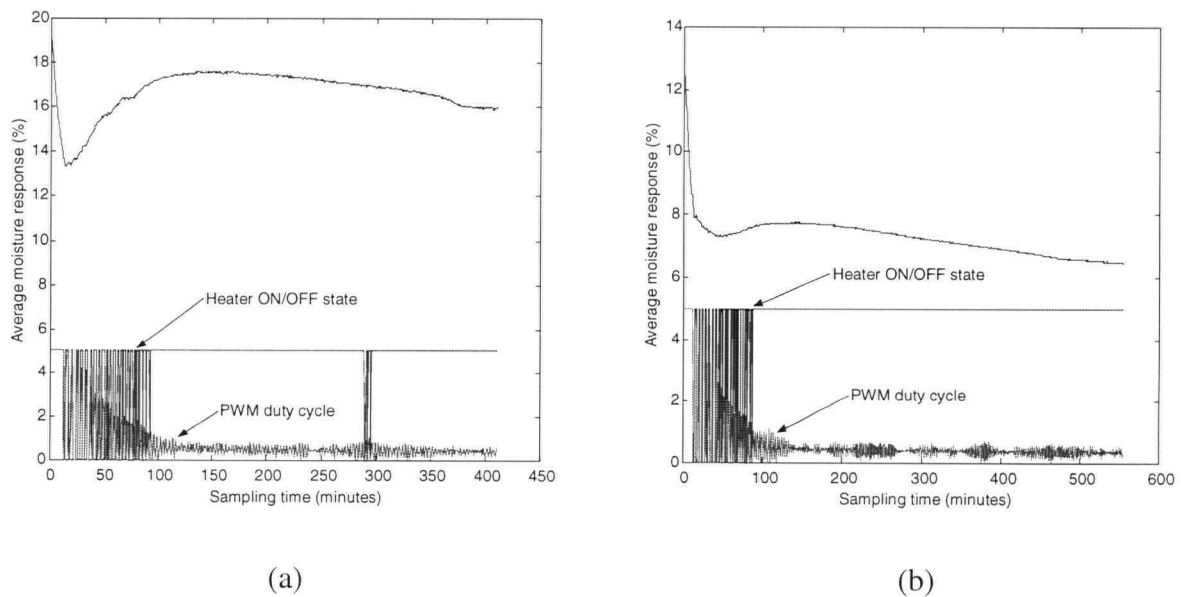
Figure 7-1   Average moisture content response under a constant temperature setting of 80 °C: (a) higher initial moisture content; (b) lower initial moisture content.

7.2 Modifications and Improvements to the Kiln System

In view of the problems outlined in the previous section, the following modifications or improvements are suggested to the physical setup of the kiln system:

- Design and install a ventilation system in the experimental setup so that excessive moisture can be removed from the interior of the kiln. Design a controller to operate the opening and closing of the air valves that determine the flow of recycled air and fresh air in the air circulation system.
- Appropriate mounting material or isolation pads should be used to reduce vibration in the fan. Springs may be placed between the mounting frame of the fan and the metal surface of the kiln. With such means of vibration reduction, the fan can be operated at a higher speed (capacity) in the long test runs.
- The relative humidity sensors should be located further away from both the heater and the plenum. They should be placed at a proper location so as to measure the humidity of the air inside the kiln. In this manner, realistic and more useful sensor information can be obtained.
- The present experimental setup has the capacity to dry larger batches of wood than what has been used in the experiments described in the thesis provided that the ventilation system is improved as suggested.

7.3 Discrepancy with Industrial Drying Kilns

In the studies described in this thesis, experiments were carried out using a laboratory prototype of a downscaled wood-drying kiln. Drying characteristics of industrial kilns can be different due to the way that stacks of wood are loaded into the kiln for drying, and furthermore the industrial kilns are of warehouse size which is far bigger than the experimental setup used in the present work. Also, the experimental setup can take no more than 20 pieces of wood (2"×4"×6") and the length is half that of normal wood pieces (2"×4"×12") dried in industry.

Besides, the species of wood used for drying experiments in the laboratory was spruce, unlike which different types of species may put together in the same load for drying in industry. The wood that was used for laboratory drying was wetted by rain in the winter season, and wetted in a water tank in the summer. In industry, freshly cut wood is directly dried in kilns. Consequently, the drying characteristic can be different in the two cases.

Even though the industrial drying process is different from the experimental wood drying in laboratory, the methodology developed for the latter can be utilized for automation and controller design for the former. The complex and nonlinear characteristics of the wood drying process which is known to have time delays make the process suitable for application of fuzzy logic control. Since it is difficult to obtain an accurate system model for such a complex process, and furthermore, since human expertise and drying knowledge are readily available in industry, integration of such knowledge into the knowledge base of fuzzy logic control, can produce highly desirable results.

7.4 Contributions of the Thesis

The main contributions of this thesis can be summarized as follows:

- A closed-loop intelligent control system using direct fuzzy logic control, with on-line in-wood moisture sensing and feedback was developed.
- The developed fuzzy logic controller was implemented in a prototype wood-drying kiln for moisture control. It demonstrated the feasibility of a knowledge-based control algorithm which does not require an explicit system model.
- Since wood drying is conventionally carried out by a schedule-based approach, a human operator has to provide the loop closing. The present approach of combining conventional control with fuzzy logic theory for overall control leads to automation of the wood drying process which has a great potential for performance improvement when applied to industrial kilns.
- Computer simulations for both conventional PID control and fuzzy PID control were developed and evaluated.

- Both conventional and fuzzy control systems were thoroughly evaluated on the physical setup in laboratory, and were tuned on line to improve the performance. Extensive experimental studies showed that the performance of both conventional and fuzzy PID controllers was satisfactory.

A complete investigation and the development of a closed-loop moisture control system with direct in-wood sensor feedback, utilizing an integrated conventional and fuzzy logic control techniques for practical wood drying kilns complete with experimental modeling, computer simulation, and thorough experimental studies has not been reported before.

7.5 Conclusions

Conventional lumber drying is considered an art rather than a science. It is a process that consumes time and energy, and is done on the basis of a pre-determined schedule. The required operating temperature, relative humidity, fan speed, the sequence of opening and closing of vents, and the time duration are all specified in an operation schedule. The entire open-loop process commonly called kiln operation requires on-line monitoring by a mill operator for some degree of feedback. The integration of expert knowledge and experience provided by the fuzzy logic theory, as done in the present thesis, has a great potential in automating the lumber drying process so that the lumber can be dried in a more cost effective way. More importantly, through automation, the utilization of the valuable resource of timber will be made more efficient. According to the present investigation on experimental modeling and development of a closed-loop control system with conventional and fuzzy PID control and feedback from wood moisture sensors, the following conclusions can be drawn:

- According to the system identification that was performed to investigate process behavior, two sub-systems of second order were found to adequately represent the drying process. Also knowledge was gained for the design of the control system.

- Computer simulations performed using MATLAB Simulink and Fuzzy Toolbox revealed the extent and limitations of controller performance. This assisted in developing the experimental system for feedback control.

- Designs of both conventional double-loop PID control, and a combination of conventional PID control with fuzzy logic control were implemented on-line in the prototype kiln system. Promising controller performance was revealed through experiments.

- Drying knowledge and experience was gained through experiments, and expressed as a set of fuzzy rules. A simple direct fuzzy logic controller for wood moisture control was developed on this basis.

- The methodology developed in this thesis is general enough to be applied to industrial wood drying kilns which are complex process where there is incomplete knowledge, and missing information, and an accurate mathematical model is very difficult to obtain.

7.6 Recommendation for Future Work

Before further experimental studies are performed with the prototype kiln, the ventilation system has to be improved. Several recommendations are made below for future work.

- Design and implement a ventilation system of the drying kiln with valve control so as to be able to determine and adjust the proportion of mixed fresh outside air and recycled air, in different drying stages.

- Develop and implement several low-level controllers (e.g., generalized predictive control, linear quadratic regulator, linear quadratic gaussian, fuzzy sliding mode) and allow the selection of different low-level controller according to different drying stages and drying conditions [36].

- Develop a more advance direct fuzzy logic control system by looking into more than one input variables (e.g., rate of change of moisture error, $\dot{e}_m$), as well as more than one output variables (e.g., fan speed) and extend its capability to control the quality of dried wood.

- Integrate the experimental experience and knowledge into the knowledge base of the fuzzy control system for automatic fuzzy rule generation and rule deletion. Specifically, fuzzy logic can incorporate a learning mode, according to the drying phenomenon in order to improve the drying quality and reduce the drying duration.

- Develop an intelligent, hierarchical, supervisory control system with multiple layers of knowledge and intelligence for an industrial wood drying kiln.

REFERENCES

[1]   Simpson, William T., *Dry Kiln Operator's Manual*, United States Department of Agriculture, 1991.

[2]   Wickramarachchi, N., *Development of a Knowledge-Based Hierarchical Control Structure for Process Automation*, Ph.D. Thesis, University of British Columbia, Vancouver, Canada, 1995.

[3]   Goulet, J. F., *Intelligent Hierarchical Control of a Deployable Manipulator*, M.A.Sc. Thesis, University of British Columbia, Vancouver, Canada, 1999.

[4]   Ljung, L., *System Identification: Theory for the User*, 2nd Edition, Prentice Hall Inc., 1999.

[5]   De Silva, C. W., *Intelligent Machines – Myths and Realities*, CRC Press Inc, Boca Raton, FL, 2000, pp.1-7.

[6]   De Silva, C. W., *Intelligent Control: Fuzzy Logic Applications*, CRC Press Inc, Boca Raton, FL, 1995.

[7]   Zadeh, L.A., "Making Computers Think Like People," *IEEE Spectrum*, August 1984, pp.26-32.

[8]   Filippidis, A., Jain, L. C., and de Silva, C. W., "Intelligent Control Techniques," Intelligent Adaptive Control, (Jain, L. C. and de Silva, C. W., Editors), CRC Press, Boca Raton, FL, 1999.

[9]   De Silva, C. W., and MacFarlane, A. G. J., *Knowledge-Based Control with Application to Robots*, Springer-Verlag, Berlin, 1989.

[10]   Basset, K.H., "Sticker Thickness and Air Velocity," *Proceedings of the Western Dry Kiln Clubs 25th Annual Meeting*, Portland, Oregon, 1974, pp. 219-225.

[11]   Pang, S., "Development and Validation of a Kiln-Wide Model for Drying of Softwood Lumber," *Proceedings of the 5th International IUFRO Wood Drying Conference*, Quebec City, Canada, 1996, pp. 103-110.

[12]   Hua, L., Bibeau, E., He, P. F., Gartshore, I., Salcudean, M., and Chow, S., "Modeling of Airflow in Wood Kilns," *Portland Wood Show*, Portland, Oregon, 1998, pp. 121-127.

[13]   Tarasiewicz, S., and Leger, F., "Industrial Lumber Drying and Its Internal Model Conception for Control System Design," *Proceedings of the 5th Internationsl IUFRO Wood Drying Conference*, Quebec City, Canada, 1996, pp. 275-281.

[14]   Wengert, G., and Bois, P., "Evaluation of Electric Moisture Meters on Kiln Dried Lumber," *Forest Products Journal*, 47(6), 1997, pp. 60-62.

[15]   Zeleniuc, O., and Ene, N., "Gravimetric System to Determine the Moisture Content of Wood During Drying Process," *Proceedings of the 5th International IUFRO Wood Drying Conference*, Quebec City, Canada, 1996, pp. 213-220.

[16]   Little, R., and Moshler, W., "An Automated Weight-Based System for Kiln Control," *Proceedings of the 5th International IUFRO Wood Drying Conference*, Quebec City, Canada, 1996, pp. 261-268.

[17]   Canteri, L., and Martin, M., "Quality Wood Drying Estimation Through Moisture, Temperature, Pressure and Shrinkage Measurements," *Proceedings of the 5th International IUFRO Wood Drying Conference*, Quebec City, Canada, 1996, pp. 245-253.

[18]   Ugolev, B. N., and Skuratov, N. V., "Application of Computer Method to Lumber Drying Schedules Development and Prong Test Analysis," *Proceedings of the 3rd International IUFRO Wood Drying Conference*, Vienna, Austria, 1992, pp. 64-68.

[19]   Dreiner, K., and Welling, J., "Self-Tuning Controllers for the Kiln Drying Process," *Proceedings of the 3rd International IUFRO Wood Drying Conference*, Vienna, Austria, 1992, pp. 205-216.

[20]   Zadeh, L. A., "Fuzzy Sets," *Information and Control*, No. 8, 1965, pp. 338-353.

[21]   Zadeh, L. A., "Outline of a New Approach to the Analysis of Complex Systems and Decision Process," *IEEE Transactions SMC*, 3 (1), 1973, pp. 28-44.

[22]   Gains, B. R., "Fuzzy Reasoning and the Logics of Uncertainty," *Proceedings of the 6th IEEE International Symposium on Multiple-Valued Logic*, 1976, pp. 179-188.

[23]   Mamdani, E. H., "Applications of Fuzzy Algorithms for Control of a Simple Dynamic Plant," *Proceedings of IEEE*, 121, 12, 1974, pp. 1585-1588.

[24]   Schwartz, D. G., and Klir, G. J., "Fuzzy Logic Flowers in Japan," *IEEE Spectrum*, July 1992, pp. 32-35.

[25]   Chevalier, F. M., and Frayret, J. M., "A Fuzzy Logic Application to Kiln Dryer Regulation," *Proceedings of the 5th International IUFRO Wood Drying Conference*, Quebec City, Canada, 1996, pp. 221-229.

[26]   Doehm, Ch., "Case Study for the Implementation of a Fuzzy Logic Controller to Control the Quality Characteristics Moisture and Color of Biscuits," *MARS GmbH*, Viersen, 1992.

[27] Krause, B., and Constantin von Altrock, "Fuzzy logic control of baking TWIX candies," *fuzzyTECH Application Paper*, http://www.fuzzytech.com,1997.

[28] Mesarovic, M. D., Macho, D., and Takahara, Y., *Theory of Hierarchical Multilevel Systems*, Academic Press, New York, 1970, pp. 34-108.

[29] Zadeh, L. A., "The Role of Fuzzy Logic in the Management of Uncertainty in Expert Systems," *Fuzzy Sets and Systems*, Vol. 11, 1976, pp. 199-227.

[30] De Silva, C. W., and MacFarlane, A. G. J., "Knowledge-Based Control Structure for Robotic Manipulators," *Proceedings of the IFAC Workshop on Artificial Intelligence in Real-Time Control*, Swansea, Wales, U.K., International Federation of Automatic Control, 1988, pp. 143-148.

[31] De Silva, C. W., "An Analytical Framework for Knowledge-Based Tuning of A Servo Controller," *Engineering Applications in Artificial Intelligence*, Vol. 4, No. 3, 1991, pp. 177-189.

[32] Saridis, G. N., "Knowledge Implementation: Structure of Intelligent Control Systems," *Journal of Robotics Systems*, Vol. 5, No. 4, 1988, pp. 255-268.

[33] De Silva, C. W., "Fuzzy Information and Degree of Resolution Within the Context of a Control Hierarchy," *Proceedings of IECON'91*, Kobe, Japan, 1991, pp. 1590-1595.

[34] Zadeh, L. A., "The concept of a Linguistic Variable and Its Application to Approximate Reasoning," Part 1-3, *Inf. Sci.*, 1975, pp. 43-80, 199-249, 301-357.

[35] Ziegler, J. G., and Nichols, N. B., "Optimum Settings for Automatic Controllers," *Transactions of the ASME*, Vol. 64, 1942, pp. 759-768.

[36] Yan, G. C. K., De Silva, C. W., and Wang X.G., "Modeling and Adaptive Control of a Kiln Dryer for Wood," *Proceedings of the Second IASTED International Conference*, Banff, Canada, 1999, pp. 144-149.